APPLICABILITY OF LASER ABLATION AND PARTIAL DISSOLUTION ICP-MS TECHNIQUES ON Mn-Fe-OXIDE COATINGS OF STREAM PEBBLES TO MINERAL EXPLORATION AND ENVIRONMENTAL MONITORING

DIANE WANDA COISH

APPLICABILITY OF LASER ABLATION AND PARTIAL DISSOLUTION ICP-MS TECHNIQUES ON Mn-Fe-OXIDE COATINGS OF STREAM PEBBLES TO MINERAL EXPLORATION AND ENVIRONMENTAL MONITORING

By
Diane Wanda Coish, B.Sc. (Hons.)

A Thesis Submitted to the School of Graduate Studies in Partial Fulfilment of the Requirements for the Degree of Master of Science

Department of Earth Science
Memorial University of Newfoundland

August, 2000

St. John's *Newfoundland*

ABSTRACT

Mn-Fe-oxide coated stream pebbles have been proposed as an alternative sampling medium for regional geochemical surveys. Partial dissolution and laser ablation microprobe analysis of these coatings were tested in this project to determine the applicability of using oxide coatings for mineral exploration and environmental monitoring projects.

The three areas covered in this project include a Au showing, a base-metal prospect and potentially harmful emissions from an oil refinery. Mn-Fe-oxide coated stream pebbles were systematically collected from stream(s) in each field area and two types of analyses were conducted on the pebble coatings. Partial dissolution Inductively Coupled Plasma-Mass Spectrometry (ICP-MS) and solid sample analysis using Laser Ablation Microprobe-Inductively Coupled Plasma-Mass Spectrometry (LAM-ICP-MS) proved successful in detecting the elements relevant to the individual disciplines. Low concentrations of elements in the stream water samples were not able to contribute to this project since most were below the detection limit (See Appendix 1) and failed the required statistical analysis of variance therefore, were not considered for further discussion.

Analysis of variance for the two approaches, digestion of oxide coatings and solid sample analysis of pebble coatings using laser ablation shows that the results from the Mn-Fe-oxide pebble coatings are encouraging. Elements that are typically used to detect and define mineralization or a potential pollutant source are present in the oxide pebble coatings and the majority of them pass the required statistics, therefore, they are graphically presented and discussed.

Comparisons between the two methods of analysis for the Mn-Fe-oxide pebble coatings suggests that there is a degree of reproducibility between the two laboratory procedures. In most cases, the partial dissolution process provides a more pronounced geochemical signature, although, these anomalies are also noted using the current LAM-ICP-MS procedure.

For this project, it appears that considering Mn-Fe-oxide coatings as a sampling medium is a viable venture. The current LAM-ICP-MS capabilities suggests that the analysis of the pebble coatings would be more reliable and cost effective if the dissolution ICP-MS method was the primary analytical procedure. Overall, the analyses of the Mn-Fe-oxide stream pebble coatings suggests that gold mineralization, base-metal Pb-Zn-Cu mineralization and potential pollutants from a smoke stack at an oil refinery and the extent of their affect on the local environment are able to be detected using the oxide pebble coatings as a sampling medium.

ACKNOWLEDGEMENTS

I would like to extend a heartfelt thanks to my supervisor Dr. Derek Wilton. Derek I know it must seem that this project has been never ending but I would really like to thank you for all of your much appreciated help. Your guidance and insight has helped me over more than one stumbling block.

Dr. Henry Longerich, thank you for all the help, the many chats and questions that only you could answer. Good luck with your retirement and any further endeavours.

Dr. Peter Davenport of the Newfoundland Department of Mines and Energy is acknowledged for his much appreciated help with statistics and very valuable corrections, which were much needed for certain areas of this thesis.

Simon Jackson, Mike, and all the ICP-MS staff and technicians, I never could have completed this without your very valuable help. Many thanks for answering all my questions and showing me the ropes around the lab.

Fellow students, Laurel McDonald, Jim Brydie, and Rod Churchill for being willing to lend a hand or ear when it was needed. To Jody Hodder for being my sounding board and letting me know when it was time for me to wind down. Thanks for everything.

I also need to thank my parents, Bruce and Patsy for their unfailing support in everything I ever aspired to do. I can never repay you, thanks and all my love.

TABLE OF CONTENTS

CHAPTER 1
INTRODUCTION

CHAPTER 2
FIELD SAMPLING AND LABORATORY PROCEDURES

CHAPTER 3
GEOLOGY AND MINERALIZATION

CHAPTER 4
RESULTS

CHAPTER 5
DISCUSSION

REFERENCES

APPENDIX 1
STREAM WATER RESULTS

APPENDIX 11
MN-FE-OXIDE COATING GEOCHEMICAL ANALYSES

APPENDIX 111
MASS OF MN-FE-OXIDE COATINGS ON THE STREAM PEBBLES

LIST OF TABLES

LIST OF FIGURES

LIST OF PLATES

CHAPTER 1: INTRODUCTION

1.1 Introduction

Classical regional geochemical surveys used in mineral exploration and environmental monitoring involve the sampling of media such as soils, stream silts, and lake bottom sediments. The concept of using oxide coated stream pebbles as a medium for these surveys was established in the 1970's when experimental studies using oxide coated pebbles have supported the supposition of such pebble coatings being a means of obtaining a regional geochemical signature. Base metals have usually been the target of these surveys with a limited number of studies concentrated on other applications such as gold exploration and environmental monitoring.

Oxide coated pebbles are ideal for use in areas where there is limited time for collection or insufficient active stream sediment. The Mn-Fe-oxide coatings absorb heavy metals from the local environment from either coprecipitation or adsorption (Carpenter and Hayes, 1978). They tend to reflect the composition of rocks and ores found in a place.

Chemical analysis of Mn-Fe-oxide coatings is commonly done by Inductively Coupled Plasma-Mass Spectrometry (ICP-MS) or Atomic Adsorption (AA) following acid dissolution. Solid sample analysis of pebble oxide coatings using laser ablation-ICP-MS is an alternative technique. In this method the coating is ablated with a laser beam and analysed until the substrate/pebble is intersected (Thompson *et. al.*, 1992; Coish, 1993). Comparison of the relative accuracy of this technique compared to ICP-MS solution analysis forms the basis of this M.Sc. study. Previous work by Coish (1993) had indicated that the laser ablation

technique worked in determining the presence of base metal mineralization in an area using Mn-Fe-oxide coated stream pebbles.

Three survey areas, covering three different objectives, (1) gold mineralization, (2) base metal mineralization and (3) an environmental study, comprise the basis of this project. Each of the surveys is a test to determine the applicability of using oxide coated pebbles to define regional geochemical dispersals. In each survey area, oxide coatings were analysed by both solution chemistry and laser ablation.

1.2 Location and access

This study is based on the geochemical analysis of pebbles from streams in three field areas. Two of these streams drain areas with known mineralization while the third is part of a network draining a possibly anthropogenically contaminated area.

The two streams with known mineralization were selected mainly because the point source of mineralization is known and each is located in or next to the streams sampled. An additional factor is the excellent background geochemical data base that has been collected from a variety of sources. The established geochemical data base provides a basis for comparison of any results obtained in this study with regards to detecting the point source of mineralization. The Come-By-Chance oil refinery, the study area for environmental monitoring, has become an object of concern for local residents and there has not been an independent study of the effects of the pollutants released from the refinery on the local environment.

1.2.1 Rocky Pond study area

Rocky Pond River drains Rocky Pond and is located approximately 7 km east-south-east of the community of Birchy Bay in northeastern Newfoundland (Fig. 1.1). The stream drains through the Duder Lake gold prospects. The study area is bounded by latitudes 49°21′N and 49°15′N and longitudes 54°41′E and 54°38′E within the Comfort Cove-Newstead map sheet (NTS 2E/7). Access to Rocky Pond River is by gravel logging roads that begin opposite the Birchy Bay turn-off on Route 340 .

1.2.2 Country Brook study area

Country Brook flows northwards into Hermitage Bay on the Hermitage Peninsula in southern Newfoundland (Fig. 1.1). The stream is located within the Gaultois map sheet (NTS 1M/12) bounded by latitudes 56°55′N and 56°30′N and longitudes 47°43′E and 47°30′E. Country Brook is approximately 33 km northeast of the community of Harbour Breton on Route 360 and was sampled for ~3 km upstream at a distance of 0.5 km from the highway. Country Brook flows from a small pond located at the base of the Winter Hill Pb-Zn volcanogenic massive sulphide deposit.

1.2.3 Come-By-Chance oil refinery study area

The network of streams that comprise area three (Fig. 1.1) drains through the area lying northeast of the Come-By-Chance oil refinery. The study area is bounded by latitudes 47°48′N and 47°51′N and longitudes 53°53′E and 54°00′E, in the Sunnyside map sheet (NTS

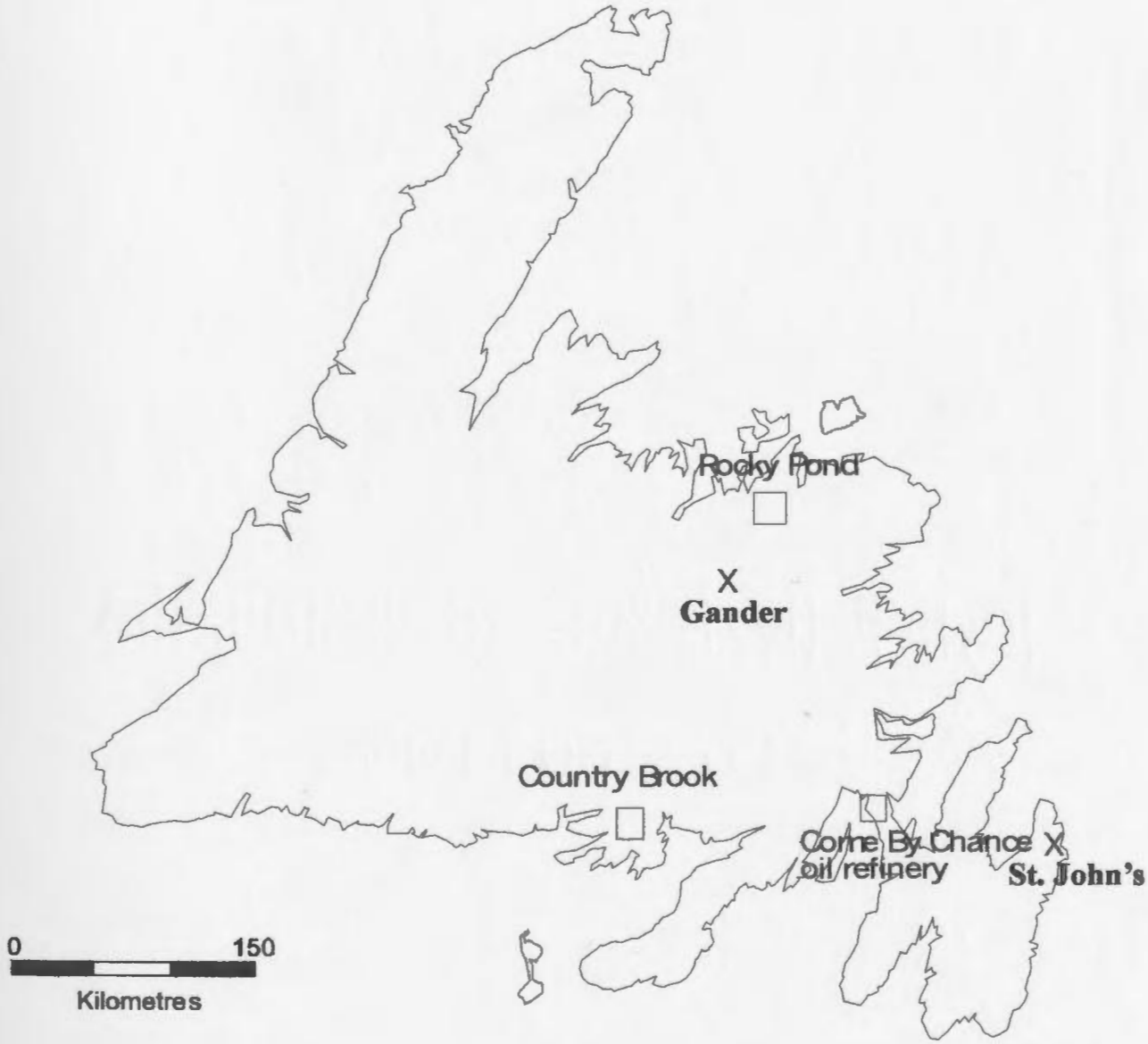

Figure 1.1: Map of Newfoundland showing the location of the three study areas, Rocky Pond, Country Brook and Come-By-Chance oil refinery.

1N/12). An abandoned railway bed provides easy access to sample locations. The streams flow southwestwards into Placentia Bay and drain an area that lies immediately downwind from the Come-By-Chance oil refinery, a sour crude refinery with the capability of processing a wide variety of crude oils and feedstocks, to produce gasoline, jet fuel and gasoil.

1.3 Physiography and vegetation

1.3.1 Rocky Pond study area

The area surrounding Rocky Pond has little bedrock exposure and is characterized mainly by bog and marsh in low-lying areas and, by elongate ridges at higher elevations. These ridges are underlain by gabbro sills and appear to be controlled by and reflect regional structures which transect the area (Churchill, 1994). Recent logging has depleted the local vegetation cover in birch, popular, and spruce trees, but the flora are relatively undisturbed along the river banks (Plate 1.1). Bog and marsh localities are dominated by grass and alder growth around their edges which is locally dense.

1.3.2 Country Brook study area

Bedrock exposure is approximately 60% along Country Brook, with close to 80% exposure in the highland regions bordering the stream. Undulating upland regions pass into steep valley walls in the southern part of the stream (Plate 1.2). The lower part of the stream, in the northern regions, lies in the low-lying area with a more gently sloped valley. Vegetation is abundant downstream but gradually thins upstream. The undulating hills on

Plate 1.1: Vegetation on the stream banks of Rocky Pond River and the relative depth and flow of the river.

either side of Country Brook are mainly covered with shrubs but stands of thick vegetation occur on hillslopes and in some valleys. Spruce, birch and alders are the dominant vegetation in the study area. Moss and shrubs are abundant along the stream banks where bedrock is not well exposed.

1.3.3 Come-By-Chance study area

Limited bedrock exposure and abundant bogs and marshes characterize the area sampled in the Come-By-Chance oil refinery area. The whole area lies at low elevation with little relief. The streams flow mainly through bogs, thus have no stream banks or bedrock exposure. The study area is wide-spread because some streams were unsuitable for sampling due to excessive mud and vegetation present with a limited amount of pebbles and/or boulders. Small shrubs, moss and grass are the dominant flora in the area with small stands of fir, alders and juniper near the lakes and ponds (Plate 1.3). Marshes and bogs have clusters of small shrubs and grass throughout the area.

1.4 Previous work

1.4.1 Rocky Pond

In the area around Rocky Pond, numerous geological studies define regional stratigraphic, tectonic and structural data (Dean, 1977, 1978; Arnott *et. al.*, 1985; Currie, 1993; Piasecki, 1993; Williams, 1993; Williams *et. al.*, 1993; Churchill, 1994). The bulk of the data collected in north-central Newfoundland were focused on the regional stratigraphy, tectonic and structural nature of the Silurian and Ordovician rocks. Most notable is the work of Dean (1977, 1978) who discussed the stratigraphy and mineralization of Notre Dame Bay. Recent works by Currie (1993), Piasecki (1993) and Williams (1993) described the structural discontinuity of the Dog Bay Line, a major tectonic boundary that separates different Silurian rock groups in this area of northeast Newfoundland (Williams *et. al.*, 1993), and revised local

Plate 1.2: Topography and vegetation surrounding Country Brook, Hermitage Peninsula.

Plate 1.3: Relatively low relief and vegetation in the area lying northwest of the Come By Chance oil refinery.

geology in the Comfort Cove-Newstead map sheet. Other recent studies have focused on the alteration assemblages and geochemistry of the Duder Lake gold showings (Evans, 1991, 1992, 1993, 1996; Churchill and Evans, 1992; Churchill *et. al.*, 1993; Churchill, 1994).

The discovery of quartz-vein-hosted gold mineralization by Blackwood (1982) in the Jonathan's Pond area prompted extensive gold exploration in north-central Newfoundland.

Results of a regional lake-sediment geochemical survey indicated that there are Au, Sb and As anomalies (Davenport and Nolan, 1988) in the eastern Dunnage Zone with the highest concentrations found at Duder Lake, Rocky Pond and Ten Mile Lake. Noranda Exploration Company (Green, 1989) undertook grass roots exploration in the area leading to the discovery of Stinger, Flirt, Goldstash and Corvette gold prospects. Noranda carried out more detailed assessment work in 1990 (Tallman, 1990) but conducted no subsequent work.

1.4.2 Country Brook

Regional mapping and reconnaissance exploration work on the Hermitage Peninsula were actively pursued during the late 1940's to mid-1950's. Two base metal prospects were discovered by NALCO Limited geologists during this time at Frenchman Head and along the Harbour Breton Highway (Sears, 1990). Throughout the 1970's more detailed mapping of the Harbour Breton (1M/5) and Gaultois (1M/12) map sheets led to the conclusion that the Connaigre Bay Group was late Precambrian (Williams, 1971). Part of the Gaultois map area was remapped by Greene and O'Driscoll (1976) who divided the Connaigre Bay Group into four formations.

The release of a lake sediment survey by the Newfoundland Department of Mines and Energy (NDME) (Butler and Davenport, 1978) resulted in a revival of mineral exploration on the Hermitage Peninsula leading to the discovery of the Winter Hill prospects. Geophysical work and diamond drilling of claims at Winter Hill by Noranda Exploration Co. Ltd. (Graves, 1985, 1986; Simpson, 1990) provided additional information regarding the size

and grade of the sulphide mineralization. Most recently, Sears (1990) and Sears and Wilton (1996) completed detailed studies of the Winter Hill sulphide showing which included the definition of the geochemical signatures that characterize the deposit type.

1.4.3 Come-By-Chance oil refinery

With the reopening of the Come-By-Chance oil refinery in 1986, residents in the area have become concerned about the effects of the production of oil products and resultant airborne emissions on the local environment. The oil refinery uses a portion of its crude oil as an energy supply for refinery operations. Gas emissions from this practice produces substantial amounts of Vanadium and Chromium to be released into the environment. Other environmental concerns are generated waste products, such as, sulphur dioxide emissions, and the potential for oil spillage into Placentia Bay from accidents on site and oil tanker traffic in the fiord.

The Department of Fisheries and Oceans published a report (Kiceniuk, 1992) concerning hydrocarbon concentrations in sediments at various localities in Placentia Bay. They discovered that some parts of the bay have elevated levels and recommended further studies be carried out. Earlier mapping projects (King, 1982) and microfossil studies (Hoffman *et. al.*, 1979) have defined the spatial distribution and geological history of the Connecting Point Group which the study area lies within.

1.5 Purpose and scope

Mn-Fe-oxide coatings on stream pebbles have been considered in mineral exploration research as an alternative sampling medium to stream sediment and water for the determination of regional geochemical patterns. These coatings absorb or co-precipitate a variety of elements (Robinson, 1981), especially heavy metals, which are relevant in mineral exploration and to the detection of potential environmental contamination of the local environment.

An earlier study by Coish (1993) analysed oxide coatings on stream pebbles to determine the dispersal of base metals in a region that has known sulphide mineralization. This earlier study was based on a compilation of ideas presented by Carpenter and Hayes (1978), Filipek *et. al.* (1981), Robinson (1981, 1984), Chao (1984), Hale *et. al.* (1984), Thompson *et. al.* (1992) and Nicholson (1992). In these other studies, the authors used either partial dissolution of the oxide coatings or laser ablation (Hale *et. al.*, 1984 and Thompson *et. al.*, 1992) to determine the heavy metals concentrated in these pebble coatings.

Coish (1993) indicated that laser ablation of oxide coated stream pebbles had the potential for mineral exploration and environmental monitoring but required further detailed refinements before it could be considered as either an inexpensive or rapid method for locating an ore deposit or a pollutant source. The purpose of this project is to test the applicability of the partial dissolution and laser ablation methods of analysing Mn-Fe-oxide coated stream pebbles for locating a gold showing, a Pb-Zn massive sulphide showing, and the detection of emissions containing heavy metals from an oil refinery and its deposition on

the surrounding environment.

CHAPTER 2: FIELD SAMPLING AND LABORATORY PROCEDURES

2.1 Field sampling

Stream pebbles and waters were systematically collected at a number of sample locations within each field area (See Figures 2.1, 2.2 and 2.3). Sample intervals were dependent on the depth, flow and accessibility to a potential sample site in the stream at locations upstream from the previous sample site. Stream waters were collected first to prevent possible contamination of the water by silt due to streambed disturbance. All samples were collected in an area of ~1 m^2 in the active part of the channel, ie: mid-stream, where the flow ranged from slow to moderate. More than twenty (20) samples were collected in areas of 2 to 4 km in length from each of the field areas. For the two mineralized areas, samples were collected upstream and downstream of the mineralization. A network of streams covering an area of approximately 4 km^2 was sampled northeast of the oil refinery, which is the prevailing wind direction in this study area.

2.1.1 Stream water collection

Waters at each sample location were collected using new B-D LuerLok 20cc syringes which were flushed with stream water three times. One-hundred (100) ml of water was filtered using a new Nalgene™ 0.45 μ syringe filter, into a previously cleaned

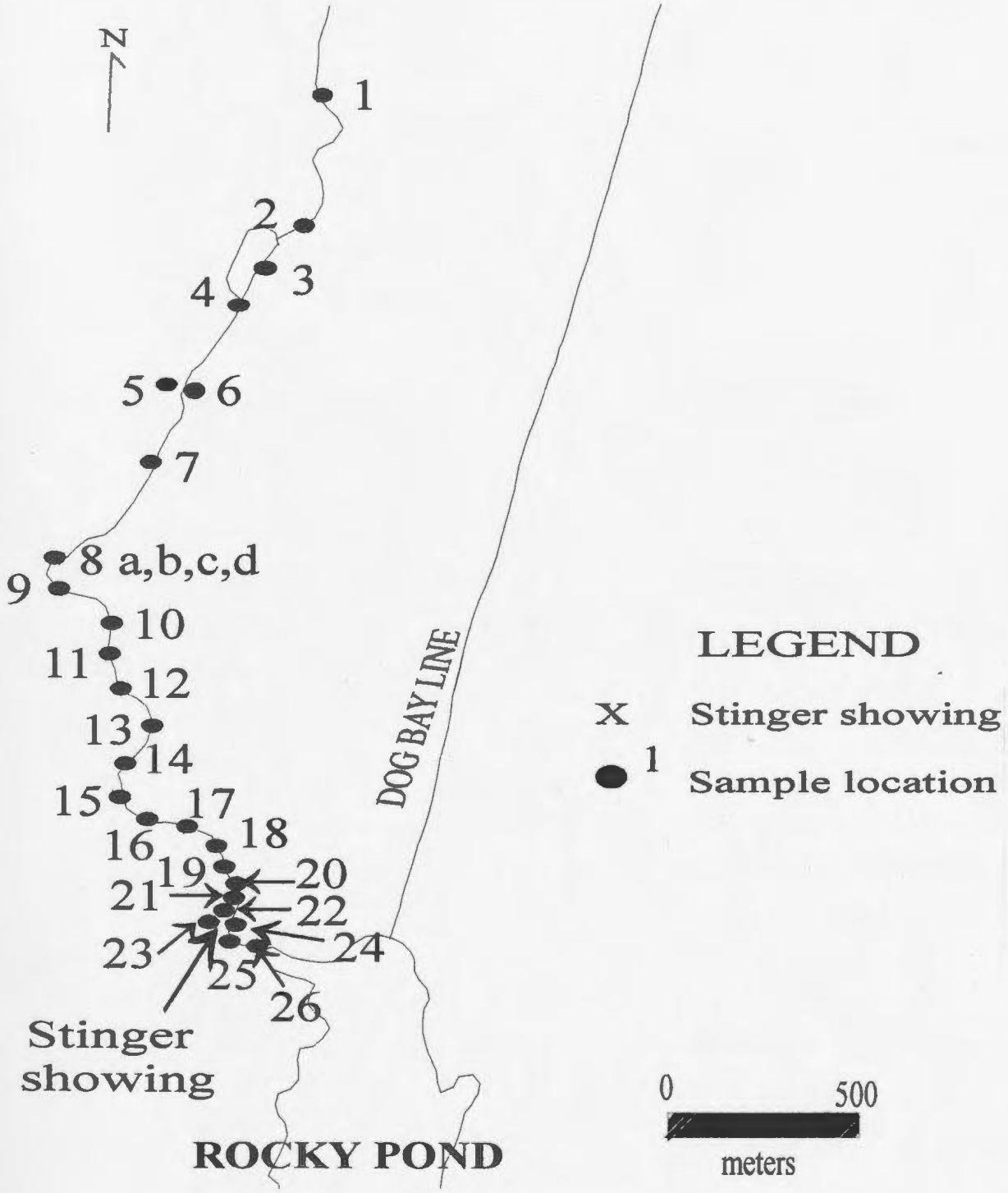

Figure 2.1: Sample locations for stream water and Mn-Fe-oxide coated stream pebble samples collected in the Duder Lake study area.

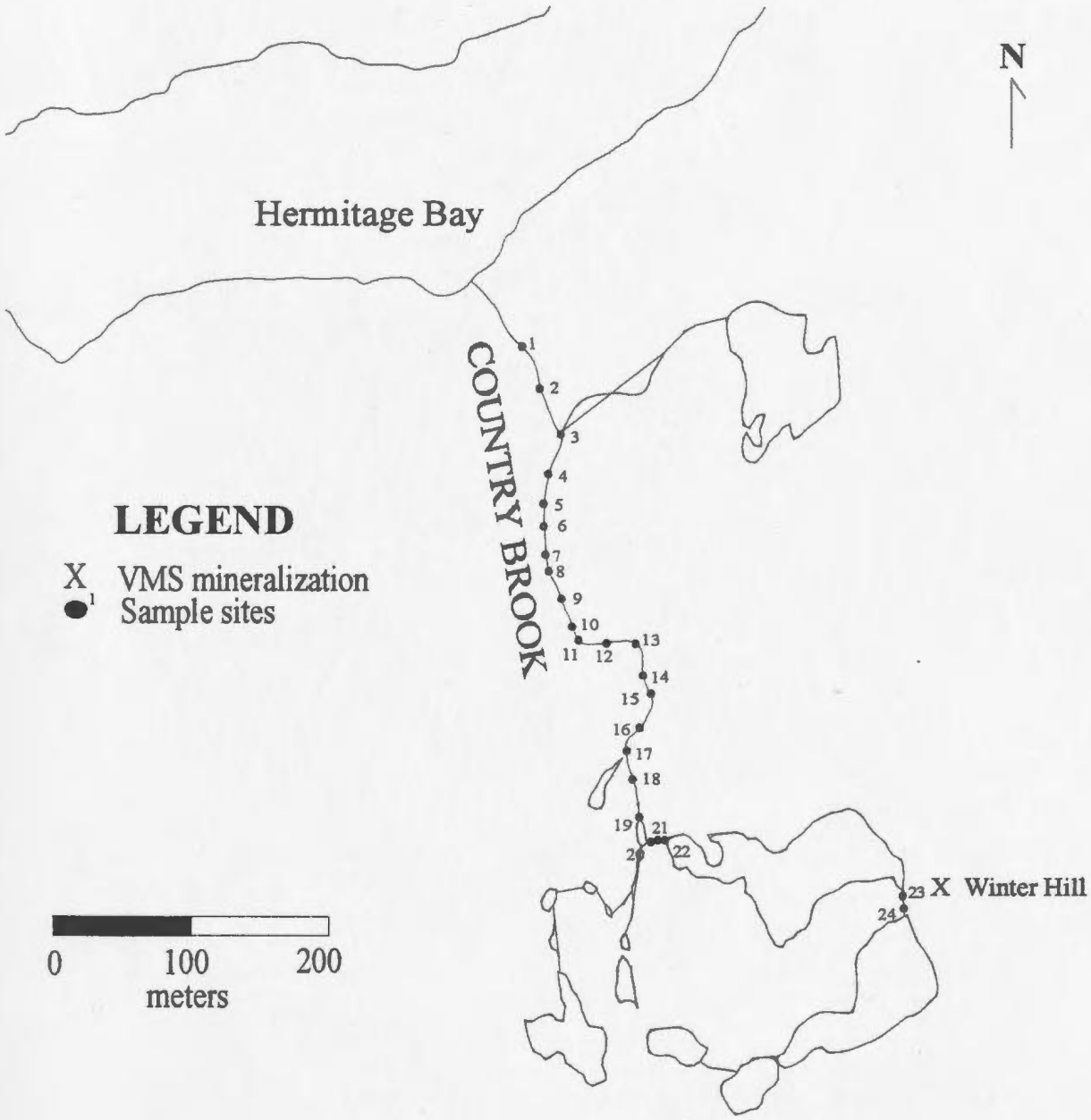

Figure 2.2: Sample locations for stream water and Mn-Fe-oxide coated stream pebble samples collected in the Winter Hill study area.

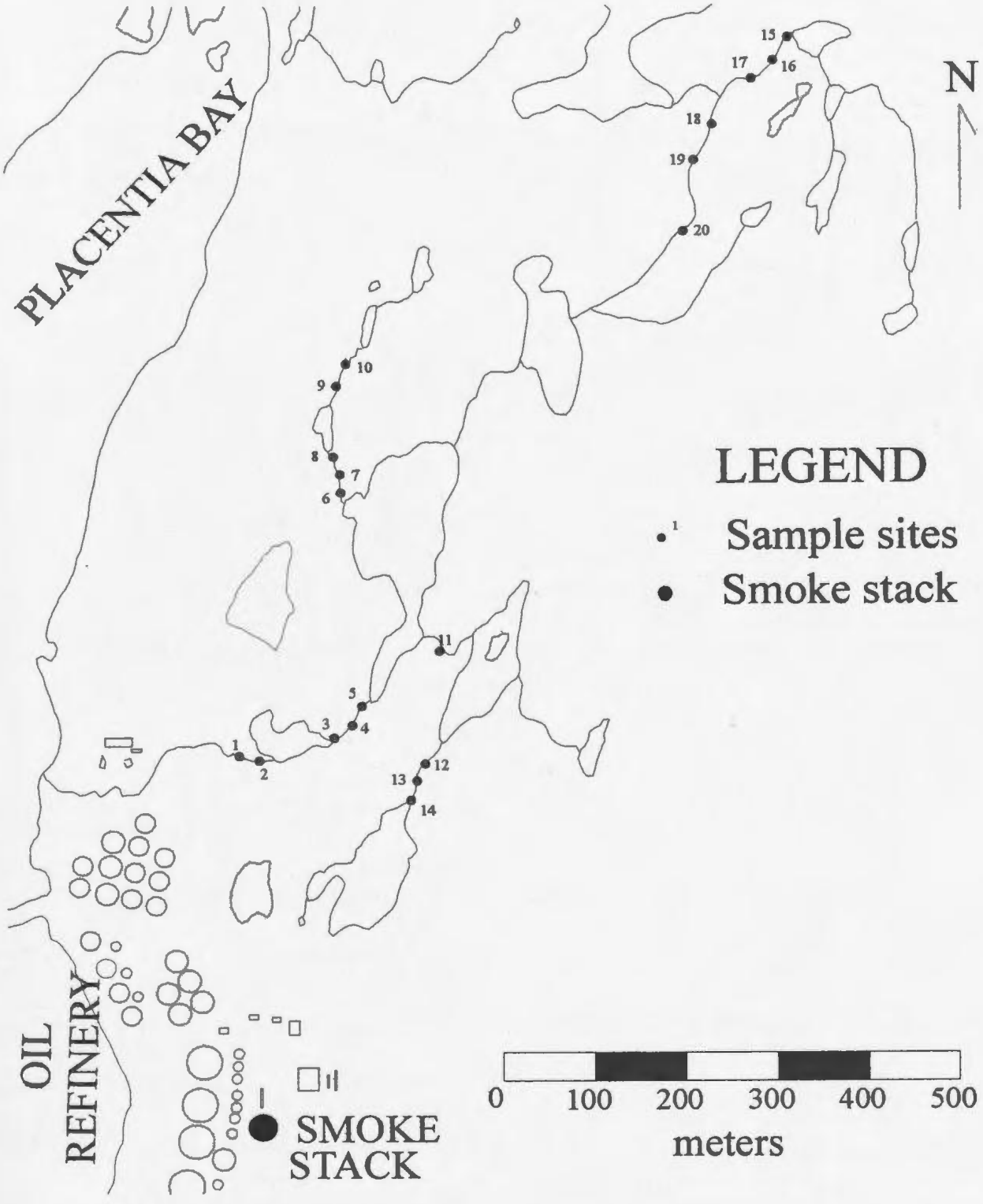

Figure 2.3: Sample locations of stream water and Mn-Fe-oxide coated stream pebble samples collected in the Come-By-Chance Oil Refinery study area.

125 ml Nalgene™ polyethylene bottle. For quality control purposes, two samples from every fourth or fifth sampling site were collected to monitor the reproducibility of the collection and preservation procedure. To prevent the absorption of metal onto the sample bottle and to prevent growth of digested materials that can remove metal from solution, the sample was acidified to *ca.* 0.2 molarity by adding two ml of pure 8N nitric acid (HNO_3) to each bottle at the end of the sample collection day. The nitric acid is ACS analytical grade from Fisher Scientific, which is diluted with distilled water then, distilled in Teflon.

Cleaning and preparation of bottles and caps were done in the lab before being used in the field. Each bottle and cap were cleaned in a 8N HNO_3 solution for twenty-four hours then rinsed three times with deionized water and dried in a filtered air-drying space.

2.1.2 Stream pebble collection

A minimum of three pebbles was collected at each site subsequent to water sample collection. Pebbles with a relatively thick and even Mn-Fe-oxide coating were the preferred samples, of the streams sampled, the pebbles from Country Brook had the thinnest and most patchy coatings (Plate 2.1). All pebbles were transported in Kraft paper sampling bags from the sampling site to the lab where they were dried. Before the dried pebbles were analyzed, they were cleaned with deionized water in the laboratory to

Plate 2.1: Mn-Fe-oxide coating on a stream pebble collected from Country Brook.

remove organisms (flora and algae) that were still attached after rinsing with stream water.

The oxide coatings harden with drying and very little of the coating is lost when washed with deionized water to remove dead organisms and algae. The cleaned pebbles were then placed in a filtered air-drying space to dry (Plate 2.2). Once dry, the samples were placed in new paper sampling bags until they were needed for analysis.

Plate 2.2: Filtered air drying of stream pebbles after cleaning with deionized water.

2.2 Laboratory procedures

2.2.1 Stream water

Stream water was analyzed using a standard waters package for the ICP-MS (Friel *et. al.*, 1990) which has been slightly modified due to the presence of significant naturally occurring Yttrium in the samples. The waters package uses Sc, Re, Th, and Rh as internal standards to correct for drift and matrix effects. For ICP-MS analysis, 10 ml of each field-acidified sample was transferred to a 12 ml test tube. Blanks were acidified in

the laboratory and 10 ml of each blank were also transferred to 12 ml test tubes for ICP-MS analysis. Collection duplicates, split sample duplicates (*i.e.*, single field samples split into two aliquots to monitor precision of the analytical measurements), reagent blanks and water reference standards were also analyzed on each run. Each water sample came directly from the field samples with no further treatment.

As a measure of the level of contamination from the equipment and HNO_3, one or more reagent blanks are prepared (at least one blank per 10 samples). To do this, a sample of deionized distilled water was "collected" using the same procedure, equipment and reagent as for the samples.

Data at each mass were acquired for 10 seconds using a dwell time of 50 ms. The following isotopes are part of the standard water package: ^{7}Li, ^{9}Be, ^{10}B, ^{12}C, ^{14}N, ^{25}Mg, ^{27}Al, ^{28}Si, ^{31}P, ^{34}S, ^{35}Cl, ^{42}Ca, ^{43}Ca, ^{49}Ti, ^{51}V, ^{52}Cr, ^{53}Cr, ^{54}Fe, ^{55}Mn, ^{56}Fe, ^{57}Fe, ^{59}Co, ^{60}Ni, ^{65}Cu, ^{66}Zn, ^{75}As, ^{79}Br, ^{82}Se, ^{85}Rb, ^{88}Sr, ^{98}Mo, ^{107}Ag, ^{111}Cd, ^{118}Sn, ^{121}Sb, ^{127}I, ^{133}Cs, ^{137}Ba, ^{139}La, ^{140}Ce, ^{201}Hg, ^{205}Tl, ^{208}Pb, ^{209}Bi and ^{238}U. Only those isotopes that were also analyzed in the partial dissolution and laser ablation procedures are noted in Appendix I.

2.2.2 Partial dissolution of oxide coatings

Several dissolution techniques have been used to dissolve a portion of a Mn-Fe-oxide coating on pebbles (Chao and Theobald, 1976; Chao, 1984) or the whole of the oxide coating (Carpenter and Hayes, 1978; Filipek *et. al.*, 1981; Robinson, 1981; 1984; Chao, 1984; Clark, 1992). A project by Coish (1993) used the results from separate

analysis of the Mn-oxide and the Fe-oxide components of the pebble coating for comparison with laser ablation data on the same pebbles. The Mn-oxide component of the coating dissolved first using a 0.1 M hydroxylamine hydrochloride solution and then dissolved the Fe-oxide component using 0.222 M oxalic acid. The data for these two separate solutions were found to be difficult to compare both with each other and with the results obtained from laser ablation, which analyzes the Mn and Fe phases simultaneously. Therefore, it was deduced that further studies were required to test these laboratory techniques using more field and laboratory duplicates and doing a statistical analysis on each of the data sets obtained.

For this present study, the collected pebbles were broken into pebble chips (5-10 mm) to provide material for partial dissolution of the oxide coatings. The solutions were subsequently analyzed using ICP-MS techniques, with the same waters package that was used for the stream water samples. The oxide coatings on the pebble chips are assumed to reflect the composition of the stream waters since the elements concentrated in the coatings are presumably derived from the stream water.

A solution of 0.25 M hydroxylamine hydrochloride in 0.25% hydrochloric acid (HCl) was used to dissolve the entire Mn-Fe-oxide coating without removing any, or any measurable amount, of the host (Chao, 1984). Prior to adding the solution to the pebble fragment(s), their weights were recorded. Three pebble fragments (5 to 10 mm), one chip from each of the three pebbles per site, were placed into a new and cleaned snap-lid polyethylene 100 ml vial with approximately 30 ml of the hydroxylamine hydrochloride/HCl solution. The solution and pebbles were then shaken for 60 minutes

on a mechanical shaker. The solutions were then filtered into previously cleaned 100 ml teflon beakers and evaporated to dryness at a temperature of 70°C on a hot plate. The remaining filtrate is composed of the pebble chip(s) and any algae or insoluble material that had been on the oxide surface. The insoluble material was discarded and the remaining pebble chip(s) were rinsed three times with deionized water, dried in an oven at 100°C overnight then weighed. Since hydrochloric acid can be a source of Cl^- interference with various elements during analysis by ICP-MS (Longerich *et. al.*, 1986), 3-6 ml of 8N HNO_3 was added to the precipitate, then evaporated to dryness. This procedure was repeated once more.

The mass of the oxide coating was determined as the difference between the pre- and post-dissolution weights (Appendix III). Each sample had a different weight but this was compensated for when each sample was made up to volume with 8N HNO_3 and deionized water. Samples where the weights of dissolved material were <0.05 g had 1 ml of 8N HNO_3 added to the precipitate, and then were made up to a volume at a ratio of 0.1 : 100 with deionized water; weights of ~0.05 g had 2 ml of 8N HNO_3 added and were made up to volume in the same ratio as above. The final weight of the solution was recorded for use in the calculating of element concentrations after analysis.

To monitor sampling precision and the precision of the analytical measurements, duplicates for half of the samples were prepared. The 143 samples (including collection and duplicate samples) were analyzed using the laboratory waters package. Fifteen blanks and a number of synthetic calibration standards, of known elemental

concentration, which determine the drift and sensitivity of the ICP-MS, were also analyzed on each run. The blanks are made using the same method as the samples; 30 ml of hydroxylamine/HCl solution is shaken on a mechanical shaker for 60 minutes then filtered into a teflon beaker and heated to dryness at 70°C; 8N HNO_3 is added to the precipitate, then evaporated to dryness. This procedure is repeated once more. Each blank is made up to volume, in a similar manner as the samples, using the oxide weights determined from the precipitates of the evaporated solutions.

Manganese concentrations were difficult to determine at first with the dilution factor stated above, 0.1 : 100. The leachate samples had to be rerun with a higher dilution factor to determine the high Mn concentrations found in the samples. These values are included in the analytical results section found in Appendix 11a.

2.2.3 Laser ablation of oxide coatings

One pebble chip from each pebble collected per sample site was used for analysis by laser ablation microprobe-inductively coupled plasma-mass spectrometry (LAM–ICP-MS). Two sites per pebble chip were ablated; to determine the repeatability of results, resulting in six analyses of a suite of isotopes collected for each individual sample site. There are exceptions to the above, for samples labeled DC-94-08a, DC-94-08b, DC-94-08c and DC-94-08d they are four samples collected across the stream from one streambank to the other to show variation in composition of the oxide coatings outside of the normally sampled mid-stream location.

Each suite of isotopes analyzed in the coatings was customized for the specific mineralization or potential environmental contribution for each study area. For Rocky Pond (Au mineralization) and Winter Hill (Pb-Zn VMS) areas, the suite of isotopes analyzed was: ^{29}Si, ^{34}S, ^{49}Ti, ^{57}Fe, ^{59}Co, ^{65}Cu, ^{66}Zn, ^{75}As, ^{82}Se, ^{98}Mo, ^{111}Cd, ^{121}Sb, ^{125}Te, ^{134}Ba, ^{181}Ta, ^{197}Au, ^{201}Hg, ^{203}Tl, ^{204}Pb, ^{209}Bi and ^{238}U. The suite of isotopes of interest for the environmental monitoring study of the Come-By-Chance oil refinery area consisted of: ^{29}Si, ^{34}S, ^{42}Ca, ^{49}Ti, ^{51}V, ^{53}Cr, ^{57}Fe, ^{59}Co, ^{60}Ni, ^{65}Cu, ^{66}Zn, ^{75}As, ^{82}Se, ^{98}Mo, ^{107}Ag, ^{111}Cd, ^{119}Sn, ^{121}Sb, ^{125}Te, ^{135}Ba, ^{140}Ce, ^{182}W, ^{201}Hg, ^{203}Tl, ^{204}Pb, ^{209}Bi and ^{238}U. This suite of isotopes was selected to closely reflect the current monitoring program of vegetation, soil and surface water that is being conducted in the vicinity of the Come-By-Chance oil refinery (Sheppard Green Engineering and Associates Limited, June, 1996). Due to the elevated concentrations of some elements in the coatings, such as Fe and Se, and the sensitivity of the ICP-MS, an isotope with lower abundance for each element was analyzed. In the case of Fe it was ^{57}Fe and for Se it was ^{82}Se. If there was analytical interference from other elements, the next lowest abundance isotope was used. Manganese values could not be determined due to Mn being monoisotopic and having extremely high concentrations, therefore, no other isotope could be used.

Three pebble chips (5-10 mm) from each sample site, a maximum of 24, were mounted on glass slides (5 by 6.5 cm) using 5 Minute® Epoxy Gel (Plate 2.3). The glass slides were cut to fit into the sample chamber of the LAM–ICP-MS system. The ablation procedure was conducted using a 266 nm laser energy beam, which is focused on and

then hits or ablates the oxide coated pebble chips three times. The coatings are to thin to allow the laser to run continuously therefore the beam hits the oxide coating three times for a couple of seconds each time at a set energy level which is dependent on the relative abundance of some of the isotopes. The ablation process is done manually, that is, the operator pushes a button to operate the beam instead of letting the laser run continuously. The energy levels of each analysis varied between 0.5 to 2.0 mJ/pulse. The energy levels used varied due to the excessive abundance of some elements such that the ICP-MS's ability to detect was hampered. The ICP-MS has an in-built cut off limit and when this limit is exceeded, by high counts, the detector shuts off to protect itself against damage (Longerich *et. al.*, 1986).

Figure 2.4 is a schematic of the laser ablation microprobe (LAM) system, which uses a Quantel (now Continuum) 1064 nm Q-switched Nd:YAG laser with frequency doubling (532 nm) and quadrupling (266 nm) hardware. Mirrors and prisms steer the laser beam through the photo tube of a petrographic microscope (Fig. 2.4). The focusing lenses are of a variety of types, including standard high quality and air spaced microscope lenses, single element quartz lenses and reflecting objectives (Günther *et. al.*, 1995). Samples can be examined with reflected or transmitted light when not ablating or by reflected light observation during ablation (Jackson *et. al.*, 1992; Günther *et. al.*, 1995). A television camera and monitor are also used for observation.

The mounted pebble chips were ablated with a diffuse or de-focused beam, meaning that the stage upon which the sample cell rests on was moved down 1 mm so that the beam was not too highly focused on one small area. The de-focusing of the beam

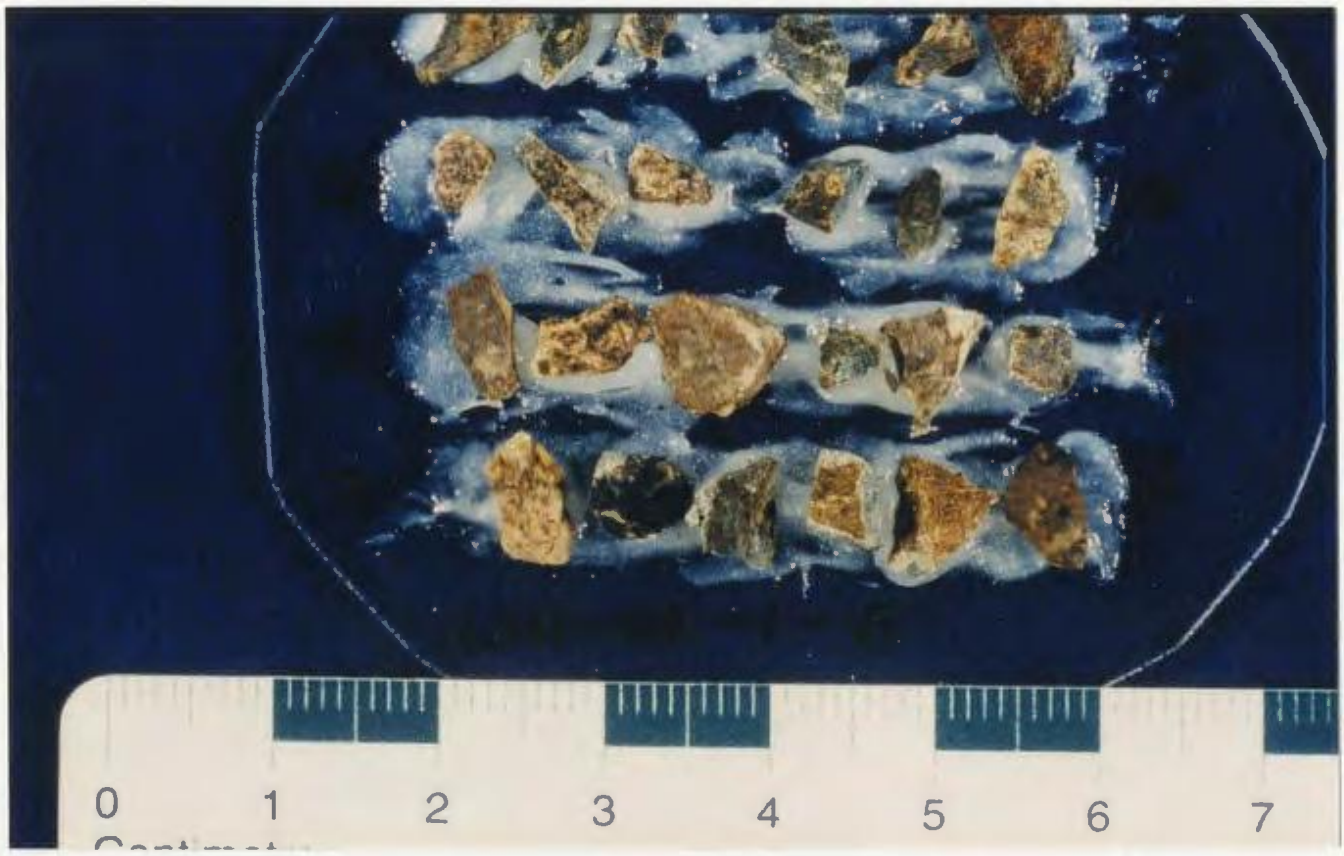

Plate 2.3: Oxide coated pebble chips mounted on a glass slide that was cut to fit into the sample chamber of the LAM – ICP - MS system.

creates a larger diameter pit, approximately 250 μm in diameter, (Plate 2.4) with the result that more of the oxide coating is ablated before the beam reaches the substrate. The smaller the suite of isotopes to be determined, the more time there is for individual determination of the isotopes. A highly focused beam reaches the substrate very quickly, hence analytical time for the analysis is greatly reduced.

A spiked silicate glass, standard reference material (NIST 610) was analyzed twice at the beginning of a suite of samples (16 samples in total per run) and two more times at the end of the run for calibration of the LAM–ICP-MS system. All results were

QWP = quarter wave plates (1064 nm)
FHG, SHG = first, second harmonic generator
M = dielectric mirror (1,2-532 nm; 3,4-266 nm; 5-1064 nm; 6,7-interchangable)
POL = dielectric polariser (1064 nm)
HWP = half wave plate (1 - 1064 nm; 2 - 532/266 nm)
GLAN = glan laser calcite prism polariser
BP = binocular prism
AN = analyser
RLM = reflected light mirror

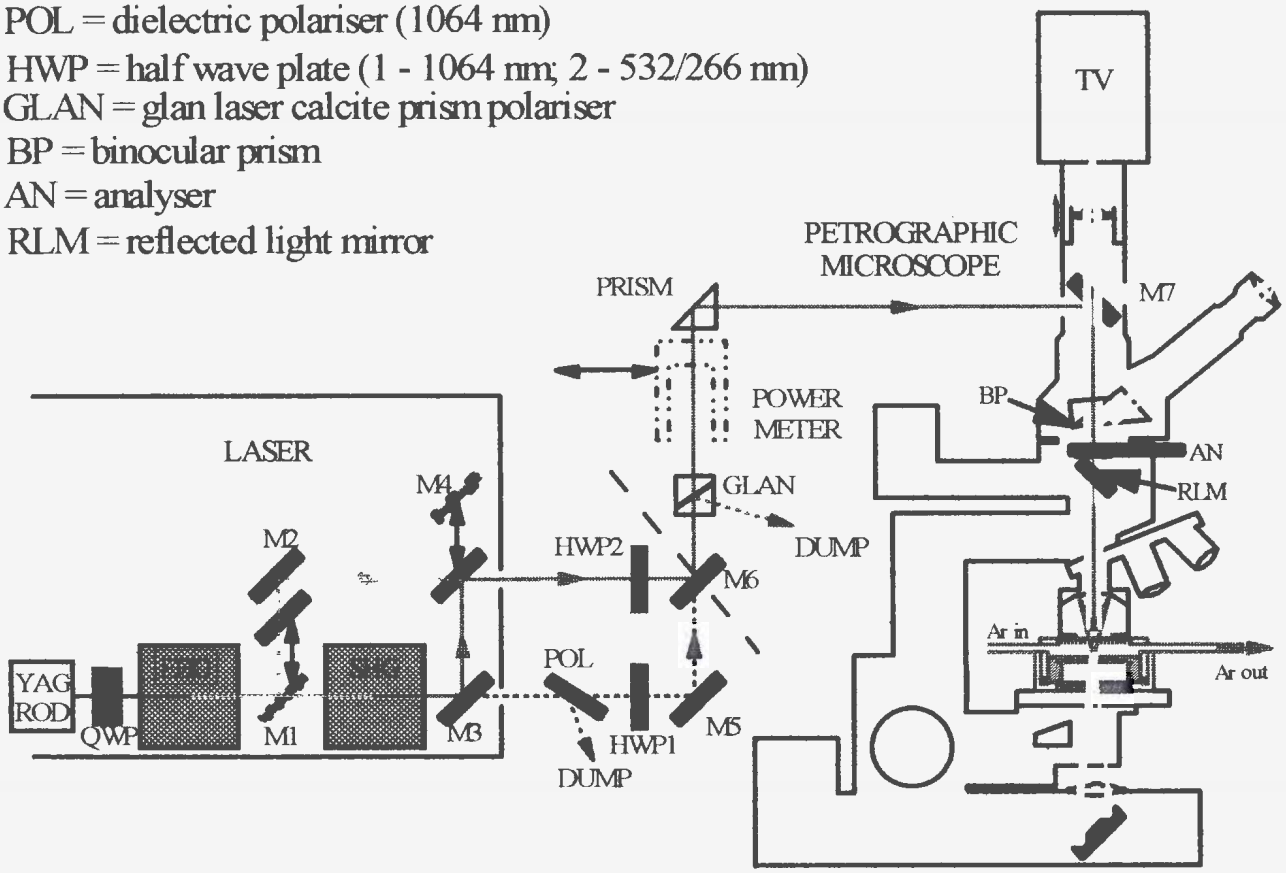

Figure 2.4: Schematic of the LAM – ICP - MS setup for solid sample analysis (modified from Jackson *et. al.*, 1992).

recorded as counts per second (cps) and acquired by peak jumping (dwell times 8.5 msec). Results are recorded in cps not concentrations because the volume of material ablated was not able to be determined. Matrix effects and drift are corrected using naturally occurring internal standards (Günther *et. al.*, 1995).

Precision and detection limits are a function of a number of variables. The two main variables are the mass of the ablated material (pit volume) and the counting time per isotope for the ablated mass (Jackson *et. al.*, 1992). Ablation time, laser intensity, and the material being ablated control the pit volume (Günther *et. al.*, 1995). Large pits allow higher count rates, lower detection limits and better precision. The counting time of individual isotopes is a function of the number of isotopes being counted since only one isotope can be counted at a time.

2.3 Statistical analysis

Statistical analysis of the data collected for the three media types were carried out using a spreadsheet program. Each data set consists of raw data obtained by analysis for each sampling medium including laboratory duplicates and/or site duplicates. All data were log-transformed to normalize the strongly positively skewed distributions as required by the analysis of variance method used for each variable; total, analytical, combined sampling and analytical, and geochemical variances and F-ratios.

Total variance of the individual data sets used the formula from Levin and Rubin (1991):

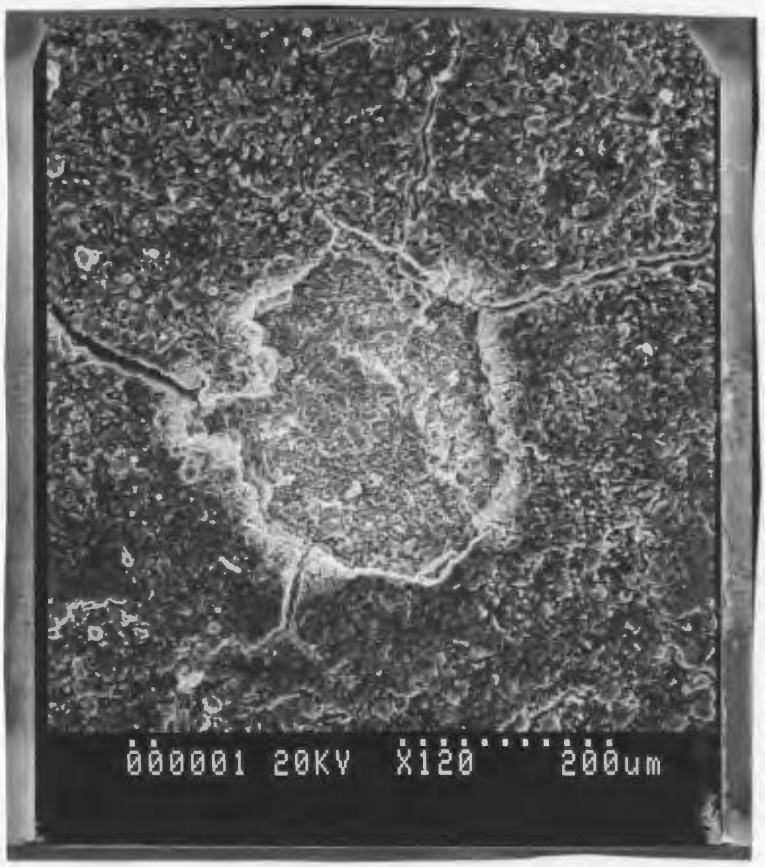

Plate 2.4: Scanning electron microscope photo of a laser ablation pit on a pebble chip.

$$\theta^2 = \frac{\sum (x - \mu)^2}{N}$$

where : θ^2 = population variance

x = the item or observation

μ = population mean

N = total number of items in the population

$\sum$ = sum of all the values $(x - \mu)^2$

For the laser ablation data subsets, total variance was calculated in two ways. All of the data from the three study areas were combined and the overall total variance and the total variance for each individual study area were calculated.

Analytical and sampling variances were calculated using the following formula (Garrett, 1973):

$$\theta^2 = \frac{\sum (x_1 - x_2)^2}{2N}$$

where : θ^2 = sampling or analytical variance

x_1 = first value of the site duplicate

x_2 = second value of the site duplicate

$\sum$ = sum of differences $(x_1 - x_2)$

N = number of site duplicate pairs

Since there were no laboratory duplicates analyzed for the stream water and leachate samples, a combined sampling and analytical variance was calculated from the field duplicates. Individual analytical and sampling variances were calculated for the laser ablation data using the Garrett (1973) formula. The data subset used for the calculation of the analytical variance consisted of the two values obtained per pebble chip of each sampled site. In most cases, six values per sample site were used since each of the three

pebble chips was analyzed twice. Sampling variance was calculated using the data subset of one value from a pebble chip and comparing it with a value of another pebble chip at the same sampling location. Analytical and sampling variance were calculated in the same way for the overall total data and for the individual study areas. Geochemical variance was calculated by subtracting the combined analytical and sampling variance from the total variance. For the stream water and partial dissolution data sets the analytical and sampling variances were already combined, so this one value was subtracted from the total variance.

The F-ratio of the stream water and leachate results was calculated using the following formula (Garrett, 1969):

$$\text{F - ratio} = \frac{\theta^2_{total}}{\theta^2_{a\&s}}$$

where: $\theta^2_{\text{total}} = \text{total population variance}$

$\theta^2_{\text{a \& s}} = \text{combined analytical and sampling variance}$

The F-ratios of analytical and combined sampling and analytical variances of the laser ablation analysis were calculated separately:

$$\text{F - ratio}_{\text{s \& a}} = \frac{\theta^2_{total}}{\theta^2_{\text{sampling \& analytical}}} \qquad \text{and} \qquad \text{F - ratio}_{\text{analytical}} = \frac{\theta^2_{total}}{\theta^2_{analytical}}$$

where: $\theta^2_{\text{total}} = \text{total variance of the data set}$

$\theta^2_{\text{sampling \&analytical}} = \text{variance of the field duplicates}$

$\theta^2_{\text{analytical}} = \text{variance of the laboratory duplicates}$

A value for F-ratios of four or greater is a generally taken to indicate an acceptably small level of experimental noise (Garrett, 1969; 1973). If the F ratio is ≥ 4, the results for that element are presumed to be sufficiently reproducible and can be considered for further discussion. When the F-ratio is < 4, the results are unlikely to show between location differences reliably due to the difference being too small to be statistically significant with respect to the sampling and/or analytical procedure used.

2.4 Data reduction

2.4.1 ICP-MS: water samples and coating solutions

Original sample values determined by ICP-MS were corrected by subtracting the value of the reagent blank from the original sample values. This same procedure was used on both the stream water and partial dissolution data sets. These corrected results are those that are presented in Appendices I and II a.

2.4.2 LAM-ICP-MS

Values obtained by the laser ablation procedure were originally recorded as counts per second with no corrections of drift, matrix effects, blanks or standards. The data, in its raw form, was transferred to a computer program that reduces the values of every time slice analyzed into one value for that sample site. These cps values are presented in Appendix II b.

CHAPTER 3: GEOLOGY AND MINERALIZATION

3.1 Rocky Pond

3.1.1 Regional Geology

The Rocky Pond/Duder Lake area and associated gold mineralization lies within the Exploits Subzone of the Dunnage Tectonostratigraphic Zone of the Newfoundland Appalachians (Williams, 1979). This zone is comprised of oceanic volcanic, plutonic and sedimentary rocks which record the development and destruction of the Iapetus Ocean during the late Cambrian to early Silurian (*op cit*). Williams *et. al.* (1988) subdivided the Dunnage Zone into two broad subzones, the Exploits and Notre Dame subzones, based on contrasts in stratigraphy, structure, lithology, fauna, plutonism, lead isotopic signatures in mineral deposits and geophysics. The Red Indian Line fault system divides the Dunnage Zone into southeastern and northwestern sections forming the Exploits Subzone and the Notre Dame Subzone, respectively (Fig. 3.1), the study area lies within the Exploits Subzone. Ordovician deep marine sedimentary, shallow marine to fluviatile sedimentary rocks, and subaerial volcanic rocks of Silurian age intruded by gabbroic bodies and Siluro-Devonian granitoid characterizes the Exploits Subzone.

Two broad stages of geological evolution have been recorded in the Dunnage Zone (Swinden, 1991). These two events are considered pre- and post-accretionary. The first stage involves pre-accretionary volcanism with pre- and syn-accretionary sedimentation in a series of Cambrian to middle Ordovician island-arcs and back-arc basins. Island-arc

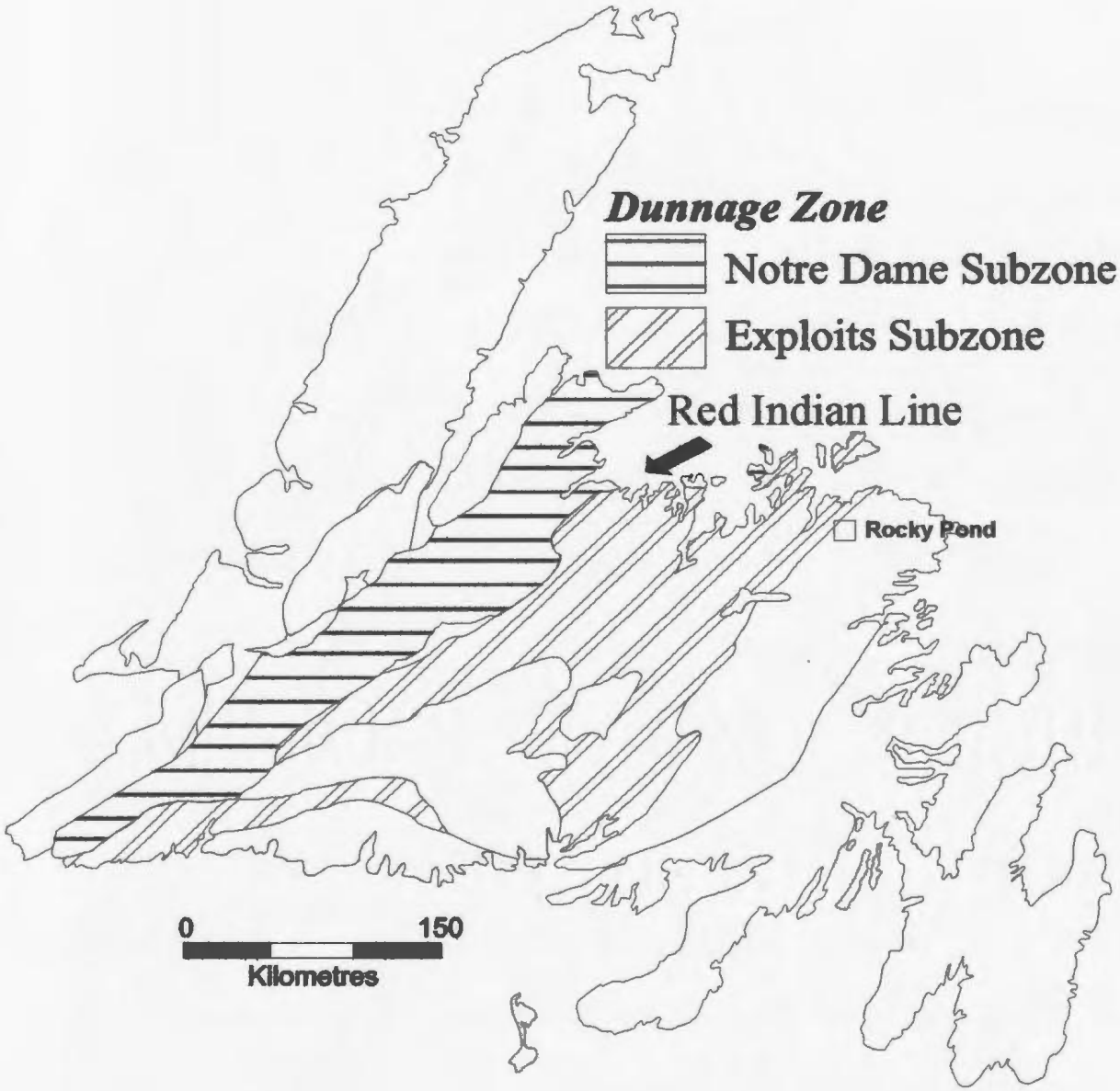

Figure 3.1: Division of the Dunnage tectonostratigraphic Zone into the Exploits and Notre Dame Subzones by the Red Indian Line.

volcanism ceased with the obduction of Taconic allochthons along the zone margins during the mid-Ordovician, the initial closure time of the Iapetus Ocean. As the Iapetus Ocean continued to close, during the Late Ordovician and Early Silurian, flyschoid sequences were deposited in fault-bounded basins of the Dunnage Zone.

The second stage consisted of syn- and post-accretionary events which resulted in crustal thickening through the deposition of Silurian subaerial fluviatile to shallow-marine sediments and epicontinental-style volcanism. Large strike-slip faults were activated or reactivated resulting in the development of pull-apart basins (Colman-Sadd and Swinden, 1984). The Silurian orogeny led to widespread deformation and deposition in the Dunnage Zone.

3.1.2 Local Geology

Recent field work (Currie, 1993; Piasecki, 1993; Williams, 1993; Williams *et. al.*, 1993) in the study area has revised the local geology and structural history. The study area was originally considered to be underlain by the Ordovician to Silurian Davidsville Group (Blackwood, 1982) in which the dominant rock types consisted of grey to black slate and/or shale with sandstone, siltstone, and greywacke. There were also occurrences of quartzite and polylithic conglomerate with minor volcanic rocks and argillaceous siltstone within the Davidsville Group. Blackwood (1982) had originally suggested that the Davidsville Group had an island-arc provenance due to the presence of thinly bedded turbidites which originated from the arc systems north and west of the area, in the Notre Dame Subzone.

Rocks that were previously assigned to the Davidsville Group probably belong to a variety of units. To the north and east of Rocky Pond these rocks have now been assigned to the Indian Islands Group (Fig. 3.2). Three formations comprise the Indian Islands Group; the basal Charles Cove Formation, and the overlying Horwood and Centennial Formations (Currie, 1993).

The Charles Cove Formation has a basal unit of limestone breccia with blocks of the crinoid *coquina* in a carbonate matrix (Currie, 1993) grading up to buff-weathered grey siltstone, shale and sandstone (Currie, 1993; Williams, 1993). Small scale thrusts obscure the relationship between the Charles Cove Formation and the overlying Horwood Formation. Grey to black shale with 1 to 5 mm beds of siltstone and sandstone comprise the Horwood Formation.

At the top of the Indian Islands Group is the Centennial Formation, consisting of red to purple, thinly bedded shale and sandstone which appear to grade downward into the Horwood Formation (Currie, 1993; Williams, 1993). Llandovery faunas found at several localities in the Charles Cove Formation (Williams, 1972) imply that all of the Indian Islands Group is Silurian.

3.1.3 Mineralization

In recent years the focus of mineral exploration in the eastern Dunnage Zone has been on gold. From 1982 to 1992, a total of 55 epithermal- and mesothermal-like gold showings were discovered (Evans, 1992; 1996). The Duder Lake area is host to four of these gold

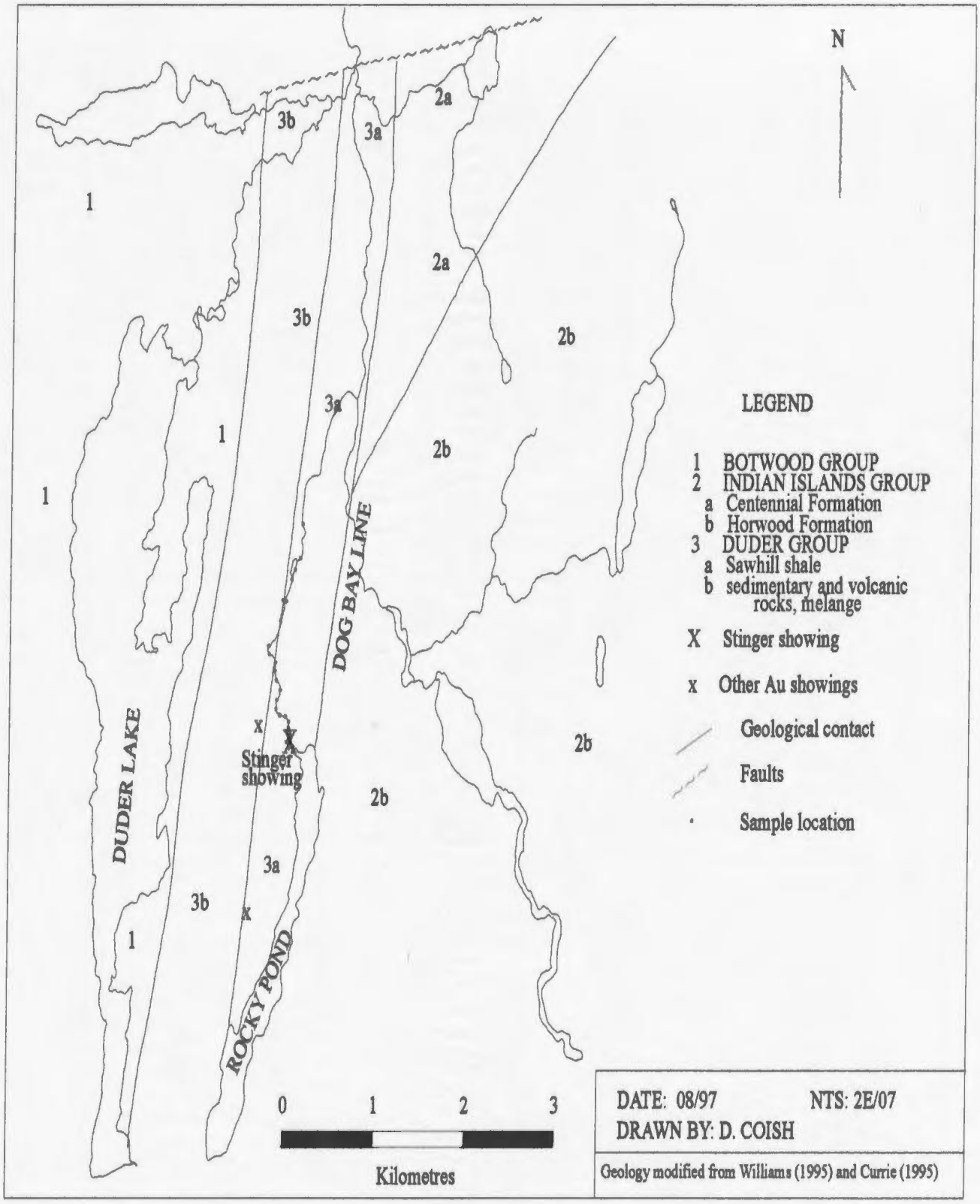

Figure 3.2: Local geology and gold mineralization of the Rocky Pond study area.

showings; the Flirt, Corvette, Goldstash and Stinger (Fig. 3.2). Each of these four mineralized zones exhibits subtle differences in their characteristics.

A study of the characteristic features associated with the various gold showings in the Dunnage Zone led Evans (1992, 1993) to develop a classification scheme (Fig. 3.3) for gold mineralization. The mineralization at Duder Lake is classified as arsenopyrite-rich, epigenetic, brittle-ductile, mesothermal-like, vein and wall rock style of mineralization (Evans, 1992; 1993; 1996).

There are three different subclassifications; types Ia, Ib and II, observed at Duder Lake. The Flirt, Corvette and Goldstash showings are considered type I mineralization. These occurrences are hosted by gabbroic rocks of inferred Siluro-Devonian age and are controlled by antithetic shears originating from a larger structure(s). Type I mineralization is further subdivided according to the mode of sulphide-gold occurrence. Corvette and Goldstash consist of shear-controlled sulphide disseminations in the highly altered gabbro host; this is considered type Ia mineralization (Churchill and Evans, 1992; Churchill, 1994). Type Ib occurs as shear-controlled quartz-carbonate veins containing blebby sulphides and minor gold (eg. Flirt) (Churchill *et. al.*, 1993; Churchill, 1994).

The Stinger showing is classified as type II mineralization and is hosted by graphitic siltstones. The deposit is comprised of quartz-carbonate veins of variable thickness (up to 30 cm) and hydrothermal breccia containing course sulphide patches with minor gold (Churchill, 1994).

The Charger Fault structure hosts the four gold showings in the Duder Lake area

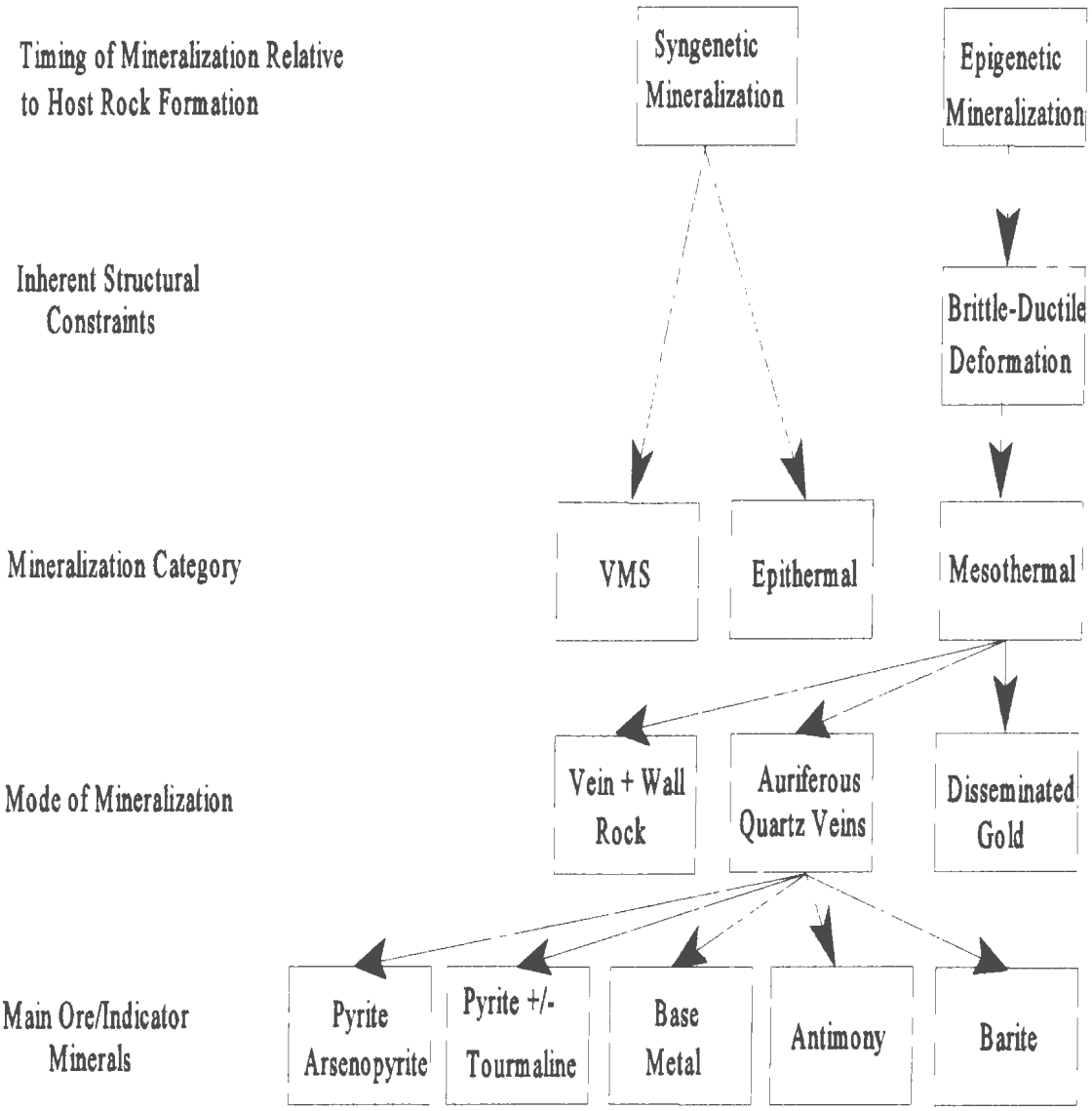

Figure 3.3 Classification scheme for gold mineralization within the Eastern Dunnage Zone (modified from Evans, 1993).

The Flirt showing is hosted by altered and sheared gabbro and consists of quartz veins from which assays of up to 9.3 g/t Au were obtained (Tallman, 1994). The shear zone has been traced for 4 km south of the Flirt showing. The Goldstash and Corvette showings occur in this shear zone and have yielded assays of 13.5 g/t Au over 2.6 m for Goldstash, and 5.6 g/t Au with channel sampling assayed 2.7 g/t Au over 3.6 m for the Corvette showing (Tallman, 1994). All three showings contain disseminated pyrite and arsenopyrite.

The Stinger showing occurs in a shear-splay from the main Charger Fault within Rocky Pond River. Quartz veins at this locality have assayed up to 30.1 g/t Au and channel sampling from the shore assayed 2.1 g/t Au over 22.8 m (Tallman, 1994). Pyrite and arsenopyrite host the gold within the quartz-carbonate veins (Evans, 1991).

The gold showings in the Duder Lake area are similar in mode of occurrence and style of mineralization to typical mesothermal gold deposits (Churchill, 1994). The most probable model for gold mineralization in this area is that it was related to regional metamorphism whereby the hydrothermal fluids were derived from metamorphic devolatilization and dehydration reactions with fluid migration along the major structures, for example the Dog Bay Line fault system (Fig. 3.4) (Churchill, 1994).

3.2 Winter Hill

3.2.1 Regional Geology

The Hermitage Peninsula constitutes the southwest margin of the Avalon Zone in Newfoundland (Williams, 1979) and is separated from the Gander Zone lithologies by the

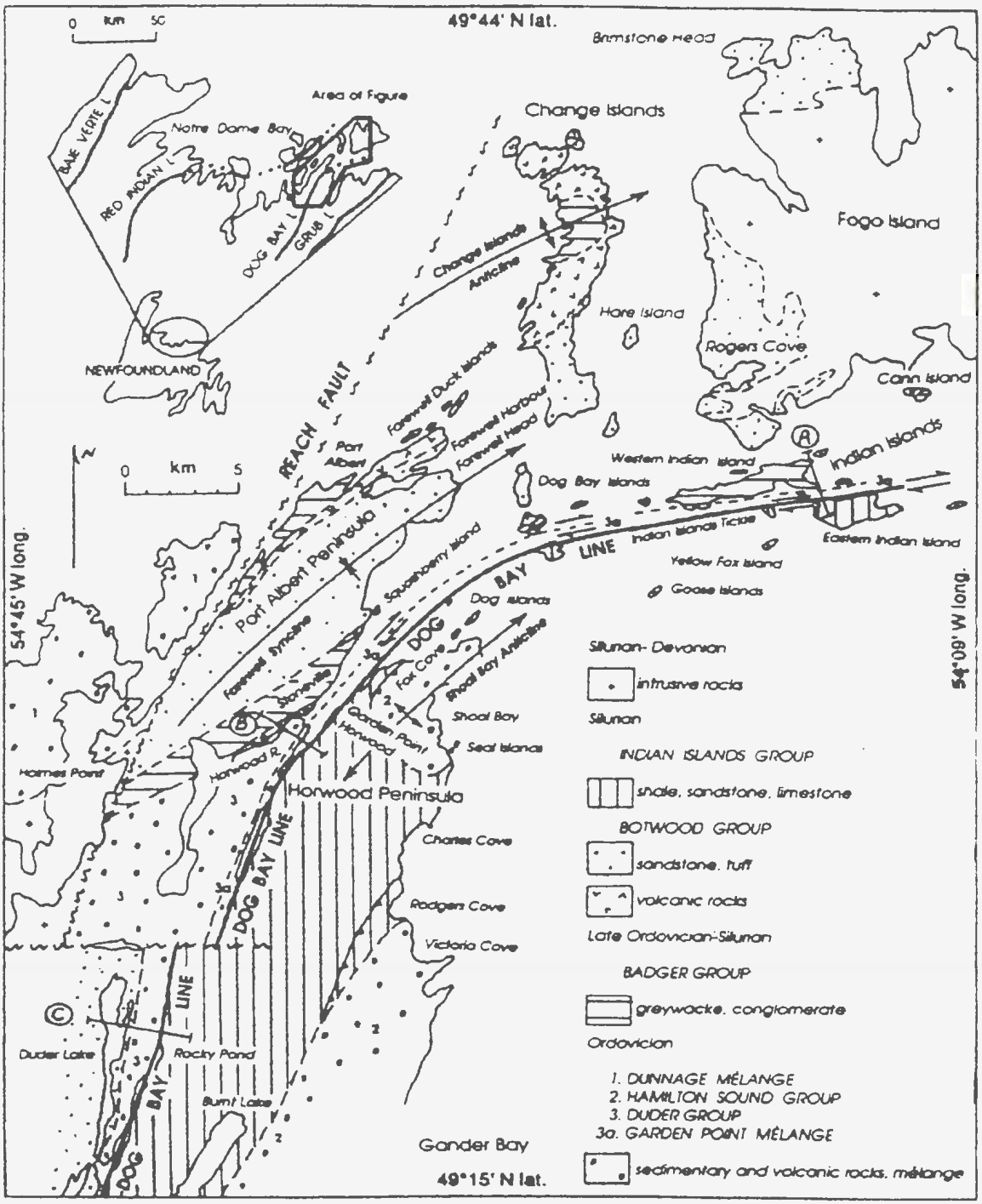

Figure 3 4 The Dog Bay Line fault system in north-central Newfoundland (adapted from Williams *et. al.*, 1993)

Hermitage Bay Fault (Fig. 3.5). The Hermitage Bay Fault is a brittle structure that trends northeast and extends offshore under Hermitage Bay. The Precambrian Avalon Tectonostratigraphic Zone developed due to either rifting and opening of the Iapetus Ocean (Papezik, 1972) or a subduction cycle that preceded the opening of Iapetus (Rast *et. al.*, 1976). During the Cambrian, the Avalon Zone was a marine shelf or a stable platform opposed to a continental margin.

Late Precambrian volcanic, sedimentary and plutonic rocks overlain by lower to mid-Palaeozoic shallow marine and terrestrial sedimentary rocks (Williams, 1978b; O'Brien *et. al.*, 1983) comprise the Avalon Zone rocks, which include the Connaigre Bay and Tickle Point Groups.

3.2.2 Local Geology

The Winter Hill study area (Fig. 3.6) is predominantly underlain by the late Precambrian Connaigre Bay Group which had been viewed as a conformable lithostratigraphic sequence with an unexposed base (O'Driscoll and Strong, 1979). It was suggested that the Connaigre Bay Group was intruded by the Ordovician or earlier Hermitage Complex consisting of, oldest to youngest, the Grole Diorite, Furby's Cove Granite and silicic to mafic dykes (O'Driscoll and Strong, 1979). O'Driscoll and Strong (1979) placed the Tickle Point Formation as the basal stratigraphic unit of the Connaigre Bay Group, comprised of a predominately bimodal volcanic assemblage with associated sedimentary rocks (Sears and Wilton, 1996). A U- Pb zircon age of 682.8 ± 1.6 Ma (Swinden and Hunt, 1991) from a

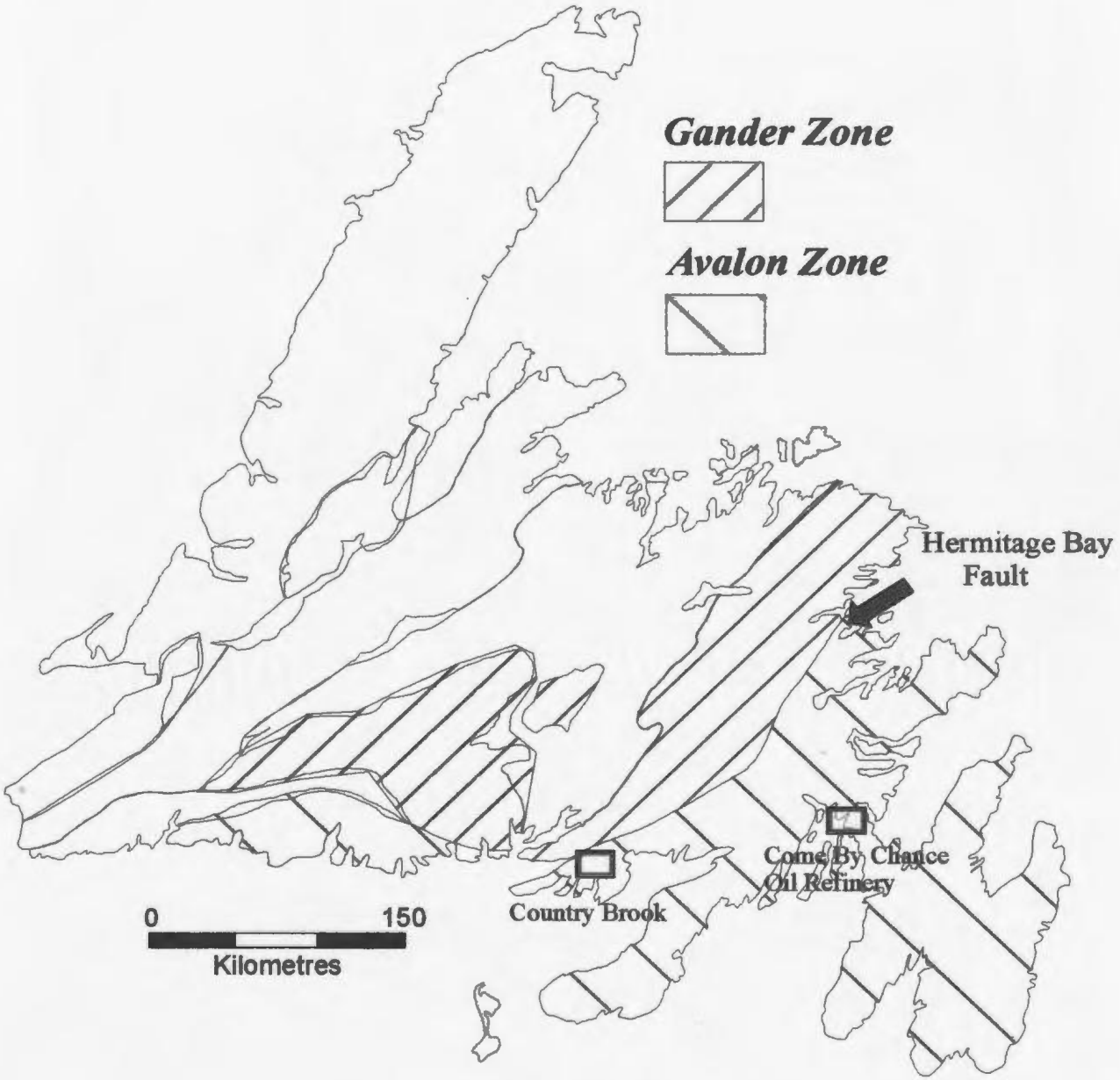

Figure 3.5: Hermitage Bay Fault, separates the Gander and Avalon tectonostratigraphic Zones.

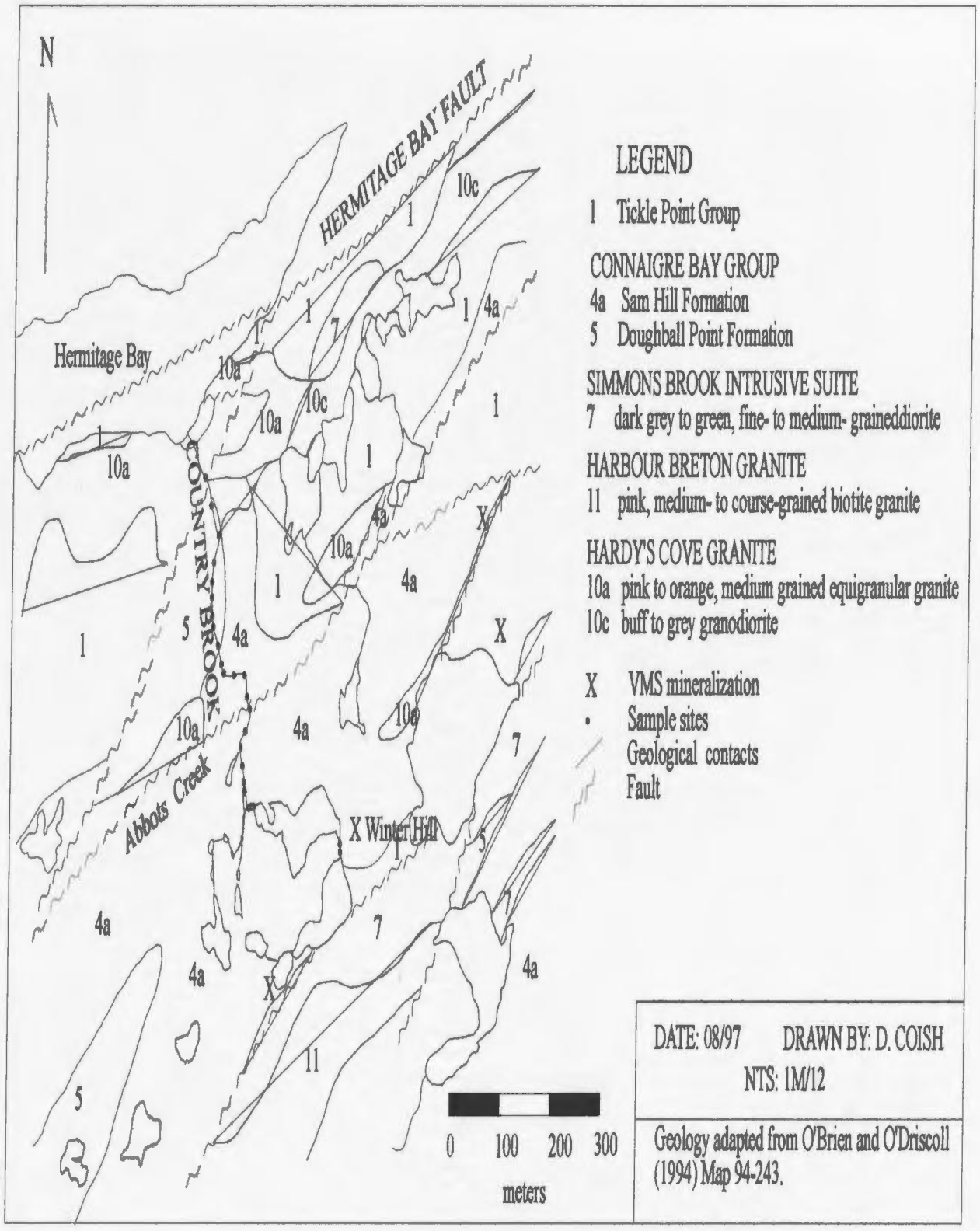

Figure 3.6: Local geology and mineralization of the Country Brook study area.

rhyolite in the Tickle Point Formation created problems for regional correlations with respect to timing of intrusions into the Connaigre Bay Group. Detailed regional mapping by O'Brien *et. al.* (1992) defined a new stratigraphy for the Connaigre Bay Group which excluded the Tickle Point Formation. The Connaigre Bay Group consists of, in ascending order, the Sam Head Formation, the Doughball Point Formation and the Down's Point Formation (O'Brien *et. al.*, 1992). An unconformity at the base of the Sam Head Formation is now considered to be the base of the Connaigre Bay Group.

Sears and Wilton (1996) proposed that the Tickle Point Formation, which hosts the Winter Hill prospect (Fig. 3.6), be known as the Tickle Point Group. The Tickle Point Group is a calcalkaline felsic volcanic suite (Sears, 1990) comprised of pink to purple and green, massive, flow banded and autobrecciated rhyolite and rhyolite lithic-crystal tuff which is interbedded with massive green andesite and basalt (Sears, 1990). Minor argillite and cherty beds have also been found throughout the Group. The Tickle Point Group was intruded by the Furby's Cove Intrusive Suite, gabbroic to granitic plutonic rocks, and both the suite and the Tickle Point Group was unconformably overlain by the Sam Head Formation of the Connaigre Bay Group.

Tholeiitic rocks of the Sam Head Formation are characterized by interbedded mafic tuffs and tuffaceous sedimentary rocks which host the base metal accumulations (Sears, 1990). Laminated grey and green argillite with purple conglomerate, sandstone and shale comprise the base of the formation (O'Driscoll, 1977; Sears, 1990). Throughout the formation are rare limestone lenses, chert and argillaceous cherty lenses.

Mafic volcanic rocks of the Doughball Point Formation conformably overlie the Sam Head Formation. The Doughball Point Formation is characterized by grey to green mafic flows and pyroclastic rocks of which the major rock types are massive andesite and basalt, with mafic tuff and agglomerate, and some interbedded silicic flows and tuffs (Sears, 1990; O'Brien *et. al.*, 1992). Both the Doughball Point Formation and the underlying Sam Head Formation have been dated at 626 ± 3 Ma (O'Brien *et. al.*, 1995).

The late Precambrian evolution of the Hermitage Peninsula involves the formation, extension, uplift and unroofing of a complex arc-like system (Sears, 1990; O'Brien *et. al.*, 1992). Following these events was deposition of the Connaigre Bay Group volcano-sedimentary rocks and the intrusion of various coeval, batholith-scale granitic to tonalitic plutons. Bimodal dykes are thought to represent a time of extension in the pre-Connaigre Bay Group basement, unrelated to the volcanism that occurred later (Sears, 1990). Adjacent to the dyke swarm is the mid-Proterozoic Hermitage Bay Fault that possibly indicates that it is located near an older, tectonically weakened zone that occurred in the pre-Connaigre Group basement.

3.2.3 Mineralization

The late Precambrian rocks of the Hermitage Peninsula host two significant volcanogenic sulphide showings and several massive base-metal-poor pyrite occurrences (Sears, 1990). The Winter Hill showings consist of three prospects which are stratabound in a limited stratigraphic thickness within felsic volcanic rocks, Winter Hill (main showing),

Winter Hill East and Winter Hill West (Fig. 3.6). The main showing, Winter Hill, will be the only one discussed here since it is the only mineralized zone that was targeted for this study. A carbonate-Ca-Mg-silicate lens within mafic tuff hosts the sulphide mineralization which occurs as massive lenses, bands and disseminations (Sears and Wilton, 1996). Diamond drilling at Winter Hill indicates that the mineralized zone is underlain by fragmental felsic and silicified rocks, indicating that this mineralization could possibly be located at the top of the Tickle Point Group (O'Brien *et. al.*, 1992).

Sulphide mineralization at the Winter Hill prospect is distributed in two zones termed upper and lower, based upon mineralogy and base-metal contents (Sears and Wilton, 1996). The lower structurally, and presumably stratigraphically, zone is considered to be a pyritic Cu-rich zone which is dominated by pyrite with lesser amounts of chalcopyrite and minor to trace abundances of sphalerite and pyrrhotite (Sears and O'Driscoll, 1989; Sears and Wilton, 1996). Thin (~ 0.5 m) lenses of massive pyrite are interbedded with disseminated and stringer pyrite and chalcopyrite which have a maximum thickness of 4 to 5 m, but are irregular in shape (Sears and O'Driscoll, 1989).

The upper zone is Zn and Pb-rich, approximately 2 to 4 m thick, and consists of disseminated to massive banded sulphides (Sears, 1990). Sphalerite is the coarsest grained and most abundant sulphide followed by galena which usually occurs with sphalerite and pyrrhotite. Next in the decreasing order of abundance is pyrrhotite, the most common Fe-sulphide (Sears, 1990). Pyrrhotite is associated with most of the sphalerite and galena mineralization in the uppermost sections of the upper zone whereas pyrite, the second least

common sulphide is found mainly in the lower section of the upper zone. Chalcopyrite is the least common sulphide and usually occurs as inclusions in sphalerite (Sears, 1990; Sears and Wilton, 1996). In the transition area, between the upper and lower zones, sphalerite is the dominant sulphide constituting 50% of the sulphides present (Sears and Wilton, 1996).

Diamond drilling by Noranda Exploration Company, Limited, in 1990 at Winter Hill provided the best Zn values of 6.17% Zn over 11.0 m including a 4.0 m section grading 10.1% Zn (Simpson, 1990).

The presence of a lower Cu-rich zone and a Zn-rich upper zone is very similar to the zonation found in many volcanogenic massive sulphide (VMS) deposits (Lydon, 1988). The presence of a lower stringer zone and a layered upper zone shows a stratabound configuration that is also a characteristic of VMS deposits. These similarities with VMS deposits suggest that the mineralization found at Winter Hill is of VMS type (Sears and Wilton, 1996).

3.3 Come-By-Chance Oil Refinery

3.3.1 Local Geology

The Isthmus of the Avalon lies in the Avalon Tectonostratigraphic Zone (Williams, 1979). The study area is contained within the Connecting Point Group (Fig. 3.7), a fault-bounded unit consisting of a thick sequence of late Precambrian sedimentary rocks (King, 1982). The total thickness is estimated to be 7.5 km since the base of the unit is not exposed.

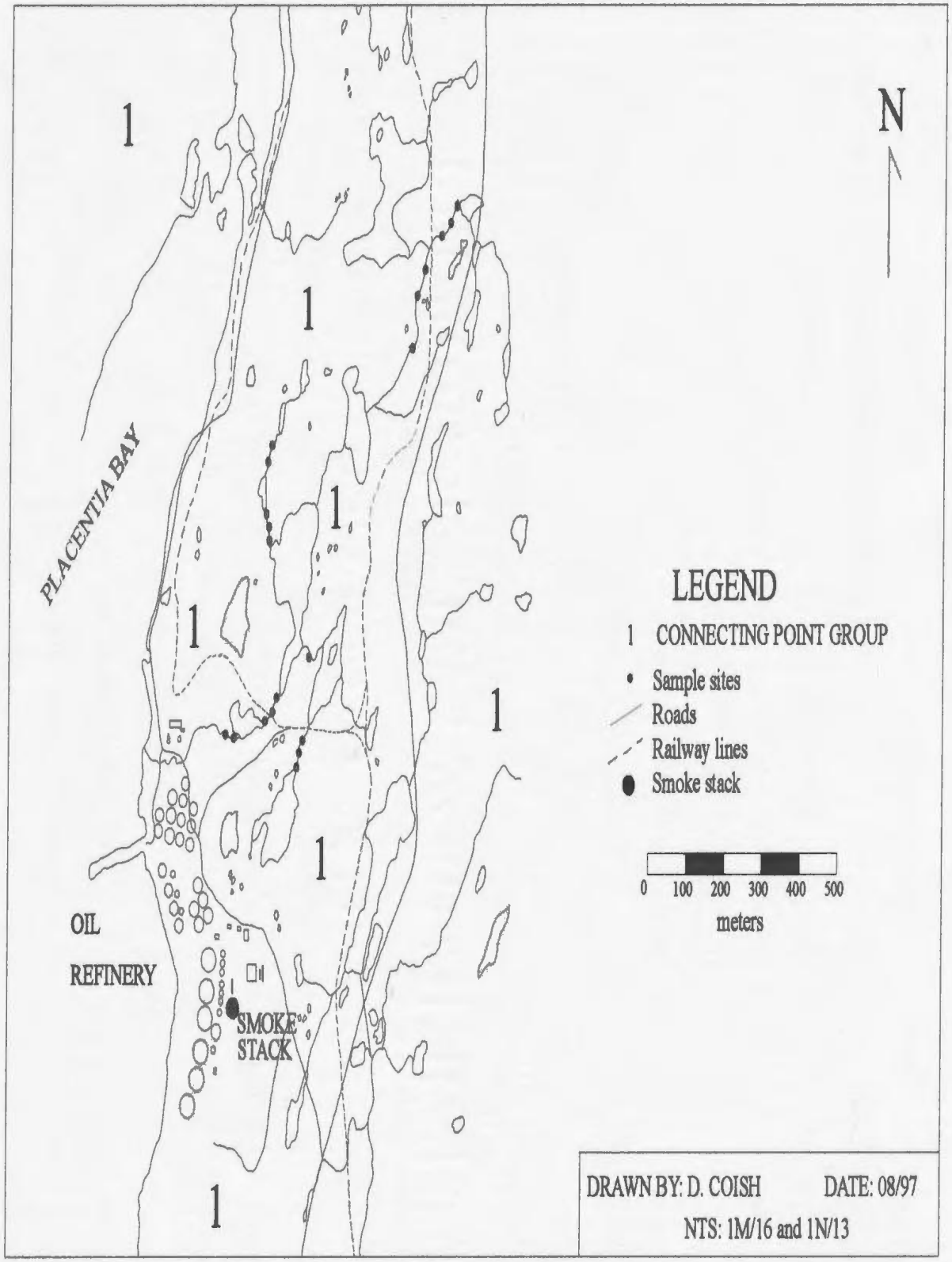

Figure 3.7: Geology of the Come By Chance oil refinery area and the location of the smoke stack responsible for emissions.

The Connecting Point Group consists of three gradational units which represent the infilling of a marine basin (O'Driscoll and Muggridge, 1979). The lowermost unit is characteristic of a deep-marine turbidite and consists of graded sandstones and siltstones, overlying this is a unit of grey shale and sandstone comprising a deltaic sequence. A green pebbly sandstone and coarse conglomerate comprise an upper shallow marine to subaerial unit considered to be the top of the Connecting Point Group.

3.3.2 Industrial activity

With a processing facility in operation at the Come-By-Chance oil refinery, considerable potential exists for contaminants to enter into the local biosphere. The flaring of waste gases is one of the most prominent pollutant sources therefore samples were collected northeast of the refinery since this is the prevailing wind direction that carries emissions from the refinery.

A preliminary stack sampling program was conducted in 1999 to estimate the rates of emission from the Sulphur Recovery Unit (SRU) for the following substances; Oxides (O_2), Carbon Dioxide (CO_2), Carbon Monoxide (CO), Nitrogen Oxide (NO_x), Total Hydrocarbons (THC), Sulphur Dioxide (SO_2), and Total Volatile Organic Compounds (Total VOCs). The SRU receives emissions from the four refining processes after crude oil distilling. The results of this sampling program are not yet available to the public. An air monitoring program of SO_2 has also been expanded to include particulate matter smaller than 10 and 2.5 microns. Additionally, monthly samples are collected and analysed for aluminum, barium, boron, iron,

lead, nickel, vanadium and zinc. These results have been documented monthly and to date show that with the exception of SO_2 do not exceed the Newfoundland air quality standards (Jacques Whitford Environment Limited, January, 2000).

The basic refinery process consists of atmospheric and vacuum crude distillation, platinum reforming, hydro cracking and associated downstream processing and conversion (Fig. 3.8). The refining process uses crude oil and bitumen as an energy source and this gas fume is another source of atmospheric pollutant. The accidental release of harmful products is possible during this process since each of these products is processed in a different unit and the various units are connected to each other, and some products are forwarded from one unit to another to complete the process. Such an occurrence happened on August 9, 1995 when approximately 60 tonnes of a Benfield solution, which is composed of 27% potassium carbonate, 4% diethanolamine and 0.6% vanadium pentoxide in a water solution, was misted from a stack and released into the atmosphere over a four hour period, causing discolouration of vegetation in the area. Vanadium pentoxide and diethanolamine are poisonous but the dilution of the solution by water greatly diminished the impact on the local environment.

The area affected by the release of the solution is shown in Figure 3.9. All the vegetation north-northwest of the refinery for a distance of approximately 1 km appeared to be dead but there was significantly less damage noted over the next kilometre. At a distance of greater than 2 km downwind from the refinery there was little or no damage sustained to the vegetation. A follow-up report by the Department of Environment, released on October 20, 1995 concluded that the discharge did not pose any threat to humans, animals or

vegetation in the area (Department of Environment, Government of Newfoundland & Labrador, Press Release, October 1995).

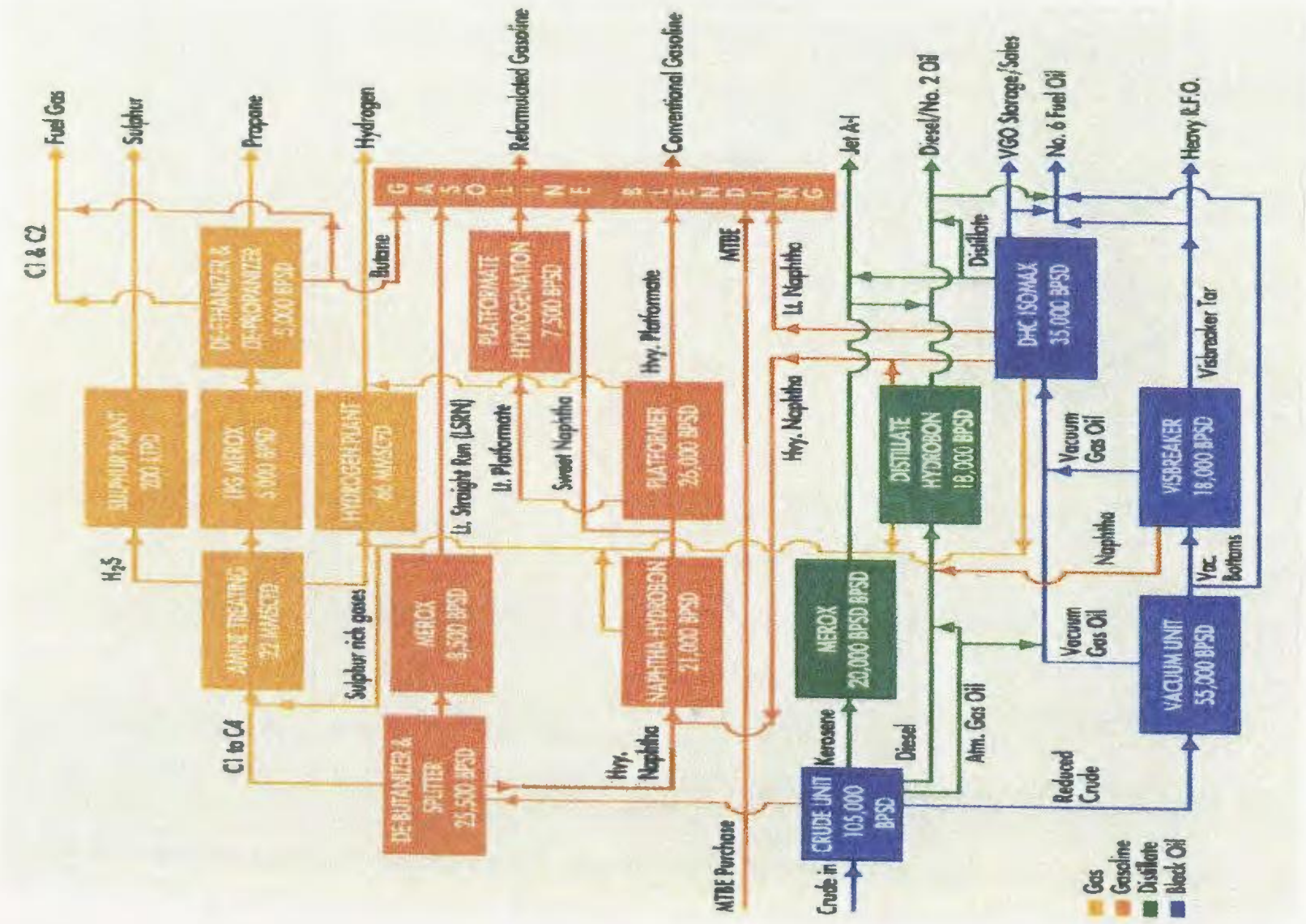

Figure 3.8: Basic refining process that occurs at the Come By Chance oil refinery (modified from Vitol information pamphlet).

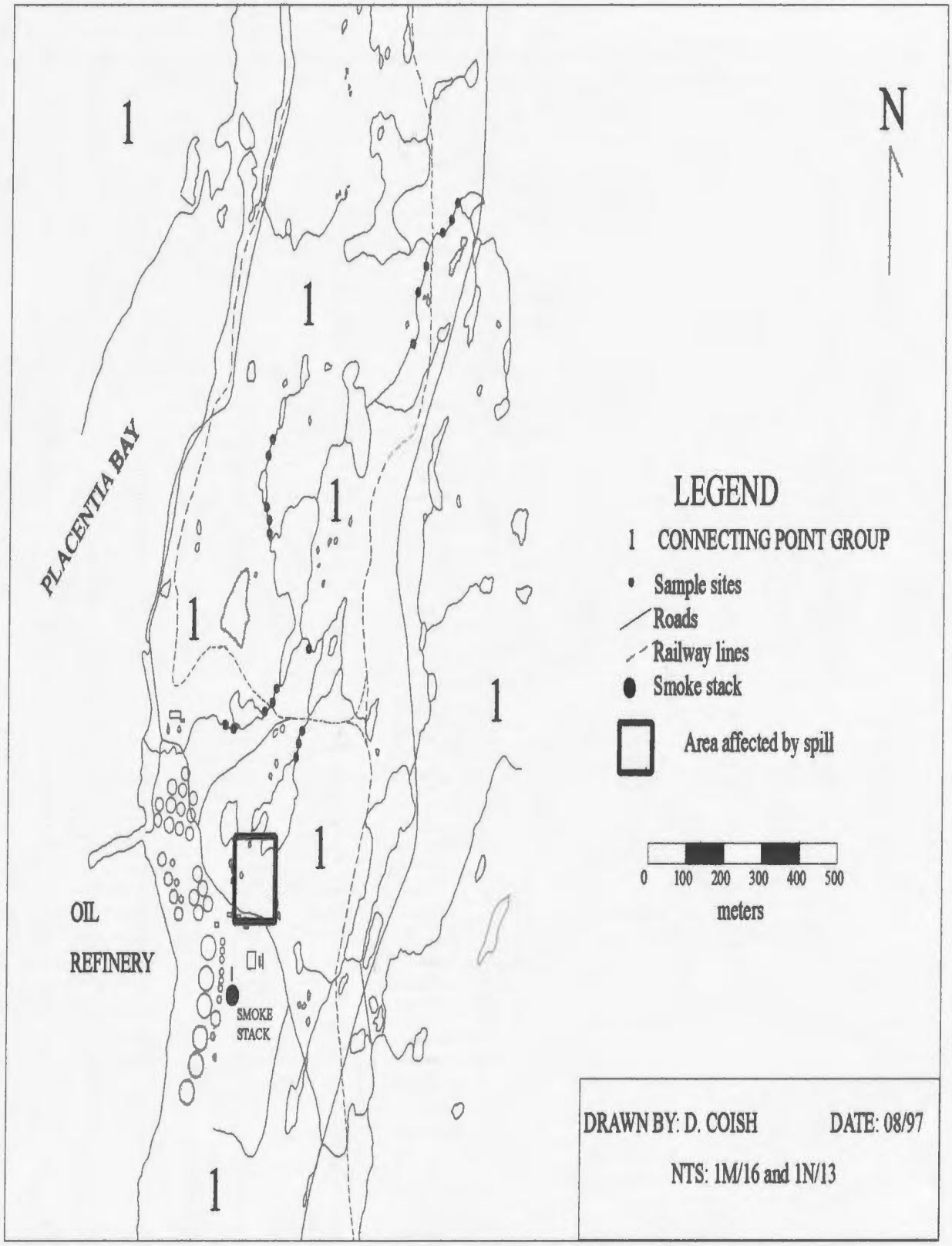

Figure 3.9: Area affected by the accidental release of a Benfield solution at the oil refinery.

CHAPTER 4: RESULTS

4.1 Statistical results

All statistical results were determined after logarithmic transformation of the data. The original values were log-transformed because they showed a log normal or skewed distribution, not a normal Gaussian curve. Plant *et. al.* (1975) suggest that in most cases geochemical distributions depart significantly from normality and show a log normal or bimodal distribution and the suggested solution to this dilemma is to log transform the data. A logarithmic transformation of the data also has the benefit of leading to an equalization of the standard errors across the range of the data (Garrett, 1973).

Statistical results calculated from the data sets for the three study areas are documented in Tables 4.1 to 4.3. Initial observations indicate that, overall, some elements yield more promising results than others. Analytical determinations for stream waters and the Mn-Fe oxide-coated stream pebbles, both partial dissolution and solid sample analysis (LAM-ICP-MS), are listed in Appendices I, II a and II b.

Table 4.1 lists the statistical results for stream waters collected in the study areas. A combined sampling and analytical variance are calculated because laboratory duplicates were not run. The ratio of total variance to the combined sampling and analytical variance was calculated for the elements. Garrett (1973) suggested that this ratio, termed F-ratio, should be >4 for the results to be viable to define real geochemical variations. Only Si, Ti, Mn, Fe, Co and Ba have ratios >4. The low number of elements with a >4 ratio can be attributed to the low concentration of most elements in the streams, since the majority have concentrations

below the detection limit. Due to the limited number of elements that pass the required statistical tests, stream water results were not considered for further analysis.

Partial dissolution statistical results of the Mn-Fe-oxide coatings for the study areas are shown in Table 4.2. Using the same rule of thumb of a F-ratio >4 suggests that the element's Ti, V, Mn, Fe, Co, Cu, Zn, As, Mo, Sb, Ba, Tl, Pb, Bi and U can be considered for further discussion. Elements such as Ni, Se, Ag and Hg have concentrations below the detection limit for the majority of the sample locations and therefore, should not be used in this study.

Analysis of variance for the laser ablation results obtained from the oxide coatings were combined from the three study areas to calculate total overall variances. For these laser ablation results, two F-ratios were calculated, one using the total variance in ratio to the combined sampling and analytical variance determined from the field duplicates (*ie.*, variance "s & a") and the other using the total variance in ratio to the analytical variance (*ie.*, variance "a") which is calculated from laboratory duplicates.

Table 4.3 lists the results determined from the total overall laser ablation data set. The results presented are excellent with the exception of Co, Au, Ce and W. The F-ratio calculated from the field duplicates was the one used to determine if an element can be considered for further discussion.

Table 4.1: Analysis of variance for stream water samples for the combined three study areas. Statistics are based on log normal data (concentration units of ppb) where "s+a" represents a combined sampling and analytical variance for 26 duplicate pairs and "g" is for geochemical variance.

element	log mean (ppb)	total variance	variance (s+a)	variance (g)	F-ratio
Si	2.39	0.06	0.01	0.06	12.13
S	2.81	0.18	0.07	0.11	2.42
Ti	-0.39	0.14	0.03	0.11	5.33
V	-0.82	0.17	0.04	0.12	3.89
Mn	0.99	0.30	0.00	0.29	364.84
Fe	1.76	0.33	0.02	0.31	14.65
Co	-1.80	0.22	0.03	0.19	7.42
Cu	-1.09	0.12	0.12	0.00	0.97
Zn	-0.05	0.34	0.16	0.18	2.10
As	-0.65	0.11	0.04	0.07	2.89
Se	-0.53	0.32	0.29	0.03	1.11
Mo	-1.50	0.21	0.09	0.12	2.35
Ag	-2.02	0.09	0.09	0.00	1.04
Cd	-1.58	0.23	0.12	0.10	1.83
Sb	-1.65	0.08	0.07	0.01	1.12
Ba	0.46	0.21	0.00	0.21	327.03
Hg	-1.24	0.19	0.24	-0.06	0.77
Tl	-2.12	0.35	0.18	0.17	1.98
Pb	-1.35	0.25	0.14	0.11	1.79
Bi	-2.07	0.24	0.25	-0.01	0.98
U	-1.75	0.11	0.15	-0.04	0.74

Table 4.2: Analysis of variance for partial dissolutions of Mn-Fe-oxide coated stream pebbles for the combined three study areas. Statistics are based on log normal data (concentration units of ppm) where "s+a" represents a combined sampling and analytical variance for 47 duplicate pairs and "g" is for geochemical variance.

element	log mean (ppm)	total variance	variance (s+a)	variance (g)	F-ratio
Si	2.94	0.27	0.08	0.19	3.30
S	3.19	0.13	0.07	0.07	1.97
Ti	1.99	0.35	0.04	0.32	9.55
V	1.52	0.17	0.02	0.15	8.16
Mn	4.62	1.12	0.06	1.07	20.12
Fe	4.31	0.21	0.02	0.19	11.11
Co	2.24	0.16	0.03	0.13	5.05
Ni	1.52	1.46	0.42	1.04	3.48
Cu	1.46	0.61	0.12	0.49	5.05
Zn	2.97	0.11	0.03	0.09	4.05
As	1.61	0.46	0.03	0.43	17.37
Se	-0.09	0.14	0.07	0.07	2.01
Mo	0.55	0.30	0.05	0.25	6.35
Ag	-1.00	0.23	0.10	0.13	2.40
Cd	0.99	0.16	0.04	0.12	3.88
Sb	-0.60	0.37	0.03	0.34	11.16
Ba	3.19	0.36	0.04	0.31	8.33
Hg	-1.23	0.06	0.03	0.04	2.39
Tl	0.36	0.20	0.04	0.16	4.67
Pb	2.11	0.26	0.02	0.24	13.24
Bi	-0.61	0.25	0.03	0.21	7.38
U	0.18	0.19	0.04	0.16	4.96

Table 4.3: Analysis of variance of laser ablation results determined from Mn-Fe-oxide coated stream pebbles for the combined three study areas. Statistics are based on log normal data (data presented as counts per second) where "s+a" represents a combined sampling and analytical variance for 78 duplicate pairs, "a" represents analytical variance for 232 duplicate pairs and "g" is for geochemical variance.

element	log mean (cps)	total variance	variance (a)	variance (s+a)	variance (g)	F-ratio (a)	F-ratio (s+a)
Si	4.64	0.79	0.08	0.19	0.52	10.24	4.08
S	3.55	0.57	0.05	0.10	0.41	10.46	5.77
Ti	4.27	0.75	0.08	0.18	0.48	9.15	4.14
Fe	5.33	0.36	0.03	0.08	0.25	12.37	4.37
Co	4.90	0.44	0.06	0.13	0.26	7.85	3.48
Cu	4.10	0.64	0.07	0.13	0.44	9.40	5.09
Zn	4.96	0.64	0.06	0.13	0.46	11.39	5.02
As	4.49	1.06	0.05	0.14	0.87	19.56	7.48
Se	2.09	1.05	0.16	0.16	0.73	6.69	6.46
Mo	3.78	0.65	0.06	0.12	0.47	11.70	5.43
Cd	2.92	1.38	0.12	0.14	1.12	11.95	9.66
Sb	3.43	1.66	0.08	0.18	1.40	20.81	9.08
Ba	4.68	1.12	0.07	0.14	0.90	15.70	7.80
Au	2.32	1.58	0.33	0.58	0.67	4.77	2.73
Hg	2.20	1.15	0.14	0.13	0.89	8.43	8.98
Tl	3.11	1.18	0.09	0.13	0.95	13.43	8.76
Pb	3.62	0.76	0.07	0.12	0.57	10.33	6.59
Bi	3.23	1.41	0.09	0.29	1.03	15.50	4.87
U	3.67	1.26	0.06	0.11	1.10	22.67	11.97
Te	1.33	1.62	0.22	0.30	1.10	7.39	5.35
Ta	2.52	1.93	0.11	0.23	1.59	17.44	8.45
Ce	4.71	0.25	0.07	0.07	0.12	3.79	3.79
W	1.99	0.25	0.08	0.19	-0.02	3.07	1.34

4.2 Analytical results

4.2.1 Introduction

This section describes the analytical results determined by ICP-MS and LAM-ICP-MS for the Mn-Fe-oxide coatings on stream pebbles. The two data sets are presented graphically for those elements that pass the F-test as shown in the previous section. The graphs (Figures 4.1 to 4.26) are X-Y plots of element/Fe ratio versus distance. The x-axis shows distance upstream (negative values) and downstream (positive values) from the sample site assigned as the showing, indicated by a distance value of zero, for the Rocky Pond River and Winter Hill study areas. The oil refinery study area has the smoke stack assigned as the origin and the sample locations are designated as distance in metres from this smoke stack.

The y-axis for the partial dissolution graphs show elements of interest as the ratio element/Fe. The elements are ratioed to Fe instead of Mn plus Fe because Mn was not able to be analysed using the laser ablation technique. The results of the ratios of element to Fe for both analytical methods would make comparisons between the two data sets more meaningful than if the partial dissolution data was presented as element/(Mn+Fe). Although the laser ablation results are presented as counts per second and not concentration values, comparisons between the two data sets can be made because presenting the data as ratios removes the factor of specific concentration units. Even though ratioing the element to Mn plus Fe would provide an overall equalization since it is presumed that it is the presence and availability of Mn and Fe that enable the elements to be adsorbed and concentrated in the coatings, the effect of ratioing elements of interest to Fe can smooth misleading results such

as false anomalies caused by high concentrations of Mn and Fe in some oxide coatings (Nowlan, 1976). Another factor is the difficulty in determining if it is only Mn and/or Fe that attracts specific elements, ie: some elements are suspected to have an affinity for either Mn- or Fe-oxides, but others are adsorbed by both. Since the degree of affinity for a specific element to either Mn or Fe is not accurately determined, ratioing the element to Fe provides a compromise for all elements and removes the factor of inflated geochemical values due to the presence of excessive Mn or Fe.

The graphs showing values of elements determined by laser ablation are ratioed to Fe since Mn levels in the oxide coatings could not be accurately measured with the current LAM-ICP-MS system. Nowlan (1976) noted that element/Fe ratios yield similar results to element/(Mn+Fe) ratios because Mn and Fe are usually highly correlated, so it is assumed here that ratioing element/Fe would be comparable to plots of element/(Mn+Fe). The y-axis show ratios of individual elements to Fe. On this axis, all six analyses determined at that sample location are plotted to show the relationship between the two analyses per pebble chip, noted as peba1 and peba2, and among the three pebbles collected at each sample site. Also, included is the median value of these six analyses for the individual sample sites. In the following sections, a median curve of the plotted results is used for discussion of trends and/or correlations between this data set and results of the solution analysis.

4.2.2 Rocky Pond

4.2.2.1 Introduction

Samples were collected above and below the area of known gold mineralization, the Stinger showing, which is located at distance zero (0) on the graphs (Figures 4.1 to 4.9). The rocks of the Sawhill shale unit, Duder Group, host the mineralization at Stinger. Lithogeochemical data for this unit has been obtained through analysis of sedimentary rock units found in various drill holes from the area (Churchill, 1994). These sedimentary rocks (siltstone, sandstone and greywacke) are located above and/or below the mineralized zone in the core, although these units contain trace amounts of sulphides (pyrite and arsenopyrite) they are considered to be relatively "fresh" and unaltered.

The relatively unaltered or slightly altered siltstones and sandstones are considered to be the "background or non-mineralized" standards upon which the current results are to be compared to determine if there is any kind of local geochemical signature to be found in Rocky Pond River. Churchill (1994) also analysed samples collected from the mineralized area, especially a quartz-carbonate vein from a trench at the Stinger showing.

4.2.2.2 Results and discussion of relevant elements

This section will discuss the results of elements that have passed the F-test, defined in section 4.1 Statistical results, for both partial dissolution and laser ablation analyses. Fe, Cu, Zn, As, Sb, Ba and Pb shows good F-ratio results for both oxide coating analyses. Other elements relevant to gold exploration; Se, Cr and Sc did not show reliable analysis of variance

or were not analysed by both analytical techniques, therefore are not discussed in this section.

All graphs of element values determined by laser ablation show element/Fe (cps) on the y-axis. These determinations show all 6 analyses for that sample location, the two analyses per pebble chip for all three pebble chips and the median value of the 6 analyses. The median value is the average of the two middle values of the 6 analyses for each sample location.

Figure 4.1 presents Mn/Fe values determined in the digestion of the pebble coatings. The results indicate high Mn concentrations near the showing which then decreases to a low near 600 m downstream which then begins to increase going further downstream. High Mn concentrations can most likely be attributed to the black shale in the study area which is highly manganiferous (Currie, 1993). All samples except 7 to 9 (approximately from 650 to 850 m downstream) are located in the Sawhill shale unit.

Iron values determined in the oxide coatings can be viewed in Figures 4.2 a and b. The general trend of Fe determined by digestion (Fig. 4.2 a) and the median values from the LAM method (Fig. 4.2 b) are similar for the majority of the stream samples. Both data sets indicate a strong increase in Fe a short distance downstream from the showing which then gradually declines with increasing distance from Stinger.

Figure 4.3 is a graph of Mn and Fe concentrations found in the dissolved oxide coatings. At all sample locations Mn is much more abundant than Fe but there appears to be a rough correlation between the two elements. Based on these results, the presentation of element/Fe for both partial dissolution and laser ablation results followed by a discussion and

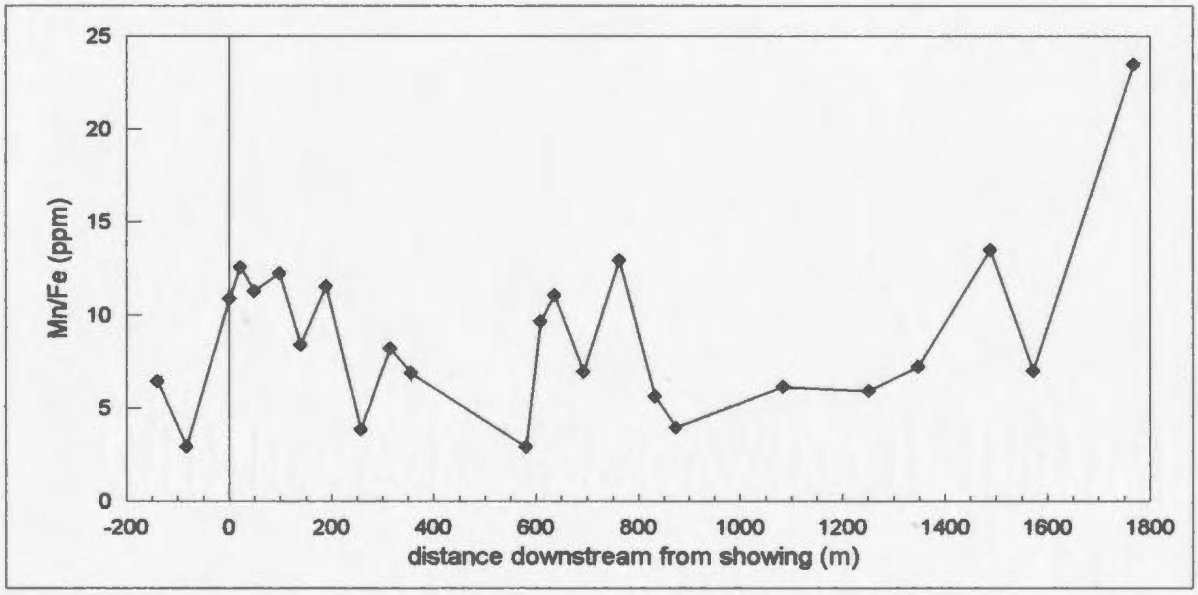

Figure 4.1: Mn/Fe (ppm) determined in the partial dissolutions of Mn-Fe-oxide pebble coatings collected from Rocky Pond River, Stinger is located at distance zero.

(a) Partial dissolution

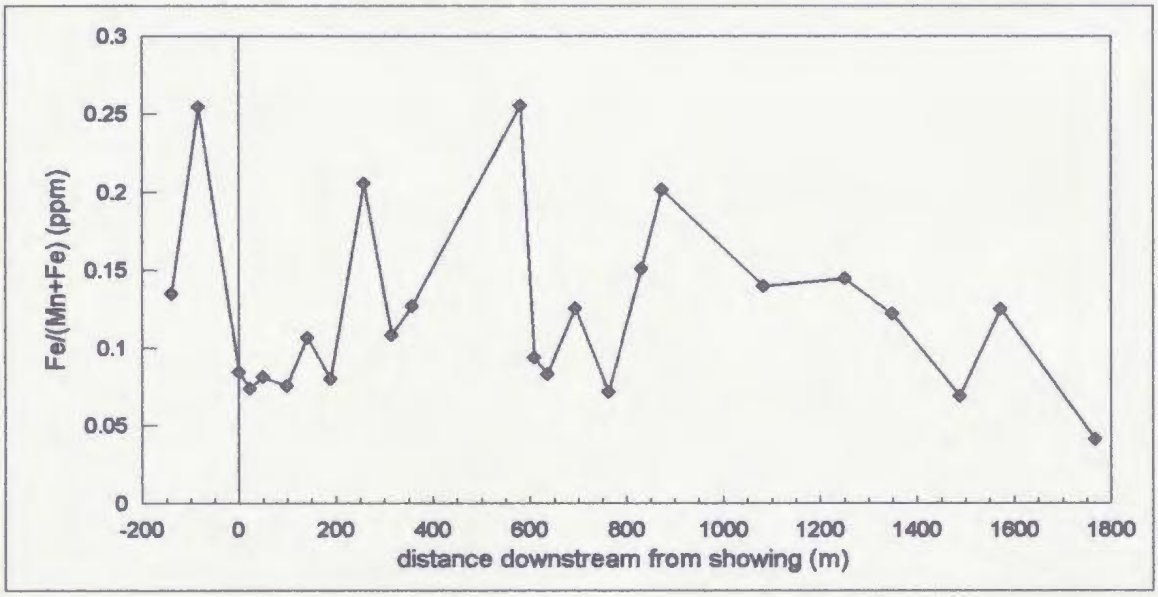

(b) Laser ablation

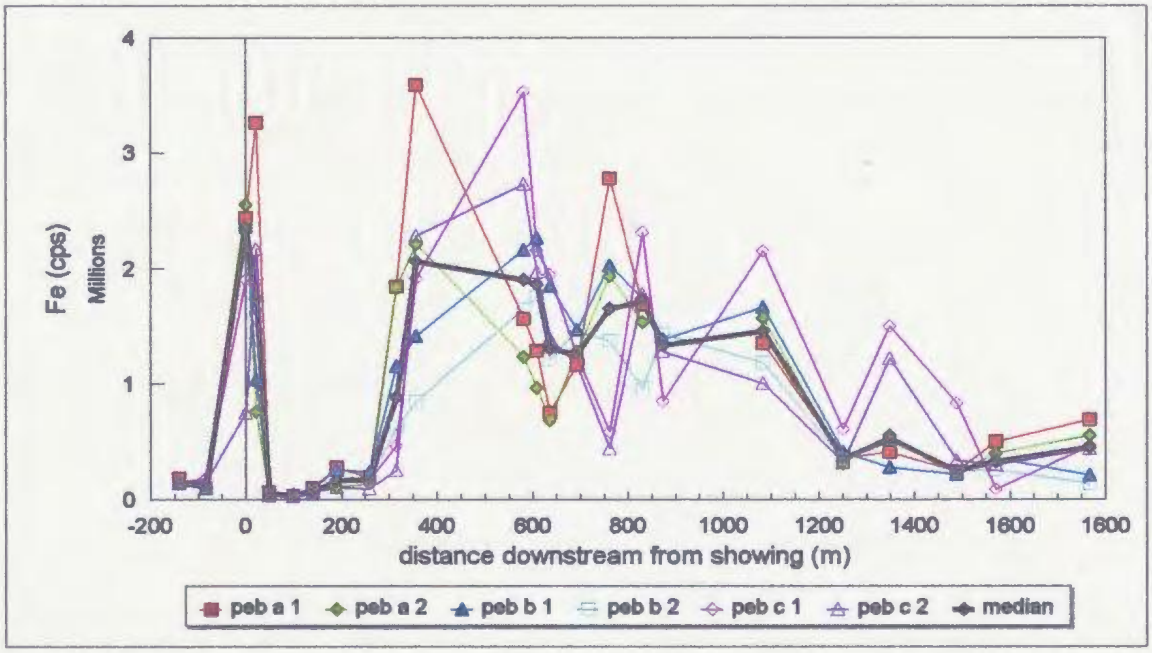

Figure 4.2: Fe determined in the oxide pebble coatings collected from Rocky Pond River; Stinger is located at distance zero. (a) Fe/(Mn+Fe) results from partial dissolutions of Mn-Fe-oxide pebble coatings and (b) Fe (cps) laser ablation results from Mn-Fe-oxide pebble coatings.

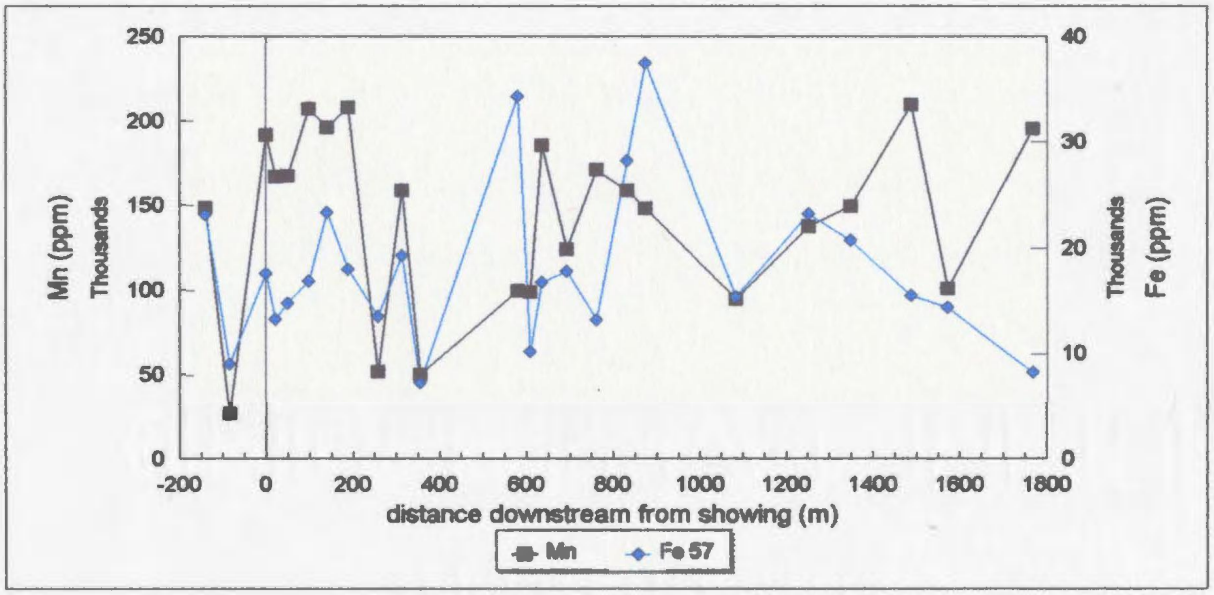

Figure 4.3: A graph of Mn and Fe concentrations determined in the partial dissolution solutions from Rocky Pond River; Stinger is located at distance zero.

comparison of the two data sets appears plausible.

Figures 4.4 a and b show Cu levels in the coatings by partial dissolution and laser ablation methods, respectively. Upstream, close to the showing, Cu values are relatively low with a general decline for approximately 600 metres, then levels are random before a sharp anomaly is noted far downstream where the digestion method also shows elevated levels of Cu for a much larger distance than the solid sample analysis by laser ablation. Copper values for the laser ablation method indicates a gradual increase in Cu with distance from the gold showing for approximately 600 m downstream. This indicates that Cu may be an indicator to Au mineralization for a limited distance from a showing using the partial dissolution method.

Zinc results are presented in Figures 4.5 a and b. Values determined by digestion (Fig. 4.5 a) show elevated levels near and slightly downstream from the showing. Overall, there is a general decline in Zn with increasing distance from the showing. Laser ablation results (Fig. 4.5 b) indicate a slight decline in Zn with distance from the showing then a relatively constant concentration in the middle part of the study area, then slightly elevated values further downstream. Both analytical methods indicate the presence of mineralization although the partial dissolution method appears to work more efficiently than the laser ablation technique.

Graphical representations of As are shown in Figures 4.6 a and b. The oxide coatings show no similarity between results obtained by digestion (Fig. 4.6 a) and laser ablation (Fig. 4.6 b). There is a general decline in As observed for a short distance downstream (~ 200 m)

(a) Partial dissolution

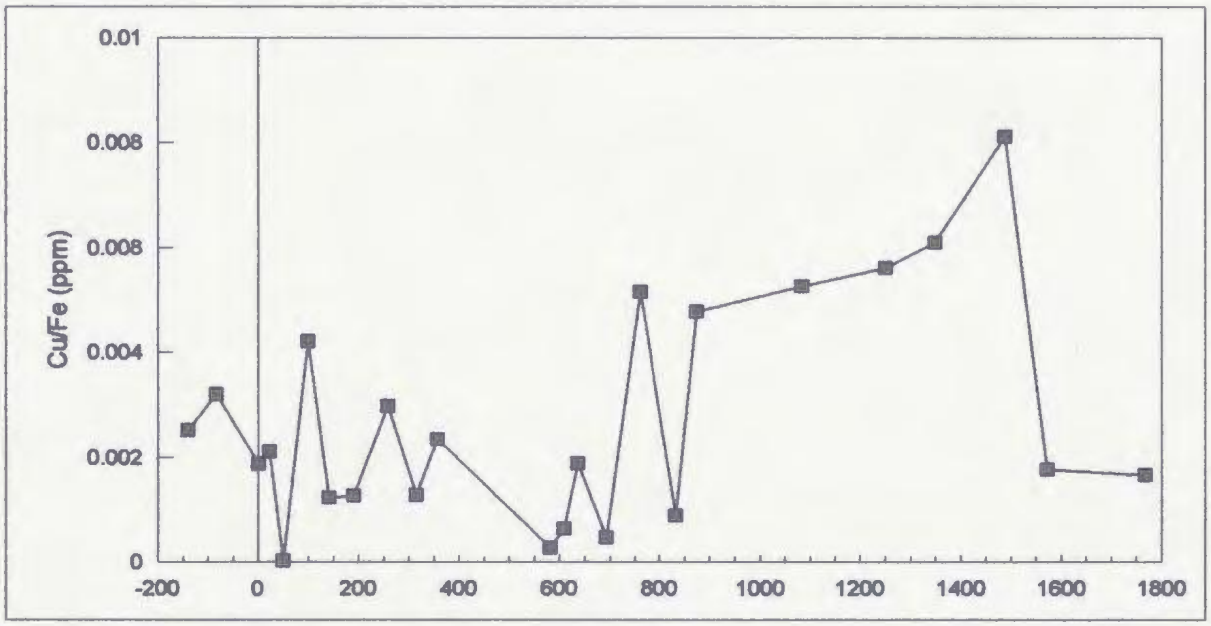

(b) Laser ablation

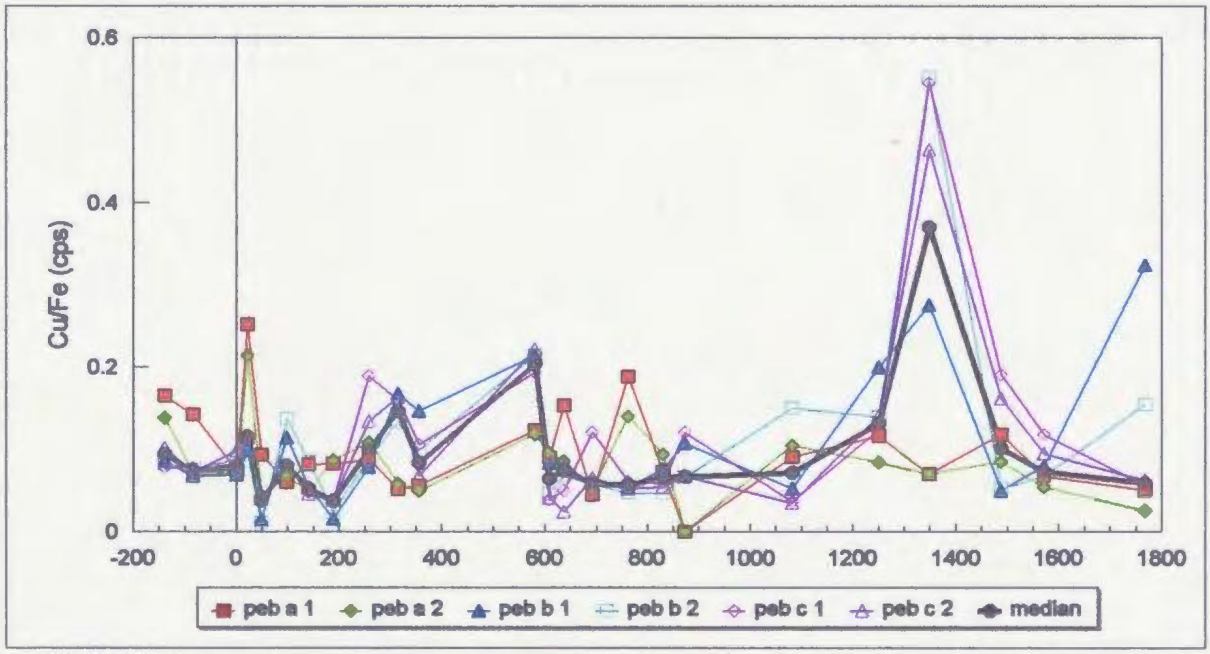

Figure 4.4: Cu determined in the oxide pebble coatings collected from Rocky Pond River; Stinger is located at distance zero. (a) Cu/Fe (ppm) results from partial dissolutions of Mn-Fe-oxide pebble coatings where data points are individual analyses of that sample location and (b) Cu/Fe (cps) laser ablation results from Mn-Fe-oxide pebble coatings where all values plotted are individual analyses and the median value is the average of the two medium values.

(a) Partial dissolution

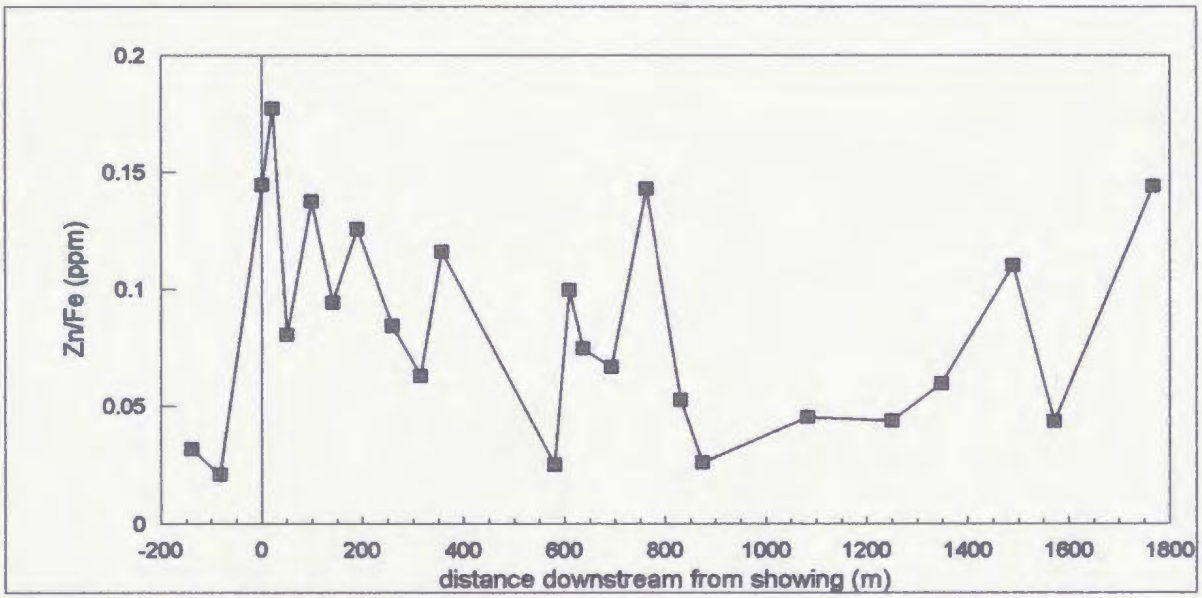

(b) Laser ablation

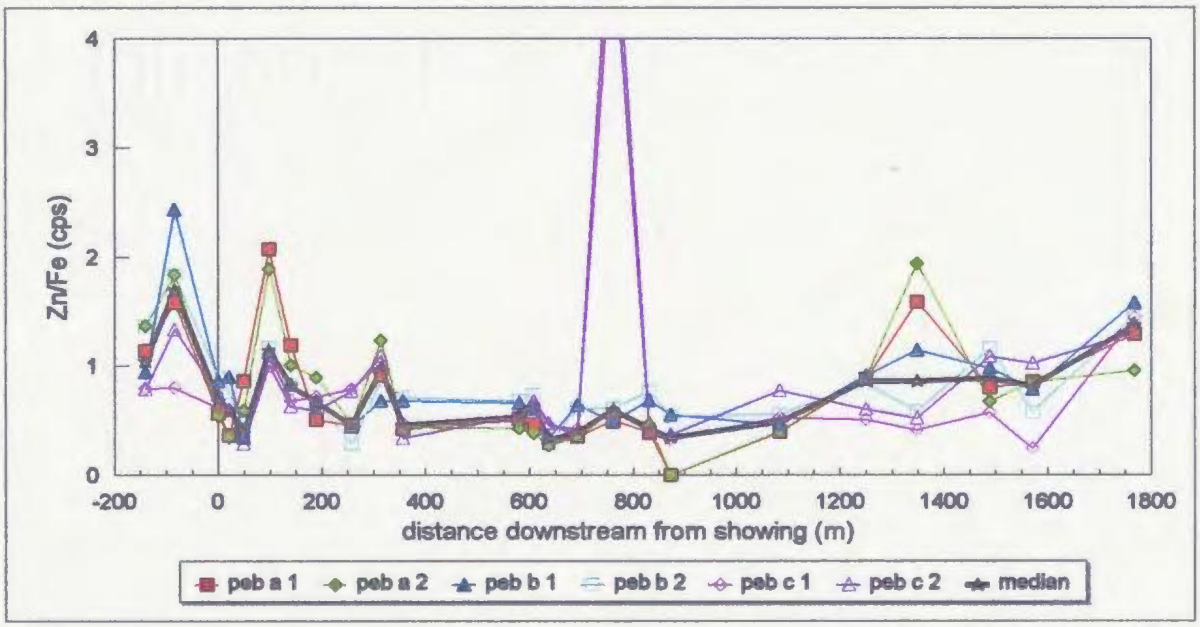

Figure 4.5: Zn determined in the oxide pebble coatings collected from Rocky Pond River; Stinger is located at distance zero. (a) Zn/Fe (ppm) results from partial dissolutions of Mn-Fe-oxide pebble coatings and (b) Zn/Fe (cps) laser ablation results from Mn-Fe-oxide pebble coatings.

(a) Partial dissolution

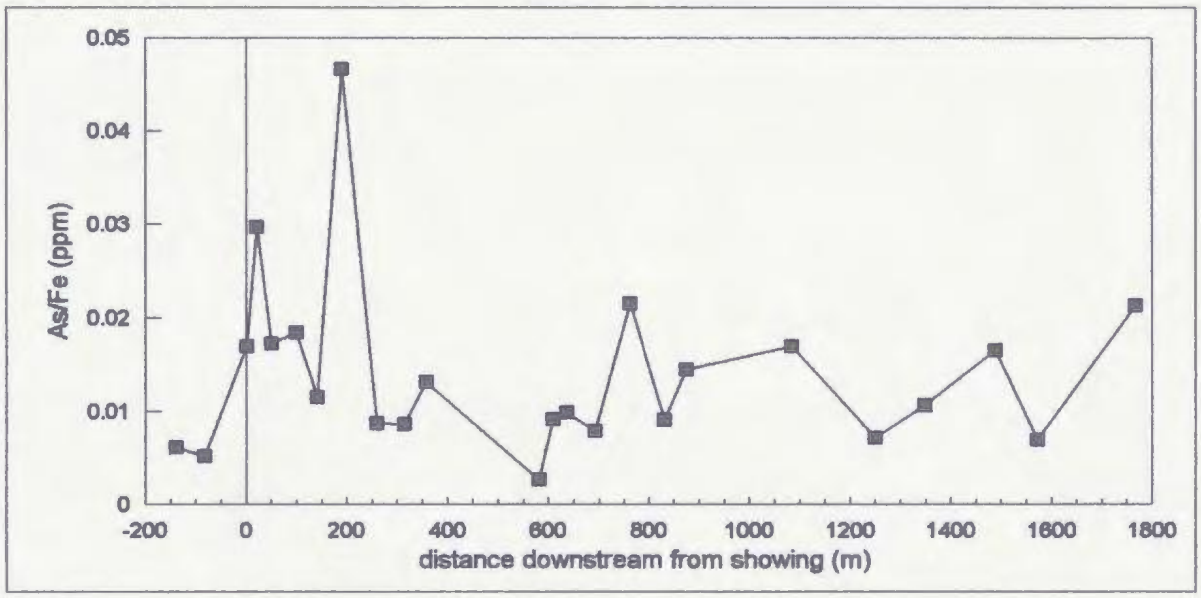

(b) Laser ablation

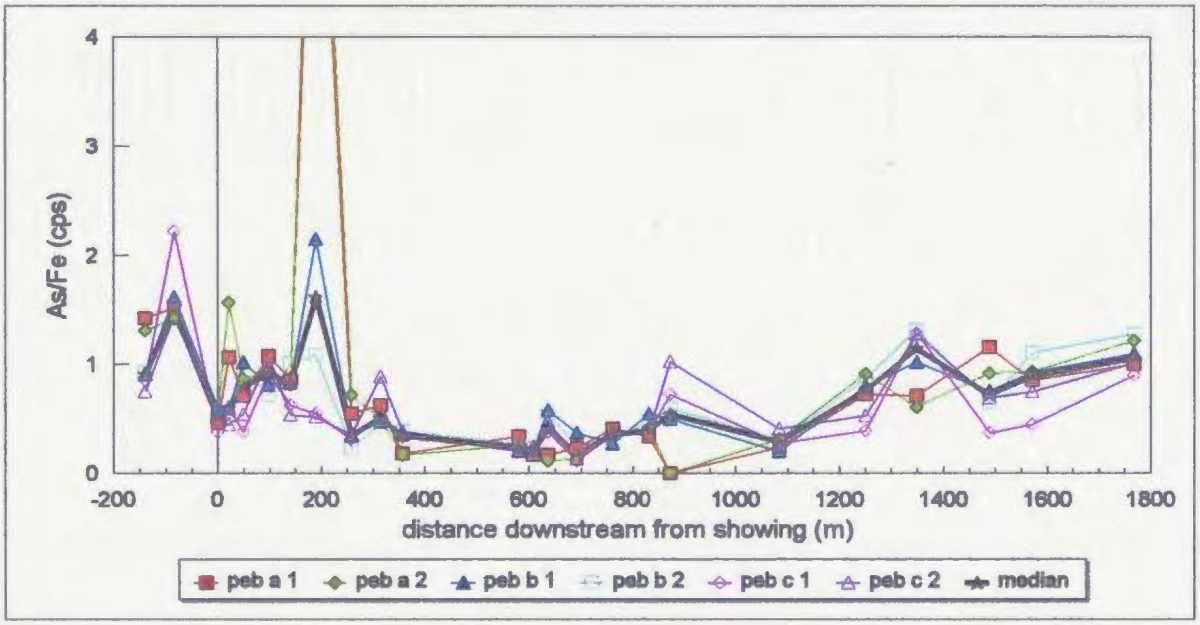

Figure 4.6: As determined in the oxide pebble coatings collected from Rocky Pond River; Stinger is located at distance zero. (a) As/Fe (ppm) results from partial dissolutions of Mn-Fe-oxide pebble coatings and (b) As/Fe (cps) laser ablation results from Mn-Fe-oxide pebble coatings.

from the showing in the laser ablation results but there is no associated decrease noted for the results of the partial dissolution of the oxide coatings, although levels are notably higher near the mineralized zone. The repeatability of the laser ablation results seem to indicate that the laser ablation method may work better than the leachate process in depicting Au mineralization using Mn-Fe-oxide coated stream pebbles.

Figures 4.7 a and b show Sb values of the oxide coated stream pebbles. The results from the partial dissolution method (Fig. 4.7 a) indicate a general decrease in Sb with increasing distance from the showing until 1 km downstream when there is a strong anomaly. The laser ablation results (Fig. 4.7 b) also indicate a gradual decline in Sb with distance downstream and a large anomaly further downstream. Both methods in this case appear to indicate mineralization with declining values with increasing distance from the showing.

Results from Ba analysis are presented in Figures 4.8 a and b. The results presented for the partial dissolution (Fig. 4.8 a) indicate higher values of Ba near the Au mineralization and downstream from it but it appears to be more of a random distribution rather than a decline in Ba with increasing distance from the showing. The pattern of Ba in the oxide coatings observed from the laser ablation results (Fig. 4.8 b) also seems to show this randomness throughout the study area. Barium does not appear to be an effective element to use in gold exploration when using Mn-Fe-oxide coated stream pebbles as a sampling medium.

Lead results are presented in Figures 4.9 a and b. There is no obvious similarity

(a) Partial dissolution

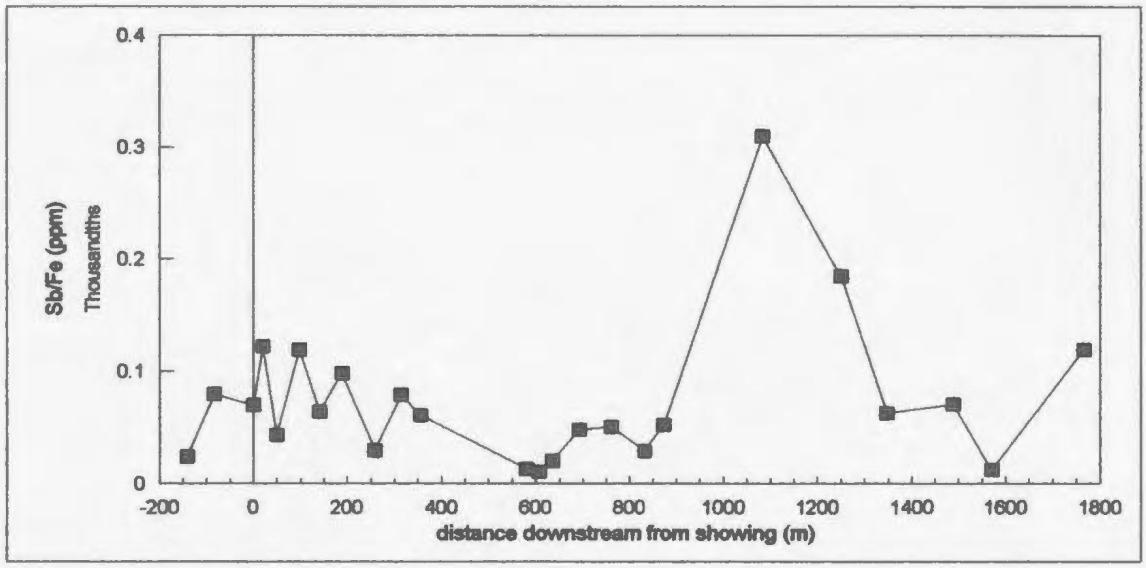

(b) Laser ablation

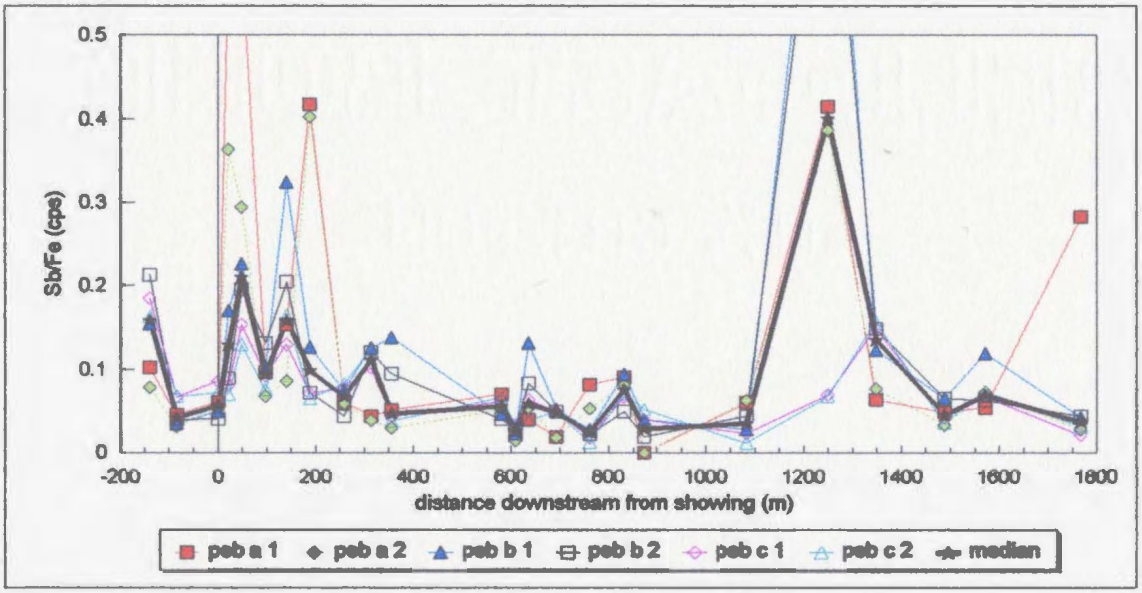

Figure 4.7: Sb determined in the oxide pebble coatings collected from Rocky Pond River; Stinger is located at distance zero. (a) Sb/Fe (ppm) results from partial dissolution of Mn-Fe-oxide pebble coatings and (b) Sb/Fe (cps) laser ablation results from Mn-Fe-oxide pebble coatings.

(a) Partial dissolution

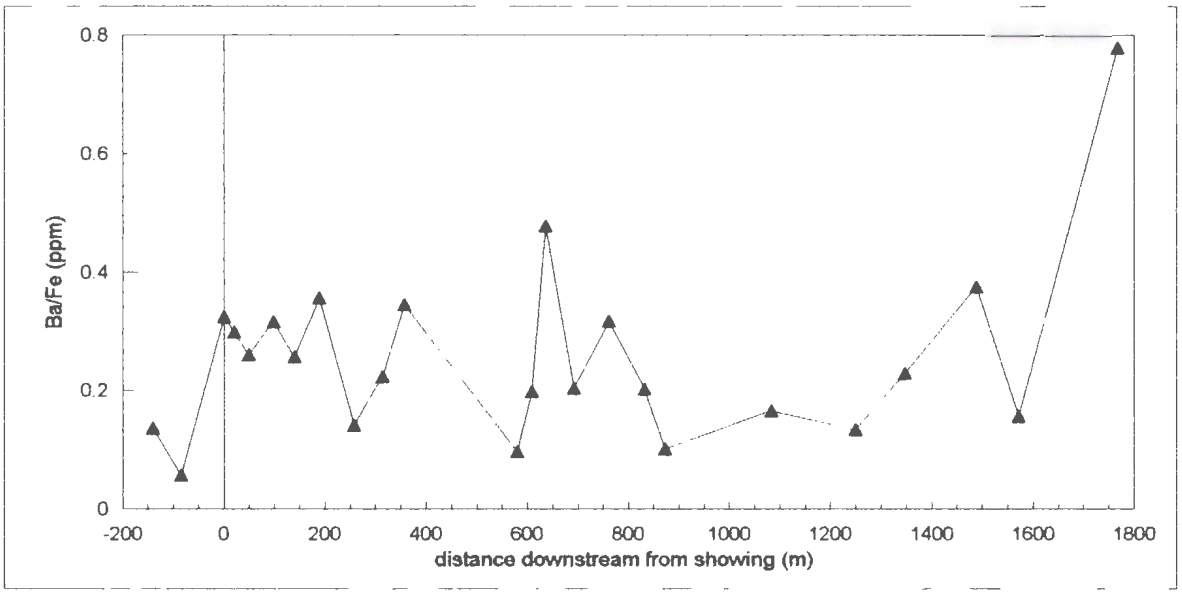

(b) Laser ablation

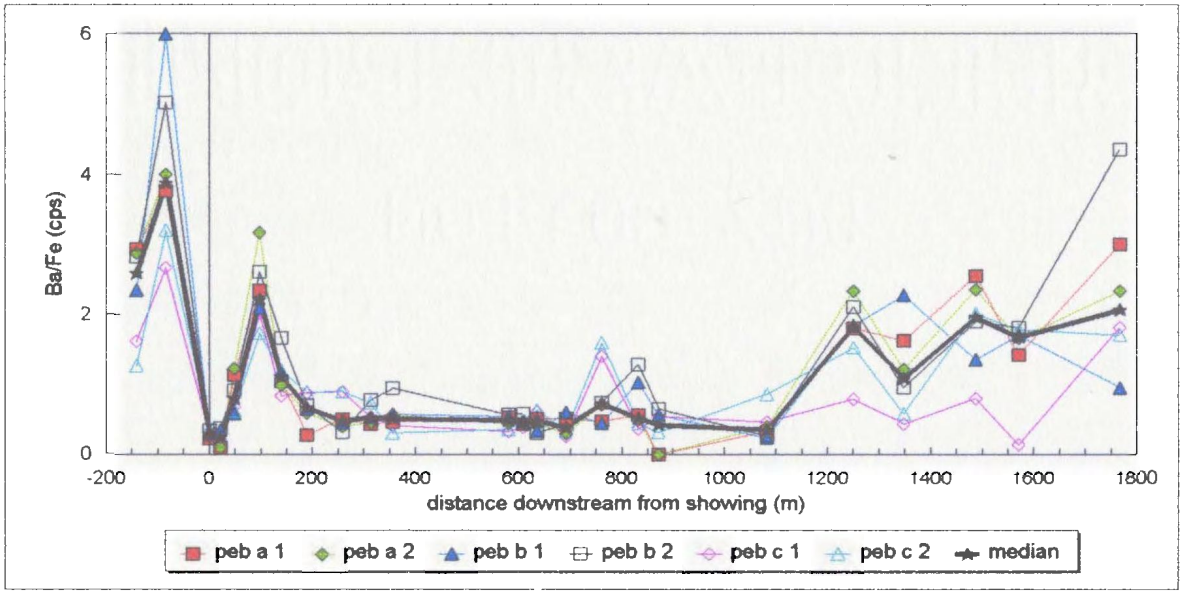

Figure 4.8: Ba determined in the oxide coated pebbles collected from Rocky Pond River; Stinger is located at distance zero. (a) Ba/Fe (ppm) results from partial dissolutions of Mn-Fe-oxide pebble coatings and (b) Ba/Fe (cps) laser ablation results from Mn-Fe-oxide pebble coatings.

between the two analytical methods for the determination of Pb in the pebble coatings. Figure 4.9 a shows Pb values from the digestion solutions which appear to be randomly distributed in the stream. Laser ablation results indicate relatively constant Pb values throughout the stream except for obvious elevated levels far downstream that covers a length of ~ 300 m. Pb does not appear to be an effective indicator mineral for Au exploration when Mn-Fe-oxide coated stream pebbles is the sampling medium.

4.2.2.3 Summary

The gold showing, Stinger, is located at distance zero on the previous graphs. The total length of the study area is underlain by the Duder Group which consists of the Sawhill Shale and a sedimentary and volcanic melange unit. Sample sites from ~ 650 m to 850 m occur in the sedimentary and volcanic unit.

The above presentations of the results indicate that there is a general correlation between the patterns of the ratioed values in the Duder Lake/Rocky Pond study area for both methods of analyses of the Mn-Fe-oxide coated stream pebbles. The partial dissolution method has been more thoroughly tested than the laser ablation method and based on previous results (Carpenter and Hayes , 1978; Filipek *et. al.*, 1981; Robinson, 1981, 1985; Chao, 1984; Hale *et. al.*, 1984 Thompson *et. al.*, 1992 and Nicholson, 1992) and the statistical analysis presented here, the LAM-ICP-MS analytical method appears to correlate well with the digestion procedure.

Graphical presentations of most of the indicator minerals for gold exploration; Fe, Cu,

(a) Partial dissolution

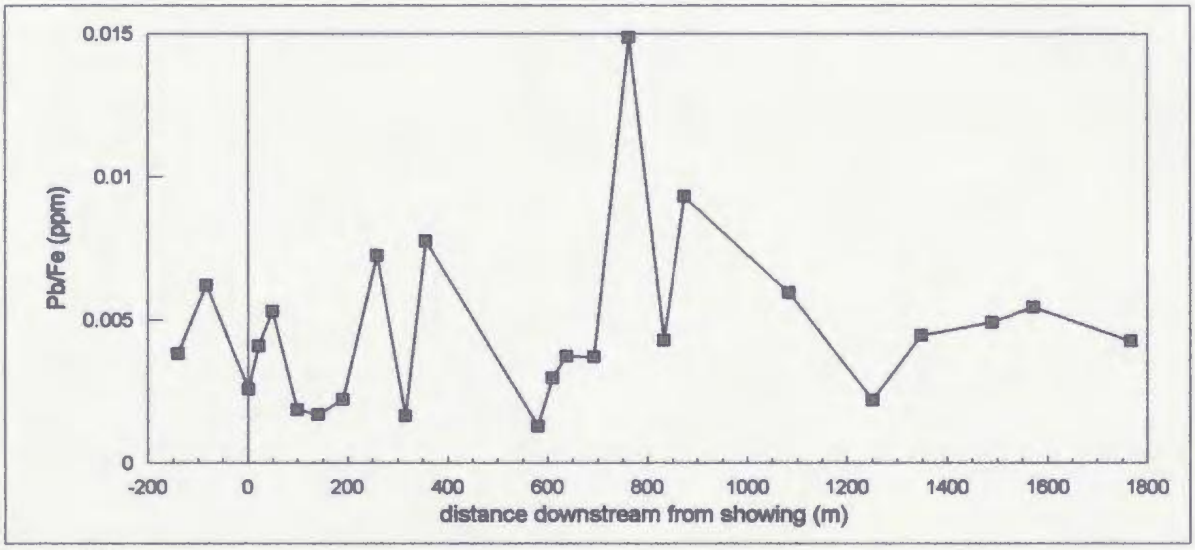

(b) Laser ablation

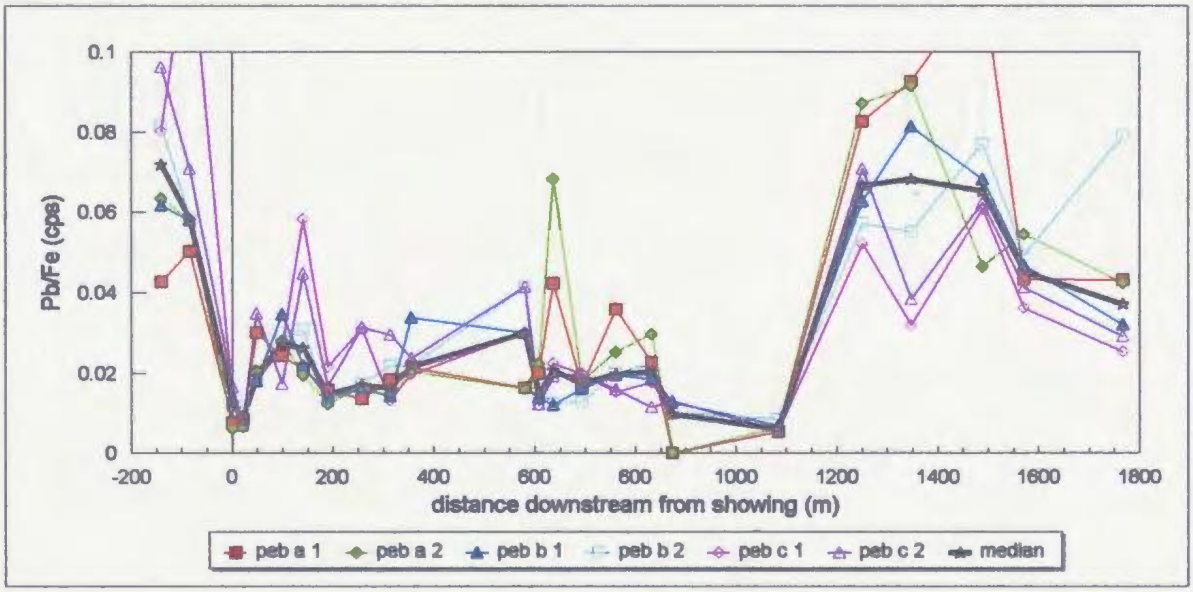

Figure 4.9: Pb determined in the oxide coated pebbles collected from Rocky Pond River; Stinger is located at distance zero. (a) Pb/Fe (ppm) results from partial dissolutions of Mn-Fe-oxide pebble coatings and (b) Pb/Fe (cps) laser ablation results from Mn-Fe-oxide pebble coatings.

Zn, As, Sb, Ba and Pb (Figures 4.1 to 4.9), indicate that most show elevated levels of that element close to and slightly downstream from the Au showing, Stinger. The degree of elevation is not always significant but indicate that Zn, As and Sb are viable for gold mineralization exploration using Mn-Fe-oxide coated stream pebbles as a sampling medium

.

4.2.3 Winter Hill

4.2.3.1 Introduction

This section follows the same outline as that described for the Rocky Pond River study area. Distance zero is the sample location closest to the Winter Hill VMS prospect. The prospect is a Pb-Zn-Cu occurrence which is hosted by the Tickle Point Group consisting of mafic tuffs and tuffaceous sedimentary rocks. The showing itself is a carbonate-calcium-magnesium silicate lens within mafic tuff. Sphalerite, galena, pyrrhotite, pyrite and chalcopyrite comprise the sulphides.

4.2.3.2 Results and discussion

The elements presented and discussed in this section (Figures 4.10 to 4.18) are based on the analysis of variance determined from the partial dissolution and laser ablation data sets (Tables 4.2 and 4.3). The elements Cu, Pb, Zn, Ba, Mo, Fe and Mn will be discussed in this section since all have passed the required statistics. Cobalt has slightly noisy data from the laser ablation procedure but will still be discussed in this section.

In Figure 4.10 Mn results from the partial dissolution of the oxide pebble coatings

from Country Brook are presented. Elevated levels, relative to Fe, are indicated near and downstream from the mineralized zone which decrease with increasing distance from the showing. A random distribution of Mn and Fe concentrations (Fig. 4.11) are noted throughout the study area when these elements are not ratioed to each other.

Similar patterns are discernable between the results presented for Fe in Figures 4.12 a and b. Higher levels of Fe are noted downstream for both partial dissolution (Fig. 4.12 a) and laser ablation (Fig. 4.12 b) methods. Laser ablation results (Fig. 4.12 b) show constant Fe values for 1.8 km downstream after which there is a steady increase then a decline. Iron values appear to be controlled by local geology rather than mineralization since they show an increase in the lower part of the stream where it enters the Connaigre Bay Group which is comprised of tholeiitic and mafic volcanic rocks. There appears to be a similar distribution of Fe noted in the pebble coatings when comparing both laboratory methods.

Results of Cu in the oxide coated stream pebble coatings can be compared in Figures 4.13 a and b. The partial dissolution method (Fig. 4.13 a) indicates a random distribution of Cu in the study area, whereas the laser ablation results (Fig. 4.13 b) show a relatively constant level of Cu throughout the stream. Cu does not appear to be an appropriate mineral to use in base metal exploration for this location when using Mn-Fe-oxide coated stream pebbles as the sampling medium since the mineralization at Winter Hill is not clearly depicted with either laboratory method. An anomalous Cu value noted at the end of the sampled area is observed for both partial dissolution and two of the pebble chips. This notable value is most likely due to the presence of tholeiitic and mafic volcanic rocks of where Cu is a common ore or

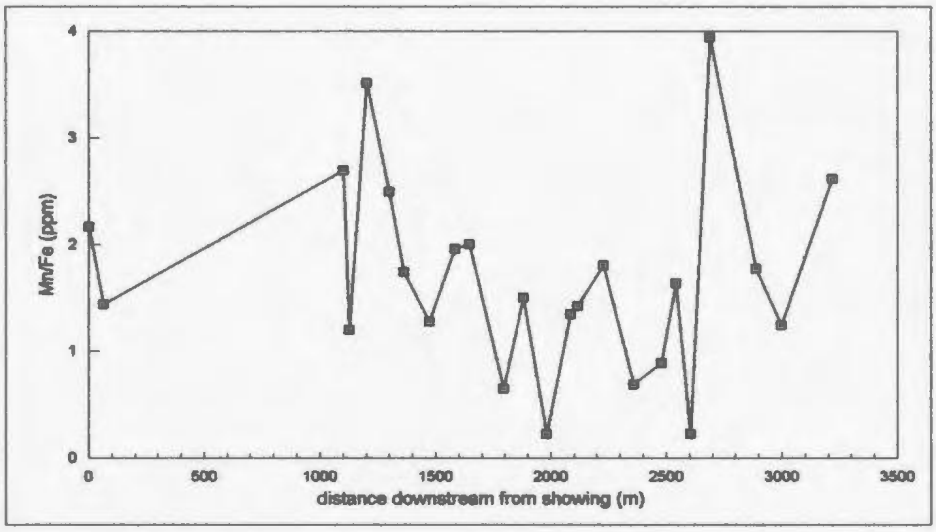

Figure 4.10: Mn/Fe (ppm) results from the partial dissolution of Mn-Fe-oxide coated stream pebbles collected from Country Brook; Winter Hill VMS prospect is located at distance zero.

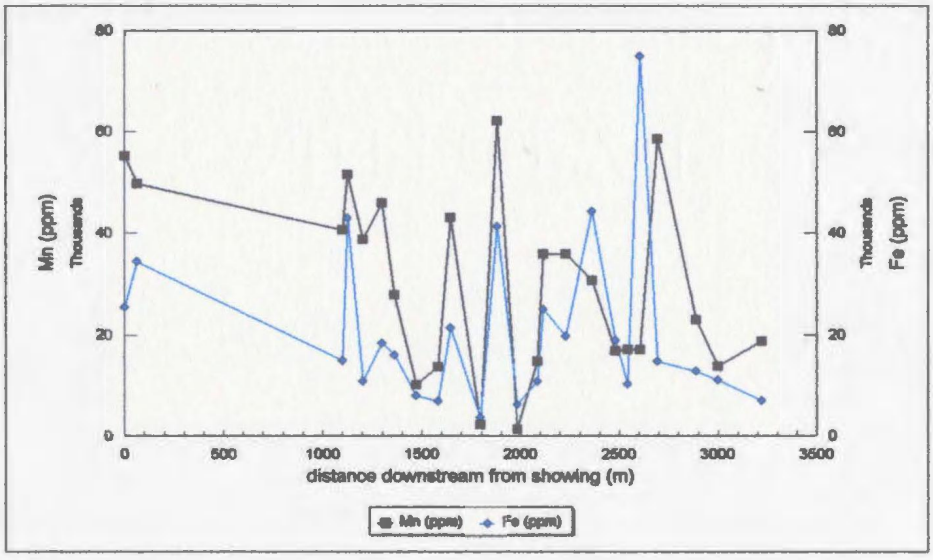

Figure 4.11: A graph of Mn and Fe concentrations determined in the partial dissolution solutions from Country Brook; Winter Hill VMS prospect is located at distance zero.

(a) Partial dissolution

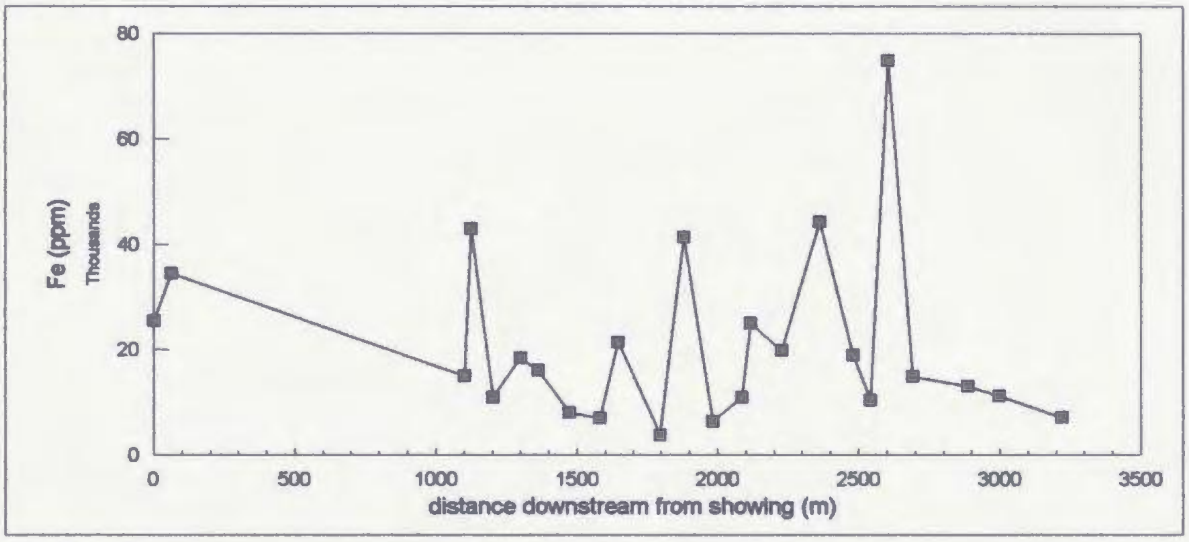

(b) Laser ablation

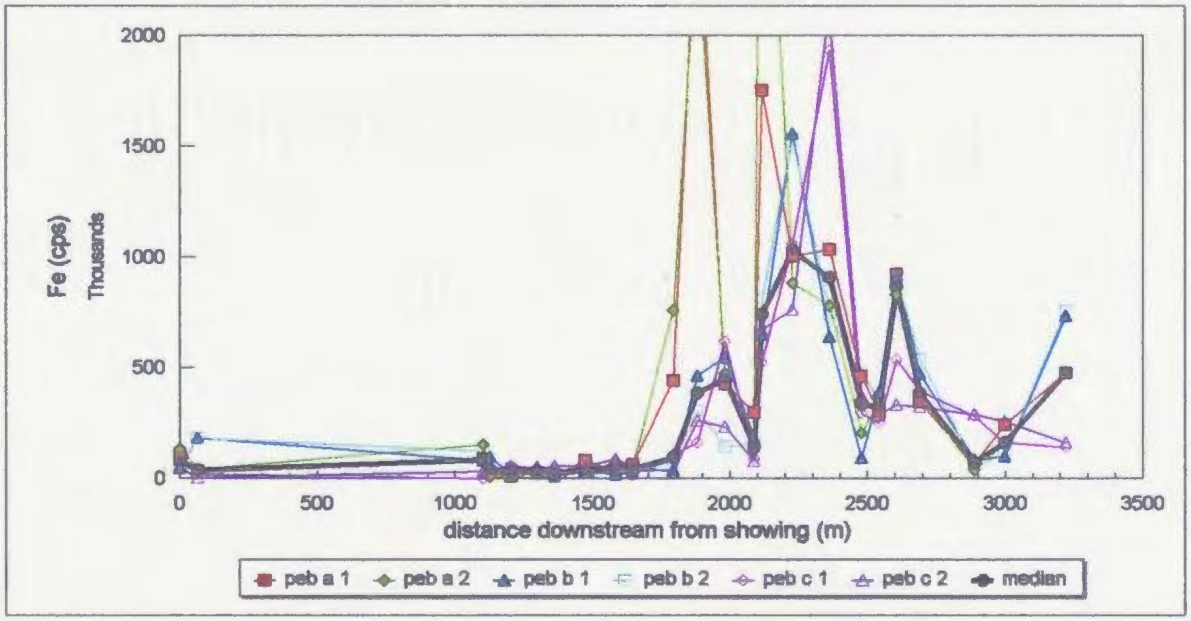

Figure 4.12: Fe determined in the oxide pebble coatings collected from Country Brook; Winter Hill VMS prospect is located at distance zero. (a) Fe (ppm) results from partial dissolutions of Mn-Fe-oxide pebble coatings and (b) Fe (cps) results from laser ablation of the Mn-Fe-oxide pebble coatings.

(a) Partial dissolution

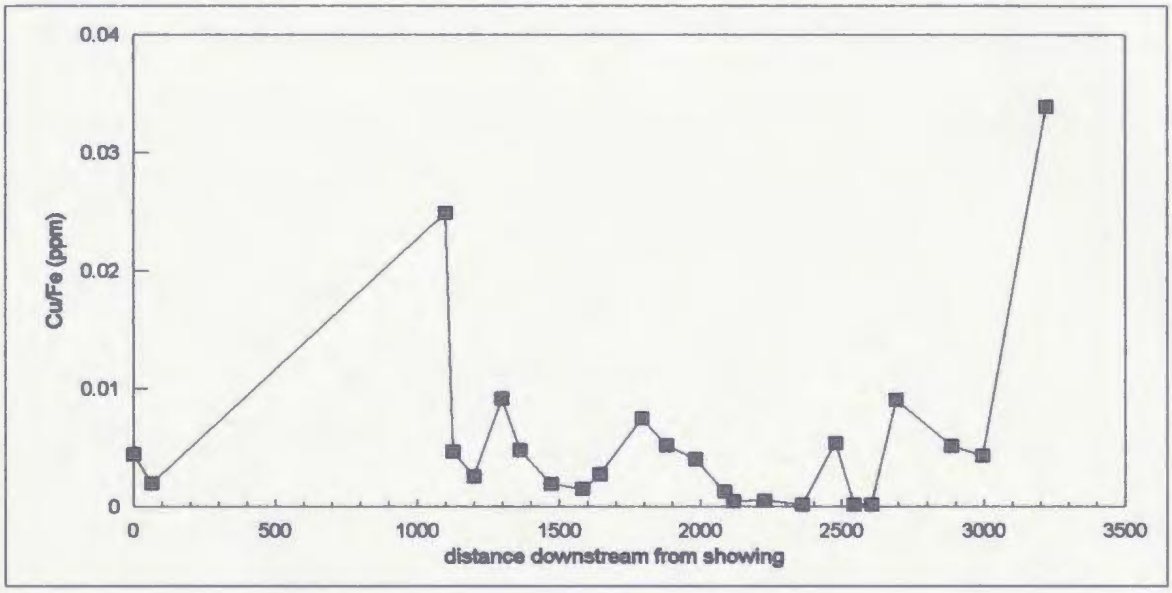

(b) Laser ablation

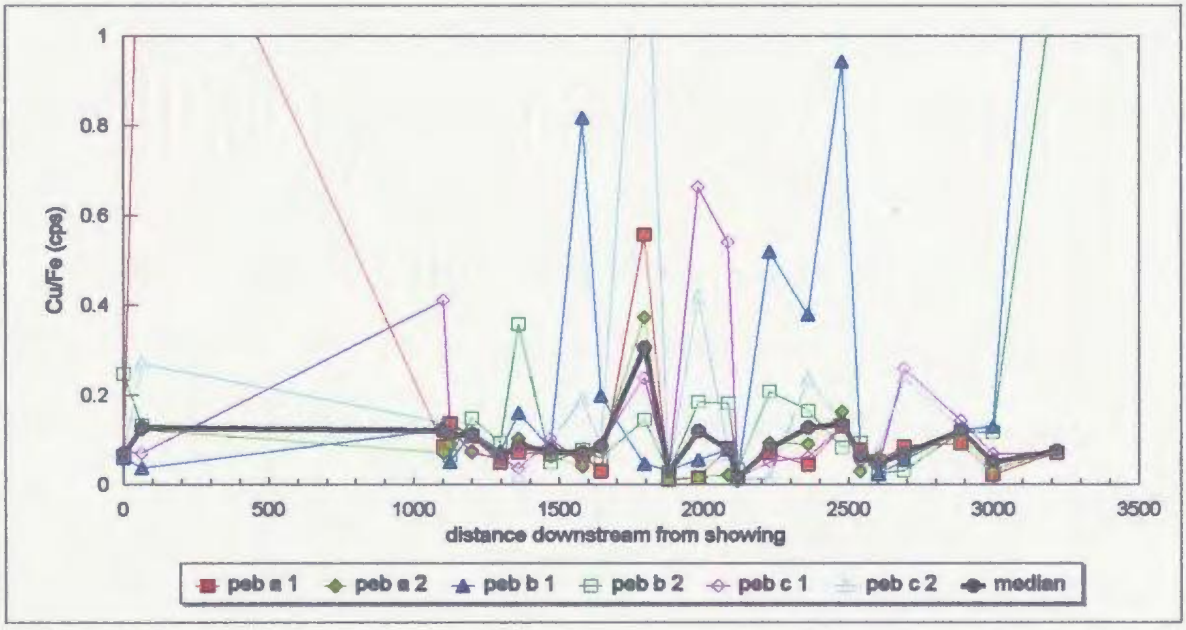

Figure 4.13: Cu determined in the oxide pebble coatings collected from Country Brook; Winter Hill VMS prospect is located at distance zero. (a) Cu/Fe (ppm) results from partial dissolutions of Mn-Fe-oxide pebble coatings where each data point is an individual analysis for each sample location and (b) Cu/Fe (cps) results from laser ablation of the Mn-Fe-oxide pebble coatings where each analyses of the pebbles are plotted and the median value is the average of the two medium values for that sample site.

replacement mineral.

Figures 4.14 a and b show the results of Pb in the oxide coatings. Partial dissolution of the coatings (Fig. 4.14 a) clearly shows elevated Pb values near and downstream from the showing with a sharp decline in values with increasing distance downstream. The laser ablation results (Fig. 4.14 b) indicate a constant level of Pb throughout the stream with an increase near the end of the study area. Slightly elevated results are noted ~ 1 km downstream but not as pronounced as the digestion method. Using Pb in base metal exploration when the sampling medium is oxide coated stream pebbles appears viable but digestion of the coatings is probably the best choice of analytical procedure not laser ablation.

Zinc results are presented in Figures 4.15 a and b. Figure 4.15 a indicates elevated Zn levels slightly downstream from the mineralized zone with a steady decline until the end of the study area where levels begin to increase. The laser ablation results (Fig. 4.15 b) also indicate a slight elevation of Zn near the showing and a gradual decline with increasing distance from the deposit. The increase in Zn near the end of the study area can be attributed to the presence of andesite and basalt which are the predominant rock type in this location.

Figures 4.16 a and b show the results of Co in the Mn-Fe-oxide coated stream pebbles. Both partial dissolution values (Fig 4.16 a) and laser ablation results (Fig 4.16 b) indicate elevated Co near and downstream from the Winter Hill showing. The remainder of the study area appears to show a random distribution of Co. The digestion procedure results indicate that the partial dissolution of oxide coated pebbles would be more effective in depicting base metal mineralization than the laser ablation method when Co is the element

(a) Partial dissloution

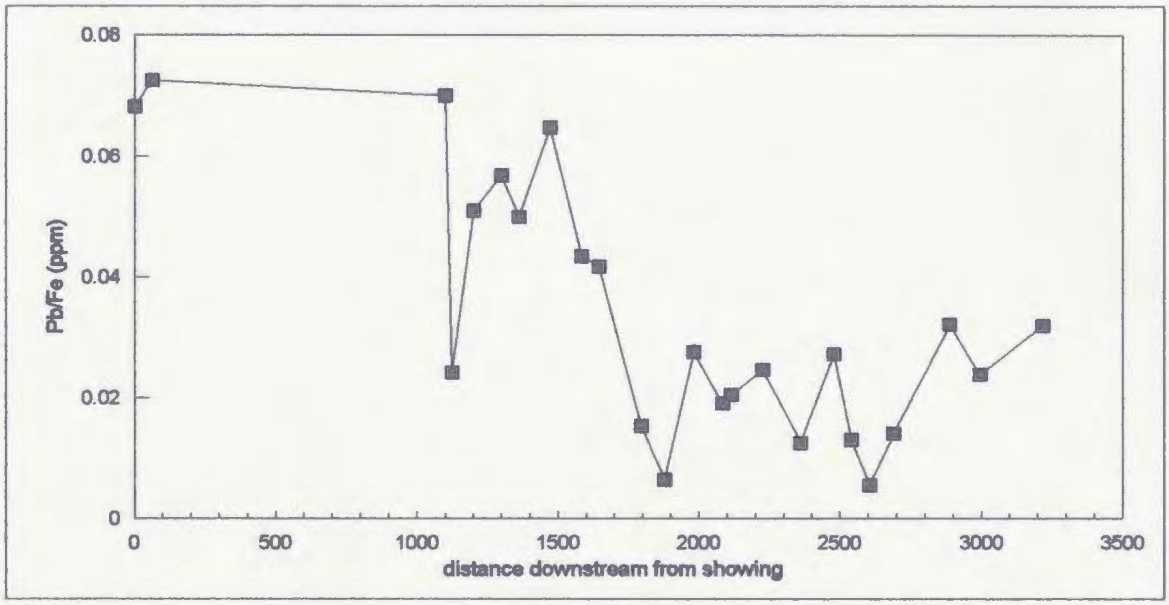

(b) Laser ablation

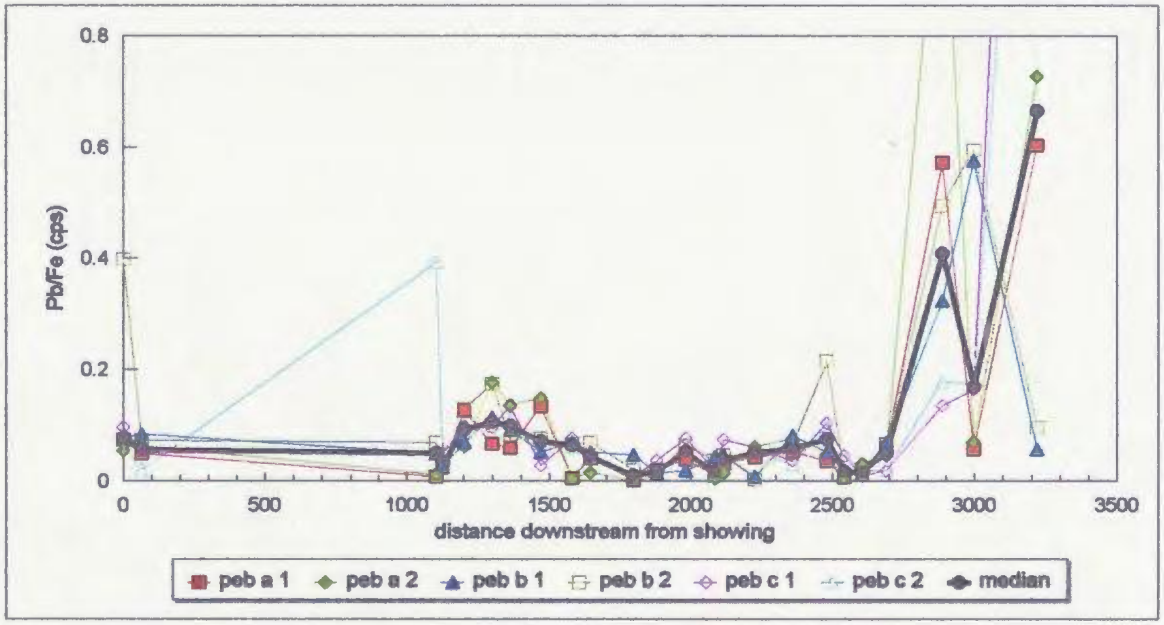

Figure 4.14: Pb determined in the oxide pebble coatings collected from Country Brook; Winter Hill VMS prospect is located at distance zero. (a) Pb/Fe (ppm) results from partial dissolutions of Mn-Fe-oxide coatings and (b) Pb/Fe (cps) results from laser ablation of the Mn-Fe-oxide pebble coatings.

(a) Partial dissolution

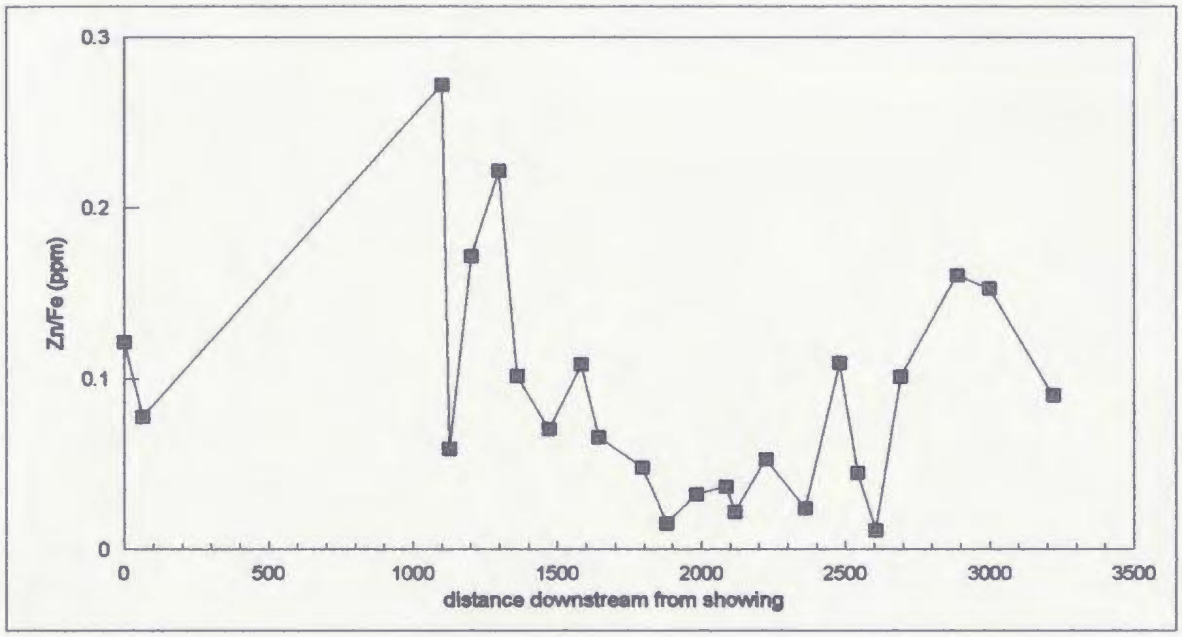

(b) Laser ablation

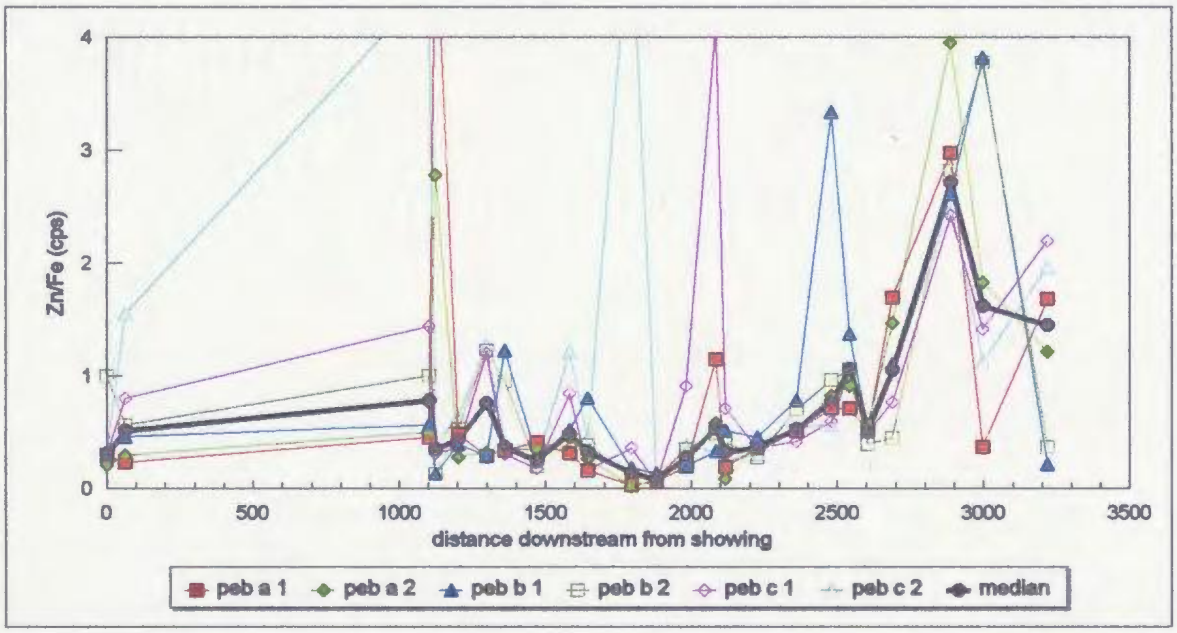

Figure 4.15: Zn determined in the oxide pebble coatings collected from Country Brook; Winter Hill VMS prospect is located at distance zero. (a) Zn/Fe (ppm) results from partial dissolutions of Mn-Fe-oxide coatings and (b) Zn/Fe (cps) results from the laser ablation of Mn-Fe-oxide pebble coatings.

(a) Partial dissolution

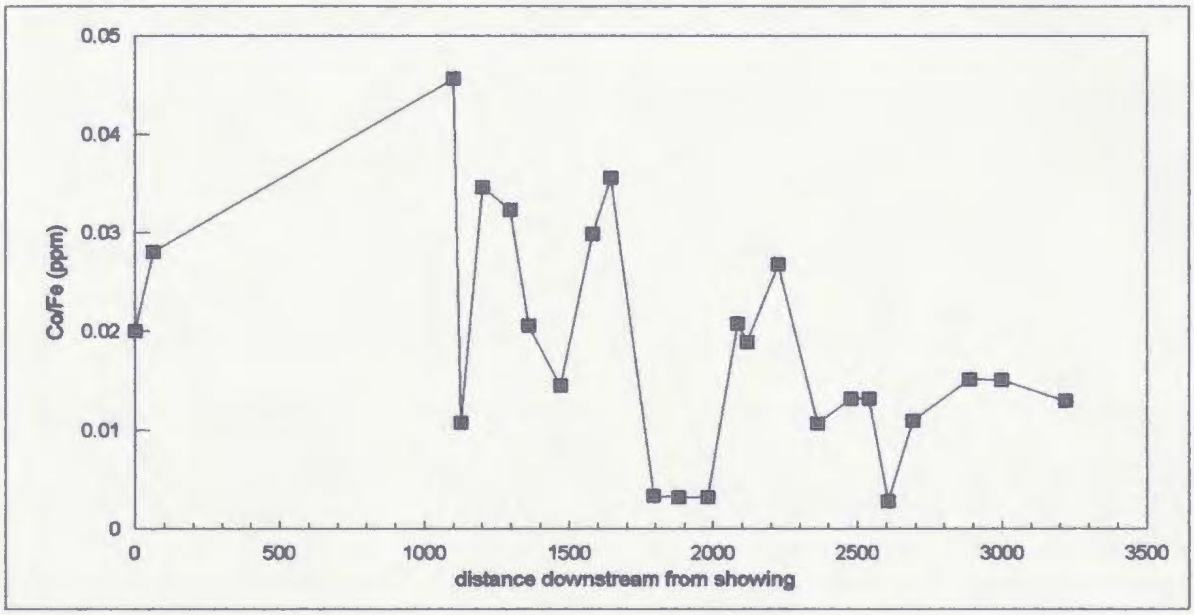

(b) Laser ablation

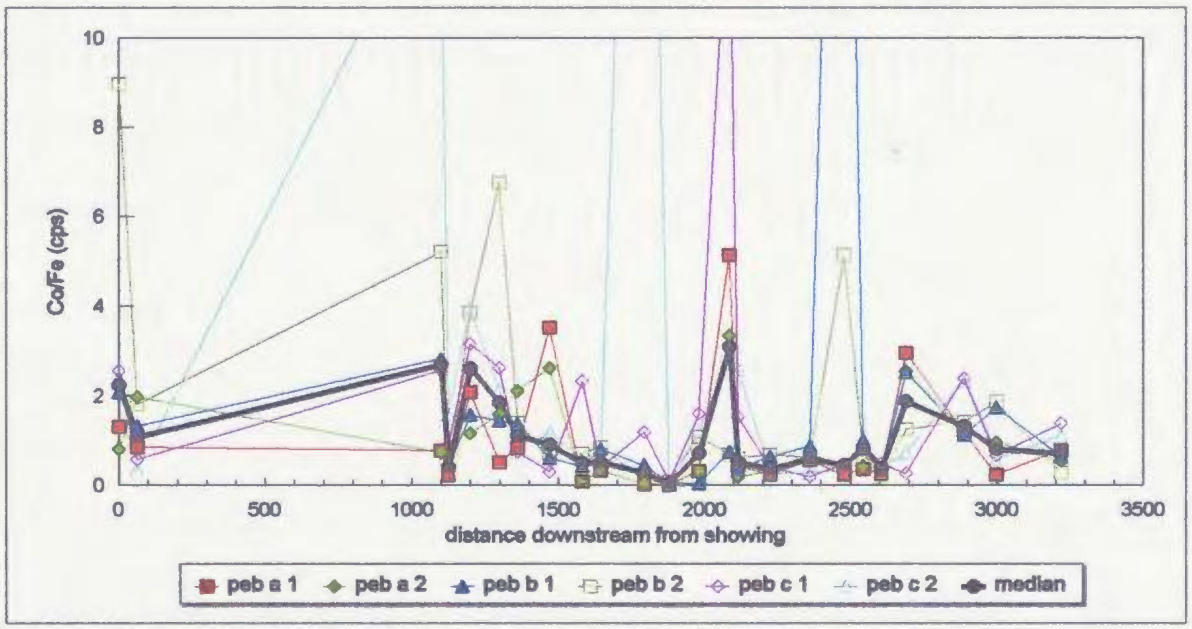

Figure 4.16: Co determined in the oxide pebble coatings collected from Country Brook; Winter Hill VMS prospect is located at distance zero. (a) Co/Fe (ppm) results from partial dissolutions of Mn-Fe-oxide coatings and (b) Co/Fe (cps) values from laser ablation of the Mn-Fe-oxide pebble coatings.

being considered.

Barium values are shown in Figures 4.17 a and b. Determinations by partial dissolution (Fig. 4.17 a) do not show elevated Ba results near the prospect. Downstream values indicate random distribution throughout the study area. Laser ablation results (Fig. 4.17 b) shows slightly declining Ba with increasing distance from the mineralized area. Barium as an indicator mineral for base metal exploration does not appear to be effective when the sampling medium is oxide coated stream pebbles.

Figures 4.18 a and b show Mo determinations from partial dissolution (Fig. 4.18 a) and laser ablation (Fig. 4.18 b) of Mn-Fe-oxide coated stream pebbles. The digestion method shows a random distribution of Mo in the study area and the laser ablation procedure indicates increasing Mo with increasing distance from the Winter Hill prospect. Using Mo as an indicator mineral, when prospecting with oxide coated pebbles as a sampling medium, does not appear to be viable for this study area.

4.2.3.3 Summary

Base-metal studies have typically been the focus for the use of Mn-Fe-oxide coated stream pebbles as a sampling medium. Country Brook drains the locality of the Pb-Zn-Cu Winter Hill occurrence. The graphical presentation of the ore and indicator minerals for the Winter Hill base metal showing in the above section suggest that not all of the elements discussed point to Pb-Zn-Cu mineralization when using Mn-Fe-oxide coated stream pebbles as a sampling medium. The partial dissolution of the oxide coatings appears to be a more

(a) Partial dissolution

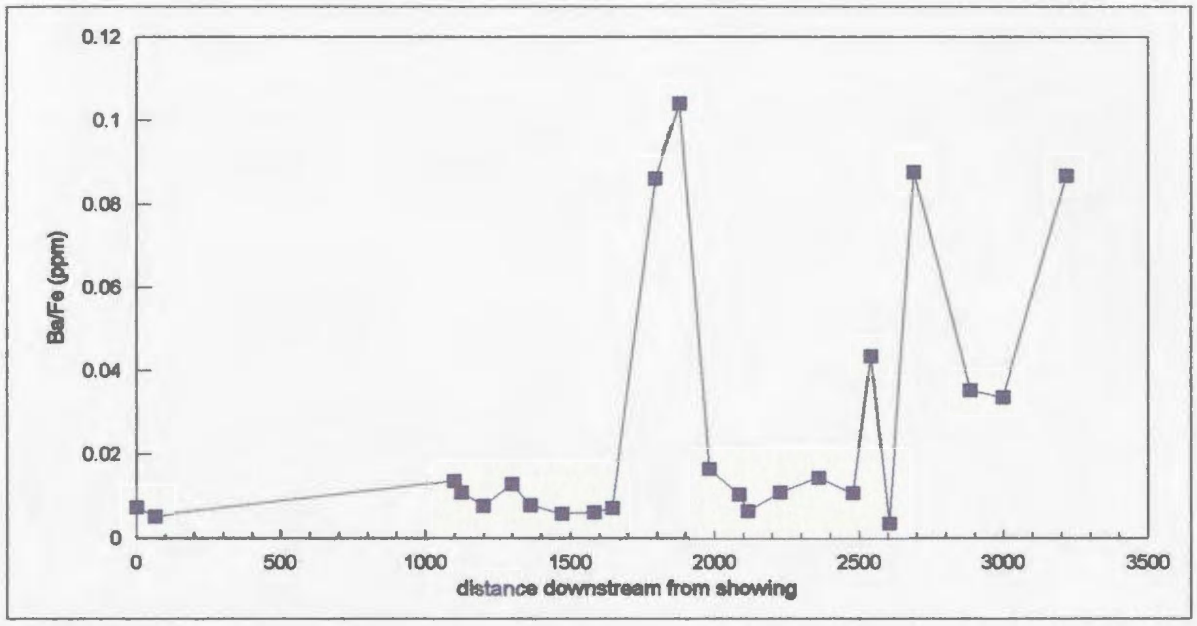

(b) Laser ablation

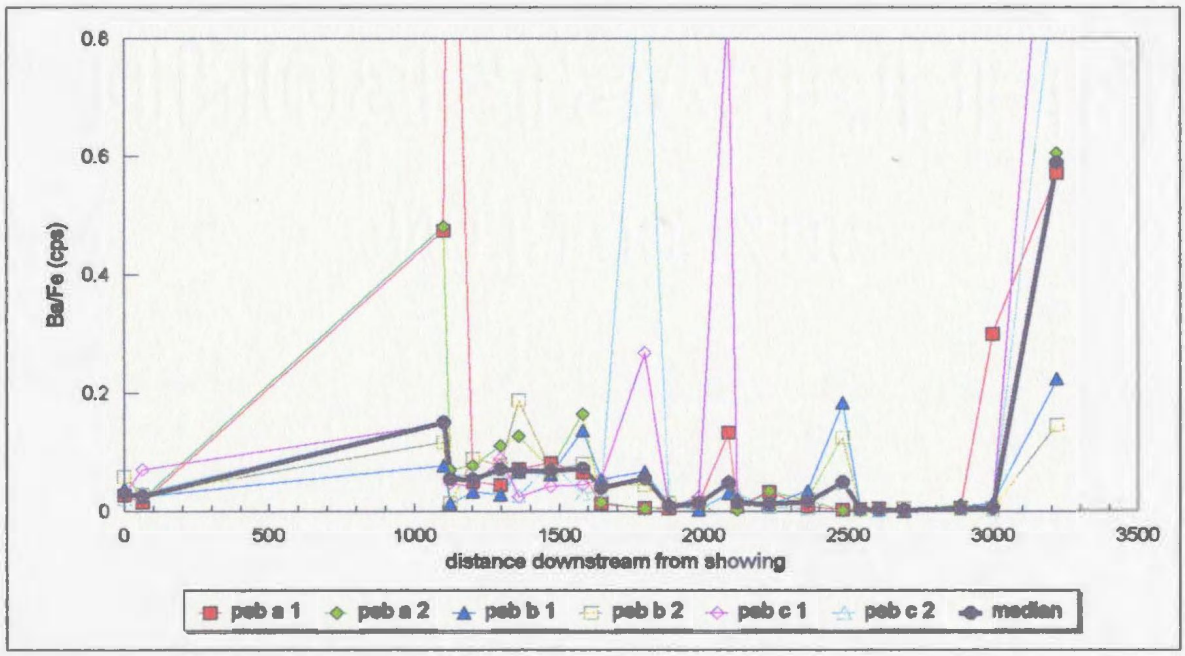

Figure 4.17: Ba determined in the oxide pebble coatings collected from Country Brook; Winter Hill VMS prospect is located at distance zero. (a) Ba/Fe (ppm) results from partial dissolutions of Mn-Fe-oxide coatings and (b) Ba/Fe (cps) results from laser ablation of the Mn-Fe-oxide pebble coatings.

(a) Partial dissolution

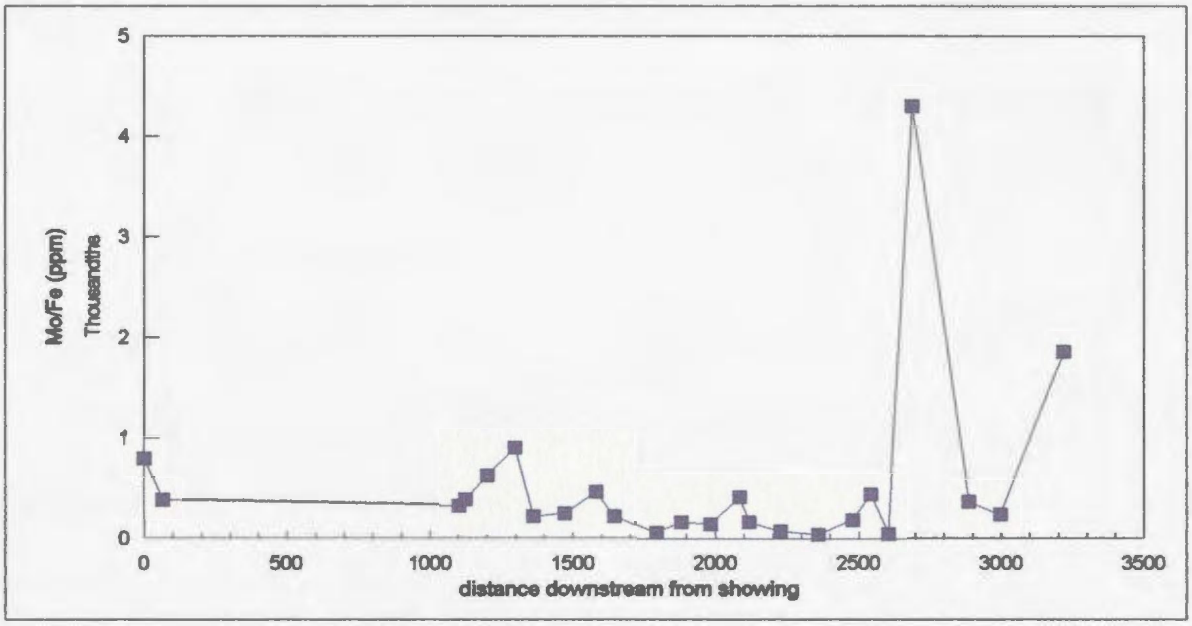

(b) Laser ablation

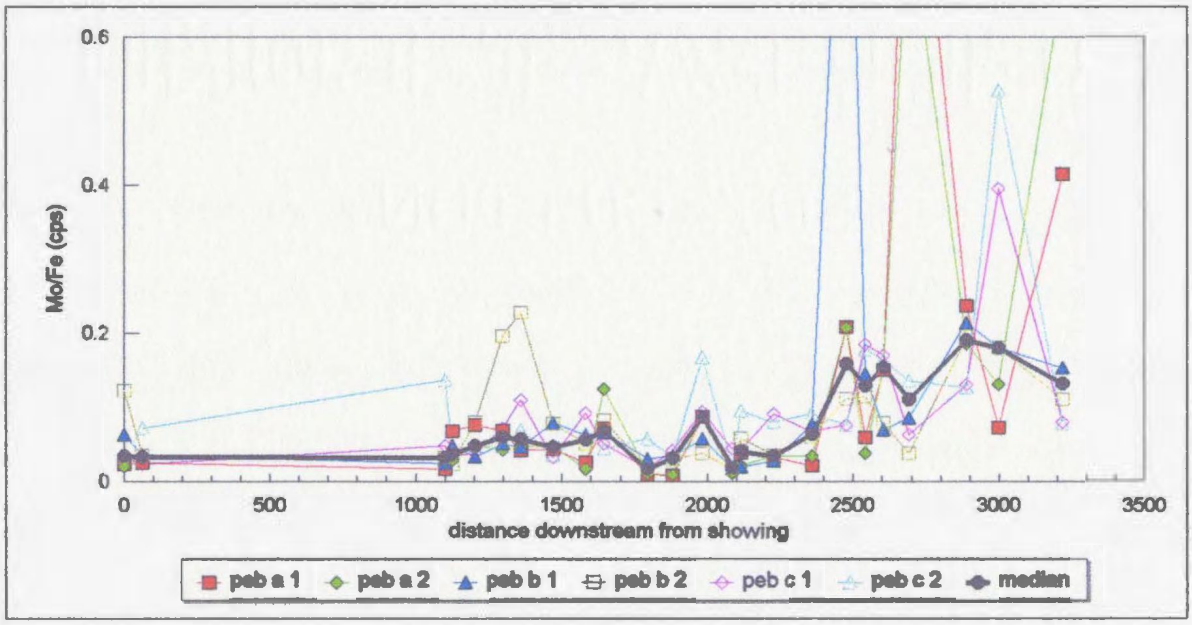

Figure 4.18: Mo determined in the oxide pebble coatings collected from Country Brook; Winter Hill VMS prospect is located at distance zero. (a) Mo/Fe (ppm) results from partial dissolutions of Mn-Fe-oxide coatings and (b) Mo/Fe (cps) results from the laser ablation of Mn-Fe-oxide pebble coatings.

viable method than laser ablation for depicting base metal mineralization. Lead, Zn and Co clearly show elevated levels near and downstream from the mineralization in the partial dissolution graphs but only Zn, Co and Ba have similar trends in the laser ablation results.

4.2.4 Come-By-Chance oil refinery

4.2.4.1 Introduction

The following section describes and discusses the analytical results derived from the oil refinery study area. The samples were collected northeast of the refinery, in the prevailing wind direction, at a distance of 1 to 4.2 km from the smoke stack which emits most of the local pollutants. The sample sites covered a network of streams that drains the area unlike the other two study areas where the samples were collected from one stream in each study area.

A stack sampling program has been implemented at the Come By Chance oil refinery but the results have not yet been made pubic. Other sampling programs (Jacqes Whitford Environment Limited, January, 2000) show that with the exception of SO_2, emissions from the smoke stack do not exceed Newfoundland air quality standards. The inorganic components in the material being burned and refined at the refinery are presumed to consist mainly of V, Ni and sulphate along with Pb, Zn, Cr, Ba, Fe, Al and others (Sheppard Green Engineering and Associates Limited, June 1996).

The graphs of relevant elements are plotted with the ratioed value of the element on the y-axes, in the same format as for the other two study areas. The x-axis is the distance of

the sample locations from the smoke stack. The graphical representation of the data sets were designed to ascertain if the smoke stack emissions are having an impact on the local environment and, if so, how large is the area being affected.

4.2.4.2 Results and discussion

The graphical presentations of elements in this section (Figures 4.19 to 4.26) are based on the analysis of variance shown in Tables 4.2 and 4.3. Since V and Ni were only included in the Come-By-Chance Oil refinery suite of isotopes for analyses using the LAM-ICP-MS procedure, there are no reliable statistical data due to a limited number of duplicate pairs. Graphs will be presented for these elements anyway as well as Mn, Fe, Zn, Pb and S which the author considers relevant to the study.

Figure 4.19 shows Mn/Fe ratio for the partial dissolution of Mn-Fe-oxide coated stream pebbles from the network of streams in the Come-By-Chance oil refinery study area. The graph indicates that Mn values are elevated from 1 to 1.5 km from the smoke stack and are greatly reduced at sample sites located at a further distance.

Iron determinations in the oxide coatings are shown in Figures 4.20 a and b. Neither the partial dissolution procedure (Fig. 4.20 a) or the laser ablation method (Fig. 4.20 b) show any significant increase in Fe at any of the sample locations with the exception of the sample site located closest to the smoke stack from the digestion analysis.

Manganese and Fe concentrations in the pebble coatings as determined from partial dissolution (Figure 4.21) suggests that Mn occurs in high concentrations for the majority of

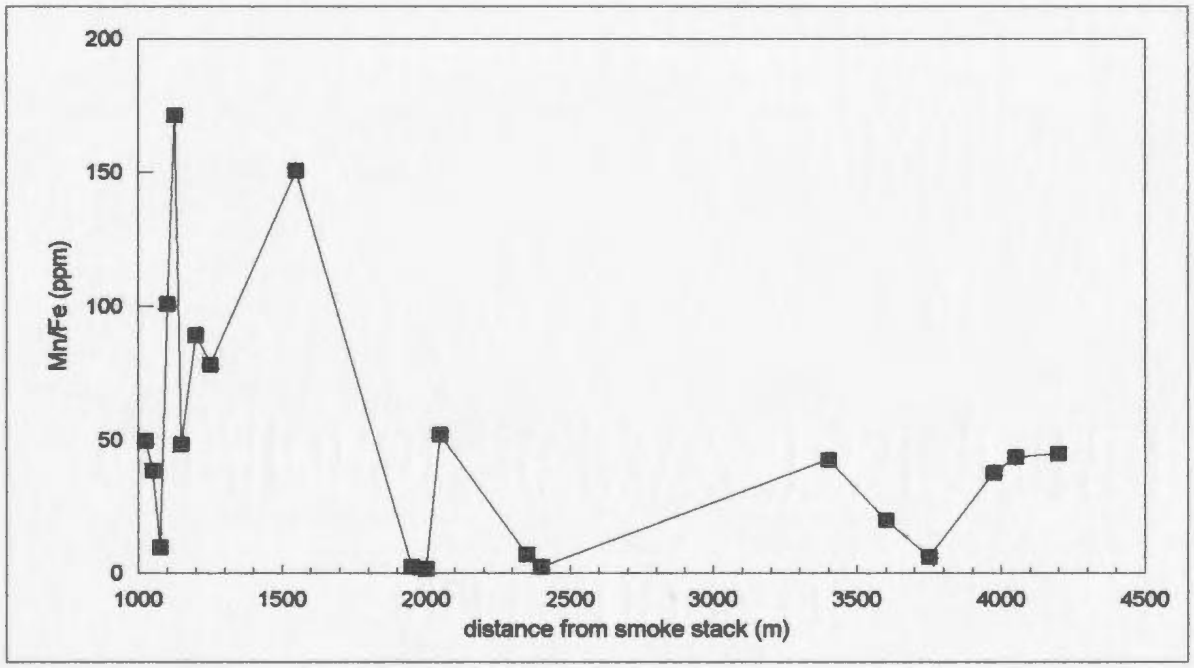

Figure 4.19: Mn/Fe (ppm) determined in partial dissolutions of Mn-Fe-oxide coated stream pebbles collected from the network of streams in the Come-By-Chance oil refinery area.

(a) Partial dissolution

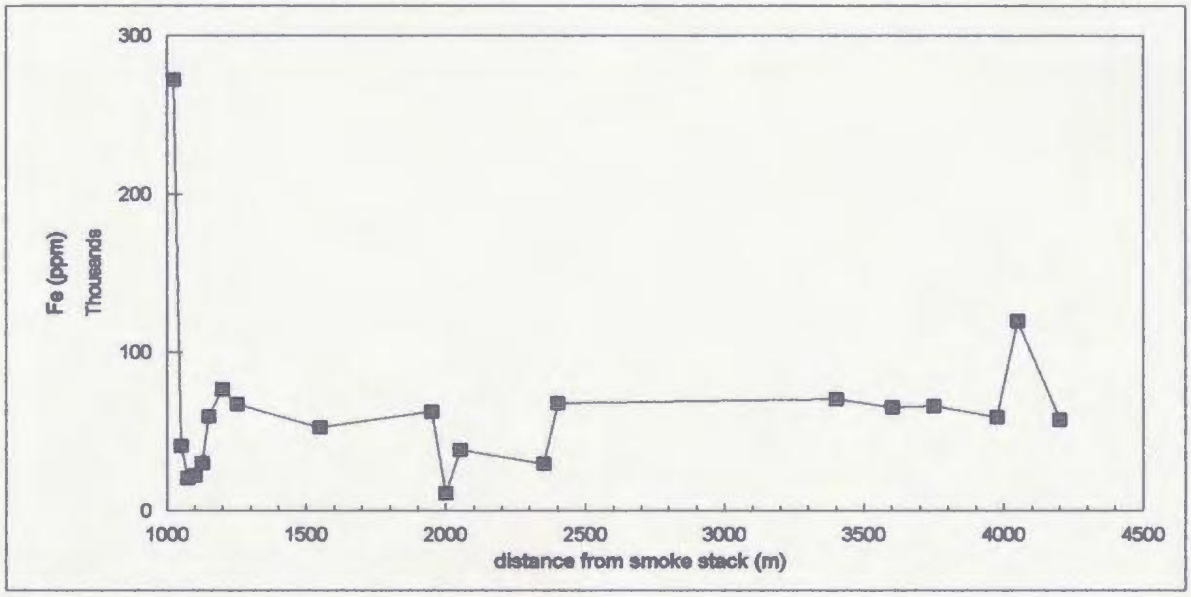

(b) Laser ablation

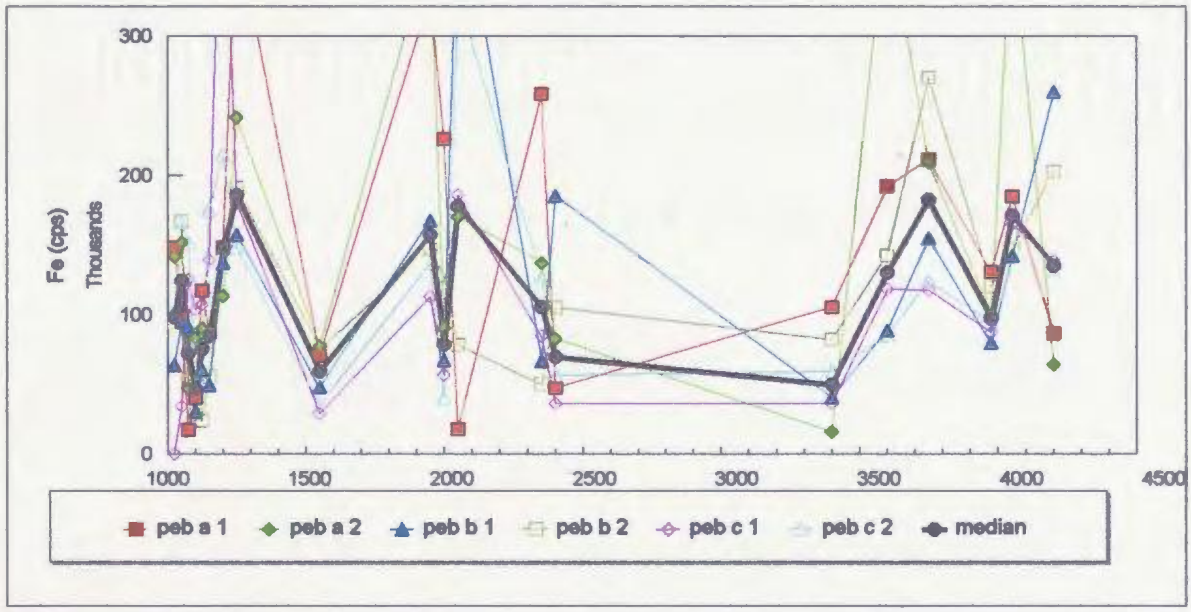

Figure 4.20: Fe results from the Mn-Fe-oxide coated stream pebbles collected from the network of streams in the Come-By-Chance oil refinery area. (a) Fe (ppm) partial dissolution results and (b) Fe (cps) results of the laser ablation of the Mn-Fe-oxide pebble coatings.

the sample locations but that Fe values are significantly lower. A monitoring report of surface water in the near vicinity of the oil refinery (Sheppard Green Engineering and Associates Limited, June 1996) also detected very high Mn in ponds within the study area but no source of contamination is clearly defined. The source for the high Fe value observed closest to the smoke stack is not known either.

Although V results determined by laser ablation do not have statistical analysis of variance to support its validity they are presented in Figure 4.22 b as a comparison to the observations of V determined by partial dissolution analysis (Fig. 4.22 a). Vanadium clearly shows significantly higher values closer to the smoke stack than those sample locations located at a distance greater than 2 km from it (Fig. 4.22 a). The laser ablation procedure indicates that the pebble coatings also have a slightly higher concentration near the smoke stack than those locations further away. These graphs indicate that V is a viable element to use for environmental monitoring in Mn-Fe-oxide coated stream pebbles using either laboratory procedure.

Table 4.2 shows that Ni did not pass the required statistical analysis for the partial dissolution data and that the data set from laser ablation was too small to be included in the analysis of variance. Nickel is included in this section though because the statistical analysis indicates that the data is only slightly noisy and may be of value. Figures 4.23 a and b indicate that Ni levels are elevated within 2 km of the smoke stack for both partial dissolution results (Fig. 4.23 a) and laser ablation determinations (Fig. 4.23 b) but are relatively low and constant beyond this range. The graphs suggest that when Ni is part of a suite of elements being

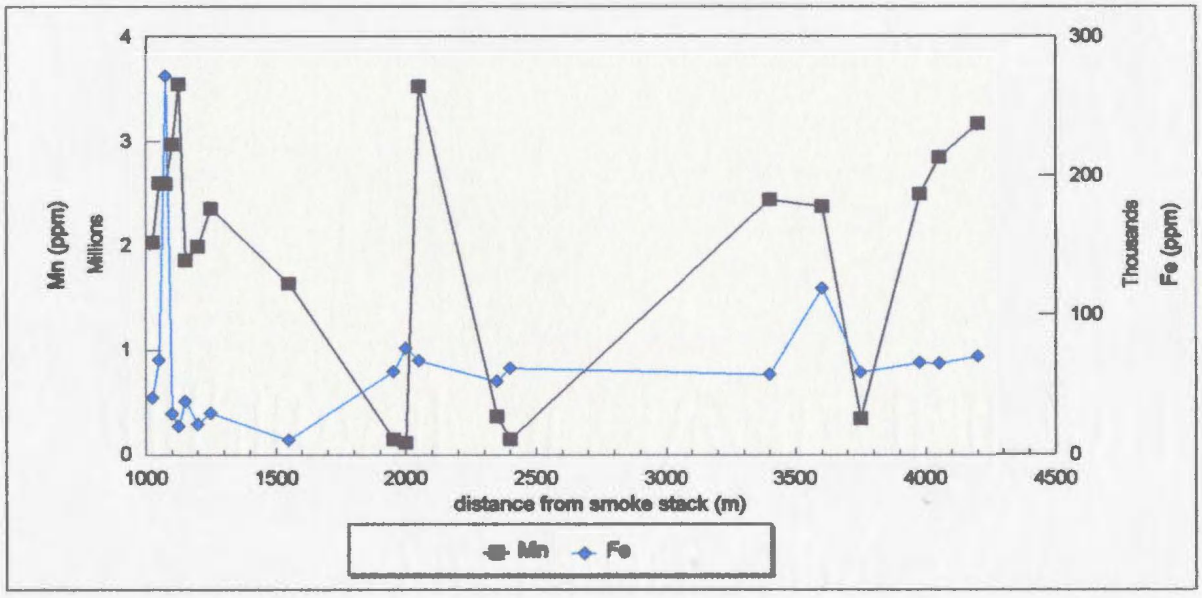

Figure 4.21: A graph of Mn and Fe concentrations determined in the partial dissolution solutions from the network of streams in the Come-By-Chance oil refinery study area.

(a) Partial dissolution

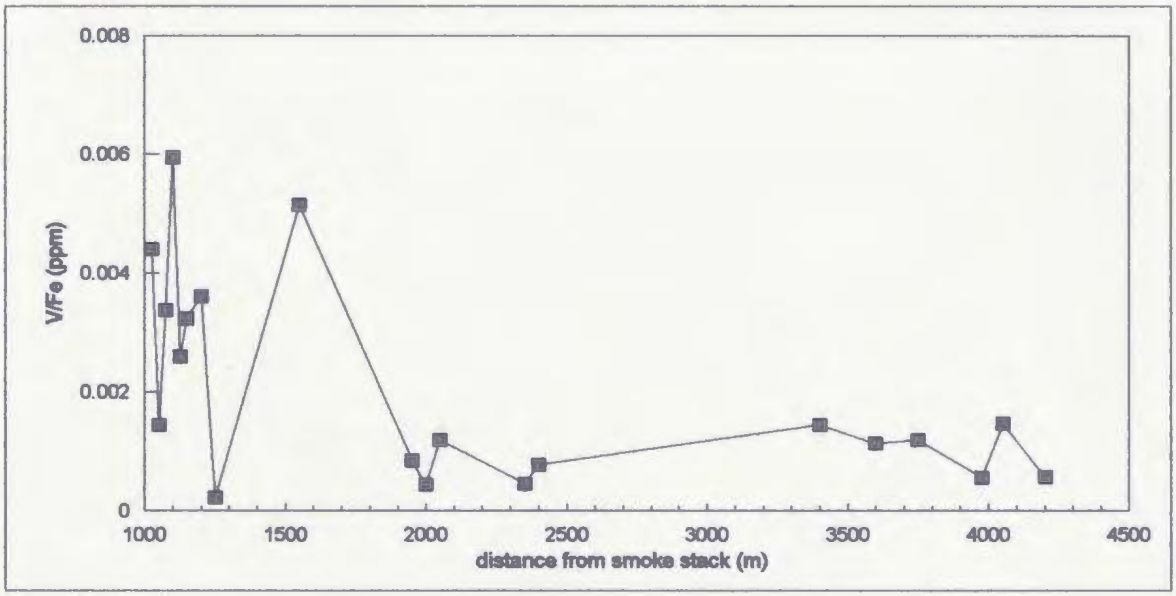

(b) Laser ablation

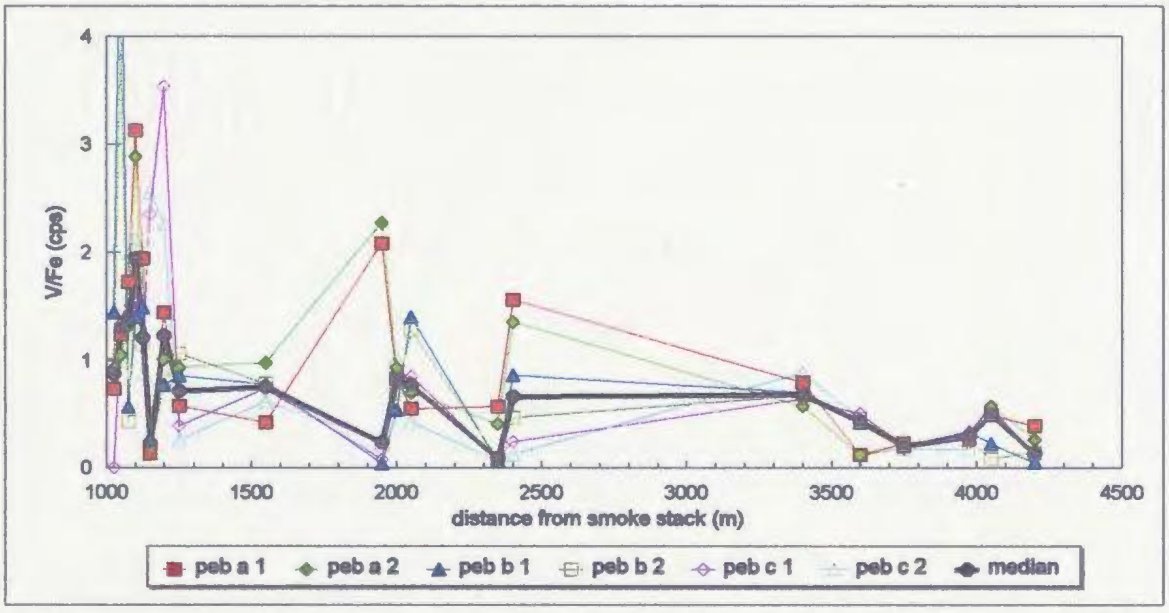

Figure 4.22: V determined in the Mn-Fe-oxide coated stream pebbles collected from the network of streams in the Come-By-Chance oil refinery study area; the smoke stack is considered distance zero. (a) V/Fe (ppm) results from partial dissolution of the pebble coatings where each data point is an individual analysis for each sample location and (b) V/Fe (cps) results from the laser ablation of the oxide coatings where each analyses of the pebbles are plotted and the median value is the average of the two medium values for that sample site.

(a) Partial dissolution

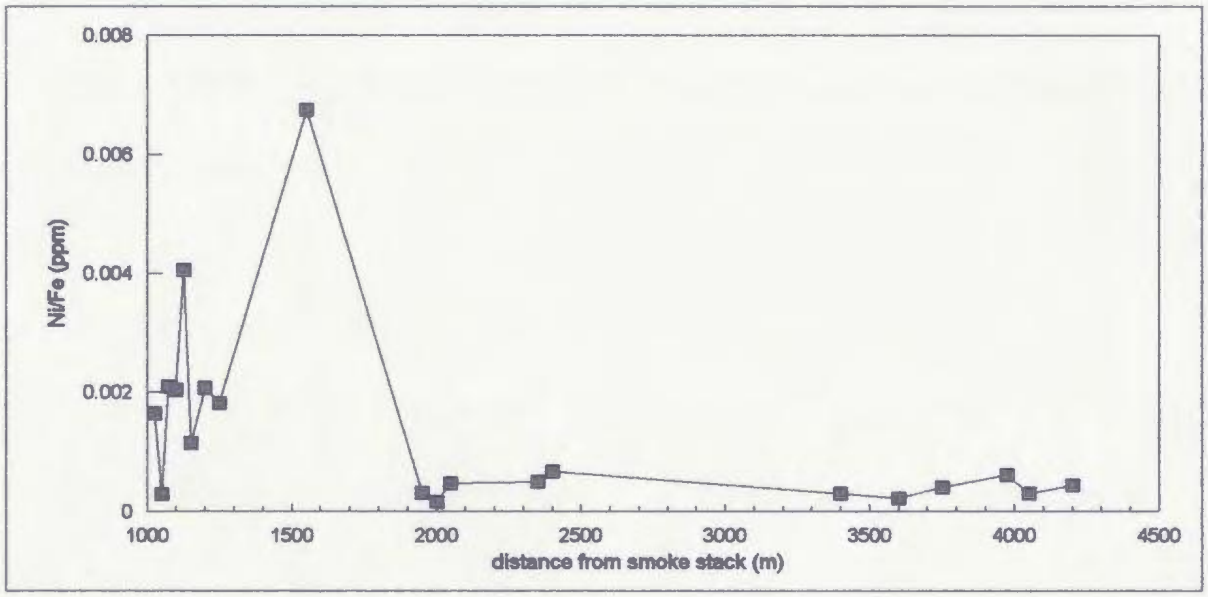

(b) Laser ablation

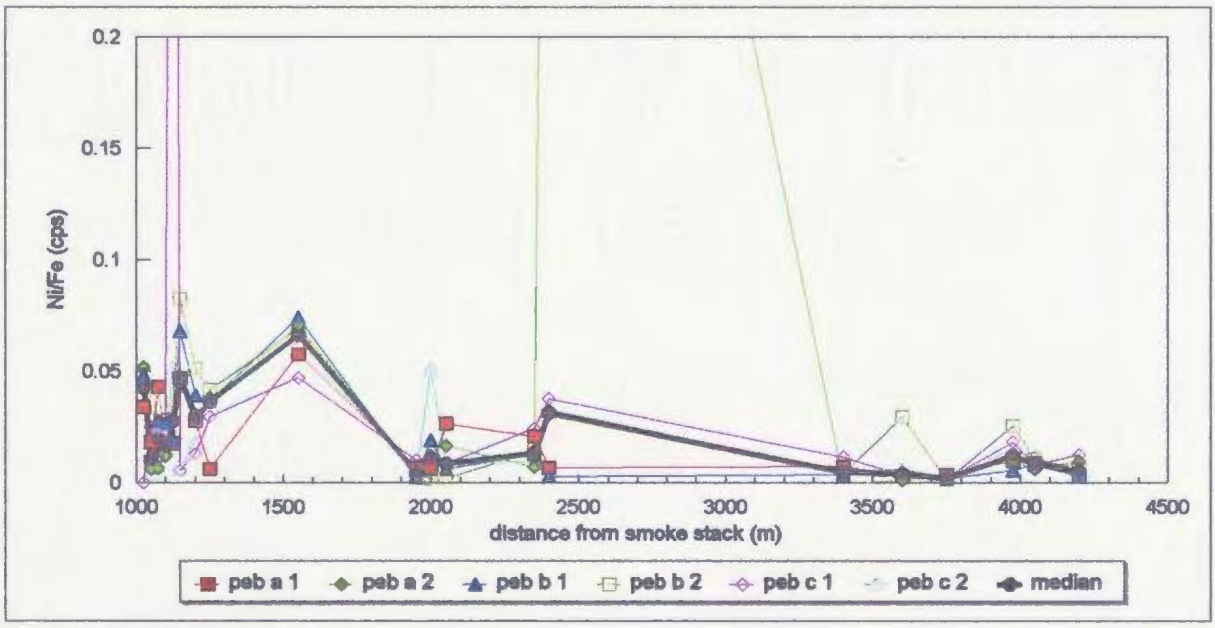

Figure 4.23: Ni determined in the Mn-Fe-oxide coated stream pebbles collected from the network of streams in the Come-By-Chance oil refinery study area; the smoke stack is considered distance zero. (a) Ni/Fe (ppm) partial dissolution results from the pebble coatings and (b) Ni/Fe (cps) results from the laser ablation of the oxide coatings.

analysed in the Mn-Fe-oxide coated stream pebbles using either dissolution or solid sample analysis, the results are viable for detecting anomalies.

Sulfur (total sulphur) data is very noisy for the partial dissolution data sets (see Table 4.2) but laser ablation results indicate that analysis of variance are good. Figures 4.24 a and b indicate elevated S (total) values within the first 2 km of the smoke stack for both partial dissolution of the pebble coatings (Fig. 4.24 a) and laser ablation of the same coatings (Fig. 4.24 b). Beyond 2 km, S levels are low and constant until at a distance of 3.5 km when both types of analyses indicate an increase in S. There is no explanation for the increase in S at this distance.

Figures 4.25 a and b are the determinations of Zn in the oil refinery study area. Elevated Zn values are noted for a distance of 1.5 km from the smoke stack in both the partial dissolution (Fig. 4.25 a) and laser ablation (Fig. 4.25 b) graphs. Beyond the 1.5 km range, Zn values are low and constant. Zinc appears to be a good candidate for environmental monitoring in the analysis of oxide coated stream pebbles by either laboratory method.

Lead results are shown in Figures 4.26 a and b. Partial dissolution of the pebble coatings (Fig. 4.26 a) indicate a relatively random distribution of Pb in the study area. Figure 4.26 b also shows a generally random pattern of Pb in the pebble coatings as determined by laser ablation analysis. Pebble c analyses by laser ablation shows significantly higher values than the other two pebbles. This anomaly is most likely due to the abundant vegetation in the stream and a heavy organic coating on the pebble along with the Mn-Fe-oxide coating. The very slow flow of the stream and the close proximity of a small lake probably contribute

(a) Partial dissolution

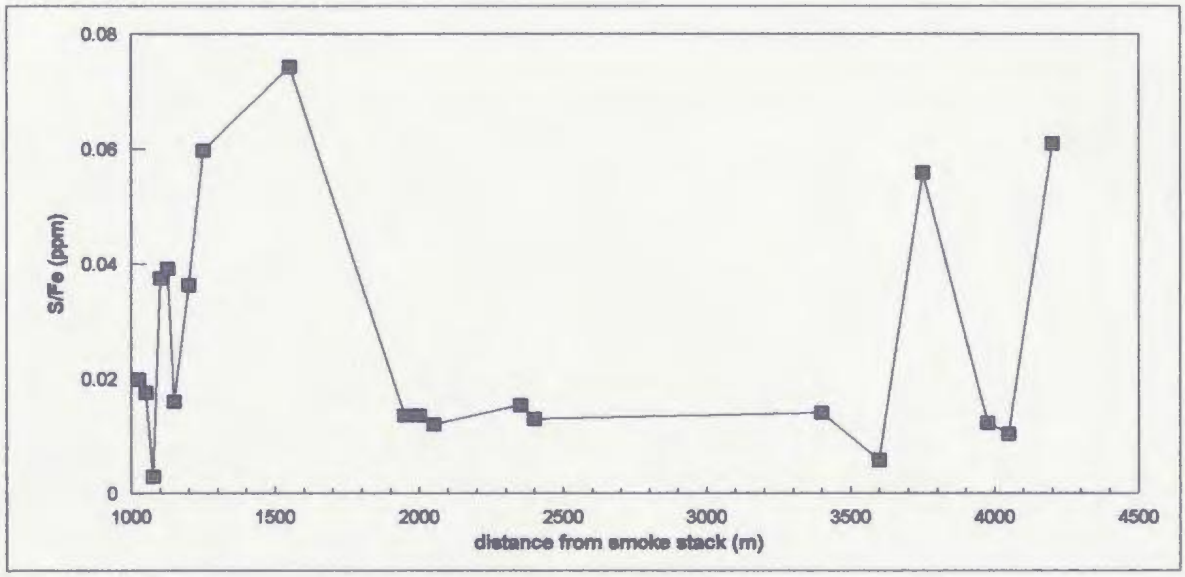

(b) Laser ablation

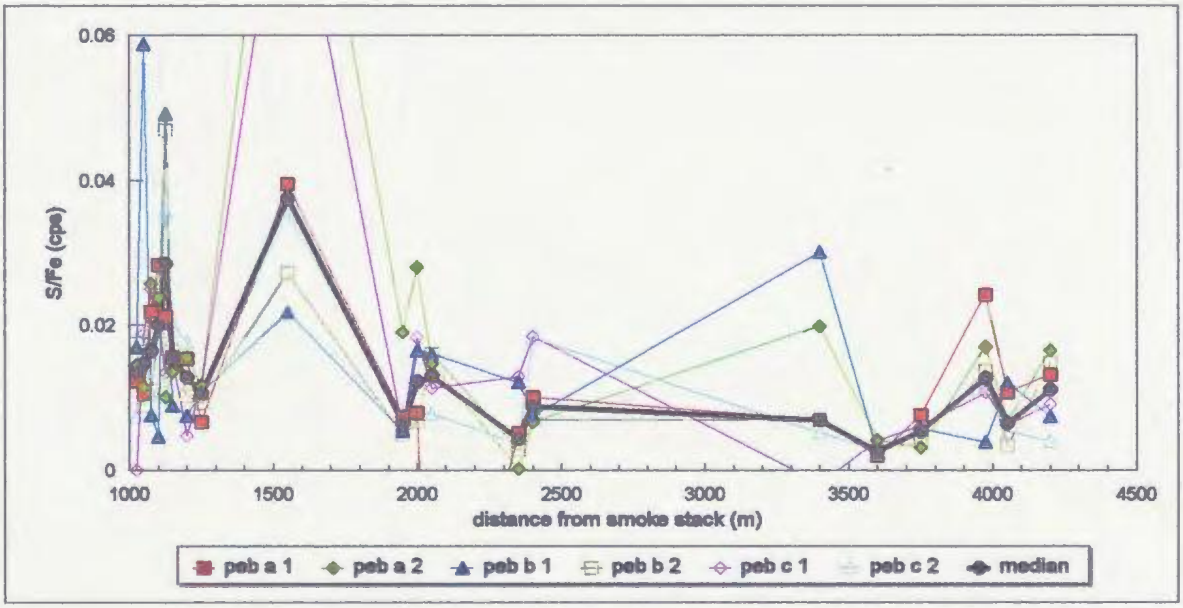

Figure 4.24: S (total) determined in the Mn-Fe-oxide coated stream pebbles collected from the network of streams in the Come-By-Chance oil refinery study area; the smoke stack is considered distance zero. (a) S/Fe (ppm) partial dissolution results from the pebble coatings and (b) S/Fe (cps) results from the laser ablation of the oxide coatings.

(a) Partial dissolution

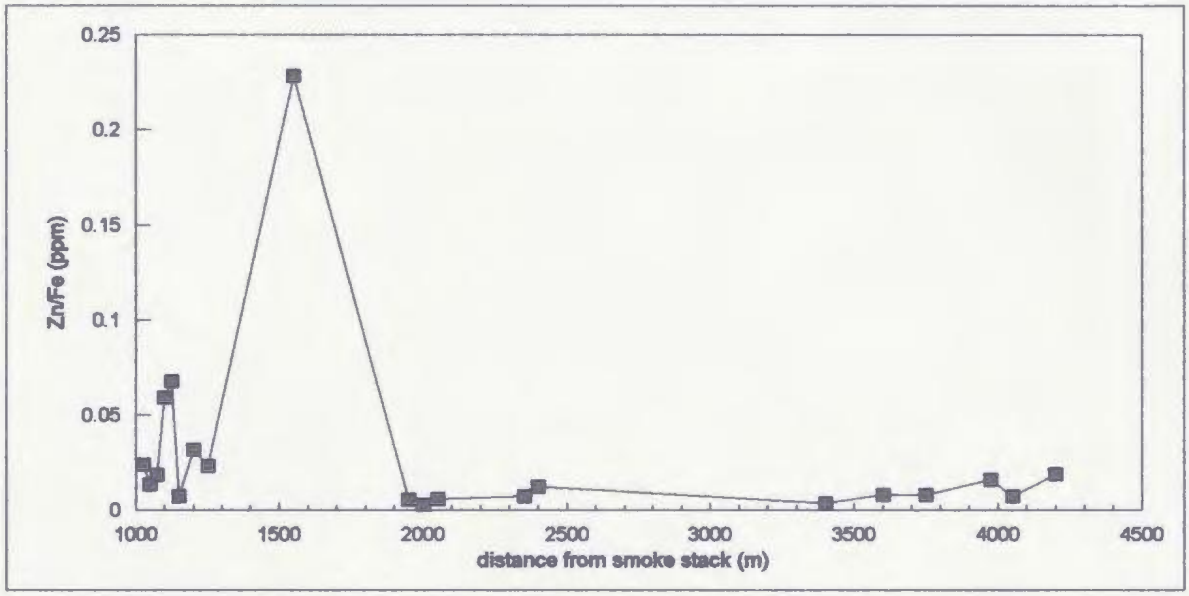

(b) Laser ablation

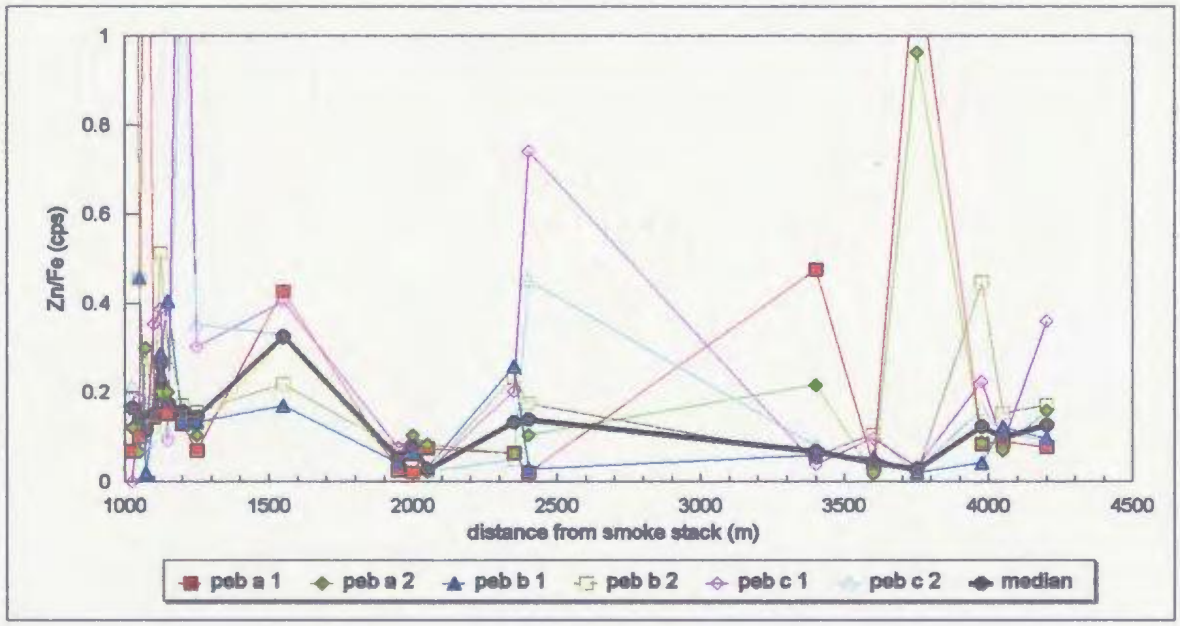

Figure 4.25: Zn determined in the Mn-Fe-oxide coated stream pebbles collected from the network of streams in the Come-By-Chance oil refinery study area; the smoke stack is considered distance zero. (a) Zn/Fe (ppm) partial dissolution results from the pebble coatings and (b) Zn/Fe (cps) results from the laser ablation of the oxide coatings.

(a) Partial dissolution

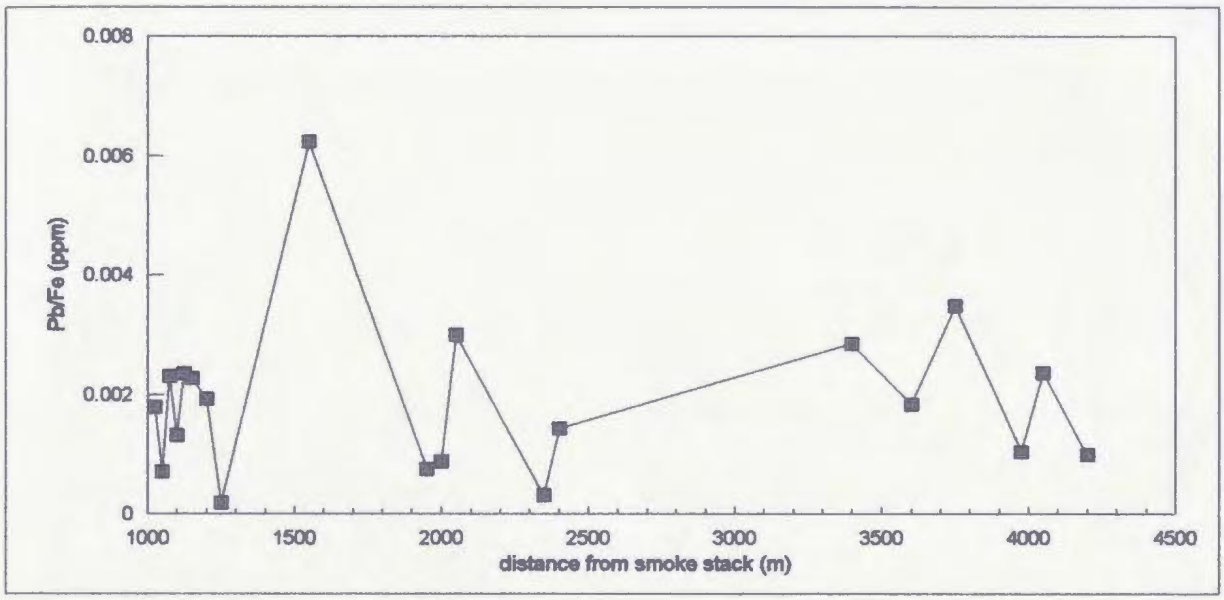

(b) Laser ablation

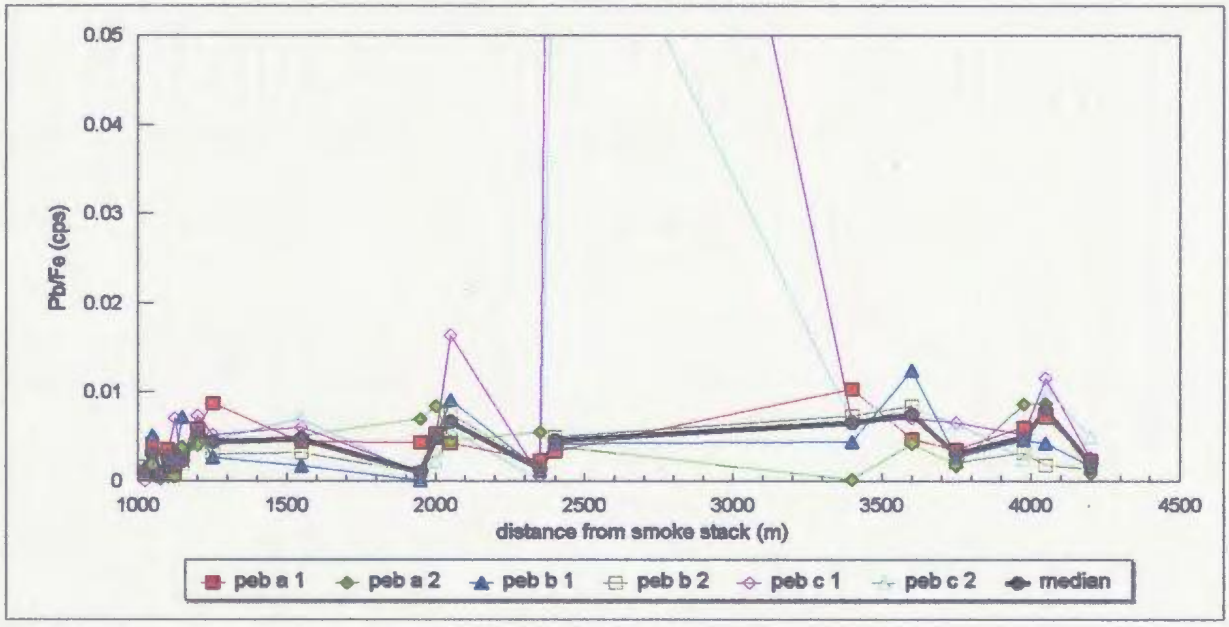

Figure 4.26: Pb determined in the Mn-Fe-oxide coated stream pebbles collected from the network of streams in the Come-By-Chance oil refinery study area; the smoke stack is considered distance zero. (a) Pb/Fe (ppm) partial dissolution results from the pebble coatings and (b) Pb/Fe (cps) results from the laser ablation of the oxide coatings.

to this elevated value on this particular stream pebble. The distribution pattern of Pb in the pebble coatings is most likely due to the local geology (shale, sandstone and siltstone) rather than contributions from the smoke stack emissions.

4.2.4.3 Summary

Emissions from the smoke stack at the Come-By-Chance oil refinery are presumed to be of the same composition as the inorganic material being burned and refined, which consists mainly of V, Ni and sulphate (H. Kelly, personal communication). The previously viewed graphs suggest that analysis of Mn-Fe-oxide coated stream pebbles in this study area is a viable method of environmental monitoring. The relevant elements discussed indicate that V, Ni, S and Zn are elevated near the smoke stack and decrease with increasing distance from it. This pattern is evident for both partial dissolution and laser ablation types of analysis.

CHAPTER 5: DISCUSSION

5.1 Introduction

The previous chapter presented and discussed the geochemical results from each study area. The following sections provide further insights into the applicability of using solution and solid sample analytical methods for determining the composition of Mn-Fe-oxide coatings on stream pebbles. These conclusions will be based on the similarity in presentation between the data sets and the ability of the selected elements to detect the mineralization or to point to the location of a potential pollutant source.

5.2 Water results

Stream water values of elements measured in the study areas are not really helpful for this project. In many cases, element concentrations are below the detection limit, and where values are more significant they fail to pass the analysis of variance F-test. Table 4.1 shows the statistical results for stream waters from the three study localities. The elements that have F-ratios ≥ 4, the general rule of thumb value (Garrett, 1973) that is used here, indicates that only Si, Ti, Mn, Fe, Co and Ba would be applicable for further discussion. Of this group, none of them are generally used as significant indicator elements in these types of mineral exploration or environmental monitoring programs. Therefore, stream water results are not presented or discussed in connection to detecting mineralization or a potential source of a pollutant.

The results presented in the previous chapter are not sufficient to conclusively say that ion concentrations in water are elevated or depleted depending on the amount of Mn and Fe concentrated as oxide coatings.

5.3 Results of the analyses of Mn-Fe-oxide stream pebble coatings

The previous chapter presented the analytical results graphically from the partial dissolution ICP-MS and LAM-ICP-MS of the Mn-Fe-oxide coated stream pebbles collected in the three study areas. As discussed, the elements shown are relevant to the individual study areas.

The Rocky Pond/Duder Lake field area concentrates on gold mineralization, more specifically the Stinger gold showing. The elements relevant in gold exploration that are presented here are Fe, Cu, Zn, As, Sb and Pb. Of these elements, Zn Sb, and Pb show elevated levels near and slightly downstream from the showing for both analytical procedures. The partial dissolutions of the oxide coatings indicate that As and Ba also depict the Au mineralization. In this study area, the partial dissolution analysis of the pebble coatings appears to be more reliable at depicting mineralization than analysis by laser ablation. The graphs of the elements analysed by the LAM-ICP-Ms procedure appears to indicate mineralization but not with the same intensity as the dissolution ICP-MS method. For this study area it would be more applicable to find Au using the partial dissolution method. Using Mn-Fe-oxide coated stream pebbles as a sampling medium is viable especially if solution ICP-MS analysis is the chosen method of analysis.

Base metal exploration in the Winter Hill study area focussed on using Cu, Pb, Zn, Ba, Mo, Fe and Mn as the ore and indicator minerals to locate Pb-Zn-Cu mineralization. Of these elements, Zn and Co show elevated levels near the base metal occurrence and decline with increasing distance from the showing for both analytical methods. Solution analysis of the pebble coatings indicate elevated Pb, Zn and Co values near the Winter Hill prospect. Only Zn and Co show a similar trend in the laser ablation presentations.

The graphical results presented in the previous chapter suggest that the Mn-Fe-oxide pebble coatings can be considered for base metal exploration but that analysis of the coatings would be best when using solution not the current LAM-ICP-MS procedure.

The Come-By-Chance oil refinery study was conducted to determined if the emissions from the smoke stack were impacting the surrounding environment and if so, the extent of that impact. Elements considered to be relevant to this type of environmental monitoring; V, Ni, Fe, Zn, Pb and S were graphically presented in the previous chapter. All of the elements shows some degree of enrichment within 1.5 to 2 km from the smoke stack. The partial dissolution procedure results have more strongly defined anomalies near the smoke stack than those observed from the laser ablation analysis of the pebble coatings. Even though small geochemical anomalies are visible in the laser ablation results they are very subtle when compared to the solution analysis of the same pebble coatings. It appears that once again the partial dissolution of the oxide pebble coatings is more effective at detecting anomalies than the laser ablation procedure.

5.4 Applicability of using Mn-Fe-oxide coatings as a sampling medium

The purpose of presenting leachate data as element/Fe ratios lessens the possibility of false anomalies due to the presence of excess Mn or Fe (Nicholson, 1992). This normalization of results against the Fe content of the oxide coatings can eliminate the appearance of a false enrichment. Nicholson (1992) states that since the Mn and Fe components have strong adsorption capabilities, trace element signatures are strongly dependent on the concentration of Mn and Fe in the pebble coatings. If there is abundant Mn and Fe in the oxide coating then the surface area is increased and adsorption of elements from the water column is elevated especially if the water is enriched in any of these elements. Therefore, if adsorption of the elements from the stream water is increased a notable geochemical signature can be detected giving rise to a false anomaly unless the elements in question can be in ratio to Fe, Mn or Mn plus Fe.

The idea that high concentrations of elements in the oxide coatings are due to higher concentrations of those elements in the stream waters is supported by experiments by Robinson (1981) and Whitney (1975). This observation by Robinson (1981) and Whitney (1975) could be considered in two different manners: (1) stream water concentrations could be depleted with adsorption of the elements onto the oxide coatings and (2) the concentrations in the water will remain high because higher concentrations in the stream water are required for the adsorption of the elements onto the coatings. For the adsorption process to continue there must be appreciable concentrations remaining in the stream water. Stabilization of the coating composition may occur and the adsorption process can stop but

this situation can quickly change with a change in pH or Eh (Chao, 1984). The previous section indicates that element concentrations in the stream water are somewhat depleted with adsorption of these elements onto the Mn-Fe-oxide coatings due to most elements being below the detection limit in the ICP-MS analysis of the stream water samples.

The purpose of this project is to determine the applicability of using Mn-Fe-oxide coated stream pebbles as a sampling medium for geochemical exploration. Overall, statistically the analysis of the coatings by digestion and laser ablation are good enough to show clear geochemical dispersion patterns in individual watersheds.

The current LAM-ICP-MS technique was not able to determine the relative amount of Mn in the oxide coatings so an alternative method was tried. The electron microprobe was able to quantatatitvity determine the amount of Mn present in the coatings. An experiment was conducted where the pebbles from two sample sites were analysed the same as they had been for the laser ablation method. Each pebble chip, three per site, was probed for Mn and Fe concentrations. The results were treated to determine a quantitative Mn value for the laser ablation method by ratioing the Mn and Fe concentrations from the probe data then cross multiplying with the Fe cps values from the laser. A Mn value was then derived based on the same ratio determined by the microprobe. Comparisons of the Mn to Fe ratios from the three analyses per sample site showed that there were large differences between the three pebbles per sample site. For example, sample site WH9417 have 0.2379, 0.0579 and 0.1251 as the Mn/Fe ratios and WH9418 have Mn/Fe ratios of 0.3807, 0.1916 and 0.0952. Based on the above results it was decided that further analysis using electron microprobe was not

warranted. Another factor was the small number of elements that passed the statistical analysis of variance for the individual studies.

The previously viewed results show that using Mn-Fe-oxide coated stream pebbles is a viable sampling medium. The current technology suggests that for now it would be best to use the partial dissolution ICP-MS analysis of the pebble coatings until high Mn concentrations can be detected and the volume of ablated material determined such that concentrations can be calculated for the elements analysed using LAM-ICP-MS.

5.5 Conclusions

Mn-Fe-oxide coated stream pebbles prove to be a viable sampling medium in gold and base metal mineral exploration and also for environmental monitoring. The previous graphical representations indicate that ore and indicator minerals can be depicted in anomalous amounts near the mineralized zone. In most cases the solution analyses of the oxide coatings show a more pronounced anomaly than the laser ablation results.

For the laser ablation of Mn-Fe-oxide coated stream pebbles to be more effective at detecting anomalies and for those levels to be more pronounced, a greater volume of coating must be ablated. Additional volumes of ablated material would be possible if the ablating time was increased and the stream pebbles analysed had thicker Mn-Fe-oxide coatings. It would make comparisons between data sets easier and more conclusive if concentration values in the ablated material could also be calculated.

Overall, the results presented for the different disciplines indicate that oxide coated

stream pebbles are a viable sampling medium but that at the current time, solution analysis would be more reliable and cost effective than using LAM-ICP-MS analysis of the same Mn-Fe-oxide coated stream pebbles.

REFERENCES

Arnott, R.J., McKerrow, W.S., and Cocks, L.R.M., 1985: The tectonics and depositional history of the Ordovician and Silurian rocks of Notre Dame Bay, Newfoundland. Canadian Journal of Earth Sciences, Volume 22, pages 607-618.

Blackwood, R.F., 1982: Geology of the Gander Lake (2D/15) and Gander River (2D/2) area. Newfoundland Department of Mines and Energy, Mineral Development Division, Report 82-4, 56 pages.

Butler, A.J. and Davenport, P.H., 1978: A lake sediment geochemical survey of the Meelpaeg Lake area, central Newfoundland. Newfoundland Department of Mines and Energy, Mineral Development Division, Open File No. 986.

Carpenter, R.H. and Hayes, W.B., 1978: Precipitation of iron, manganese, zinc and copper on clean, ceramic surfaces in a stream draining a poly-metallic sulfide deposit. In Journal of Geochemical Exploration, Volume 9, pages 31-37.

Chao, T.T., 1984: Use of partial dissolution techniques in geochemical exploration. Journal of Geochemical Exploration, vol. 20, pages 101-135.

Chao, T.T. and Theobald, Jr., P.K., 1976: The significance of secondary iron and manganese oxides in geochemical exploration. Economic Geology, vol. 71, pages 1560-1569.

Churchill, R.A., 1994: An integrated study of epigenetic gold mineralization, Duder Lake area, northeastern Newfoundland. Unpublished M.Sc. dissertation, Memorial University of Newfoundland, St. John's, Newfoundland, 233 p.

Churchill, R.A. and Evans, D.T.W., 1992: Geology and gold mineralization of the Duder Lake gold showings, eastern Notre Dame Bay, Newfoundland. In Current Research. Newfoundland Department of Mines and Energy, Geological Survey Branch, Report 92-1, pages 211-220.

Churchill, R.A., Wilton, D.H.C., and Evans, D.T.W., 1993: Geology, alteration assemblages and geochemistry of the Duder Lake gold showings, northeastern Newfoundland. In Current Research. Newfoundland Department of Mines and Energy, Geological Survey Branch, Report 93-1, pages 317-334.

Clark, J.R., 1992: Detection of bedrock-related geochemical anomalies at the surface of transported overburden. In Explore, number 76, pages 1-11.

Coish, D.W., 1993: Analysis of Mn and Fe coatings on stream pebbles by laser ablation microprobe-inductively coupled plasma mass spectrometer (LAM-ICP-MS): A tool for environmental monitoring and mineral exploration. Unpublished B.Sc (hons) dissertation, Memorial University of Newfoundland, St. John's, Newfoundland. 97 p.

Colman-Sadd, S. and Swinden, H.S., 1984: A tectonic window in Central Newfoundland? Geological evidence that the Appalachian Dunnage Zone may be allochthonous. Canadian Journal of Earth Sciences, Volume 21, pages 1349-1367.

Currie, K.L., 1993: Ordovician-Silurian stratigraphy between Gander Bay and Birchy Bay, Newfoundland. In Current Research, Part D; Geological Survey of Canada, Paper 93-1D, pages 11-18.

Davenport, P.H. and Nolan, L.W., 1988: Gold and associated elements in lake-sediment from regional surveys in the Botwood map area (NTS 2E).Newfoundland Department of Mines, Mineral Development Division. Open File 2E/563.

Dean, P.L., 1977: A report on the geology and metallogy of the Notre Dame Bay area, to accompany maps 12H/1,8,9 and 2E/3,4,5,6,7,8,9,10,11 and 12. Newfoundland Department of Mines and Energy, Mineral Development Division, Report 77-10, 17 pages.

Dean, P.L., 1978: The volcanic stratigraphy and metallogy of Notre Dame Bay, Newfoundland. Unpublished M.Sc. Thesis, Memorial University of Newfoundland, St. John's, Newfoundland, 205 pages.

Department of Environment, Government of Newfoundland & Labrador, Press Release, October 1995.

Evans, D.T.W., 1991: Gold metallogeny Eastern Dunnage Zone, Central Newfoundland. In Current Research. Newfoundland Department of Mines and Energy, Geological Survey Branch, Report 91-1, pages 310-318.

Evans, D.T.W., 1992: Gold mineralization in the eastern Dunnage Zone, Central Newfoundland. In Current Research. Newfoundland Department of Mines and Energy, Geological Survey Branch, Report 92-1, pages 339-349.

Evans, D.T.W., 1993: Gold metallogeny of the eastern Dunnage Zone, Central Newfoundland. In Current Research. Newfoundland Department of Mines and Energy, Geological Survey Branch, Report 93-1, pages 231-243.

Evans, D.T.W., 1996: Epigenetic Gold Occurrences, Eastern and Central Dunnage Zone, Newfoundland. Mineral Resource Report 9, Government of Newfoundland and Labrador, Department of Mines and Energy, Geological Survey, 135 pages.

Filipek, L.H., Chao, T.T. and Carpenter, R.H., 1981: Factors affecting the partitioning of Cu, Zn and Pb in boulder coatings and stream sediments in the vicinity of a polymetallic sulfide deposit. In Chemical Geology, Volume 33, pages 45-64.

Friel, J.K., Skinner, C.S., Jackson, S.E. and Longerich, H.P., 1990: Analysis of biological reference materials prepared by microwave digestion using inductively coupled plasma-mass spectrometry (ICP-MS). Analyst, vol. 115, pages 269-273.

Garrett, R.G., 1969: The determination of sampling and analytical errors in exploration geochemistry. Economic Geology, volume 64, pages 568-569.

Garrett, R.G., 1973: The determination of sampling and analytical errors in exploration geochemistry - a reply. Economic Geology, volume 68, pages 282-283.

Graves, G., 1985: Second year assessment report, Licence 2474, on diamond drilling at Winter Hill, NTS 1M/12. Unpublished Noranda Exploration Co. Ltd. report, 63 pages.

Graves, G., 1986: Report on diamond drilling, Licence 2474 and 2539, Hermitage and Frenchman Head claim groups, NTS 1M/12, Project No. 4A81. Unpublished Noranda Exploration Co. Ltd. report, 42 pages.

Green, K., 1989: First year assessment report on Licences 3411, 3429, 3449, 3453, 3493, 3494, 3502, 3503 and 3504. NTS 2D/15, 2E/2, 2E/7. Noranda Exploration Company, Confidential Report, 39 pages. [NFLD (1890)]

Greene, B.A. and O'Driscoll, C.F., 1976: Gaultois map area. Report of Activities, 1975, Newfoundland Department of Mines and Energy, Mineral Development Division, Report 75-1, pages 3-9.

Günther, D., Longerich, H.P., Forsythe, L. and Jackson, S.E., 1995: Laser ablation microprobe-inductively coupled plasma-mass spectrometry. American Laboratory, vol. 27, pages 24-29.

Hale, M., Thompson, M. and Wheatley, M.R., 1984: Laser ablation of stream-sediment pebble coatings for simultaneous multi-element analysis in geochemical exploration. Journal of Geochemical Exploration, vol. 21, pages 361-371.

Hofmann, H.J., Hill, J. and King, A.F., 1979: Late Precambrian microfossils, southeastern Newfoundland. Geological Survey of Canada, vol. 79 1B, pages 83-98.

Jackson, S.E., Longerich, H.P., Dunning G.R. and Fryer, B.J., 1992: The application of laser-ablation microprobe-inductively coupled plasma-mass spectrometry (LAM-ICP-MS) to insitu trace-element determinations in minerals. Canadian Mineralogist, vol. 30, pages 1049-1064.

Jacques Whitford Environment Limited, January 2000: Synthesis of Environmental Studies by North Atlantic Refining Limited.

Kiceniuk, J.W., 1992: Aromatic hydrocarbon concentrations in sediments of Placentia Bay, Newfoundland. Canadian technical report of fisheries and aquatic sciences, no. 1888, 12 pages.

King, A.F., 1982: Guidebook for Avalon and Meguma Zones of Atlantic Canada. IGCP Project 27, The Caledonide Orogen. Memorial University of Newfoundland, Department of Earth Sciences, Report 9.

Levin, R.I. and Rubin, D.S., 1991: Statistics for management. 5th ed., Englewood Cliffs, New Jersey, Prentice-Hall, Inc..

Longerich, H.P., Strong, D.F. and Kantipuly, C.J., 1986: Progress in evaluation of instrumental and other parameters affecting chemical and isotopic analysis by inductively coupled plasma-mass spectrometry (ICP-MS). Canadian Journal of Spectroscopy, vol. 31, no. 5, pages 111-121.

Lydon, J.W., 1988: Volcanogenic massive sulphide deposits. Part 2: Genetic models. Geoscience Canada, vol. 15, no. 1, pages 43-65.

Nicholson, K., 1992: Contrasting mineralogical-geochemical signatures of manganese oxides: Guides to metallogenesis. In Economic Geology, vol. 87, pages 1253-1264.

Nowlan, G.A., 1976: Concretionary manganese-iron oxides in streams and their usefulness as a sample medium for geochemical prospecting. Journal of Geochemical Exploration, vol. 6, pages 193-210.

O'Brien, S.J., O'Driscoll, C.F. and Tucker, R.D., 1992: A reinterpretation of the geology of parts of the Hermitage Peninsula, southwestern Avalon Zone, Newfoundland. In Current Research, Newfoundland Department of Mines and Energy, Geological Survey Branch, Report 92-1, pages 185-194.

O'Brien, S.J., Wardle, R.J. and King, A.F., 1983: The Avalon Zone: a Pan-African terrane in the Appalachian Orogen of Canada. Geological Journal, vol. 18, pages 195-222.

O'Brien, S.J., O'Driscoll, C.F., Greene, B.A. and Tucker, R.D., 1995: Pre-Carboniferous geology of the Connaigre Peninsula and the adjacent coast of Fortune Bay, southern Newfoundland. Current Research, Newfoundland Department of Natural Resources, Geological Survey, Report 95-1, pages 267-297.

O'Driscoll, C.F., 1977: Geology, petrology and geochemistry of the Hermitage Peninsula, southern Newfoundland. Unpublished M.Sc., Memorial University of Newfoundland, 144 pages.

O'Driscoll, C.F. and Muggridge, W.W., 1979: Geology of Merasheen (1M/8) and Harbour Buffett (1M/9 E1/2), Newfoundland. Report of Activities for 1978, Mineral Development Division, Department of Mines and Energy, Government of Newfoundland and Labrador, Report 79-1, pages 82-89.

O'Driscoll, C.F. and Strong, D.F., 1979: Geology and geochemistry of the late Precambrian volcanic and intrusive rocks of southwestern Avalon Zone in Newfoundland. Precambrian Research, vol. 8, pages 19-48.

Papezik, V.S., 1972: Late Precambrian ignimbrites in eastern Newfoundland and their tectonic significance. In Proceedings of the 24th International Geological Congress, Montreal, Section 1, pages 147-152.

Piasecki, M.A.J., 1993: Tectonics along the Dog Bay Line - a Silurian terrane boundary in northeastern Newfoundland. In current Research, Part E; Geological Survey of Canada, Paper 93-1E, pages 291-298.

Plant, J., Jeffery, E.G. and Fage, C., 1975: The systematic determination of accuracy and precision in geochemical exploration data. Journal of Geochemical Exploration, vol. 4, pages 467-486.

Rast, N., O'Brien, B.H. and Wardle, R.J., 1976: Relationships between Precambrian and lower Paleozoic rocks of the Avalon Platform in New Brunswick, the northeastern Appalachians and the British Isles. Tectonophysics, Volume 30, pages 315-338.

Robinson, G.D., 1981: Adsorption of Cu, Zn and Pb near sulfide deposits by hydrous manganese-iron oxide coatings on stream alluvium. In Chemical Geology, Volume 33, pages 65-79.

Robinson, G.D., 1984: Sequential chemical extractions and metal partitioning in hydrous Mn-Fe-oxide coatings: reagent choice and substrate composition affect results. Chemical Geology, vol. 47, pages 97-112.

Sears, W.A., 1990: A geochemical, petrographic, and metallogenic analysis of volcanogenic sulphide deposition within the Connaigre Bay Group, Hermitage Peninsula, southern Newfoundland. Unpublished M.Sc. thesis, Memorial University of Newfoundland, 282 pages.

Sears, W.A. and O'Driscoll, C.F., 1989: Metallogeny of the Connaigre Bay Group, Southwestern Newfoundland. In Current Research, Newfoundland Department of Mines and Energy, Geological Survey of Newfoundland, Report 89-1, pages 193-199.

Sears, W.A. and Wilton, D.H.C., 1995: Reinterpretation of the Avalon Zone, southern Newfoundland, as a complex arc terrane through identification of base metal massive sulphide deposits at the Winter Hill and Frenchman Head Prospects, unpublished report, Memorial University of Newfoundland.

Sheppard Green Engineering and Associates Limited in association with G.R. Ringius and Associates, June 1996; Terrestrial effects monitoring of SO_2 impact on vegetation, soil and surface water in the near vicinity of North Atlantic Refining Limited at Come-By-Chance, Newfoundland.

Simpson, A., 1990: Sixth year assessment report on diamond drilling, Hermitage (6602) Licence 2474 NTS 1M/12. Unpublished Noranda Exploration Company, Ltd. report, file no. 1M/12 (320).

Swinden, H.S., 1991: Paleotectonic settings of volcanogenic massive sulphide deposits in the Dunnage Zone, Newfoundland Appalachians. CIM Bulletin, vol. 84, no. 946, pages 59-69.

Swinden, H.S. and Hunt, P.A., 1991: A U-Pb zircon age from the Connaigre Bay Group, southwestern Avalon Zone, Newfoundland: implications for regional correlations and metallogenesis. In Radiogenic Age and Isotopic Studies: Report 4, Geological Survey of Canada, Paper 90-2, pages 3-10.

Tallman, P., 1990: Second year assessment report on geological and diamond drilling exploration for the Noranda/Noront GRUB Line North Project for licence 3989 on claim blocks 6077, 6080-6081, 7184 and 7187-7188 in the Duder Lake area, Newfoundland (6721). NTS 2E/2 and 2E/7. Noranda Exploration Company Limited, Confidential Report, 50 pages. [2E/02(0744)]

Tallman, P., 1994: A proposal for diamond drill testing of the goldstash showing Duder Lake property, north-central Newfoundland. NTS 2E/07. Noront Resources Limited, 11 pages.

Thompson, M., Hale, M. and Coles, B., 1992: Geochemical reconnaissance using stream-sediment pebble coatings and laser ablation ICP-AES. In Trans. Instn Min.Metall. (Section B: Applied earth science), 101, pages B9-14.

Whitney, P.R., 1975: Relationship of manganese-iron oxides and associated heavy metal to grain size in stream sediments. Journal of Geochemical Exploration, vol.4, pages 251-263.

Williams, H., 1971: geology of the Belleoram map area, Newfoundland (1M/11). Geological Survey of Canada, Paper 70-65, 39 pages.

Williams, H., 1972: Stratigraphy of the Botwood map area, northeastern Newfoundland. Geological Survey of Canada, Open File 113, 103 pages.

Williams, H., 1978b: Geological development of the northern Appalachians: its bearing on the evolution of the British Isles. In Bowes, D.R., and Leake, B.E. (eds.), Crustal evolution in northwestern Britain and adjacent regions. Geological Journal, Special Issue No. 10, pages 1-22.

Williams, H., 1979: Appalachian orogen in Canada. Canadian Journal of Earth Sciences, vol. 16, pages 792-807.

Williams, H., 1993: Stratigraphy and structure of the Botwood belt and definition of the Dog Bay Line in northeastern Newfoundland. In Current Research, Part D; Geological Survey of Canada, Paper 93-1D, pages 19-27.

Williams, H., Colman-Sadd, S.P. and Swinden, H.S., 1988: Tectonic-stratigraphic subdivisions of central Newfoundland. In Current Research, Part B, Geological Survey of Canada, Paper 88-1B, pages 91-98.

Williams, H., Currie, K.L. and Piasecki, M.A.J., 1993: The Dog Bay Line: a major Silurian boundary in northeast Newfoundland. Canadian Journal of Earth Sciences, vol.30, pages 2481-2494.

Vitol information pamphlet, North Atlantic Refining, North Atlantic Refining Limited, 1995.

APPENDIX 1

STREAM WATER GEOCHEMICAL ANALYSES

dp indicates duplicate of sample; - indicates below detection limit.

ppb	dc-94-1	dc-94-2	dc-94-3	dc-94-4	dc-94-5	dc-94-5dp	dc-94-6
Si	152	151	153	154	144	153	148
S	-	-	-	-	-	-	-
Cl	2306	2325	2296	2345	2156	2458	2239
Ti	-	-	-	-	-	-	-
V	0.06	0.06	0.05	-	0.05	-	0.05
Mn	4.7	4.7	4.5	4.6	4.3	4.3	4.7
Fe	-	-	-	-	-	-	-
Co	-	0.01	-	-	-	-	-
Ni	-	-	-	-	-	-	-
Cu	-	-	-	-	-	-	-
Zn	0.6	0.7	0.7	0.3	0.3	0.5	0.5
As	0.5	0.5	0.4	0.4	0.4	0.4	0.5
Se	-	-	-	-	-	-	-
Mo	0.03	0.02	0.02	0.02	0.02	0.03	0.03
Ag	-	-	-	-	-	-	-
Cd	-	-	-	-	-	-	-
Sb	0.04	0.04	0.04	0.04	0.04	0.03	0.04
Ba	1.3	1.1	1.2	1.1	1.2	1.1	1.2
Hg	-	-	-	-	-	-	-
Pb	-	-	-	-	-	-	-
Bi	-	-	-	-	-	-	-
U	-	-	-	-	-	0.02	-

Appendix 1: (continued)

ppb	dc-94-7	dc-94-8a	dc-94-8b	dc-94-8c	dc-94-8d	dc-94-9	dc-94-10
Si	146	152	149	154	152	147	150
S	-	-	-	-	-	-	-
Cl	2366	2282	2256	2300	2289	2205	2182
Ti	-	-	-	-	-	-	-
V	0.05	-	-	-	-	-	0.05
Mn	4.0	4.1	4.3	4.3	4.3	4.2	4.3
Fe	-	-	-	-	-	-	-
Co	0.00	-	-	-	-	0.01	-
Ni	-	-	-	-	-	-	-
Cu	-	-	-	-	-	-	-
Zn	0.4	0.5	0.6	0.7	0.5	1.2	0.6
As	0.4	0.5	0.5	0.5	0.5	0.5	0.5
Se	-	-	-	-	-	-	-
Mo	0.04	0.04	0.03	0.03	0.04	0.03	0.02
Ag	-	-	-	-	-	-	-
Cd	-	-	-	-	-	-	-
Sb	0.04	0.04	0.03	0.03	0.03	0.04	0.03
Ba	1.1	1.2	1.1	1.2	1.0	1.1	1.1
Hg	-	-	-	0.09	-	-	-
Pb	-	-	-	-	-	-	-
Bi	-	-	-	-	0.02	-	-
U	-	-	0.04	-	0.02	-	-

Appendix 1: (continued)

ppb	dc-94-10dp	dc-94-11	dc-94-12	dc-94-13	dc-94-14	dc-94-15	dc-94-15dp
Si	144	157	134	134	135	136	138
S	-	-	-	-	-	-	-
Cl	2170	2278	2206	2307	2171	2150	2313
Ti	-	-	-	-	-	-	-
V	0.05	-	-	0.05	0.05	0.05	0.05
Mn	4.2	4.5	4.7	3.9	3.9	5.0	4.3
Fe	-	-	-	-	-	-	-
Co	-	0.01	0.01	-	-	0.00	-
Ni	-	0.5	-	-	-	-	-
Cu	-	-	-	-	-	-	-
Zn	9.4	0.9	1.3	0.6	0.4	-	0.5
As	0.4	0.5	0.4	0.5	0.5	0.5	0.5
Se	-	-	-	-	-	-	-
Mo	0.03	0.03	0.04	0.03	0.03	0.04	0.03
Ag	-	-	-	-	-	-	-
Cd	-	-	-	-	-	-	-
Sb	0.03	0.05	0.04	0.04	0.04	0.05	0.02
Ba	1.2	1.1	1.2	1.2	1.2	1.1	1.2
Hg	-	-	-	-	-	-	-
Pb	-	-	-	-	-	-	-
Bi	-	-	-	-	-	-	-
U	0.04	-	-	-	-	0.04	-

Appendix 1: (continued)

ppb	dc-94-16	dc-94-17	dc-94-18	dc-94-19	dc-94-20	dc-94-20dp	dc-94-21
Si	136	142	140	151	147	142	151
S	-	-	-	-	-	-	-
Cl	2260	2266	2228	2284	2281	2162	2205
Ti	-	-	-	0.3	0.2	-	-
V	0.05	0.05	0.09	-	0.07	0.05	-
Mn	3.5	3.5	3.6	3.6	3.7	3.7	4.0
Fe	-	-	-	-	-	-	-
Co	-	-	-	-	-	-	-
Ni	-	-	-	-	-	-	-
Cu	-	-	-	-	-	-	-
Zn	0.7	0.6	0.7	0.5	0.5	0.4	0.3
As	0.5	0.5	0.5	0.5	0.5	0.5	0.5
Se	-	-	-	-	-	-	-
Mo	0.02	0.03	0.03	0.03	0.03	0.02	0.04
Ag	-	-	-	-	-	-	-
Cd	-	-	-	-	-	-	-
Sb	0.03	0.03	0.04	0.03	0.03	0.03	0.03
Ba	1.2	1.1	1.2	1.2	1.1	1.2	1.3
Hg	-	-	-	0.08	-	-	-
Pb	-	-	-	-	-	-	-
Bi	-	-	-	-	-	-	-
U	-	-	-	0.03	0.03	-	0.06

Appendix 1: (continued)

ppb	dc-94-22	dc-94-23	dc-94-24	dc-94-24dp	dc-94-25	dc-94-25dp	dc-94-26
Si	145	152	157	501	152	153	151
S	-	-	-	-	-	-	-
Cl	2158	2273	2418	4148	2199	2298	2279
Ti	-	-	0.2	0.3	-	0.3	-
V	0.05	0.05	-	0.15	0.05	-	0.05
Mn	3.8	3.6	4.3	3.0	3.6	3.5	3.5
Fe	-	-	-	-	-	-	-
Co	0.01	-	-	0.01	-	-	-
Ni	-	-	-	-	-	-	-
Cu	-	-	-	-	-	-	-
Zn	1.6	1.0	0.3	11.4	0.7	0.6	1.0
As	0.5	0.5	0.5	-	0.5	0.5	0.5
Se	-	-	-	-	-	-	-
Mo	0.04	0.02	0.03	0.03	0.03	0.03	0.04
Ag	-	-	-	-	-	0.01	-
Cd	-	-	-	0.06	-	-	-
Sb	0.05	0.03	0.03	0.01	0.04	0.04	0.03
Ba	1.2	1.1	1.0	1.4	1.1	1.1	1.2
Hg	-	-	-	-	-	-	-
Pb	-	-	-	0.14	-	-	-
Bi	-	-	-	-	-	-	-
U	0.04	-	0.02	-	-	-	-

Appendix 1: (continued)

ppb	dl-94-01	dl-94-02	dl-94-02dp	wh-94-1	wh-94-1dp	wh-94-2	wh-94-3
Si	202	199	201	458	442	409	399
S	-	-	-	-	-	-	-
Cl	4292	4167	4292	3829	3618	3592	3845
Ti	-	-	-	0.4	0.7	0.7	0.6
V	-	0.1	0.1	0.2	0.2	0.2	0.2
Mn	4.5	4.7	4.8	1.5	1.6	1.8	1.8
Fe	-	-	-	-	-	60	-
Co	-	-	-	0.02	-	0.02	0.02
Ni	-	-	-	-	-	-	-
Cu	-	-	-	-	-	-	-
Zn	0.5	0.2	0.8	3.3	2.8	2.8	3.9
As	0.3	0.3	0.3	0.1	0.1	-	-
Se	-	-	-	-	-	-	-
Mo	0.02	0.03	0.01	0.09	0.10	0.08	0.10
Ag	-	-	-	-	-	-	-
Cd	-	-	-	-	-	0.04	-
Sb	0.03	0.02	0.04	0.02	0.02	-	0.01
Ba	2.8	2.5	2.8	2.2	2.3	2.2	2.1
Hg	-	-	-	-	-	-	-
Pb	-	-	-	0.1	0.1	0.1	0.1
Bi	-	0.02	-	-	-	-	-
U	0.03	0.03	-	0.03	0.04	0.10	-

Appendix 1: (continued)

ppb	wh-94-4	wh-94-5	wh-94-5dp	wh-94-6	wh-94-7	wh-94-8	wh-94-9
Si	442	429	430	428	289	289	274
S	-	-	-	-	-	-	-
Cl	3779	3820	3652	3623	3392	3511	3419
Ti	0.7	0.7	0.7	0.6	0.3	0.6	0.5
V	0.2	0.2	0.2	0.2	0.2	0.2	0.2
Mn	1.8	1.9	1.9	1.9	1.9	2.1	2.2
Fe	-	-	-	-	-	-	-
Co	0.02	0.03	0.02	0.03	0.02	0.02	0.02
Ni	-	-	-	-	-	-	-
Cu	-	-	-	-	-	-	-
Zn	5.0	3.9	4.6	3.7	7.8	4.8	5.3
As	0.1	-	0.1	0.1	-	0.1	-
Se	0.8	-	-	-	-	-	-
Mo	0.1	0.1	0.1	0.1	0.1	0.1	0.1
Ag	-	-	-	-	-	-	-
Cd	-	-	-	0.04	-	0.04	-
Sb	0.02	0.02	0.03	0.01	-	0.03	0.03
Ba	2.3	1.9	2.1	2.2	1.4	1.4	1.2
Hg	-	-	-	-	-	-	-
Pb	0.2	0.1	0.2	0.1	0.1	0.1	0.1
Bi	-	-	-	-	-	-	-
U	0.06	-	-	-	-	-	-

Appendix 1: (continued)

ppb	wh-94-10	wh-94-10dp	wh-94-11	wh-94-12	wh-94-13	wh-94-14	wh-94-15
Si	271	274	270	289	294	299	377
S	-	-	-	-	-	-	-
Cl	3362	3378	3123	3377	3461	3420	3774
Ti	0.5	0.5	0.5	0.5	0.4	0.4	0.3
V	0.2	0.3	0.2	0.2	0.2	0.1	0.2
Mn	2.3	2.9	2.4	2.5	2.4	2.1	1.9
Fe	-	117	-	-	-	-	-
Co	-	0.03	0.02	0.03	0.02	0.01	-
Ni	-	-	-	-	-	-	-
Cu	-	-	-	-	-	-	-
Zn	4.5	5.0	5.0	4.7	4.5	5.2	6.3
As	0.1	-	-	-	0.1	-	0.1
Se	-	-	-	-	-	-	-
Mo	0.1	0.1	0.1	0.1	0.1	0.1	0.1
Ag	-	-	-	-	-	-	-
Cd	-	-	-	-	-	-	0.05
Sb	0.03	0.04	0.26	0.02	0.02	0.02	0.02
Ba	1.4	1.2	1.2	1.2	1.3	1.1	1.1
Hg	-	-	-	-	-	-	-
Pb	0.1	0.2	0.1	0.1	0.1	8.0	0.1
Bi	-	-	-	-	-	-	-
U	-	0.05	-	-	-	-	-

Appendix 1: (continued)

ppb	wh-94-15dp	wh-94-16	wh-94-17	wh-94-18	wh-94-19	wh-94-20	wh-94-20dp
Si	386	403	455	486	511	486	496
S	-	-	-	-	-	-	-
Cl	3738	3798	3759	3869	3878	3736	3781
Ti	0.4	0.3	-	0.4	0.3	-	0.4
V	0.1	0.1	0.1	0.2	0.1	0.1	0.1
Mn	1.9	2.2	2.6	3.1	3.6	3.8	3.8
Fe	-	-	-	-	-	-	-
Co	-	-	0.02	0.01	0.03	0.03	0.02
Ni	-	-	-	-	-	-	-
Cu	-	-	-	-	-	-	-
Zn	6.6	6.2	7.5	7.2	7.8	7.8	8.7
As	0.08	0.07	-	-	0.13	-	-
Se	-	-	-	-	-	-	-
Mo	0.09	0.09	0.09	0.09	0.09	0.05	0.06
Ag	-	-	-	-	-	-	-
Cd	0.06	0.41	-	-	0.07	-	0.05
Sb	0.01	0.03	0.02	-	0.01	0.01	-
Ba	1.2	1.1	1.2	1.3	1.2	1.1	1.2
Hg	0.11	-	-	-	-	-	-
Pb	0.1	0.1	0.1	0.1	0.1	0.1	0.2
Bi	-	-	-	-	-	-	-
U	-	0.02	-	-	-	-	-

Appendix 1: (continued)

ppb	wh-94-21	wh-94-22	wh-94-23	wh-94-24	hb-94-1	hb-94-2	hb-94-02dp
Si	497	505	482	500	551	486	484
S	-	-	-	-	-	-	-
Cl	3876	3641	3974	4025	8926	8749	8662
Ti	0.5	0.4	-	0.2	0.9	0.8	0.9
V	0.1	0.1	0.2	0.1	0.2	0.2	0.2
Mn	3.7	3.8	2.9	2.9	5.5	9.9	10.3
Fe	-	-	-	-	74	94	82
Co	0.03	0.02	0.02	0.02	0.01	0.03	0.03
Ni	-	-	-	-	-	-	-
Cu	-	-	-	-	-	-	-
Zn	7.7	7.5	10.4	10.7	1.2	0.7	0.6
As	0.1	-	0.1	0.1	-	0.1	0.1
Se	-	-	-	-	-	-	-
Mo	0.05	0.04	0.06	0.04	0.12	0.12	0.13
Ag	-	-	-	-	-	-	-
Cd	-	-	0.11	0.07	-	-	-
Sb	0.02	-	0.02	0.01	0.02	0.02	0.02
Ba	1.2	1.3	1.6	1.5	2.2	2.2	2.2
Hg	-	-	-	-	-	-	-
Pb	0.12	0.19	0.18	0.15	-	-	-
Bi	-	-	-	-	-	-	-
U	-	-	-	-	0.07	-	-

Appendix 1: (continued)

ppb	hb-94-3	ss-95-01	ss-95-01dp	ss-95-02	ss-95-02dp	ss-95-03	ss-95-04
Si	474	686	699	365	356	190	188
S	-	-	-	-	-	-	-
Cl	8593	13652	13489	8899	8608	9259	9118
Ti	0.7	0.9	0.6	0.9	1.1	-	-
V	0.2	0.2	0.2	0.1	0.2	-	0.4
Mn	6.2	148.5	147.6	31.3	31.3	26.1	25.6
Fe	69	110	114	40	38	93	95
Co	0.03	0.08	0.05	0.04	0.04	0.01	-
Ni	-	0.3	0.4	-	-	-	-
Cu	-	0.1	0.1	-	-	-	-
Zn	0.6	1.6	1.9	0.7	0.5	0.6	-
As	0.1	0.2	-	-	-	0.2	-
Se	-	-	-	-	-	-	-
Mo	0.11	-	-	0.07	-	-	-
Ag	-	-	-	-	-	-	-
Cd	-	-	-	-	-	-	-
Sb	0.03	-	-	0.04	-	0.02	-
Ba	2.2	11.4	11.1	9.4	9.5	4.2	3.8
Hg	-	-	-	-	-	-	-
Pb	-	-	-	-	0.13	-	-
Bi	-	-	-	-	-	-	-
U	0.05	-	-	-	-	-	-

Appendix 1: (continued)

ppb	ss-95-04dp	ss-95-05	ss-95-05dp	ss-95-06	ss-95-06dp	ss-95-07	ss-95-08
Si	185	197	184	136	140	122	108
S	-	-	-	-	-	-	-
Cl	9226	9531	9462	4660	4510	4162	4283
Ti	0.9	-	-	1.4	1.2	1.1	1.3
V	0.3	-	-	0.8	0.7	-	-
Mn	25.9	31.7	31.1	18.9	18.9	19.7	16.0
Fe	92	99	98	459	465	395	357
Co	-	0.01	-	0.05	0.04	0.06	0.04
Ni	0.2	-	-	0.3	0.2	0.2	0.2
Cu	-	-	-	-	-	-	-
Zn	0.6	0.4	0.5	1.0	0.5	0.7	0.6
As	0.2	0.1	0.2	0.7	0.5	0.4	0.4
Se	-	-	-	-	-	-	-
Mo	-	-	0.04	-	0.04	0.05	0.05
Ag	-	-	-	-	-	-	-
Cd	-	-	-	-	-	-	-
Sb	-	0.01	-	-	-	0.02	0.02
Ba	3.8	3.8	3.8	1.6	1.6	1.7	1.7
Hg	-	-	-	-	-	-	-
Pb	-	-	-	0.2	0.1	0.1	0.1
Bi	0.05	-	-	0.07	-	-	-
U	-	-	-	-	-	-	-

Appendix 1: (continued)

ppb	ss-95-08dp	ss-95-09	ss-95-09dp	ss-95-10	ss-95-11	ss-95-11dp	ss-95-12
Si	108	339	342	252	215	240	354
S	-	-	-	-	-	3212	3344
Cl	4435	4491	4480	4486	6927	7847	7145
Ti	1.1	1.3	1.4	1.6	-	-	-
V	0.6	-	-	0.7	-	0.3	-
Mn	16.3	82.4	81.7	30.2	8.0	9.2	155.9
Fe	352	591	608	582	-	-	169
Co	0.05	0.11	0.11	0.06	-	-	0.04
Ni	-	-	0.2	0.2	-	-	-
Cu	-	-	-	-	-	0.4	-
Zn	6.4	0.8	0.5	0.7	-	-	0.9
As	0.5	0.6	0.6	0.8	-	0.2	0.2
Se	-	-	-	-	-	-	-
Mo	0.05	-	0.03	0.06	0.03	-	0.05
Ag	-	-	-	-	-	-	-
Cd	-	-	-	-	-	-	-
Sb	-	0.04	0.02	-	0.04	0.05	0.02
Ba	1.8	1.8	1.8	1.8	46.1	46.8	22.3
Hg	-	-	-	-	0.15	-	-
Pb	0.2	0.1	0.2	0.2	-	-	-
Bi	-	0.08	-	-	-	-	-
U	-	-	-	-	0.02	-	-

Appendix 1: (continued)

ppb	ss-95-13	ss-95-13dp	ss-95-14	ss-95-15	ss-95-15dp	ss-95-16	ss-95-17
Si	217	227	203	119	117	168	203
S	2226	3353	3194	-	-	-	-
Cl	7595	7516	7614	26762	25744	26889	26695
Ti	-	-	0.7	0.7	1.0	0.8	0.8
V	0.3	-	0.3	-	-	0.2	-
Mn	59.9	58.5	78.9	14.7	14.6	66.4	15.9
Fe	110	107	79	231	225	269	253
Co	-	0.03	-	-	0.02	0.05	-
Ni	0.3	-	-	-	-	-	-
Cu	-	-	-	-	-	-	-
Zn	0.3	0.4	1.3	0.8	0.6	0.7	0.6
As	0.2	-	0.2	0.3	0.2	0.4	0.3
Se	-	-	-	-	-	-	-
Mo	0.05	0.07	0.05	0.05	0.03	0.05	0.07
Ag	-	-	-	-	-	-	-
Cd	-	-	-	-	-	-	-
Sb	-	0.01	0.03	-	0.04	-	0.03
Ba	22.8	22.9	22.8	8.3	8.0	8.4	7.8
Hg	-	0.2	-	-	0.2	-	-
Pb	-	-	-	-	0.1	0.1	-
Bi	-	-	0.06	-	-	-	-
U	-	-	-	-	-	-	-

Appendix 1: (continued)

ppb	ss-95-17dp	ss-95-18	ss-95-18dp	ss-95-19	ss-95-20	ss-95-20dp
Si	200	881	899	428	399	409
S	-	-	-	-	-	-
Cl	24703	21903	21334	11410	11131	11272
Ti	-	1.6	0.9	0.7	0.5	1.0
V	-	0.4	-	0.2	0.3	0.3
Mn	15.7	82.3	80.1	39.1	27.9	28.7
Fe	248	396	413	202	221	217
Co	0.03	0.08	0.08	-	0.04	0.04
Ni	-	0.2	-	-	-	0.2
Cu	-	-	-	-	-	-
Zn	0.4	2.5	3.8	0.2	0.4	3.1
As	0.3	0.3	0.5	0.2	0.3	0.3
Se	-	-	-	-	-	-
Mo	0.03	0.04	0.04	0.03	-	-
Ag	-	-	-	-	-	-
Cd	-	-	-	-	-	-
Sb	0.02	-	0.02	-	-	-
Ba	8.1	14.5	14.1	6.4	5.7	5.6
Hg	-	-	-	-	-	-
Pb	0.1	0.1	0.1	-	0.1	0.1
Bi	-	0.05	-	-	-	-
U	-	-	-	-	0.07	-

APPENDIX 11

MN-FE-OXIDE COATING GEOCHEMICAL ANALYSES

Appendix 11a: Geochemical analyses by partial dissolution.

dp represents sample duplicate; - indicates below detection limit; A,B,C,D indicates other individual pebbles from that sample location were also analysed.

ppm	dc-94-1	dc-94-1 dp	dc-94-2	dc-94-2 dp	dc-94-3	dc-94-3 dp
Si	275	156	799	1369	364	1473
S	-	-	-	-	-	-
Ti	39	19	80	150	37	28
V	9	11	23	29	15	22
Mn	195301	143894	101059	57347	209558	153999
Fe 57	8323	10429	14431	17526	15522	21187
Co	69	103	72	62	136	163
Ni	240	191	119	77	298	228
Cu	14	16	26	12	126	158
Zn	1199	1212	631	484	1713	1377
As	177	225	101	101	257	242
Se	-	-	-	-	-	1.5
Mo	17	8	1	1	8	6
Ag	0.03	0.02	0.06	0.09	0.16	0.10
Cd	15	12	7	5	20	12
Sb	1.0	1.1	0.2	0.2	1.0	0.8
Ba	6485	4377	2261	2142	5840	4504
Hg	-	-	-	-	-	-
Tl	4.3	4.3	1.7	1.4	4.8	2.9
Pb	36	32	79	65	77	89
Bi	0.06	0.07	0.15	0.17	0.35	0.45
U	7.1	0.8	2.5	3.2	1.5	3.0

Appendix 11a: Geochemical analyses by partial dissolution (continued)

ppm	dc-94-4	dc-94-5	dc-94-5 dp	dc-94-6	dc-94-7	dc-94-7 dp
Si	767	1946	1589	757	896	617
S	-	-	-	-	-	-
Ti	28	54	85	52	67	43
V	13	17	13	12	15	10
Mn	149691	137734	129815	161389	95077	68449
Fe57	20758	23231	18987	13839	15448	13038
Co	321	217	156	129	275	205
Ni	343	190	263	293	207	204
Cu	127	131	166	119	81	20
Zn	1240	1023	1045	1744	701	1163
As	220	166	178	312	262	216
Se	1.6	1.8	-	-	-	-
Mo	6	3	3	14	5	5
Ag	0.09	0.56	0.14	0.11	0.10	0.08
Cd	15	12	12	19	7	9
Sb	1.3	4.3	15.8	1.0	4.8	5.0
Ba	4769	3108	3631	4757	2560	2178
Hg	-	-	-	-	-	-
Tl	3.0	2.1	2.1	4.6	1.0	2.8
Pb	93	52	50	220	92	66
Bi	0.14	0.17	0.15	0.97	0.32	0.25
U	1.2	2.1	2.1	3.9	1.9	1.0

Appendix 11a: Geochemical analyses by partial dissolution (continued)

ppm	dc-94-8A	dc-94-8B	dc-94-8B dp	dc-94-8C	dc-94-8C dp	dc-94-8D
Si	1943	486	278	340	399	562
S	-	-	-	-	-	-
Ti	44	28	12	15	12	33
V	18	10	7	4	7	13
Mn	148508	134612	99584	-0.5	-0.5	199455
Fe57	37456	12367	9032	34920	34893	23648
Co	320	145	146	112	117	189
Ni	280	308	284	214	234	367
Cu	179	103	91	31	42	50
Zn	977	1222	863	723	658	2132
As	542	277	192	80	85	604
Se	4.0	-	1.5	-	-	-
Mo	5	4	2	2	3	21
Ag	0.3	0.1	0.1	0.0	0.0	0.1
Cd	11	10	8	7	7	24
Sb	2.0	2.0	1.2	0.6	0.7	1.2
Ba	3806	5606	3829	3142	3949	6405
Hg	-	-	-	-	-	-
Tl	2.1	2.8	2.0	2.4	2.2	6.7
Pb	349	113	116	47	51	119
Bi	1.3	0.6	0.6	0.1	0.1	0.5
U	8.5	2.7	2.6	0.9	1.1	1.8

Appendix 11a: Geochemical analyses by partial dissolution (continued)

ppm	dc-94-8D dp	dc-94-9	dc-94-10	dc-94-10dp	dc-94-11	dc-94-11B
Si	389	2314	607	490	923	715
S	-	-	-	-	-	-
Ti	24	410	171	107	89	11
V	10	64	13	15	19	25
Mn	179706	159154	171341	-1.6	124361	148410
Fe	20923	28294	13238	14571	17859	24174
Co	153	163	175	146	117	170
Ni	255	189	417	440	261	263
Cu	68	25	68	61	9	8
Zn	1552	1497	1893	2154	1193	942
As	369	257	285	315	141	118
Se	-	1.9	1.7	2.2	-	-
Mo	11	3	6	5	6	2
Ag	1.3	0.2	0.1	0.3	0.1	0.2
Cd	16	14	23	26	13	12
Sb	1.2	0.8	0.7	2.2	0.9	1.2
Ba	4675	5718	4210	5240	3644	5547
Hg	-	-	-	-	-	-
Tl	3.9	2.9	5.8	6.5	4.0	3.0
Pb	113	122	197	151	66	49
Bi	0.5	0.5	0.5	0.3	0.2	0.4
U	1.6	3.6	1.7	2.1	2.4	4.6

Appendix 11a: Geochemical analyses by partial dissolution (continued)

ppm	dc-94-11Bdp	dc-94-12	dc-94-12dp	dc-94-13	dc-94-14	dc-94-14dp
Si	1190	890	565	305	279	486
S	-	-	-	-	-	-
Ti	11	44	122	5	12	11
V	31	15	11	6	10	14
Mn	75317	185488	55177	99082	100182	128488
Fe	19879	16794	11947	10255	34332	31762
Co	221	124	71	34	129	235
Ni	514	350	79	163	192	252
Cu	3	32	18	7	9	33
Zn	890	1259	291	1024	870	882
As	107	166	61	94	93	94
Se	-	-	-	-	-	-
Mo	3	4	1	1	3	3
Ag	0.1	0.3	0.0	0.1	0.1	0.2
Cd	12	16	3	12	9	10
Sb	0.9	0.3	0.9	0.1	0.4	0.3
Ba	7119	8037	1620	2034	3310	4347
Hg	-	-	-	-	-	-
Tl	2.3	4.9	0.9	3.1	2.6	3.2
Pb	57	63	83	31	45	65
Bi	0.2	0.2	0.2	0.1	0.1	0.2
U	5.3	1.8	1.5	0.6	0.6	1.1

Appendix 11a: Geochemical analyses by partial dissolution (continued)

ppm	dc-94-15	dc-94-15dp	dc-94-16	dc-94-16dp	dc-94-17	dc-94-18
Si	125	438	249	1013	631	102
S	-	-	-	-	-	-
Ti	11	29	30	39	13	46
V	5	17	16	15	8	13
Mn	50575	-1	158946	173697	52501	207908
Fe	7353	17589	19347	18976	13596	18019
Co	121	178	111	142	88	114
Ni	183	428	295	362	172	642
Cu	17	23	25	26	40	23
Zn	855	2461	1218	1337	1148	2270
As	97	219	167	210	119	841
Se	-	-	-	-	-	-
Mo	3	11	14	13	3	13
Ag	0.04	0.16	0.10	0.10	0.10	0.05
Cd	9	24	15	19	9	35
Sb	0.5	0.8	1.5	1.3	0.4	1.8
Ba	2542	11646	4334	5278	1921	6436
Hg	-	-	-	-	-	-
Tl	3.2	9.8	5.0	7.4	2.0	10.8
Pb	57	83	32	43	99	41
Bi	0.1	0.2	0.2	0.2	0.3	0.1
U	0.8	3.7	1.0	1.2	2.3	1.5

Appendix 11a: Geochemical analyses by partial dissolution (continued)

ppm	dc-94-18dp	dc-94-19	dc-94-20	dc-94-20dp	dc-94-21	dc-94-21dp
Si	343	297	506	7106	560	864
S	-	-	-	-	-	-
Ti	48	51	100	83	17	45
V	15	17	22	21	10	11
Mn	209946	196016	207343	140155	167455	160922
Fe	23642	23357	16937	16340	14828	17803
Co	151	115	92	84	200	233
Ni	557	679	569	409	304	385
Cu	23	29	71	103	0.3	0.3
Zn	1745	2206	2329	1592	1199	1422
As	1059	269	312	236	256	249
Se	-	-	-	1.2	-	-
Mo	14	14	13	9	3	5
Ag	0.06	0.06	0.08	0.13	0.10	0.45
Cd	28	35	31	22	12	13
Sb	1.8	1.5	2.0	1.5	0.6	0.8
Ba	6287	6018	5366	5091	3873	4039
Hg	-	-	-	-	-	-
Tl	10	12	14	11	3	3
Pb	35	40	32	32	79	100
Bi	0.1	0.1	0.1	0.1	0.2	0.4
U	1.5	1.3	1.1	1.3	1.1	1.7

Appendix 11a: Geochemical analyses by partial dissolution (continued)

ppm	dc-94-22	dc-94-22dp	dc-94-23	dc-94-24	dc-94-24dp	dc-94-25
Si	131	209	284	281	295	725
S	-	-	-	-	-	-
Ti	31	45	125	36	42	6
V	13	13	22	14	15	7
Mn	167128	-0.5	191628	175357	215687	26635
Fe	13309	15000	17643	20652	20986	9097
Co	120	106	116	122	118	17
Ni	476	565	545	421	453	42
Cu	28	27	33	18	19	29
Zn	2359	2502	2552	1693	1976	192
As	396	349	299	202	225	47
Se	-	-	1.2	-	-	3.2
Mo	10	12	7	9	12	2
Ag	0.09	0.08	0.07	0.03	0.03	0.08
Cd	29	32	31	24	28	2
Sb	1.6	1.7	1.2	0.8	1.2	0.8
Ba	3984	4441	5731	7400	7220	519
Hg	-	-	-	-	-	-
Tl	11	13	10	7	8	0.6
Pb	55	45	46	44	42	57
Bi	0.3	0.3	0.1	0.1	0.1	0.6
U	0.9	1.0	1.0	1.0	1.0	4.1

Appendix 11a: Geochemical analyses by partial dissolution (continued)

ppm	dc-94-25dp	dc-94-26	dc-94-26dp	dl-94-01	dl-94-01B	dl-94-1Bdp
Si	1220	1671	524	4208	1333	1593
S	-	-	-	-	-	-
Ti	28	20	12	443	1364	346
V	13	20	8	31	41	43
Mn	48640	149110	32081	63055	127980	98676
Fe 57	14154	23195	8172	18174	22225	20016
Co	71	111	29	138	256	346
Ni	160	132	40	322	296	753
Cu	154	59	19	91	173	240
Zn	797	744	205	916	701	1582
As	124	142	47	166	177	230
Se	-	-	-	-	-	-
Mo	2	4	1	3	8	5
Ag	0.12	0.14	-	0.16	0.17	0.60
Cd	8	7	2	10	5	14
Sb	0.8	0.6	0.3	0.3	0.7	1.2
Ba	1862	3157	865	1845	1742	2189
Hg	-	-	-	-	-	-
Tl	2.2	1.8	0.6	1.7	1.8	3.0
Pb	69	89	27	276	439	1002
Bi	0.4	0.4	0.1	0.7	1.3	3.6
U	2.1	2.6	0.8	3.0	9.0	7.9

Appendix 11a: Geochemical analyses by partial dissolution (continued)

ppm	dl-94-02	dl-94-02dp	wh-94-1	wh-94-1dp	wh-94-2	wh-94-3
Si	66	702	50474	37294	693	3427
S	-	-	-	-	-	-
Ti	12	67	63	46	60	127
V	4	9	20	17	28	36
Mn	17171	60062	18849	21962	13956	23122
Fe	3372	9046	7199	6320	11209	13039
Co	12	32	93	180	169	197
Ni	36	179	13	7	22	21
Cu	4	0.3	244	233	49	67
Zn	203	627	648	562	1710	2091
As	30	104	8	4	8	10
Se	-	-	-	-	-	-
Mo	0.4	2	13	26	3	5
Ag	-	0.08	1.45	0.77	0.09	0.29
Cd	1	8	10	9	10	13
Sb	0.2	0.3	0.1	0.1	0.1	0.1
Ba	622	1887	626	472	377	461
Hg	-	-	-	-	-	-
Tl	0.2	1.2	1.4	0.9	1.7	2.3
Pb	23	95	230	162	267	420
Bi	0.1	0.6	1.1	0.5	0.5	0.6
U	0.6	2.0	13.5	32.9	3.6	5.8

Appendix 11a: Geochemical analyses by partial dissolution (continued)

ppm	wh-94-3dp	wh-94-4	wh-94-4dp	wh-94-5	wh-94-5dp	wh-94-6
Si	32533	2421	36537	1124	870	30846
S	-	-	-	-	-	-
Ti	137	414	298	116	197	99
V	32	64	53	80	105	31
Mn	16992	58626	23612	17268	23311	17230
Fe	12781	14878	12278	74969	39263	10516
Co	138	163	90	205	284	138
Ni	24	18	11	6	4	5
Cu	60	135	109	13	54	2
Zn	1330	1503	852	816	835	468
As	10	11	10	4	7	13
Se	-	-	-	-	-	-
Mo	3	64	28	4	5	5
Ag	0.09	0.24	0.29	1.54	1.48	0.15
Cd	8	24	11	9	11	8
Sb	0.2	0.1	0.1	0.1	0.1	0.0
Ba	282	1306	729	271	358	458
Hg	-	-	-	-	-	-
Tl	1.8	2.0	0.9	1.6	1.7	0.7
Pb	273	209	132	412	619	137
Bi	0.5	0.5	0.6	0.6	0.8	0.1
U	3.7	14.2	13.6	7.3	5.9	3.7

Appendix 11a: Geochemical analyses by partial dissolution (continued)

ppm	wh-94-7	wh-94-7dp	wh-94-8	wh-94-8C	wh-94-8Cdp	wh-94-9
Si	3214	2166	2153	1430	3623	1075
S	-	-	-	-	-	-
Ti	513	450	289	89	326	1130
V	71	45	72	32	176	202
Mn	16932	39642	30788	73684	55236	35956
Fe	18955	9642	44408	4	103759	19859
Co	250	642	474	1139	1074	532
Ni	11	0.0	0.0	4	27	0.0
Cu	102	120	9	46	151	10
Zn	2070	1260	1056	766	1527	1049
As	5	6	9	4	9	8
Se	-	-	-	-	-	-
Mo	3.5	19.7	1.9	6.6	8.2	1.5
Ag	0.09	0.08	0.14	0.04	0.23	0.05
Cd	10	12	10	13	22	15
Sb	0.1	0.1	0.1	0.2	0.2	0.0
Ba	206	259	644	1509	1243	218
Hg	-	-	-	-	-	-
Tl	2.4	2.9	2.0	1.9	3.7	2.8
Pb	517	461	552	247	1139	490
Bi	0.2	0.2	0.4	0.2	0.4	0.2
U	10.1	8.4	12.2	9.2	35.0	2.0

Appendix 11a: Geochemical analyses by partial dissolution (continued)

ppm	wh-94-9dp	wh-94-10	wh-94-11	wh-94-11dp	wh-94-12
Si	342	581	893	1220	788
S	-	-	-	-	-
Ti	296	486	292	809	83
V	57	113	40	57	24
Mn	17389	35971	14879	46830	1438
Fe	8992	25153	11012	24085	6394
Co	298	476	229	697	20
Ni	0.1	0.1	0.0	0.5	0.5
Cu	0.8	12.0	14.3	32.4	25.9
Zn	618	549	404	682	204
As	4	11	8	24	3
Se	-	-	-	-	-
Mo	1.1	4.3	4.6	6.3	0.9
Ag	0.02	0.03	0.04	0.14	0.02
Cd	8	13	7	15	1
Sb	0.0	0.1	0.1	0.3	0.0
Ba	114	163	115	320	106
Hg	-	-	-	-	-
Tl	1.6	3.0	1.5	4.4	0.4
Pb	258	514	210	525	177
Bi	0.2	0.1	0.1	0.4	0.1
U	0.7	0.8	0.5	1.0	0.8

Appendix 11a: Geochemical analyses by partial dissolution (continued)

ppm	wh-94-13	wh-94-13dp	wh-94-14	wh-94-14C	wh-94-14Cdp	wh-94-15
Si	1357	251	1035	233	1154	2176
S	-	-	-	-	-	-
Ti	122	58	117	157	118	1037
V	54	25	15	17	28	67
Mn	62217	10310	2495	7592	10265	43153
Fe	41404	22740	3801	3108	4660	21483
Co	133	49	13	25	57	765
Ni	11	0.0	0.0	0.0	0.0	1.4
Cu	215	27	29	0.0	2.1	58
Zn	617	291	182	175	630	1408
As	8	5	3	2	4	8
Se	-	-	-	-	-	-
Mo	7	2	0.2	0.9	1	5
Ag	0.11	0.04	0.08	0.01	0.02	0.11
Cd	8	4	1	1	3	15
Sb	0.1	0.0	0.0	0.0	0.0	0.1
Ba	4315	428	328	574	743	159
Hg	-	-	-	-	-	-
Tl	2.2	0.5	0.3	0.5	0.8	2.9
Pb	263	104	58	78	84	896
Bi	0.3	0.1	0.2	0.0	0.1	0.4
U	3.0	1.0	0.2	0.2	0.3	1.4

Appendix 11a: Geochemical analyses by partial dissolution (continued)

ppm	wh-94-15dp	wh-94-16	wh-94-17	wh-94-17dp	wh-94-18	wh-94-19
Si	3402	1177	1632	2612	2190	7636
S	-	-	-	-	-	-
Ti	1089	228	266	620	829	821
V	68	27	35	76	60	56
Mn	36073	13883	10320	20022	27978	46064
Fe	22869	7067	8090	19954	16079	18427
Co	565	211	117	247	331	596
Ni	11	0.1	0.0	3	0.0	12633
Cu	43	10	15	30	77	169
Zn	1207	765	568	1376	1630	4084
As	10	5	3	8	4	9
Se	-	-	-	-	0.9	-
Mo	5	3	2	5	4	17
Ag	0.10	0.01	0.18	0.37	0.12	0.18
Cd	12	7	8	19	19	23
Sb	0.1	0.1	0.0	0.1	0.1	0.2
Ba	121	45	49	127	129	239
Hg	-	-	-	-	-	-
Tl	2.5	1.3	1.6	3.6	2.7	4.3
Pb	674	307	524	989	803	1047
Bi	0.5	0.2	0.5	0.7	0.6	0.7
U	1.1	0.5	0.7	1.5	1.0	1.6

Appendix 11a: Geochemical analyses by partial dissolution (continued)

ppm	wh-94-19dp	wh-94-20	wh-94-20dp	wh-94-21	wh-94-22	wh-94-22dp
Si	2821	1207	3301	2971	2145	1015
S	-	-	-	-	-	-
Ti	645	1120	2462	1014	1424	911
V	78	35	72	70	56	51
Mn	61177	38811	77026	51614	40717	53354
Fe	21400	11044	24001	43045	15108	9896
Co	828	382	834	463	689	736
Ni	21	5	12	35	21	22
Cu	84	28	71	201	375	115
Zn	3480	1894	3802	2521	4110	4206
As	15	10	13	14	9	19
Se	2.1	-	0.7	3.0	1.5	-
Mo	21	7	9	17	5	11
Ag	0.19	0.05	0.15	0.13	0.24	0.20
Cd	36	27	59	30	47	60
Sb	0.2	0.1	0.1	0.1	0.1	0.1
Ba	183	86	159	472	205	172
Hg	-	-	-	-	-	-
Tl	5.4	2.8	6.8	4.7	4.3	5.9
Pb	893	563	1280	1040	1058	971
Bi	0.6	0.3	0.6	1.6	1.0	0.5
U	1.4	0.6	1.4	3.4	2.5	1.7

Appendix 11a: Geochemical analyses by partial dissolution (continued)

ppm	wh-94-23	wh-94-23B	wh-94-23Bdp	wh-94-24	wh-94-24dp	hb-94-1
Si	2226	3239	1719	3823	4676	1161
S	-	-	-	-	-	-
Ti	2052	1755	688	1263	1104	206
V	113	107	59	87	90	28
Mn	49740	70256	38566	55282	52116	58647
Fe	34529	28164	15402	25458	25316	21547
Co	970	1161	727	511	568	81
Ni	12	23	49	1918	22	61
Cu	69	102	144	113	90	65
Zn	2689	3398	3245	3082	2251	750
As	20	24	10	31	24	10
Se	3.2	-	-	-	-	-
Mo	13	20	7	20	10	11
Ag	0.60	0.81	0.91	0.35	0.69	0.15
Cd	40	39	17	63	60	10
Sb	0.1	0.2	0.9	0.3	0.2	0.2
Ba	186	237	195	190	175	1276
Hg	-	-	-	-	-	-
Tl	5.4	3.9	2.2	7.4	6.3	1.0
Pb	2505	2631	1473	1736	2007	58
Bi	1.5	0.9	1.0	1.2	1.9	0.2
U	1.5	1.8	1.8	1.4	1.3	2.1

Appendix 11a: Geochemical analyses by partial dissolution (continued)

ppm	hb-94-1 dp	hb-94-2	hb-94-3	hb-94-3 dp	ss-95-1	ss-95-2
Si	1076	1652	904	1311	16890	7401
S	-	-	-	-	-	-
Ti	245	218	108	78	497	304
V	32	77	50	33	917	180
Mn	48562	72717	86230	82616	1080367	129364
Fe	28682	51920	28780	19871	271805	40836
Co	108	110	130	116	1469	163
Ni	68	59	66	146	570	67
Cu	68	38	105	81	592	350
Zn	847	1008	989	1490	4990	975
As	9	17	8	7	300	40
Se	-	-	-	-	11.8	7.1
Mo	11	7	14	18	37	4
Ag	0.10	0.40	0.27	0.24	1.19	0.41
Cd	11	12	13	22	40	5
Sb	0.1	0.1	0.2	0.1	1.5	0.2
Ba	1283	2151	1301	1683	25208	3273
Hg	-	-	-	-	-	-
Tl	1.0	0.8	1.1	2.0	10.7	1.1
Pb	66	60	148	96	626	73
Bi	0.2	0.2	1.0	0.6	5.5	0.1
U	3.0	1.8	2.3	1.9	7.0	3.5

Appendix 11a: Geochemical analyses by partial dissolution (continued)

ppm	ss-95-2 dp	ss-95-03	ss-95-4	ss-95-4 dp	ss-95-5	ss-95-5A
Si	3967	776	448	428	834	446
S	-	-	-	-	1806	1255
Ti	168	507	34	40	167	303
V	75	54	80	98	7	97
Mn	35022	163665	148700	184348	97496	41359
Fe	18176	20669	22345	27588	30248	10474
Co	50	116	159	211	78	43
Ni	24	84	46	63	55	21
Cu	119	103	135	58	53	7
Zn	467	1400	713	1040	702	218
As	16	37	57	78	2	4
Se	1.5	1.4	0.9	-	-	-
Mo	2	5	2	5	0	0
Ag	0.18	0.06	0.16	0.17	0.16	0.02
Cd	2	14	6	7	5	2
Sb	0.1	0.2	0.1	0.2	0.0	0.0
Ba	973	5960	3526	4149	3486	1104
Hg	-	-	-	-	-	-
Tl	0.4	2.9	1.2	2.0	0.1	0.5
Pb	29	49	43	56	6	31
Bi	0.1	0.1	0.3	0.2	-	0.1
U	1.7	0.8	1.0	0.8	0.5	0.5

Appendix 11a: Geochemical analyses by partial dissolution (continued)

ppm	ss-95-5A dp	ss-95-06	ss-96-6 dp	ss-95-7	ss-95-8	ss-95-8 dp
Si	360	268	479	450	324	553
S	-	-	-	1040	-	3576
Ti	206	84	110	48	79	83
V	69	50	76	33	81	73
Mn	77303	229056	-1	248568	143982	127025
Fe	14307	59652	94497	76611	67544	68727
Co	72	363	685	381	414	304
Ni	26	18	30	12	32	26
Cu	2	34	41	4	28	54
Zn	259	317	491	233	389	302
As	12	38	56	13	83	139
Se	-	0.2	-	-	-	-
Mo	1	1	1	-	1	2
Ag	0.04	0.03	0.03	0.02	0.06	0.14
Cd	2	6	9	5	9	8
Sb	0.1	0.1	0.1	-	0.3	0.3
Ba	1378	3168	5161	4163	2878	1946
Hg	-	-	-	-	-	0.1
Tl	0.6	8.6	12.1	6.9	8.4	6.7
Pb	35	44	66	67	202	180
Bi	0.1	0.0	0.1	-	0.1	0.1
U	0.5	0.2	0.3	0.9	0.2	0.3

Appendix 11a: Geochemical analyses by partial dissolution (continued)

ppm	ss-95-9	ss-95-10	ss-95-10 dp	ss-95-11	ss-95-11B	ss-95-12
Si	296	350	112	667	778	1340
S	809	-	1465	-	-	615
Ti	46	51	68	46	89	35
V	24	48	57	56	24	125
Mn	278751	313910	182978	102084	50750	40351
Fe	52763	62433	68121	10886	3313	38542
Co	262	416	473	124	50	109
Ni	26	42	37	73	29	44
Cu	0	6	19	129	73	115
Zn	391	765	689	2485	229	275
As	4	100	222	6	4	18
Se	-	-	-	5.1	-	2.5
Mo	0.0	0.7	1.7	1.5	0.9	1.7
Ag	0.01	0.02	0.02	0.10	0.03	0.07
Cd	6	14	13	5	2	1
Sb	0.0	0.1	0.3	0.2	0.1	0.2
Ba	4143	4343	4472	5481	2822	1997
Hg	-	-	-	-	-	-
Tl	4.4	10.9	10.9	0.4	0.1	0.2
Pb	16	89	114	68	24	87
Bi	0.0	0.1	0.1	0.4	0.3	0.8
U	0.1	0.4	0.8	1.1	0.7	0.9

Appendix 11a: Geochemical analyses by partial dissolution (continued)

ppm	ss-95-12 dp	ss-95-13	ss-95-14	ss-95-14 dp	ss-95-15	ss-95-15C
Si	1307	249	277	560	283	544
S	-	1106	1191	303	4298	809
Ti	51	25	29	34	37	38
V	85	175	98	130	40	43
Mn	48211	146162	156507	121154	159502	176428
Fe	24973	29494	67931	103973	70552	57085
Co	317	114	145	172	417	328
Ni	82	60	20	15	31	33
Cu	237	50	10	0	26	0
Zn	266	1737	913	719	1323	1558
As	26	19	31	28	88	200
Se	-	-	-	-	-	1.0
Mo	5	3	4	3	1	2
Ag	0.11	0.04	0.06	0.06	0.06	0.03
Cd	3	4	3	2	17	19
Sb	0.3	0.1	0.2	0.2	0.1	0.2
Ba	2418	9506	11485	9221	8377	7717
Hg	-	-	-	-	-	-
Tl	0.4	0.6	1.2	0.7	6.6	8.0
Pb	128	39	48	48	70	26
Bi	1.3	0.4	0.2	0.3	0.1	0.1
U	0.9	0.6	0.5	0.6	0.9	0.5

Appendix 11a: Geochemical analyses by partial dissolution (continued)

ppm	ss-95-15C dp	ss-95-16	ss-95-16 dp	ss-95-17	ss-95-18	ss-95-18 dp
Si	195	803	569	287	446	176
S	-	678	1600	-	3300	-
Ti	36	42	35	33	59	24
V	41	96	93	37	71	84
Mn	155946	58217	57208	187612	9526	15512
Fe	76416	65467	53190	66129	59010	75722
Co	417	279	246	398	62	46
Ni	37	20	18	41	24	15
Cu	3	47	160	19	93	50
Zn	1763	475	643	1045	466	647
As	80	54	79	46	32	29
Se	-	-	-	1.4	-	-
Mo	1	1	2	1	1	0
Ag	0.01	0.14	0.66	0.05	0.29	0.16
Cd	21	5	4	15	4	2
Sb	0.6	0.3	0.4	0.3	0.3	0.1
Ba	7445	2655	2459	7706	1561	1151
Hg	-	-	-	-	-	-
Tl	8.7	1.1	1.0	8.7	0.5	0.5
Pb	69	155	120	68	206	262
Bi	0.1	0.6	0.5	0.1	0.9	0.5
U	0.5	0.9	1.1	0.6	1.3	1.1

Appendix 11a: Geochemical analyses by partial dissolution (continued)

ppm	ss-95-19	ss-95-20	ss-95-20 dp	ss-95-20A	ss-95-20A dp
Si	245	223	303	252	466
S	693	-	809	1123	2900
Ti	112	160	130	151	213
V	136	83	125	116	74
Mn	107296	42204	81607	47424	26935
Fe	119360	57593	75338	50321	35854
Co	265	140	155	134	92
Ni	27	17	32	27	13
Cu	0	11	16	13	55
Zn	933	200	315	265	170
As	81	36	46	51	33
Se	-	-	-	-	-
Mo	1	1	1	1	1
Ag	0.08	0.06	0.13	0.07	0.04
Cd	5	2	5	3	1
Sb	0.3	0.1	0.2	0.1	0.2
Ba	2145	1464	1660	1612	1361
Hg	-	-	-	-	-
Tl	2.7	0.8	1.8	1.0	0.5
Pb	219	164	148	151	157
Bi	0.3	0.2	0.4	0.4	0.3
U	0.9	0.9	0.6	0.8	1.2

APPENDIX 11

MN-FE-OXIDE COATING GEOCHEMICAL ANALYSES

Appendix 11b: Geochemical analyses by laser ablation.

cps	DC-94-01A	DC-94-01A	DC-94-01B	DC-94-01B
Si	135268	317386	43665	112354
S	16715	18304	7054	12587
Ti	158469	156926	6061	7635
Fe	688974	549707	452059	213085
Co	320581	370182	279721	104023
Cu	35145	14327	20028	69074
Zn	890906	526723	928154	336724
As	693202	669610	503694	234103
Se	-43	308	51	567
Mo	23830	21338	24094	4071
Cd	17233	6283	13493	2098
Sb	195022	15387	14204	8986
Te	281	335	341	70
Ba	2066293	1279628	1601915	200741
Ta	4024	4443	235	995
Au	260	120	156	9535
Hg	2010	1273	1177	495
Tl	23721	10916	24512	2056
Pb	29809	23291	7509	6846
Bi	2957	5223	1320	1354
U	23652	27042	9149	4707

Appendix 11b: Geochemical analyses by laser ablation (continued)

cps	DC-94-01B	DC-94-01B	DC-94-01C	DC-94-01C
Si	17814	63642	99631	166136
S	4915	21131	27678	14297
Ti	6276	6580	20964	32970
Fe	137517	246727	461397	437060
Co	57933	89372	150139	166479
Cu	21243	28026	25996	27097
Zn	199962	394544	666425	571722
As	175202	273665	416272	445091
Se	298	-30	86	9
Mo	5168	6119	12671	10414
Cd	4340	7175	15286	13084
Sb	6055	6522	9989	13780
Te	91	16	54	151
Ba	598621	516628	834179	743916
Ta	2192	136	1263	443
Au	711	210	105	845
Hg	1588	937	1429	1757
Tl	18435	14309	11211	9426
Pb	10856	5092	11748	12767
Bi	3656	1636	6201	3142
U	30034	9965	7318	15241

Appendix 11b: Geochemical analyses by laser ablation (continued)

cps	DC-94-02A	DC-94-02A	DC-94-02B	DC-94-02B	DC-94-02C
Si	132735	114456	221752	81098	95272
S	17018	13457	10557	11513	88006
Ti	92633	57052	78291	38354	5954
Fe	497842	398392	358803	253811	90900
Co	150908	110023	116006	87965	8020
Cu	33456	21525	28656	17134	10739
Zn	426238	339437	283518	146496	22771
As	428714	371605	332711	280616	40931
Se	564	12	-9	293	292
Mo	15893	12075	9888	8745	2321
Cd	10128	8054	4693	2486	713
Sb	26864	28746	42503	15869	6078
Te	487	232	166	181	187
Ba	704897	659269	608003	457912	12430
Ta	2772	1190	1855	1430	1386
Au	439	1395	440	116	478
Hg	2035	1722	1974	1491	1588
Tl	11266	8257	13173	7210	1396
Pb	21658	21716	16847	12527	3292
Bi	8253	9909	6182	2454	2692
U	43759	26273	68113	48895	5471

Appendix 11b: Geochemical analyses by laser ablation (continued)

cps	DC-94-02C	DC-94-03A	DC-94-03A	DC-94-03B	DC-94-03B
Si	49327	91966	78602	64868	85121
S	6074	6464	7861	3760	4589
Ti	10160	46399	10794	10972	38494
Fe	300489	252564	232593	217932	252015
Co	58807	126010	92891	51759	66432
Cu	28543	29928	19829	10865	12907
Zn	308721	201784	156533	213688	291700
As	226609	293270	214897	164453	163711
Se	254	204	74	215	216
Mo	13366	6878	4419	10310	8231
Cd	3844	4197	3384	5255	9629
Sb	22139	12309	7566	14229	16357
Te	79	580	117	268	149
Ba	533252	643988	546602	293097	478776
Ta	836	3186	556	4496	3525
Au	325	63	241	4567	537
Hg	1849	1665	1382	1782	3240
Tl	17412	7797	7948	8521	14429
Pb	12444	29769	10829	14896	19403
Bi	6105	28032	8392	18907	16595
U	34451	79545	43289	34811	31846

Appendix 11b: Geochemical analyses by laser ablation (continued)

cps	DC-94-03C	DC-94-03C	DC-94-04A	DC-94-04A	DC-94-04B
Si	160977	41320	171024	259079	63590
S	6380	3739	10586	11931	6563
Ti	46106	20655	62726	84715	23954
Fe	834497	338574	409030	554410	279124
Co	180322	98384	105057	138212	71456
Cu	159425	54842	28646	38925	76805
Zn	478991	369285	648901	1077380	320931
As	313452	234633	291199	337229	284917
Se	277	92	194	245	346
Mo	16962	12940	16699	17367	8714
Cd	12651	13236	22013	20161	10929
Sb	34898	11896	25796	42582	34155
Te	643	286	941	1330	226
Ba	664736	679496	664558	671626	633548
Ta	7549	1070	11967	10701	5813
Au	830	235	1047	2049	10765
Hg	3222	1890	1967	1648	1920
Tl	23619	21986	40797	38793	17344
Pb	50848	21163	37892	50760	22748
Bi	33739	8284	38897	40558	26676
U	118925	27498	100025	125434	40172

Appendix 11b: Geochemical analyses by laser ablation (continued)

cps	DC-94-04B	DC-94-04C	DC-94-04C	DC-94-05A	DC-94-05A
Si	68288	111183	94060	216417	208045
S	10049	23824	23393	5554	7829
Ti	13341	58395	33938	65920	58668
Fe	499483	1499439	1218727	363894	310856
Co	87100	290732	303733	83295	84368
Cu	275248	817426	565339	42416	26311
Zn	289137	625801	638542	322071	277779
As	655323	1927806	1557206	264534	284890
Se	143	581	523	36	157
Mo	9273	25835	25364	12732	11338
Cd	8313	23683	26553	14215	7977
Sb	74249	223570	189558	150904	120147
Te	534	824	653	619	559
Ba	472995	642413	701557	655700	723784
Ta	4582	8238	5969	6116	4589
Au	19327	768	789	3975	3953
Hg	1452	2213	1936	2027	2409
Tl	13672	33792	41020	48287	39156
Pb	27497	47920	46945	30077	27127
Bi	14145	37994	24038	19946	14198
U	63255	100102	75190	88759	74077

Appendix 11b: Geochemical analyses by laser ablation (continued)

cps	DC-94-05B	DC-94-05B	DC-94-05C	DC-94-05C	DC-94-06A
Si	106901	63084	234239	150592	105983
S	9898	10909	7667	6233	5313
Ti	38145	12761	124457	65233	39842
Fe	411927	341068	605154	321809	265632
Co	105834	91357	103915	78278	74410
Cu	82337	47423	75362	45496	51481
Zn	377639	286814	308930	196016	290197
As	330242	295912	235669	169960	289595
Se	289	333	254	21	200
Mo	21175	14143	24115	6827	10991
Cd	9669	10017	7570	4959	10205
Sb	363553	276596	41791	21678	38347
Te	246	493	554	348	849
Ba	758335	718176	474452	490046	664737
Ta	5180	2207	10917	6240	7447
Au	2923	1878	9460	1842	1502
Hg	1975	2979	1858	1655	1196
Tl	25001	23313	26506	20881	20984
Pb	25849	19573	31579	22802	27683
Bi	17179	11463	35034	23537	21718
U	84240	51811	152624	82079	104221

Appendix 11b: Geochemical analyses by laser ablation (continued)

cps	DC-94-06A	DC-94-06B	DC-94-06B	DC-94-06C	DC-94-06C
Si	55177	81700	103016	302736	250504
S	4162	5662	4101	6932	6547
Ti	31748	22722	31700	125447	78585
Fe	191291	278760	295289	401572	314136
Co	60255	72018	67741	154132	113450
Cu	88216	35717	60009	174333	109251
Zn	240205	369911	318396	461318	421076
As	311120	213213	218109	342491	273830
Se	99	40	313	333	367
Mo	9162	16159	11879	55833	43636
Cd	7835	14532	10315	15791	14834
Sb	30101	37301	33272	56017	45603
Te	369	601	794	1628	1189
Ba	537369	752142	645978	715765	812528
Ta	4847	10276	8143	21664	14452
Au	19288	70369	2259	39766	2091
Hg	1628	2210	1724	1612	1795
Tl	15265	44220	37105	65531	58891
Pb	24902	26474	29200	138928	121019
Bi	17087	25046	33056	119551	97957
U	54729	124586	134152	434038	357189

Appendix 11b: Geochemical analyses by laser ablation (continued)

cps	DC-94-07A	DC-94-07A	DC-94-07B	DC-94-07B	DC-94-07C
Si	1158371	1259156	1991063	1698303	1410406
S	23948	47894	28963	27466	90126
Ti	281694	250282	297541	308213	271049
Fe	1350325	1571269	1669312	1181025	2154123
Co	440192	478457	375254	334209	506243
Cu	122596	164419	87547	176945	78308
Zn	537690	639015	769951	653572	1140473
As	329524	497971	334963	357324	599143
Se	110	379	754	456	-240
Mo	13550	21022	46897	37243	75163
Cd	4073	6305	12929	15690	21236
Sb	80789	97926	46049	51765	49949
Te	97	590	1472	1176	295
Ba	434429	605823	388433	311312	991477
Ta	2456	1841	5712	7994	4587
Au	1216	5749	453	985	381
Hg	1110	1466	1011	1235	1576
Tl	3257	5414	7080	7659	22643
Pb	7307	9779	11405	10017	12190
Bi	2599	13091	14725	24130	11922
U	27973	38215	42124	51039	40977

Appendix 11b: Geochemical analyses by laser ablation (continued)

cps	DC-94-07C	DC-94-08aB	DC-94-08aB	DC-94-08aB	DC-94-08aC
Si	998355	1518193	1525768	1324025	618857
S	89663	31162	33739	28364	66946
Ti	87625	264486	284466	289981	145117
Fe	1006934	1459502	1384417	1432967	828999
Co	303505	405630	408415	575668	292318
Cu	35522	83604	148533	93982	151588
Zn	782829	749268	765481	770039	265733
As	411132	579266	694521	845206	622491
Se	226	710	253	-161	430
Mo	24201	26031	30129	27154	18158
Cd	13355	8180	9924	7625	6066
Sb	11566	36733	53994	27272	34534
Te	254	246	389	209	82
Ba	862036	827733	777384	925127	390686
Ta	930	2460	3153	5955	663
Au	352	3700	140	3947	378
Hg	1386	709	814	844	1119
Tl	14194	9856	10175	7659	1991
Pb	5718	12573	17707	14451	13526
Bi	12151	5942	6374	5298	4404
U	14059	46750	38998	37977	8968

Appendix 11b: Geochemical analyses by laser ablation (continued)

cps	DC-94-08aC	DC-94-08aC	DC-94-08bA	DC-94-08bA	DC-94-08bB
Si	858197	901692	745264	1437030	2282171
S	49938	86645	22963	33890	66230
Ti	133083	301169	461586	1114115	576802
Fe	849193	1282189	1137708	2001794	1884144
Co	314318	344397	393605	625140	566635
Cu	103020	86791	183506	197927	236258
Zn	279923	477557	666059	1021861	1644520
As	616198	1314418	1254520	1900669	1172343
Se	263	656	485	1555	684
Mo	19120	27507	32777	58798	67890
Cd	2904	7038	13886	19854	39460
Sb	33381	66140	143206	335328	139829
Te	-6	155	2127	2538	3759
Ba	454696	397669	1163425	1201772	2404455
Ta	1110	1279	13792	17180	24375
Au	99	56	2503	2524	1476
Hg	458	523	1459	2028	2594
Tl	2540	2415	27608	42724	126174
Pb	8218	16774	79854	119869	88166
Bi	4853	12136	24306	47225	168442
U	30280	17080	198900	410093	674390

Appendix 11b: Geochemical analyses by laser ablation (continued)

cps	DC-94-08bB	DC-94-08bC	DC-94-08bC	DC-94-08cA	DC-94-08cA
Si	1978168	838713	958012	1694383	920651
S	93282	34428	23363	43226	35481
Ti	261239	307316	259847	1003099	410087
Fe	1606298	1108591	1130215	2524683	1542749
Co	476298	359010	359186	660087	401855
Cu	123170	51063	80832	181548	93718
Zn	1575400	456421	552978	942346	694801
As	1050496	811092	817272	677096	542835
Se	739	222	252	615	1040
Mo	59039	28217	30013	45291	29617
Cd	35286	7900	8027	15075	8857
Sb	106188	30902	38849	111146	42010
Te	1167	505	806	1507	156
Ba	2665357	801318	975319	1144198	1087369
Ta	9744	3425	4903	16652	7816
Au	2335	5539	1866	1055	1053
Hg	2847	1462	1485	3607	2393
Tl	110555	12868	15573	69041	35119
Pb	56834	24737	32479	86112	29914
Bi	81766	15441	17762	63007	18868
U	432428	136595	157232	292085	166303

Appendix 11b: Geochemical analyses by laser ablation (continued)

cps	DC-94-08cB	DC-94-08cB	DC-94-08cC	DC-94-08cC	DC-94-08dA
Si	780429	845212	527712	184684	791650
S	136817	52424	34720	25703	28148
Ti	111676	246128	133685	49323	248862
Fe	2108127	1820003	976850	674566	1580083
Co	989040	500946	334256	228925	333143
Cu	294152	120878	88312	55588	119532
Zn	1726424	1047888	1023256	816321	754879
As	977107	1865845	566428	520299	2305767
Se	2577	2204	1178	1200	1042
Mo	102836	41110	32704	23427	61211
Cd	45729	19535	20886	16309	14463
Sb	122824	97080	22645	11019	86640
Te	3416	1981	337	169	1093
Ba	2733132	1147551	1409434	1268369	646275
Ta	4505	7076	2875	1217	7755
Au	435	388	246	130	193
Hg	3098	1962	2950	2170	2129
Tl	113003	33019	44455	23999	20856
Pb	148451	56959	29517	15356	71832
Bi	107221	67622	24447	4348	44459
U	191929	80233	143777	53296	130169

Appendix 11b: Geochemical analyses by laser ablation (continued)

cps	DC-94-08dA	DC-94-08dB	DC-94-08dB	DC-94-8dC	DC-94-8dC
Si	227987	411246	374044	972272	862476
S	11878	22294	23227	45767	36696
Ti	182813	82746	89565	307964	236890
Fe	856283	857701	796488	1460061	1245010
Co	155936	320125	224689	516527	481200
Cu	42194	48570	41034	82070	85877
Zn	316385	608571	707588	1740464	1327959
As	1919563	318388	359496	799992	557988
Se	366	260	619	345	524
Mo	30902	19541	22295	110160	49733
Cd	6126	9699	11298	65016	37427
Sb	31462	25480	25203	86657	65481
Te	147	321	203	2966	1927
Ba	394890	1060421	911237	2214856	1638735
Ta	3009	1901	1827	26155	14557
Au	537	371	920	3121	1368
Hg	828	1770	1638	2831	1267
Tl	5176	24287	19719	105280	60572
Pb	13879	19940	22863	46023	30079
Bi	12162	12942	9660	82450	29650
U	56731	34791	35927	171109	128810

Appendix 11b: Geochemical analyses by laser ablation (continued)

cps	DC-94-09A	DC-94-09A	DC-94-09B	DC-94-09B	DC-94-09C
Si	1605690	1483435	424245	159085	1700646
S	32092	39986	44249	23860	62959
Ti	824169	786280	225450	103702	276364
Fe	1688932	1534856	1741758	949830	2315237
Co	443683	496301	625945	325708	481170
Cu	122989	144737	131954	44544	136463
Zn	670897	718355	1198173	726436	881198
As	580407	633731	958324	452908	870810
Se	1229	786	1019	461	313
Mo	79285	52258	77766	30305	54492
Cd	24653	17050	33877	14957	14513
Sb	152463	124935	163615	47066	154129
Te	4712	2067	996	673	856
Ba	938385	746093	1771456	1213085	845858
Ta	65824	60566	8887	2309	24179
Au	16050	2993	2652	714	5177
Hg	1733	2082	2609	2644	2402
Tl	35026	30024	49590	25822	29625
Pb	38242	45725	32369	21201	41114
Bi	183301	87395	33914	9848	32938
U	471576	436675	102729	46959	226518

Appendix 11b: Geochemical analyses by laser ablation (continued)

cps	DC-94-09C	DC-94-10A	DC-94-10A	DC-94-10B	DC-94-10B
Si	1063758	2345172	1478251	1408409	978203
S	45166	54296	34658	32176	60692
Ti	287919	1272975	548376	401783	288713
Fe	1778232	2783728	1937659	2033228	1369910
Co	418484	1232042	852852	534052	464453
Cu	95681	525212	271036	107556	63448
Zn	684694	1401623	1136791	1003164	841517
As	648347	1152491	709536	553620	412811
Se	596	1159	753	556	637
Mo	48417	46620	35587	37819	27536
Cd	14042	30069	18262	17472	13271
Sb	125829	225796	101856	54571	30093
Te	1115	853	491	467	424
Ba	786561	1309718	1373180	884122	1013512
Ta	4984	19230	9391	5670	3615
Au	4768	15777	30507	1035	482
Hg	2011	3956	2871	3128	2954
Tl	23193	68994	39962	44545	28160
Pb	20407	99861	49056	39806	27291
Bi	47638	38947	22048	23300	12902
U	162541	396962	165371	159455	84405

Appendix 11b: Geochemical analyses by laser ablation (continued)

cps	DC-94-10C	DC-94-10C	DC-94-11A	DC-94-11A	DC-94-11B
Si	135672	56394	1017301	1146297	640827
S	15396	11236	25093	29670	49556
Ti	51731	13391	352830	370298	216876
Fe	585366	439351	1164510	1278463	1469202
Co	204668	152086	296278	232896	304885
Cu	35616	23177	52360	65568	84970
Zn	2946623	2462153	416753	456980	945913
As	210018	175534	273547	168399	551486
Se	976	984	72	340	1276
Mo	23094	17819	13712	20855	38211
Cd	12233	9456	7441	6554	19257
Sb	10771	5397	21923	23678	76326
Te	74	12	221	247	391
Ba	818695	700868	597768	377580	875789
Ta	399	267	3959	3477	3700
Au	101	169	171	3233	1819
Hg	5728	4342	610	1195	1797
Tl	23116	17316	15377	18927	26849
Pb	8914	7020	19671	23018	23749
Bi	4115	1800	8796	8634	8484
U	36385	25161	73286	76499	144313

Appendix 11b: Geochemical analyses by laser ablation (continued)

cps	DC-94-11B	DC-94-11C	DC-94-11C	DC-94-12A	DC-94-12A
Si	704856	1263064	963213	796053	842093
S	40676	38222	31899	22792	10524
Ti	336893	241593	319783	85684	135261
Fe	1456326	1238302	1162696	748077	687195
Co	340468	285308	324714	231036	148844
Cu	85257	149356	75595	114987	58832
Zn	888722	523056	428023	225189	188751
As	350624	142271	159315	128850	79895
Se	1175	192	424	106	255
Mo	27251	15297	16663	9867	6794
Cd	24183	4977	4995	2072	1900
Sb	71955	60866	56076	29279	37091
Te	266	192	68	228	255
Ba	624878	315425	387056	379438	303978
Ta	6007	3677	3212	2085	4142
Au	2507	5738	535	843	619
Hg	1790	1231	1370	910	449
Tl	22467	11825	8950	13940	12931
Pb	18459	24779	22975	31700	46941
Bi	13508	8939	7165	16491	13366
U	105154	92512	86887	172195	139174

Appendix 11b: Geochemical analyses by laser ablation (continued)

cps	DC-94-12B	DC-94-12B	DC-94-12C	DC-94-12C	DC-94-13A
Si	1646059	1103722	763921	524016	705607
S	30526	18911	32699	18772	41976
Ti	773195	589556	227424	119155	475123
Fe	1851776	1206831	1947781	1395205	1284395
Co	447746	266706	538366	449557	323483
Cu	150235	81852	97410	33137	115724
Zn	634972	354848	897000	668804	597693
As	1070596	640782	743244	651989	221900
Se	1354	723	653	74	489
Mo	190947	93003	77332	48527	34931
Cd	17493	7889	15178	8734	10185
Sb	242988	100185	122784	53610	26974
Te	2588	1470	1331	937	417
Ba	610335	359578	1181140	876282	546108
Ta	46812	22497	15326	13598	7079
Au	3679	12969	1310	773	728
Hg	869	621	1552	1662	2047
Tl	32672	13705	22826	11976	18839
Pb	22432	14854	43835	26763	25611
Bi	83449	25423	33084	11621	14754
U	312552	140922	180016	89280	75013

Appendix 11b: Geochemical analyses by laser ablation (continued)

cps	DC-94-13A	DC-94-13B	DC-94-13B	DC-94-13C	DC-94-13C
Si	401585	798366	799475	1949345	1662482
S	28756	36880	32454	37667	58056
Ti	334321	193545	233236	456046	380242
Fe	962062	2271941	1756052	2164724	1970408
Co	244127	391268	393129	529320	496711
Cu	92443	188449	80142	84472	79405
Zn	371468	1379279	1286757	1391773	1344659
As	200112	468535	412770	403374	491886
Se	203	560	391	587	526
Mo	53377	73578	35830	101193	122957
Cd	8326	31190	39196	48589	34345
Sb	14468	53228	51012	72190	61589
Te	76	298	449	579	711
Ba	414262	1041419	1015999	817784	956022
Ta	2936	4070	3641	6616	5324
Au	1655	2207	1232	3603	2389
Hg	1080	1998	2095	1153	1430
Tl	13330	48080	53608	69041	53642
Pb	21469	31773	26799	25596	23958
Bi	13237	15163	8923	18641	10683
U	39185	98136	60900	152741	91506

Appendix 11b: Geochemical analyses by laser ablation (continued)

cps	DC-94-14A	DC-94-14A	DC-94-14B	DC-94-14B	DC-94-14C
Si	465955	276949	346173	236726	638049
S	34178	21701	26546	14633	29234
Ti	185295	53291	222270	123130	266376
Fe	1566256	1232740	2165760	1646015	3533368
Co	323887	251252	443306	342852	845541
Cu	193182	145745	465353	352777	684236
Zn	815393	530416	1435798	1127736	1760466
As	532858	318846	451243	434279	800064
Se	178	296	1358	1046	543
Mo	37980	27328	49952	23297	50639
Cd	15125	9179	40932	24937	27807
Sb	110051	63079	99241	66820	214094
Te	571	480	465	452	447
Ba	823800	545140	1170304	928624	1140839
Ta	5239	2485	2186	3104	7911
Au	882	2696	996	1329	1951
Hg	1821	1093	1656	1656	3718
Tl	21351	11473	60276	38382	37298
Pb	25515	19847	65079	68156	105896
Bi	17426	9922	33381	19503	58337
U	44070	25579	56542	36651	81518

Appendix 11b: Geochemical analyses by laser ablation (continued)

cps	DC-94-14C	DC-94-15A	DC-94-15A	DC-94-15B	DC-94-15B
Si	441498	868020	404823	409716	194589
S	22699	24339	13073	20102	14356
Ti	210298	469965	219615	146012	59652
Fe	2732936	3593894	2216348	1414993	844981
Co	605679	926602	495929	339593	254383
Cu	605533	201086	109519	208174	83946
Zn	1501784	1521438	978532	961804	597123
As	557167	652401	379095	506206	325967
Se	442	814	286	773	499
Mo	40720	179324	79101	39226	28616
Cd	20106	28413	14226	14530	13236
Sb	179534	182494	65039	194619	79972
Te	396	655	320	213	213
Ba	966670	1639045	1243416	805322	796925
Ta	2385	9455	6726	1829	744
Au	1367	374	3404	188	282
Hg	2635	2271	1698	1900	1275
Tl	28551	48640	25205	30408	31536
Pb	113417	77058	45368	47931	18486
Bi	32298	12044	7182	11123	2809
U	77731	189416	90722	55329	24106

Appendix 11b: Geochemical analyses by laser ablation (continued)

cps	DC-94-15C	DC-94-15C	DC-94-16A	DC-94-16A	DC-94-16B
Si	369377	362405	240753	144611	208095
S	10917	14127	33858	26185	14270
Ti	263609	367237	84538	41933	72142
Fe	1919515	2285261	1848816	1832703	1156177
Co	548492	603218	534297	461664	307001
Cu	203990	153905	95920	107170	194022
Zn	916845	780802	1694219	2268815	791528
As	648749	885087	1160759	919603	544766
Se	645	555	560	927	408
Mo	38781	48661	215202	238880	37844
Cd	9979	10567	65164	75166	12387
Sb	84015	87476	80202	70744	144770
Te	193	410	212	245	208
Ba	778703	695119	786248	821749	609056
Ta	6263	4944	1271	2108	1044
Au	152	194	864	571	1962
Hg	1389	1528	1875	1595	979
Tl	12315	12766	84722	68588	23337
Pb	37849	54076	34095	26225	16508
Bi	10022	23934	16973	12291	14437
U	62691	76055	28755	34213	24486

Appendix 11b: Geochemical analyses by laser ablation (continued)

cps	DC-94-16B	DC-94-16C	DC-94-16C	DC-94-17A	DC-94-17A
Si	98597	84948	33093	29659	22577
S	10848	3210	1425	2247	636
Ti	59755	25531	12699	3737	7098
Fe	620282	465287	255239	194720	142428
Co	171878	114520	62485	47364	44186
Cu	82851	74538	41803	17073	15468
Zn	539789	477455	280593	90183	66401
As	284134	244058	227474	107410	102684
Se	543	139	168	98	-19
Mo	19197	18455	8791	4760	4739
Cd	6121	7825	6023	1429	757
Sb	74764	47615	31607	11729	8371
Te	61	130	41	1	0
Ba	481099	245455	188880	97268	54809
Ta	523	2119	687	102	33
Au	1356	21747	14843	41	931
Hg	471	281	351	223	47
Tl	10280	9475	6485	2822	868
Pb	13521	6149	7531	2625	2383
Bi	5328	4230	2606	1375	520
U	13105	22835	9358	9729	6837

Appendix 11b: Geochemical analyses by laser ablation (continued)

cps	DC-94-17B	DC-94-17B	DC-94-17C	DC-94-17C	DC-94-18A
Si	61654	52314	40625	20921	31884
S	1887	448	667	406	1791
Ti	17179	24675	28634	10138	4031
Fe	237629	180117	170673	96705	277652
Co	42298	36727	36561	19575	74130
Cu	18538	16044	32355	13007	22852
Zn	106054	51299	134666	74369	142262
As	82864	41381	54357	34050	1919071
Se	191	51	170	11	64
Mo	4772	2246	5900	2441	15005
Cd	1713	935	2150	1623	3286
Sb	17810	7871	13282	7961	115744
Te	141	47	66	17	13
Ba	106906	56572	153178	85822	74074
Ta	307	347	612	461	706
Au	17	770	3420	623	1480
Hg	171	196	327	112	781
Tl	3553	1952	5229	1921	3977
Pb	3857	3078	5291	3034	4393
Bi	1366	5139	2391	1911	818
U	32531	23397	24045	7185	15102

Appendix 11b: Geochemical analyses by laser ablation (continued)

cps	DC-94-18A	DC-94-18B	DC-94-18B	DC-94-18C	DC-94-18C
Si	14931	30730	25805	56031	28260
S	599	1134	705	749	459
Ti	3328	19180	13161	25467	13638
Fe	103629	258701	166390	168243	106870
Co	32678	50566	30308	30365	22153
Cu	8938	4103	3896	6156	4049
Zn	92906	177072	110274	120683	63276
As	797800	555719	180698	92486	55254
Se	12	15	5	-1	8
Mo	5039	8013	5102	4779	3534
Cd	1724	5482	4401	3994	2441
Sb	41727	32684	11894	11898	6957
Te	3	45	-10	85	17
Ba	61203	166807	115824	146764	94686
Ta	109	617	510	879	318
Au	814	493	408	579	169
Hg	281	199	192	240	142
Tl	2380	7566	4302	7893	3271
Pb	1270	3553	2108	3627	1786
Bi	1034	1048	1027	1849	1068
U	7455	11582	13208	21724	13232

Appendix 11b: Geochemical analyses by laser ablation (continued)

cps	DC-94-19A	DC-94-19A	DC-94-19B	DC-94-19B	DC-94-19C
Si	12611	6943	16242	8706	5772
S	894	848	618	461	296
Ti	3874	1866	7036	2558	2470
Fe	101919	70686	102748	46566	44916
Co	31793	21613	24106	14512	8643
Cu	8308	3546	5478	3953	2179
Zn	121520	71356	85850	37242	30656
As	87094	57472	85905	46900	27929
Se	-4	108	21	56	15
Mo	13355	6827	4954	2352	4042
Cd	5056	3448	4558	1617	1514
Sb	15625	6064	33272	9533	5816
Te	197	38	129	0	25
Ba	105590	69642	119074	77346	37560
Ta	434	213	717	184	387
Au	412	1985	79	70	95
Hg	144	100	321	103	155
Tl	8146	4782	6996	2496	1792
Pb	2146	1376	2239	1430	2620
Bi	2330	819	2400	3542	850
U	8672	4147	7574	2640	4250

Appendix 11b: Geochemical analyses by laser ablation (continued)

cps	DC-94-19C	DC-94-20A	DC-94-20A	DC-94-20B	DC-94-20B
Si	9916	3346	2434	10176	7576
S	483	399	347	349	355
Ti	7789	568	673	3279	3130
Fe	65582	34477	28909	49207	35261
Co	15228	8778	8428	14358	11925
Cu	2983	2078	1918	5633	4836
Zn	41236	71534	54646	55700	41096
As	35017	37186	27037	40130	25213
Se	-40	-3	32	47	20
Mo	5617	3620	2735	5323	3141
Cd	2143	3327	4008	2279	1872
Sb	10730	3328	1955	4961	4628
Te	105	-15	4	-7	75
Ba	78073	80773	91714	102794	92030
Ta	566	63	101	206	228
Au	273	59	57	1414	9
Hg	261	123	116	218	112
Tl	2409	7075	8067	5080	2554
Pb	2944	839	808	1710	1016
Bi	1500	288	83	377	466
U	8183	1365	1057	4037	3227

Appendix 11b: Geochemical analyses by laser ablation (continued)

cps	DC-94-20C	DC-94-20C	DC-94-21A	DC-94-21A	DC-94-21B
Si	7290	2807	13584	9679	21520
S	484	136	369	320	268
Ti	3497	691	4410	4026	7117
Fe	46501	31491	61964	45609	67009
Co	14213	10342	9469	7257	5282
Cu	3709	2542	5798	1951	1020
Zn	51451	31720	53518	26981	23407
As	42644	33624	44126	39539	68513
Se	30	-3	78	27	80
Mo	6027	6140	3329	1500	1406
Cd	4788	2230	1721	885	714
Sb	4296	2371	37055	13427	15121
Te	59	-8	45	-16	33
Ba	93647	54519	70176	55743	38594
Ta	90	8	265	273	571
Au	28	-5	515	97	88
Hg	211	111	78	64	60
Tl	6918	3408	2819	1724	1626
Pb	1235	545	1857	943	1208
Bi	763	314	4458	1001	18132
U	3682	2038	8605	4416	11238

Appendix 11b: Geochemical analyses by laser ablation (continued)

cps	DC-94-21B	DC-94-21C	DC-94-21C	DC-94-22A	DC-94-22A
Si	14670	12481	11736	1413345	235081
S	232	659	863	87710	18921
Ti	4637	2002	1680	155307	27686
Fe	59301	39988	36288	3261810	759314
Co	4043	3956	2813	2869107	617474
Cu	635	1448	1437	823019	162888
Zn	25224	14345	10593	1192904	264564
As	55404	15288	19663	3474485	1192412
Se	-5	52	19	1545	290
Mo	1590	836	525	200440	29458
Cd	1003	368	255	30502	6632
Sb	11557	6121	4683	1798503	275894
Te	24	29	4	2088	297
Ba	54161	27014	22248	310414	69389
Ta	421	120	115	19143	2769
Au	203	179	7	4467	1280
Hg	103	51	87	1912	514
Tl	1404	765	410	29262	7398
Pb	1022	722	1262	27707	4953
Bi	945	741	392	98687	15686
U	7527	4768	4167	165176	32888

Appendix 11b: Geochemical analyses by laser ablation (continued)

cps	DC-94-22B	DC-94-22B	DC-94-22C	DC-94-22C	DC-94-23A
Si	805832	823726	892131	773996	825582
S	28453	36967	46678	62285	104777
Ti	105424	160810	129374	207240	214754
Fe	1039691	1589249	1888443	2171093	2439121
Co	300023	469693	461286	556696	833549
Cu	102683	148369	220725	249089	177895
Zn	936403	1205154	1130868	1304502	1392293
As	625488	780127	1124841	976991	1141546
Se	1597	1469	1937	2108	1024
Mo	35386	43724	59204	56163	104129
Cd	19031	30249	35542	33833	28849
Sb	176742	140803	152521	151568	148242
Te	555	541	719	881	753
Ba	351387	583327	444683	533426	542900
Ta	4873	4774	5887	5532	5117
Au	5775	2185	702	5859	1047
Hg	1024	999	1234	2115	1414
Tl	26334	37676	34665	37675	36881
Pb	8600	18538	17650	14870	18508
Bi	17582	15263	19715	31276	21519
U	44292	70975	68731	61407	83953

Appendix 11b: Geochemical analyses by laser ablation (continued)

cps	DC-94-23A	DC-94-23B	DC-94-23B	DC-94-23C	DC-94-23C
Si	786143	1270183	1827720	1251456	498943
S	125189	98668	82983	38662	24049
Ti	240736	254130	580554	251229	79227
Fe	2555296	2370065	2345367	1904333	747861
Co	724147	531499	551550	395403	174324
Cu	182967	164043	206481	154896	73418
Zn	1392639	2055479	2105881	1175805	559765
As	1485771	1391255	1338120	726963	343129
Se	796	2065	1979	2091	612
Mo	94434	85352	87495	262898	89359
Cd	31950	55180	49487	18550	9203
Sb	134922	116646	95057	162945	53495
Te	608	545	733	676	127
Ba	638738	696669	796228	530756	276659
Ta	6413	7214	7340	4485	771
Au	969	9626	1115	789	1060
Hg	1336	2358	2185	2306	857
Tl	41623	60199	63307	35006	14060
Pb	15281	31427	27359	24478	12367
Bi	12360	26126	37403	15748	6508
U	92096	164057	157319	165244	54068

Appendix 11b: Geochemical analyses by laser ablation (continued)

cps	DC-94-24A	DC-94-24A	DC-94-24B	DC-94-24B	DC-94-24C
Si	1161456	623528	1519596	1628580	15686
S	90496	49625	34773	68271	1851
Ti	168005	82103	317756	347905	9229
Fe	2877040	1433251	1991670	2683942	160616
Co	604320	285453	431695	598700	35499
Cu	108471	45238	79677	110175	10156
Zn	1372860	776188	1305329	2029651	185038
As	1697183	827204	615183	909434	311212
Se	1169	346	520	479	533
Mo	99969	35352	74950	95894	18448
Cd	32167	12527	35441	57054	6786
Sb	124787	48095	120738	96818	14752
Te	534	310	521	593	337
Ba	697420	457400	350866	826819	244500
Ta	4245	1370	3499	5066	1514
Au	2001	219	576	350	241
Hg	1608	789	661	1190	2607
Tl	40063	18446	31088	59154	7663
Pb	18338	7541	14903	23524	5707
Bi	10494	3939	19308	13464	4363
U	71985	30672	74898	85292	34152

Appendix 11b: Geochemical analyses by laser ablation (continued)

cps	DC-94-24C	DC-94-25A	DC-94-25A	DC-94-25B	DC-94-25B
Si	14959	4333	10478	2647	5985
S	1994	1760	3259	1326	1500
Ti	3546	962	1052	1088	3037
Fe	164942	108859	128062	98818	107137
Co	79259	32230	46040	40624	42211
Cu	9463	15536	9099	6645	8005
Zn	248300	171971	235636	241067	195807
As	308377	165561	181248	160331	158104
Se	466	188	512	503	249
Mo	15159	6486	8697	7735	6902
Cd	9462	3677	6125	4024	5481
Sb	7827	4913	3962	3434	4200
Te	133	84	143	42	27
Ba	702825	409000	511753	592182	537809
Ta	844	191	485	243	865
Au	19681	228	204	105	1477
Hg	3146	1868	2084	2173	2289
Tl	12598	15700	23397	16598	10709
Pb	14795	5478	7465	5747	6264
Bi	6164	2468	2517	2653	3998
U	33076	21154	20524	15166	22450

Appendix 11b: Geochemical analyses by laser ablation (continued)

cps	DC-94-25C	DC-94-25C	DC-94-26A	DC-94-26A	DC-94-26B
Si	4865	5751	10538	8911	41793
S	2098	1816	1735	1756	9971
Ti	10001	6177	19685	5414	5793
Fe	184447	155091	184094	151154	149163
Co	75657	47863	53846	48346	35406
Cu	14103	11134	30422	20919	12845
Zn	148368	207608	210733	207069	141660
As	409320	225469	261982	198158	135191
Se	351	261	137	248	142
Mo	14580	16221	12354	14297	10476
Cd	3518	6024	5436	5023	4487
Sb	12228	10514	18753	11791	22953
Te	219	91	413	81	90
Ba	490797	495343	539832	434057	349361
Ta	945	840	1365	295	986
Au	3254	1712	1599	521	464
Hg	1898	1408	1954	2516	1792
Tl	3532	10759	10582	11431	8862
Pb	23865	10987	7872	9591	9228
Bi	18148	14175	8083	4835	5204
U	21739	22512	20095	27118	36787

Appendix 11b: Geochemical analyses by laser ablation (continued)

cps	DC-94-26B	DC-94-26C	DC-94-26C	DL-94-01A	DL-94-01A
Si	32716	14936	14917	16734	12220
S	7787	1668	1367	664	1542
Ti	6767	20831	34940	18717	12983
Fe	139622	154191	141862	122349	204909
Co	57621	34946	50951	36832	49997
Cu	11473	11914	14476	9601	14313
Zn	189738	123058	112337	143207	255059
As	128857	132003	106234	65623	129394
Se	318	146	365	301	553
Mo	21598	7710	9775	4398	7570
Cd	8743	2710	2965	6618	13069
Sb	29684	28456	22991	7557	10071
Te	248	86	199	93	87
Ba	394421	247945	178665	325816	534394
Ta	1391	2398	3644	1146	334
Au	1377	9144	1188	159	91
Hg	2004	1279	1267	1160	1345
Tl	13795	5449	6154	5310	12025
Pb	11392	12397	13670	14515	11130
Bi	6583	6082	3556	5375	5519
U	34681	47010	49306	29703	34420

Appendix 11b: Geochemical analyses by laser ablation (continued)

cps	DL-94-01B	DL-94-01B	DL-94-01C	DL-94-01C	DL-94-02A
Si	7865	8484	19473	7406	20163
S	2280	2690	768	1530	973
Ti	5412	7711	9838	2550	6274
Fe	103913	120503	76057	88638	106695
Co	47366	35281	38925	49569	38872
Cu	8459	9399	5078	7202	8768
Zn	155445	91503	92227	136347	136416
As	104664	75627	45092	59527	72099
Se	112	143	161	248	226
Mo	7463	5419	5535	5963	5311
Cd	4232	3285	3248	5866	5674
Sb	8326	10662	9169	4981	11350
Te	327	113	643	222	328
Ba	521327	302535	282957	402624	489380
Ta	2985	1873	1999	1008	5050
Au	596	793	721	2941	5063
Hg	669	659	625	948	1857
Tl	4439	3272	2615	3483	10572
Pb	10929	10345	12820	14014	11278
Bi	5261	6861	8861	5734	24662
U	19835	31160	24903	19096	69158

Appendix 11b: Geochemical analyses by laser ablation (continued)

cps	DL-94-02A	DL-94-02B	DL-94-02B	DL-94-02C	DL-94-02C
Si	16884	21426	21062	2935	3786
S	1012	1340	1056	445	906
Ti	6791	14814	11944	1764	3731
Fe	98112	103507	103670	98871	114388
Co	36532	35537	43512	48723	47512
Cu	6410	8310	5154	6456	6599
Zn	125530	85841	150006	159581	158811
As	70374	64390	58237	68829	73609
Se	229	154	138	303	115
Mo	5629	7409	6962	4878	5263
Cd	5069	3451	4066	8758	9539
Sb	12952	15793	12589	7806	9327
Te	235	189	393	40	116
Ba	510384	483515	471405	419125	430548
Ta	2507	2354	1714	1259	948
Au	290	507	321	2201	1249
Hg	1779	704	1148	982	577
Tl	10442	3968	6077	8607	9587
Pb	7478	8123	8634	10003	11844
Bi	29515	6770	5779	3177	3175
U	57539	39586	29188	7683	8888

Appendix 11b: Geochemical analyses by laser ablation (continued)

cps	WH-94-01-A	WH-94-01-A	WH-94-01-B	WH-94-01-B	WH-94-01-C	WH-94-01-C
Si	24192	23766	35548	35693	14288	23200
S	3352	2699	5104	4290	671	1078
Ti	29198	41256	39676	48792	11139	18860
Fe	474745	477961	733892	753574	141396	162427
Co	369114	261538	463368	210445	195461	178274
Cu	33618	34988	1524799	880320	10133	12572
Zn	800336	580052	156812	276689	310150	318074
As	51157	95231	68691	40663	18106	13228
Se	1619	1330	275	64	684	739
Mo	196653	321587	112417	83125	11314	12670
Cd	54116	43898	3525	9771	11132	8488
Sb	36694	39883	13943	8797	6538	5385
Te	42563	20240	31624	9918	532	684
Ba	271743	289891	163839	109558	184049	150081
Ta	6870	5497	6243	6426	2065	2279
Au	2997	9295	698	345	67	59
Hg	3047	1775	2207	2632	2207	2570
Tl	34413	16281	11067	16649	72534	42328
Pb	286425	347529	41876	71279	366160	310241
Bi	155586	98144	324708	881436	56547	56289
U	504965	1128138	158842	160830	114720	80164

Appendix 11b: Geochemical analyses by laser ablation (continued)

cps	WH-94-02-A	WH-94-02-A	WH-94-02-B	WH-94-02-B	WH-94-02-C
Si	23680	13265	10121	3523	8619
S	132	684	1244	1066	1365
Ti	62959	8486	5693	5953	4600
Fe	244333	159235	102336	105406	164150
Co	59354	153268	178564	196925	107977
Cu	5200	5289	13164	12317	11270
Zn	88871	291300	390402	397820	232777
As	13203	6123	17186	19136	8044
Se	72	450	483	563	425
Mo	17723	20800	18417	19030	64842
Cd	2236	723	1944	2202	1031
Sb	19712	8041	24225	21979	18994
Te	187	8462	6548	5448	8427
Ba	73354	1170	1262	548	315
Ta	3024	120067	139959	147935	58005
Au	111	2246	8423	4350	1849
Hg	1921	1497	408	208	255
Tl	8588	3393	2914	2977	2122
Pb	14042	11193	58979	62636	27003
Bi	3045	627080	496535	570703	26873
U	92083	79217	94106	85777	16438

Appendix 11b: Geochemical analyses by laser ablation (continued)

cps	WH-94-02-C	WH-94-03-A	WH-94-03-A	WH-94-03-B	WH-94-03-B
Si	4946	15545	13211	9971	12924
S	2635	770	277	648	722
Ti	2387	6143	2609	9480	8685
Fe	258047	62515	38040	85421	61264
Co	145348	74605	46817	96484	86675
Cu	8679	5797	4077	10377	7241
Zn	289374	185906	150317	222804	172742
As	5666	11486	9623	29151	14253
Se	856	1144	669	654	600
Mo	136054	14836	7063	18269	11971
Cd	1242	2692	922	3109	1879
Sb	31373	7423	4959	8828	6631
Te	19409	3937	2309	2244	4513
Ba	742	364	387	742	245
Ta	95435	102414	89705	58232	68480
Au	2043	5582	7979	4900	3987
Hg	529	244	83	119	174
Tl	2793	2710	1928	3445	1651
Pb	44680	35784	45424	27616	30287
Bi	41554	356258	240979	296664	268358
U	21114	65415	41488	93885	77570

Appendix 11b: Geochemical analyses by laser ablation (continued)

cps	WH-94-03-C	WH-94-03-C	WH-94-04-A	WH-94-04-A	WH-94-04-B
Si	71772	57906	21305	33794	55325
S	1499	2076	4761	5350	6692
Ti	27916	22595	12464	19190	216078
Fe	282806	290682	345801	374658	471913
Co	676382	677543	1019615	951860	1188938
Cu	40254	36163	30033	20843	26216
Zn	684903	731574	587130	551805	519473
As	25221	47528	11421	13832	26259
Se	1614	1235	459	72	131
Mo	36826	36665	341910	291431	40483
Cd	3529	4663	658	513	3682
Sb	8109	11807	64179	46983	30488
Te	4705	6007	13083	9234	12974
Ba	1069	913	103	303	930
Ta	81327	110829	490993	441194	104789
Au	1834	1691	589	504	4692
Hg	775	565	308	753	1803
Tl	3219	3023	3509	4863	3261
Pb	38079	51831	20400	17030	32874
Bi	223760	377668	51048	49794	27953
U	40954	55199	2198	834	12278

Appendix 11b: Geochemical analyses by laser ablation (continued)

cps	WH-94-04-B	WH-94-04-C	WH-94-04-C	WH-94-05-A	WH-94-05-A
Si	40384	60602	29480	76698	93991
S	5133	1168	874	2416	2731
Ti	81780	230317	34567	99809	115290
Fe	538122	395452	324108	922705	830884
Co	671419	103732	233321	228197	307699
Cu	16374	102283	77224	48112	49758
Zn	240765	300663	329032	472411	468161
As	38876	14772	19289	238221	192161
Se	92	326	1040	1102	1549
Mo	20189	24830	43901	138548	129918
Cd	776	1778	3147	20430	4752
Sb	11020	3812	7246	9117	10668
Te	26358	2594	4409	18057	15731
Ba	2455	891	857	4012	3124
Ta	165419	72255	55655	60437	105012
Au	925	10672	3404	7725	5629
Hg	28	21	968	181	189
Tl	1030	1578	1345	1175	1218
Pb	35728	7430	6032	15588	25234
Bi	21515	68412	205217	262464	281148
U	34028	12563	40475	138344	100093

Appendix 11b: Geochemical analyses by laser ablation (continued)

cps	WH-94-05-B	WH-94-05-B	WH-94-05-C	WH-94-05-C	WH-94-06-A
Si	53058	38130	60242	57830	23057
S	3014	3819	2092	468	1413
Ti	44068	13218	26371	23744	10178
Fe	912742	898268	533748	333397	297966
Co	329754	150615	257113	127933	107585
Cu	21621	22750	23435	24179	23569
Zn	466660	350621	261782	192494	211864
As	48895	30462	35302	16124	8858
Se	1591	1179	1052	539	215
Mo	63157	71001	90632	54359	17511
Cd	31374	25051	2020	4918	1763
Sb	9196	7673	5021	4664	4631
Te	6974	9665	4762	3946	4584
Ba	707	894	1359	519	986
Ta	87189	69257	65890	38633	32197
Au	2805	1455	2158	2193	1016
Hg	358	19677	94	219	4622
Tl	1150	999	813	977	1127
Pb	13512	12629	4636	6247	1858
Bi	214013	218883	225436	138823	77724
U	66099	38509	41714	30239	13213

Appendix 11b: Geochemical analyses by laser ablation (continued)

cps	WH-94-06-A	WH-94-06B	WH-94-06B	WH-94-06C	WH-94-06C
Si	41496	37606	35237	18681	23968
S	1384	2901	1403	1386	2124
Ti	11704	35106	31464	36397	22007
Fe	342171	388432	363057	253061	286806
Co	145036	388447	260254	226751	256493
Cu	9845	29886	34169	13139	11316
Zn	311905	531811	382530	270921	305409
As	9228	24515	37124	44085	51922
Se	245	1378	1229	564	376
Mo	13124	56223	41287	46811	50791
Cd	4102	7781	4674	1524	745
Sb	3996	21198	14536	18655	21887
Te	3878	7492	7567	4675	4466
Ba	437	1261	1031	1044	982
Ta	35365	184403	104358	93122	80430
Au	856	3112	2549	3128	1704
Hg	16522	1375	299	706	405
Tl	1477	1903	1097	2432	2016
Pb	1652	7273	4394	11157	13497
Bi	70219	269480	187610	345694	323718
U	7386	65849	44421	54925	53436

Appendix 11b: Geochemical analyses by laser ablation (continued)

cps	WH-94-07A	WH-94-07A	WH-94-07B	WH-94-07B	WH-94-07C
Si	21204	19613	33511	31456	33926
S	6294	1398	5386	32995	7319
Ti	21396	13669	48355	189022	146529
Fe	461801	205892	93234	465608	297410
Co	105721	93222	2560161	2389968	137088
Cu	59937	33416	87906	38430	38743
Zn	327133	169421	311140	449403	175418
As	14748	4748	25539	25349	31575
Se	674	549	877	-431	2362
Mo	95885	42596	99335	51935	22559
Cd	3930	7259	2075	2131	7018
Sb	3146	1701	33962	58077	66523
Te	5021	3250	50	136	76
Ba	1149	324	17074	57877	14487
Ta	20699	28201	293	998	462
Au	1512	680	-15	275	196
Hg	2544	56208	269	278	386
Tl	2775	2861	2889	5241	613
Pb	16313	9797	4748	99921	31007
Bi	217765	212104	393	4883	7554
U	46981	21900	6820	9057	41043

Appendix 11b: Geochemical analyses by laser ablation (continued)

cps	WH-94-07C	WH-94-08A	WH-94-08A	WH-94-08B	WH-94-08B
Si	65417	364311	129026	137293	97296
S	13607	25361	25500	25539	27348
Ti	101110	137923	116977	126994	105287
Fe	373250	1035880	780329	639628	738745
Co	121215	583904	527667	554770	455509
Cu	52011	46804	70708	242351	121352
Zn	209155	527648	405487	500446	513378
As	42187	56989	34755	120406	116210
Se	4138	7757	11280	12261	13710
Mo	28453	22239	26648	49018	44452
Cd	1142	1705	2118	2183	2617
Sb	100386	73621	114567	103798	131350
Te	103	302	194	498	429
Ba	18067	8719	14474	21517	15625
Ta	753	1261	775	1182	656
Au	161	290	441	570	156
Hg	615	968	1238	1349	1216
Tl	951	1401	3583	3557	4584
Pb	37020	55026	58738	52465	47943
Bi	12720	23946	18226	14149	12443
U	58629	19155	37458	61735	60157

Appendix 11b: Geochemical analyses by laser ablation (continued)

cps	WH-94-08C	WH-94-08C	WH-94-09-A	WH-94-09-A	WH-94-09-B
Si	254309	180324	512027	427312	482048
S	41405	47384	25236	20678	35984
Ti	297825	313697	302181	579093	2925924
Fe	1932338	2107625	1005035	882458	1557548
Co	360341	542834	236993	266749	983607
Cu	118151	494929	70397	83340	806660
Zn	806566	1118482	362720	350779	707542
As	259281	222760	62865	60347	66645
Se	4531	3295	12741	6238	1036
Mo	130933	192121	32135	30141	43440
Cd	4373	4702	2401	3922	3539
Sb	119112	120970	201148	185271	112804
Te	1180	1767	193	252	739
Ba	27327	8795	32224	29991	16206
Ta	1548	1806	2970	11445	7907
Au	1487	3614	398	8728	-17
Hg	507	2082	1296	1004	97
Tl	2440	2519	3944	2964	5106
Pb	68255	60527	42551	55090	10736
Bi	30197	30293	19861	29820	1557
U	50725	50335	48851	44336	55454

Appendix 11b: Geochemical analyses by laser ablation (continued)

cps	WH-94-09-B	WH-94-09-C	WH-94-09-C	WH-94-10-A	WH-94-10-A
Si	253664	208811	151974	242132	482091
S	35833	25882	16263	43052	64808
Ti	2658740	984955	1145041	192783	132471
Fe	1533028	1060456	761623	1753297	3721315
Co	1045287	434144	197665	750467	704173
Cu	318048	54046	9886	25356	26962
Zn	425665	377977	227724	333030	319269
As	55065	347817	176572	241969	326865
Se	-491	4564	1516	3911	1840
Mo	52985	96057	60562	68511	78073
Cd	5410	2798	4804	4096	2088
Sb	87258	91774	64234	86412	109610
Te	734	2835	1320	966	610
Ba	13650	16084	5215	14047	7028
Ta	5406	4496	4540	1182	349
Au	28	-7	27	806	-20
Hg	231	82	289	391	74
Tl	5338	2319	981	1872	2711
Pb	3852	66070	44397	54474	52313
Bi	969	50158	42418	12552	1520
U	61138	11213	5387	6709	4933

Appendix 11b: Geochemical analyses by laser ablation (continued)

cps	WH-94-10-B	WH-94-10-B	WH-94-10-C	WH-94-10-C	WH-94-11-A
Si	369300	472611	280934	167106	215241
S	12574	17779	34254	12625	24910
Ti	1467819	982344	1328046	1567526	56441
Fe	651414	810139	522048	671858	298013
Co	227834	485975	798894	1729146	1531388
Cu	14007	27180	8417	6956	24272
Zn	333397	333209	369872	160648	341130
As	24653	61583	60103	30789	8943
Se	4181	4041	2325	2059	2524
Mo	12273	46835	22406	63379	5172
Cd	855	1050	3361	1503	1464
Sb	39698	74247	40618	53407	17641
Te	145	300	71	161	0
Ba	13619	10255	8078	19129	39731
Ta	2068	1349	2936	3171	150
Au	23	4692	-8	36	172
Hg	222	692	-130	455	289
Tl	589	1466	2943	4549	2580
Pb	29680	38230	38806	18280	3118
Bi	1102	8028	292	144	327
U	4735	8591	5730	4132	2182

Appendix 11b: Geochemical analyses by laser ablation (continued)

cps	WH-94-11-A	WH-94-11-B	WH-94-11-B	WH-94-11-C	WH-94-11-C
Si	96019	214022	156219	8568	3517
S	5731	5932	9327	7561	3096
Ti	16808	46605	51867	48452	139882
Fe	128482	179381	157331	87663	80030
Co	428461	132569	107909	1208645	228547
Cu	2888	14157	28548	47280	5530
Zn	74409	59395	75985	359949	25901
As	3357	9889	4265	5193	7426
Se	2502	4430	1310	415	385
Mo	1396	3269	2657	3887	1619
Cd	569	196	495	8377	292
Sb	4014	24463	21570	1490	757
Te	-39	18	133	49	-14
Ba	6408	5350	-2574	75089	3688
Ta	160	122	93	397	1596
Au	-23	55	14879	0	10
Hg	186	345	459	391	426
Tl	682	439	911	8998	544
Pb	411	7722	5866	1749	554
Bi	15	1830	1542	85	283
U	429	2043	2252	1664	2463

Appendix 11b: Geochemical analyses by laser ablation (continued)

cps	WH-94-12-A	WH-94-12-A	WH-94-12-B	WH-94-12-B	WH-94-12-C
Si	59349	112569	27941	59942	57837
S	5261	7999	5042	4315	28210
Ti	80429	67143	22488	24162	129156
Fe	425125	472070	548402	144913	619502
Co	130353	153981	20356	156992	987522
Cu	6727	7255	30480	26617	410467
Zn	84364	92056	111688	50456	561628
As	72865	48147	40100	4423	107641
Se	360	881	1176	1321	791
Mo	36885	41281	31642	5456	57954
Cd	608	485	250	305	5329
Sb	1272	1634	956	719	7716
Te	230	163	157	13	323
Ba	5903	7261	1026	2093	14773
Ta	322	367	129	185	377
Au	1	25	-15	4915	22
Hg	-60	62	213	89	112
Tl	616	293	308	441	1095
Pb	16369	25995	10156	9323	47554
Bi	4852	5849	622	1397	722
U	1968	1458	1834	2027	39812

Appendix 11b: Geochemical analyses by laser ablation (continued)

cps	WH-94-12-C	WH-94-13-A	WH-94-13-A	WH-94-13-B	WH-94-13-B
Si	27300	124751	93052	32831	11404
S	5943	61521	55283	7335	5597
Ti	215440	19648	15980	8694	4600
Fe	233118	2705018	2455345	463453	305938
Co	279265	19753	47371	19352	27046
Cu	97774	29626	24818	14852	8546
Zn	86657	173275	181224	63245	27694
As	37389	174938	91772	25029	14618
Se	53	3995	2739	513	412
Mo	39048	22910	20917	15619	9032
Cd	4080	4035	2617	376	90
Sb	2026	2366	1330	742	545
Te	137	188	72	24	-1
Ba	3243	12894	15925	6003	4352
Ta	368	38	31	51	35
Au	7	-16	238	1274	-17
Hg	-25	275	232	125	669
Tl	264	564	798	216	226
Pb	11677	54188	25685	6028	4593
Bi	937	2066	1693	394	539
U	19958	7042	5357	1192	803

Appendix 11b: Geochemical analyses by laser ablation (continued)

cps	WH-94-13-C	WH-94-13-C	WH-94-14-A	WH-94-14-A	WH-94-14-B
Si	70905	58286	59868	110667	1729
S	4013	4420	4629	5359	660
Ti	11197	47462	714957	856122	5411
Fe	163741	262726	441733	759027	39868
Co	12547	5955	6219	15808	18101
Cu	4763	7247	246123	282991	1836
Zn	7654	24969	13894	16797	7411
As	18026	25578	26443	46118	1161
Se	799	1524	350	492	396
Mo	6839	8765	3900	7384	1209
Cd	162	119	-17	52	-1
Sb	217	233	1886	2076	69
Te	45	0	268	294	2
Ba	943	2775	2621	3687	2659
Ta	70	527	88	37	31
Au	-14	40	177	188	-9
Hg	145	285	-80	725	87
Tl	214	182	205	222	85
Pb	6089	7001	456	328	1880
Bi	2149	6111	292	158	971
U	1060	1738	4363	5070	1321

Appendix 11b: Geochemical analyses by laser ablation (continued)

cps	WH-94-14-B	WH-94-14-C	WH-94-14-C	WH-94-15-A	WH-94-15-A
Si	5591	42338	4213	15248	24188
S	2410	10063	5576	1539	480
Ti	4741	251250	55522	170950	84566
Fe	82536	107484	31349	61417	52143
Co	7986	128068	927423	19929	16729
Cu	11974	25588	45248	1843	4433
Zn	7611	38526	161743	9746	13598
As	986	6906	2296	1386	693
Se	655	-25	181	-103	54
Mo	1435	1719	1787	4370	6501
Cd	73	727	1494	114	35
Sb	330	776	290	302	336
Te	-11	7	26	36	17
Ba	3705	28806	31333	787	814
Ta	34	296	27	889	467
Au	18	14352	101	-2	-8
Hg	219	12	162	37	-30
Tl	170	1025	3005	114	86
Pb	1623	792	367	2505	791
Bi	1072	100	28	3060	4267
U	2244	675	582	430	2098

Appendix 11b: Geochemical analyses by laser ablation (continued)

cps	WH-94-15-B	WH-94-15-B	WH-94-15-C	WH-94-15-C	WH-94-16-A
Si	68049	6952	4697	7833	62516
S	1898	813	411	836	2286
Ti	23783	11577	3057	11960	9038
Fe	34750	18847	17066	52022	31773
Co	27718	15864	6522	33439	2725
Cu	6890	1137	1511	4595	2100
Zn	27880	7233	2851	23141	9914
As	1047	1299	294	1486	3077
Se	251	-253	91	346	98
Mo	2297	1550	867	2313	828
Cd	56	45	79	80	83
Sb	203	119	81	55	153
Te	16	-30	47	-31	-13
Ba	1850	837	914	1810	2083
Ta	242	287	14	74	118
Au	4740	226	-9	-11	8976
Hg	114	23	-4	281	78
Tl	192	385	50	173	21
Pb	1823	1297	773	2285	159
Bi	207	471	264	819	-8
U	1509	204	749	865	452

Appendix 11b: Geochemical analyses by laser ablation (continued)

cps	WH-94-16-A	WH-94-16-B	WH-94-16-B	WH-94-16-C	WH-94-16-C
Si	70789	33977	31824	19154	69676
S	2314	749	1146	1616	2265
Ti	49758	17240	10975	36168	42430
Fe	66556	20363	23214	72938	87940
Co	6337	8568	16406	169295	50784
Cu	2708	16639	1816	3349	16555
Zn	29885	10505	9349	61295	106046
As	2402	329	244	4696	5031
Se	91	442	131	-44	352
Mo	1113	1276	1174	6725	5578
Cd	181	38	31	273	401
Sb	238	498	606	403	565
Te	-23	-18	26	40	-2
Ba	10937	2779	1852	3210	2588
Ta	132	75	152	315	350
Au	641	1079	944	21	721
Hg	2	161	43	73	380
Tl	42	257	268	404	248
Pb	242	1408	1555	5589	5344
Bi	23	291	141	2316	2909
U	501	173	326	1283	1932

Appendix 11b: Geochemical analyses by laser ablation (continued)

cps	WH-94-17-A	WH-94-17-A	WH-94-17-B	WH-94-17-B	WH-94-17-C
Si	10491	2475	4898	66833	9857
S	3348	1583	1067	1391	577
Ti	11573	7453	9183	88021	5732
Fe	80248	41370	31801	43344	26702
Co	282840	108209	19237	28854	7740
Cu	5471	2599	2596	2153	2764
Zn	33036	14060	8371	8564	4729
As	1185	865	440	1589	1095
Se	692	496	250	188	-96
Mo	3505	1990	2506	3370	871
Cd	176	70	-26	78	19
Sb	263	107	214	182	73
Te	17	-3	9	-2	15
Ba	6587	2949	1970	2922	1126
Ta	61	22	132	635	49
Au	-6	-13	81	25	32
Hg	25	68	103	-13	-32
Tl	862	235	230	291	28
Pb	10703	6152	1661	3335	718
Bi	1701	1343	313	995	301
U	1765	1060	1269	9035	481

Appendix 11b: Geochemical analyses by laser ablation (continued)

cps	WH-94-17-C	WH-94-18-A	WH-94-18-A	WH-94-18-B	WH-94-18-B
Si	9586	4179	5559	13217	8453
S	1784	415	1376	506	192
Ti	9412	2468	4236	1895	3765
Fe	53078	10163	31974	9960	6494
Co	61769	8471	67401	13715	9129
Cu	5164	745	3290	1598	2322
Zn	12616	3398	11275	12222	6169
As	1828	263	274	212	176
Se	80	30	209	-76	-95
Mo	1859	419	1466	458	1480
Cd	139	20	109	52	-4
Sb	15	133	18	1770	-52
Te	-29	-8	-14	7	-16
Ba	4354	723	4078	662	1215
Ta	81	16	45	3	72
Au	22	13	1	-2	283
Hg	203	-82	92	-26	47
Tl	86	39	409	124	66
Pb	3583	609	4337	910	481
Bi	574	180	534	271	92
U	799	82	630	228	175

Appendix 11b: Geochemical analyses by laser ablation (continued)

cps	WH-94-18-C	WH-94-18-C	WH-94-19-A	WH-94-19-A	WH-94-19-B
Si	64230	13738	1206	2696	12467
S	2423	1657	1200	605	1115
Ti	26186	38312	10774	4970	21638
Fe	44555	58488	25123	23446	49796
Co	33167	43741	12627	37070	72340
Cu	1570	1300	1222	1317	3772
Zn	13499	22328	7154	7459	14598
As	1401	2095	1413	495	904
Se	82	-48	164	176	226
Mo	4879	4010	1715	1003	2534
Cd	281	295	26	50	182
Sb	100	23	71	53	107
Te	-15	13	4	18	-14
Ba	1114	1517	1120	2603	1412
Ta	196	354	73	50	128
Au	30	-8	-5	-8	10
Hg	31	44	-9	130	54
Tl	162	292	93	160	530
Pb	5957	6284	1677	4138	5663
Bi	1529	3947	1039	479	1858
U	329	886	1135	471	712

Appendix 11b: Geochemical analyses by laser ablation (continued)

cps	WH-94-19-B	WH-94-19C	WH-94-19C	WH-94-20A	WH-94-20A
Si	38154	6573	2726	1022	4659
S	296	704	524	-542	583
Ti	5221	13169	5158	3795	2176
Fe	16701	43953	37757	9841	10571
Co	112697	115249	80036	20496	12242
Cu	1563	2616	2535	1069	796
Zn	20532	52691	47648	4737	2920
As	248	521	388	353	188
Se	15	246	418	111	125
Mo	3268	3132	1782	748	513
Cd	116	178	114	71	50
Sb	72	71	51	-31	-107
Te	27	0	-18	11	-6
Ba	1310	3887	2387	488	813
Ta	33	99	61	22	21
Au	184	1	9	10	1
Hg	17	81	31	87	50
Tl	456	228	214	68	8
Pb	2912	4222	3732	1243	654
Bi	328	944	531	198	108
U	270	176	135	294	152

Appendix 11b: Geochemical analyses by laser ablation (continued)

cps	WH-94-20B	WH-94-20B	WH-94-20C	WH-94-20C	WH-94-21A
Si	17675	24269	21701	28128	161172
S	300	1363	1190	2686	1931
Ti	7945	17149	11165	9903	5985
Fe	21765	43649	58564	51016	27703
Co	34200	168047	184431	199921	5913
Cu	2547	6447	4192	5997	3808
Zn	8529	23026	20966	31953	143694
As	349	1355	1238	2032	568
Se	234	350	566	129	208
Mo	727	3499	2207	2429	1866
Cd	68	324	191	160	127
Sb	119	145	336	117	208
Te	8	21	16	37	24
Ba	701	3855	2353	2952	38153
Ta	45	87	23	84	64
Au	9	24	12	2	4415
Hg	-9	-10	79	95	102
Tl	149	660	591	345	30
Pb	1511	5636	5741	4432	678
Bi	233	706	870	677	204
U	383	1320	908	1283	1127

Appendix 11b: Geochemical analyses by laser ablation (continued)

cps	WH-94-21A	WH-94-21B	WH-94-21B	WH-94-21C	WH-94-21C
Si	2865	9976	8742	43735	58428
S	568	2005	389	1689	1613
Ti	622	17971	11655	9286	7184
Fe	7548	95995	47623	38684	42916
Co	2737	41171	13002	34389	67547
Cu	703	4920	3081	4999	5459
Zn	20998	12290	5993	11934	16522
As	171	3765	1280	751	762
Se	16	315	329	59	279
Mo	212	4643	1076	1322	1724
Cd	18	92	57	94	165
Sb	-23	362	172	274	198
Te	7	0	-3	0	0
Ba	526	1263	671	1842	2635
Ta	3	74	48	25	25
Au	9	13	0	-2	3
Hg	13	149	-15	26	-1
Tl	-1	250	99	190	157
Pb	284	2521	1046	1928	2379
Bi	62	1521	472	427	400
U	110	938	258	290	300

Appendix 11b: Geochemical analyses by laser ablation (continued)

cps	WH-94-22A	WH-94-22A	WH-94-22B	WH-94-22B	WH-94-22C
Si	9444	55368	9632	15076	7555
S	2685	5019	2985	5858	1294
Ti	5425	18121	16240	23796	418
Fe	86984	152097	81287	123580	2840
Co	66532	110245	229092	645318	7265
Cu	7533	10753	9992	14995	1166
Zn	39131	75300	45848	123903	4084
As	894	1925	2393	2344	33
Se	119	130	226	398	-60
Mo	1406	4953	1967	3951	137
Cd	435	281	439	641	4
Sb	82	287	399	185	102
Te	25	5	12	-3	-1
Ba	41230	73226	6291	14360	421
Ta	22	45	54	50	4
Au	18	101	-6	-3	267
Hg	58	69	7	144	-13
Tl	181	179	967	1107	40
Pb	701	1737	4055	8508	144
Bi	219	349	798	869	8
U	773	1072	1209	1667	16

Appendix 11b: Geochemical analyses by laser ablation (continued)

cps	wh-94-22C	wh-94-23A	wh-94-23A	wh-94-23B	wh-94-23B
Si	19413	17099	9372	29588	50688
S	3246	1687	1726	8792	5469
Ti	3262	19141	12786	103426	118311
Fe	32402	36403	42107	185480	181416
Co	445279	30784	82858	245632	328439
Cu	4470	57020	5191	6815	24017
Zn	143750	8475	12326	85043	102265
As	3031	799	1572	7690	7679
Se	179	11	535	671	13
Mo	4434	899	1328	6725	6301
Cd	1433	31	53	252	213
Sb	31	172	135	698	942
Te	20	13	8	100	129
Ba	4952	545	878	4519	5035
Ta	9	18	31	169	250
Au	-2	372	62	6321	4974
Hg	130	12	73	157	110
Tl	1081	102	193	331	147
Pb	12707	1797	2653	15490	13143
Bi	93	624	679	4509	3775
U	95	233	268	466	411

Appendix 11b: Geochemical analyses by laser ablation (continued)

cps	WH-94-23C	WH-94-23C	WH-94-24A	WH-94-24A	WH-94-24B
Si	22118	10711	14509	24266	22858
S	1878	849	2304	3766	1151
Ti	1856	4081	42443	76834	9595
Fe	19963	4843	100477	135013	48263
Co	11348	1608	131625	108970	100455
Cu	1398	1304	6523	7999	2886
Zn	15959	7499	30342	27802	13765
As	212	99	3542	4976	524
Se	541	136	-101	492	213
Mo	463	345	2300	2671	3057
Cd	112	33	172	238	26
Sb	19	45	32	92	193
Te	5	8	21	41	16
Ba	1398	147	2718	4431	1790
Ta	0	33	143	135	17
Au	19	51	43	527	2
Hg	-30	48	86	125	-2
Tl	5	15	318	180	299
Pb	1020	99	7401	7333	3699
Bi	84	1	2077	2984	358
U	54	42	658	1318	246

Appendix 11b: Geochemical analyses by laser ablation (continued)

cps	WH-94-24B	WH-94-24C	WH-94-24C	HB-94-01A	HB-94-01A
Si	44488	9487	20484	44589	43098
S	3442	3971	1009	8259	10672
Ti	19448	45582	20068	21599	11139
Fe	54590	94903	51835	256969	227321
Co	489407	243144	124227	110053	123337
Cu	13459	7211	3835	11738	12889
Zn	54607	29836	17257	119490	98399
As	944	4246	2147	3418	3765
Se	266	119	498	94	207
Mo	6662	3188	1764	29390	16962
Cd	891	202	181	730	738
Sb	152	244	14	188	440
Te	-23	5	32	47	22
Ba	3199	2602	994	106721	98784
Ta	28	114	19	91	112
Au	-9	-5	-10	12	175
Hg	196	66	-41	156	179
Tl	454	542	204	308	344
Pb	21735	9163	3261	3154	2265
Bi	220	2031	707	717	534
U	144	342	407	3051	2838

Appendix 11b: Geochemical analyses by laser ablation (continued)

cps	HB-94-01B	HB-94-01B	HB-94-01C	HB-94-01C	HB-94-02A
Si	93340	52935	213962	79987	65734
S	10098	9952	10287	5087	5061
Ti	51554	44223	7147	7782	12181
Fe	257326	284979	193264	115956	251745
Co	93683	85683	45808	31556	37880
Cu	11844	11673	9272	8922	6402
Zn	134110	119914	84142	66737	65573
As	3549	3659	3374	1270	4206
Se	3	181	-447	872	121
Mo	1822	2013	1515	1110	1971
Cd	1762	1588	1815	920	822
Sb	160	448	343	160	344
Te	31	0	15	1	12
Ba	116528	111204	61707	47829	54718
Ta	87	79	86	-9	59
Au	2	-1	626	0	-12
Hg	276	233	144	305	207
Tl	339	398	544	369	161
Pb	2076	2311	1221	570	1091
Bi	699	947	408	232	363
U	3133	2884	1212	912	1126

Appendix 11b: Geochemical analyses by laser ablation (continued)

cps	HB-94-02A	HB-94-02B	HB-94-02B	HB-94-02C	HB-94-02C
Si	156185	50321	190937	320759	636148
S	17512	10181	17163	7365	10835
Ti	25320	7149	18048	37763	112353
Fe	341243	266571	329922	199480	661571
Co	62135	74720	105334	56991	99264
Cu	10778	17023	45686	7540	18512
Zn	120127	83634	191955	107937	164879
As	10188	2046	5251	3530	6927
Se	-116	269	71	241	-40
Mo	22253	1299	8848	1838	4342
Cd	1866	594	2581	972	3381
Sb	424	194	650	137	348
Te	52	29	-4	16	38
Ba	96488	98909	251110	67700	88060
Ta	27	15	64	10	96
Au	55	-4	21	24	-8
Hg	261	179	240	141	252
Tl	348	203	1414	225	367
Pb	1128	905	1054	592	1716
Bi	356	283	358	106	417
U	2706	1930	5247	996	3195

Appendix 11b: Geochemical analyses by laser ablation (continued)

cps	HB-94-03A	HB-94-03A	HB-94-03B	HB-94-03B	HB-94-03C	HB-94-03C
Si	37223	27927	45498	56986	29011	26502
S	7825	5432	2061	11393	996	1596
Ti	4336	5356	3645	2754	4749	6152
Fe	142901	129456	65910	108961	21949	18395
Co	71396	78469	25607	67081	26105	38137
Cu	10500	5843	2887	9436	5065	33753
Zn	164311	46723	28927	194135	13042	16596
As	1414	2406	2609	3180	330	381
Se	-201	59	-11	437	116	175
Mo	11155	2382	2913	22875	954	965
Cd	1837	836	274	3451	21	337
Sb	123	159	195	218	10	325
Te	2	8	-4	18	3	18
Ba	91954	57454	30360	108016	1490	1637
Ta	36	39	19	2	1095	80
Au	0	-4	7	6	-9	25
Hg	138	119	153	91	18	52
Tl	543	255	60	561	26	90
Pb	589	1314	1151	1058	1024	1151
Bi	200	390	242	194	170	228
U	1694	1047	4601	909	217	565

Appendix 11b: Geochemical analyses by laser ablation (continued)

cps	SS-95-01A	SS-95-01A	SS-95-01B	SS-95-01B	SS-95-01C	SS-95-01C
Si	1860	3163	12000	6488	13949	9876
S	382	1216	695	602	3127	1585
Ti	411	680	2816	1674	2485	2775
Fe	17490	47284	90755	54525	125071	151547
Co	4704	5048	58634	32539	33880	31527
Cu	717	1087	1313	2172	3549	4848
Zn	43269	14144	1661	7531	9907	13545
As	1199	1879	2431	1829	3597	7237
Se	231	126	143	111	504	250
Mo	333	171	641	1000	738	815
Cd	30	5	81	27	77	50
Sb	53	6	178	52	56	91
Te	3	1	7	-5	6	25
Ba	17319	15948	18900	45993	43048	53537
Ta	-8	-1	16	45	10	31
Au	56	-6	9	-5	8	5
Hg	8	26	0	62	35	70
Tl	53	5	64	256	40	51
Pb	120	248	84	51	844	1291
Bi	-1	13	71	52	90	64
U	25	40	1149	754	215	177
Ce						
W						

Appendix 11b: Geochemical analyses by laser ablation (continued)

cps	SS-95-02A	SS-95-02A	SS-95-02B	SS-95-02B	SS-95-02C	SS-95-03A
Si	7942	17657	13881	15377	16439	23482
S	1827	2061	1085	1644	753	2485
Ti	3484	5191	3375	21878	2982	1882
Fe	148395	141512	63772	94030	102478	117513
Co	46406	62930	34404	55861	45975	47648
Cu	3077	9008	2562	3445	4860	2902
Zn	9992	16997	831843	831142	21557	17921
As	7135	6300	1991	3405	3461	16838
Se	134	-219	132	92	-147	110
Mo	1550	2421	876	929	1543	646
Cd	82	-8	27	137	33	66
Sb	160	38	111	150	247	120
Te	8	4	10	-21	4	38
Ba	114994	149257	55815	119101	144187	98768
Ta	23	7	12	9	49	0
Au	50	6	8	-1	11	-6
Hg	-45	14	380	736	96	39
Tl	117	235	105	261	153	164
Pb	889	1129	1152	1525	784	1174
Bi	153	104	94	153	79	84
U	708	666	416	561	556	142
Ce						
W						

Appendix 11b: Geochemical analyses by laser ablation (continued)

cps	SS-95-03A	SS-95-03B	SS-95-03B	SS-95-03-C	SS-95-03-C	SS-95-04-A
Si	35534	7630	3711	25943	2602	29573
S	909	2978	1134	1453	2079	2273
Ti	1475	2309	538	54832	1567	5589
Fe	90285	60649	24184	107582	58126	148143
Co	25088	14373	4202	37496	21904	52286
Cu	6414	1614	1591	16335	1837	7453
Zn	18041	17273	12387	41741	14060	18874
As	6269	3189	811	5626	3134	8010
Se	95	-109	121	-370	152	170
Mo	364	418	253	4802	758	2262
Cd	2	63	47	321	43	89
Sb	197	168	79	3130	1343	200
Te	-9	19	-3	4	-7	13
Ba	46124	41899	18063	146691	97667	131137
Ta	2	11	6			
Au	1	1	2			
Hg	47	53	37	15	-5	46
Tl	115	137	32	188	121	183
Pb	705	303	130	758	192	868
Bi	41	137	10	81	44	122
U	235	143	113	286	60	276
Ce				264162	41222	148701
W				353	104	522

Appendix 11b: Geochemical analyses by laser ablation (continued)

cps	SS-95-04-A	SS-95-04-B	SS-95-04-B	SS-95-04-C	SS-95-04-C	SS-95-05-A
Si	1203	20652	8775	378405	118044	31474
S	1760	1029	1512	2248	3781	2536
Ti	4610	3297	3203	25919	5815	3988
Fe	113337	137102	147099	469857	215242	381165
Co	35039	39095	48517	110058	36296	54428
Cu	3919	5008	5718	14386	8432	7013
Zn	16200	18125	25136	888551	269811	26078
As	3470	9314	7775	43923	7810	45345
Se	310	-12	487	107	191	62
Mo	1811	2155	2518	3611	1712	2230
Cd	-53	164	193	84	28	173
Sb	60	74	305	1306	1292	704
Te	46	-18	30	45	7	-4
Ba	60738	155742	205188	157151	119362	51275
Ta						
Au						
Hg	30	46	161	274	151	-32
Tl	358	368	369	467	95	216
Pb	455	794	693	3457	890	3326
Bi	167	106	111	405	291	325
U	283	448	556	2761	726	1120
Ce	102959	166880	157152	80528	73918	186581
W	202	189	246	643	320	405

Appendix 11b: Geochemical analyses by laser ablation (continued)

cps	SS-95-05-A	SS-95-05-B	SS-95-05-B	SS-95-05-C	SS-95-05-C	SS-95-06-A
Si	17690	19146	14458	62302	15078	12055
S	2858	1696	1762	2098	1559	2410
Ti	11820	7128	5607	1905	7087	8896
Fe	241751	157355	191549	180374	147668	328745
Co	59623	48497	65002	66398	64341	35110
Cu	3679	2881	3175	2506	2012	3207
Zn	24804	20905	29833	54169	51955	8243
As	6207	3038	7467	32782	26220	69273
Se	167	-462	526	339	139	726
Mo	3857	2213	3381	13075	10176	4724
Cd	161	6	112	184	111	115
Sb	137	113	293	422	266	514
Te	13	29	21	-8	49	29
Ba	151252	139022	233697	135319	170231	13639
Ta						
Au						
Hg	-6	101	53	40	19	65
Tl	290	105	171	409	441	195
Pb	1038	408	581	933	677	1431
Bi	92	46	126	63	92	493
U	400	320	219	439	431	361
Ce	110708	85830	96097	82679	78662	49166
W	367	318	341	71	52	230

Appendix 11b: Geochemical analyses by laser ablation (continued)

cps	SS-95-06-A	SS-95-06-B	SS-95-06-B	SS-95-06-C	SS-95-06-C	SS-95-07-A
Si	14256	4752	10077	-666	3089	46638
S	7007	912	721	628	1080	1799
Ti	5195	2460	2810	2630	14475	6890
Fe	368120	167884	146325	112951	136562	226543
Co	79404	103097	120450	52202	118358	29739
Cu	2073	191	260	336	1967	1507
Zn	13990	6690	10337	8581	8385	4448
As	90514	17405	66637	17397	89338	28241
Se	395	68	339	-310	481	738
Mo	8066	905	1057	2185	1132	1733
Cd	37	72	63	219	74	13
Sb	689	36	45	1037	75	191
Te	-8	10	10	12	-13	45
Ba	30528	88953	118431	31055	82842	17415
Ta						
Au						
Hg	48	41	80	-32	78	56
Tl	214	2296	1930	581	482	41
Pb	2561	14	138	118	76	1215
Bi	1027	83	53	20	12	89
U	652	-37	225	328	305	65
Ce	77658	94985	73115	148277	56209	15951
W	419	59	14	47	22	139

Appendix 11b: Geochemical analyses by laser ablation (continued)

cps	SS-95-07-A	SS-95-07-B	SS-95-07-B	SS-95-07-C	SS-95-07-C	SS-95-08-A
Si	16643	2931	2883	5324	1714	15819
S	2521	1112	852	1041	304	-752
Ti	1440	3159	5426	2721	1067	618
Fe	90113	67397	127995	57000	39471	18149
Co	46977	3463	5633	12887	3065	5984
Cu	730	768	891	452	280	1742
Zn	9294	4134	2626	5077	3499	1342
As	12094	7325	34084	5585	2948	2260
Se	599	96	-166	70	-472	155
Mo	1068	745	2468	573	321	175
Cd	115	36	-14	-2	-15	-41
Sb	46	-10	1475	145	-49	77
Te	22	-9	8	-1	-7	10
Ba	33580	2831	3690	9463	1591	3485
Ta						
Au						
Hg	53	132	-41	33	47	-40
Tl	374	9	17	128	6	22
Pb	758	327	438	286	84	78
Bi	86	-267	205	35	18	-7
U	16	351	295	161	32	36
Ce	19161	6573	8973	8789	3232	3151
W	85	93	113	20	44	-5

Appendix 11b: Geochemical analyses by laser ablation (continued)

cps	SS-95-08-A	SS-95-08-B	SS-95-08-B	SS-95-08-C	SS-95-08-C	SS-95-09-A
Si	33157	93486	31962	29576	2092	626809
S	2517	6716	1260	2107	2537	1325
Ti	4584	11241	2562	7904	4299	13168
Fe	170324	417621	78365	186000	328656	258712
Co	91344	112482	18139	79247	115339	80361
Cu	2590	3578	509	1486	2979	2559
Zn	14085	12901	1665	4029	7119	16215
As	29251	285736	36402	22313	24268	94068
Se	366	820	87	614	-72	171
Mo	2194	10434	889	1709	2273	1997
Cd	142	184	-47	33	63	68
Sb	2279	858	55	166	136	1280
Te	-26	57	35	6	39	-2
Ba	67860	54299	8280	24311	25227	28491
Ta						
Au						
Hg	-26	31	-2	-3	44	-17
Tl	1567	616	69	127	277	520
Pb	750	3791	587	3050	1881	596
Bi	104	691	137	231	199	133
U	600	356	176	314	105	504
Ce	65630	111163	15819	65322	201615	99434
W	182	342	73	222	254	311

Appendix 11b: Geochemical analyses by laser ablation (continued)

cps	SS-95-09-A	SS-95-09-B	SS-95-09-B	SS-95-09-C	SS-95-09-C	SS-95-10-A
Si	7245	2036	6256	14790	22848	23851
S	36	811	144	1090	457	481
Ti	2114	944	852	2815	2166	939
Fe	137055	66684	49985	84641	125851	47794
Co	68493	149105	64874	181507	42052	10001
Cu	382	222	127	892	424	354
Zn	8453	17166	11639	17158	6016	967
As	87779	21177	10419	9044	17537	20540
Se	-397	207	4	825	135	-202
Mo	1544	1066	561	4225	975	662
Cd	367	298	88	74	372	-15
Sb	131	1252	290	529	192	63
Te	31	-3	-10	47	0	-14
Ba	37186	32053	26299	55223	46004	3666
Ta						
Au						
Hg	39	-53	-2	-31	18	73
Tl	466	198	215	143	212	28
Pb	754	78	77	46	-3	159
Bi	126	53	70	1279	359	36
U	68	54	30	234	1161	33
Ce	51773	60767	33993	26226	8696	6132
W	66	43	-5	258	42	101

Appendix 11b: Geochemical analyses by laser ablation (continued)

cps	SS-95-10-A	SS-95-10-B	SS-95-10-B	SS-95-10-C	SS-95-10-C	SS-95-11-A
Si	1043	9269	2877	8245	27186	86119
S	549	1396	726	668	1029	2805
Ti	2134	2299	1720	942	1078	2346
Fe	82723	185324	105022	36224	56748	71037
Co	17344	35902	80357	85863	165299	22181
Cu	4306	888	444	25655	24242	13298
Zn	8579	5184	18362	26859	25531	30255
As	42321	43424	58641	3372	3095	1659
Se	128	17	-125	-189	-95	-215
Mo	989	1041	1086	524	491	647
Cd	8	48	103	126	55	273
Sb	80	178	117	67	58	136
Te	-3	-5	-8	14	-13	51
Ba	7559	9912	50815	12882	21438	160450
Ta						
Au						
Hg	19	102	3	-9	-24	58
Tl	770	79	737	242	243	98
Pb	319	767	516	6061	4265	313
Bi	15	239	77	35	20	161
U	39	179	76	596	879	465
Ce	8936	41599	50905	93422	82433	97211
W	66	81	23	27	26	152

Appendix 11b: Geochemical analyses by laser ablation (continued)

cps	SS-95-11-A	SS-95-11-B	SS-95-11-B	SS-95-11-C	SS-95-11-C	SS-95-12-A
Si	95211	42289	82395	54523	37276	92134
S	8480	1052	2035	2584	1231	1346
Ti	4683	35908	2949	4612	2528	7306
Fe	77445	48364	75089	29035	34732	86571
Co	31345	17065	21388	10751	13691	158621
Cu	17389	8402	14077	8013	7047	17338
Zn	24889	8217	16355	11749	11439	13063
As	1427	1904	8492	466	1218	8258
Se	-66	284	4	60	-371	-14
Mo	629	301	662	189	227	1388
Cd	180	48	70	168	5	49
Sb	312	134	196	195	98	651
Te	5	12	25	34	-11	20
Ba	211397	183825	240578	76298	158946	14207
Ta						
Au						
Hg	15	14	57	48	61	6
Tl	55	166	188	12	10	168
Pb	389	80	239	175	241	206
Bi	362	51	64	239	85	207
U	314	230	488	172	435	2525
Ce	144202	64052	132711	66342	79048	433860
W	152	102	281	32	201	1802

Appendix 11b: Geochemical analyses by laser ablation (continued)

cps	SS-95-12-A	SS-95-12-B	SS-95-12-B	SS-95-12-C	SS-95-12-C	SS-95-13-A
Si	94401	71444	28327	34919	25565	14914
S	1146	448	931	2155	3536	1140
Ti	9198	11700	2672	2863	11145	16469
Fe	84194	49837	55701	139104	174936	40333
Co	189266	102485	129636	4361	13586	2747
Cu	12157	92304	131451	1282	3294	510
Zn	16914	20127	17106	12725	19487	5791
As	17163	2264	4295	8607	10215	849
Se	-180	-355	109	-67	119	320
Mo	1114	142	160	275	464	195
Cd	154	477	1035	69	-19	15
Sb	1396	484	358	90	-10	-1
Te	79	69	-3	15	7	-6
Ba	12591	45215	44385	26789	62747	32132
Ta						
Au						
Hg	20	36	-14	20	83	37
Tl	107	108	113	-4	1	19
Pb	319	356	105	318	395	144
Bi	1068	77	91	89	68	25
U	1520	891	630	314	264	132
Ce	986802	111368	181862	15776	25313	6988
W	256	122	79	276	115	69

Appendix 11b: Geochemical analyses by laser ablation (continued)

cps	SS-95-13-A	SS-95-13-B	SS-95-13-B	SS-95-13-C	SS-95-13-C	SS-95-14-A
Si	54133	18884	23845	80572	42044	10267
S	1973	142	566	2058	1004	1017
Ti	3185	4038	5026	10408	1537	1245
Fe	83255	30410	28185	103247	52695	97374
Co	5950	1644	1936	8755	3209	4576
Cu	1404	771	1211	6364	1470	1197
Zn	12410	4669	3452	36503	9837	9640
As	2750	1170	468	2164	1872	4866
Se	-51	-25	166	-172	-104	138
Mo	339	51	70	123	138	1213
Cd	12	-1	4	36	4	-32
Sb	120	17	20	278	40	77
Te	-19	-6	-13	25	-1	-3
Ba	60837	22627	20386	63542	27398	63815
Ta						
Au						
Hg	-18	18	-39	-14	25	3
Tl	46	39	-4	10	14	108
Pb	205	83	48	296	138	391
Bi	67	26	22	40	27	41
U	300	300	120	785	155	290
Ce	12634	4240	6187	15468	9844	12381
W	89	29	10	153	119	79

Appendix 11b: Geochemical analyses by laser ablation (continued)

cps	SS-95-14-A	SS-95-14-B	SS-95-14-B	SS-95-14-C	SS-95-14-C	SS-95-15-A
Si	18093	25246	58589	20702	33250	6374
S	1738	5567	1474	644	2988	1146
Ti	1676	2660	2805	822	11333	1243
Fe	151621	94827	166741	34259	165770	86663
Co	11114	3646	11244	1504	8566	22088
Cu	1213	624	1393	702	1311	923
Zn	10098	43339	75476	6269	16414	6597
As	7217	2956	5235	1028	4881	5599
Se	-259	19	151	-120	92	-54
Mo	884	288	645	199	843	372
Cd	113	5	211	-6	-14	15
Sb	6	163	1732	-10	73	95
Te	-6	-7	16	29	11	-4
Ba	63949	20126	63040	29235	33228	12616
Ta						
Au						
Hg	11	-3	6	35	14	-29
Tl	51	1	76	43	51	-7
Pb	262	483	695	42	363	200
Bi	117	79	159	20	62	17
U	470	194	711	153	238	150
Ce	21834	9497	13803	5326	14545	69019
W	34	122	308	55	62	95

Appendix 11b: Geochemical analyses by laser ablation (continued)

cps	SS-95-15-A	SS-95-15-B	SS-95-15-B	SS-95-15-C	SS-95-15-C
Si	9832	11309	14302	3506	12709
S	1066	1930	3008	1262	531
Ti	2718	853	2561	1185	1301
Fe	64561	260061	202829	138758	131679
Co	9955	86272	84469	111880	15021
Cu	986	905	1267	1962	995
Zn	10268	24672	34731	49839	11959
As	6230	37190	90613	41138	15602
Se	285	15	-223	-20	12
Mo	292	1015	589	716	1507
Cd	32	170	218	500	89
Sb	62	557	367	327	254
Te	23	12	1	19	-1
Ba	20328	141384	59166	180865	17549
Ta					
Au					
Hg	-64	20	15	-48	-24
Tl	79	1043	1079	1328	127
Pb	53	417	275	362	642
Bi	4	86	52	102	53
U	89	239	369	330	190
Ce	64812	91659	57886	145735	83517
W	69	54	37	58	156

Appendix 11b: Geochemical analyses by laser ablation (continued)

cps	SS-95-16-A	SS-95-16-A	SS-95-16-B	SS-95-16-B	SS-95-16-C
Si	46321	31474	32315	17465	9495
S	1992	2536	1708	494	1034
Ti	2823	3988	5393	1540	3774
Fe	185099	381165	141839	146838	164527
Co	48855	54428	77447	18344	35788
Cu	3009	7013	2807	10289	4000
Zn	16401	26078	17340	22481	13770
As	21339	45345	21421	18947	34308
Se	58	62	-72	55	265
Mo	923	2230	1674	458	1344
Cd	61	173	85	52	96
Sb	621	704	3727	316	385
Te	8	-4	23	1	-5
Ba	40857	51275	36081	37361	41882
Ta					
Au					
Hg	43	-32	68	1	-23
Tl	142	216	158	211	205
Pb	1332	3326	597	255	1906
Bi	125	325	58	359	361
U	1562	1120	788	1153	757
Ce	161798	186581	155515	74566	155677
W	258	405	131	113	819

Appendix 11b: Geochemical analyses by laser ablation (continued)

cps	SS-95-16-C	SS-95-17-A	SS-95-17-A	SS-95-17-B	SS-95-17-B
Si	12514	3136	6718	2578	5249
S	947	3155	1698	311	1644
Ti	60301	1272	4308	977	1049
Fe	177543	130472	99801	79584	120291
Co	36240	54509	30368	14204	67282
Cu	10185	3333	2172	1375	2180
Zn	19154	10841	8664	3265	53690
As	13920	11135	6463	6837	16248
Se	295	317	333	80	-172
Mo	1580	547	595	429	1315
Cd	73	113	8	24	330
Sb	538	149	106	105	252
Te	14	1	7	-3	27
Ba	59220	62694	32092	18593	104951
Ta					
Au					
Hg	114	98	93	38	125
Tl	343	539	105	104	547
Pb	1869	790	862	364	383
Bi	281	120	99	127	96
U	826	509	184	262	346
Ce	198848	115433	138739	107423	235677
W	1668	73	82	38	258

Appendix 11b: Geochemical analyses by laser ablation (continued)

cps	SS-95-17-C	SS-95-17-C	SS-95-18-A	SS-95-18-A	SS-95-18-B
Si	7363	7849	648	-748	3953
S	938	1119	1606	663	885
Ti	1049	1286	934	487	4405
Fe	87269	94157	211609	209799	154978
Co	47224	28099	22003	19054	15066
Cu	2302	2395	2045	2658	1538
Zn	19522	15211	253821	202183	3091
As	30827	7165	10593	6756	6053
Se	-209	-17	113	38	-149
Mo	953	633	808	580	227
Cd	73	198	115	101	24
Sb	124	73	190	210	193
Te	533	-1	-1	7	16
Ba	48936	40416	71694	35554	17814
Ta					
Au					
Hg	56	-7	83	179	126
Tl	495	280	134	113	37
Pb	456	227	745	358	404
Bi	108	59	83	74	35
U	566	477	222	211	185
Ce	131049	109109	199775	99821	38447
W	121	95	176	108	43

Appendix 11b: Geochemical analyses by laser ablation (continued)

cps	SS-95-18-B	SS-95-18-C	SS-95-18-C	SS-95-19-A	SS-95-19-A
Si	2128	309	2911	7659	17689
S	1086	715	647	380	1635
Ti	650	408	692	2013	1462
Fe	269853	117741	123880	192283	386285
Co	15642	15944	15036	7059	7933
Cu	1194	1598	1540	1306	1973
Zn	4883	3711	2966	6524	6324
As	10418	4014	2919	7530	25118
Se	-118	114	-136	33	50
Mo	899	200	179	471	609
Cd	24	16	2	31	87
Sb	274	142	211	292	814
Te	4	0	28	-8	4
Ba	21320	15890	10743	13409	12859
Ta					
Au					
Hg	49	70	0	-17	28
Tl	41	25	45	93	83
Pb	558	776	807	901	1598
Bi	56	110	35	610	106
U	302	196	108	424	1431
Ce	71656	99611	67632	51355	73461
W	88	68	53	69	54

Appendix 11b: Geochemical analyses by laser ablation (continued)

cps	SS-95-19-B	SS-95-19-B	SS-95-19-C	SS-95-19-C	SS-95-20-A
Si	8584	6897	9863	1549	7134
S	223	382	488	232	733
Ti	2395	22958	3876	583	1041
Fe	88652	142499	118244	84641	105245
Co	26323	20877	11965	13340	14192
Cu	814	8775	1566	915	10897
Zn	4722	14835	11324	2882	50055
As	13561	10085	23787	5401	7707
Se	-81	51	108	87	105
Mo	308	647	518	390	1057
Cd	33	822	70	51	150
Sb	286	236	568	263	270
Te	-10	27	9	9	2
Ba	28871	40312	11223	9549	34456
Ta					
Au					
Hg	21	-5	93	-78	53
Tl	47	177	68	23	62
Pb	1099	1202	827	680	1088
Bi	108	85	132	29	117
U	170	269	307	148	260
Ce	97687	118700	43420	57501	48143
W	62	149	126	64	149

Appendix 11b: Geochemical analyses by laser ablation (continued)

cps	SS-95-20-A	SS-95-20-B	SS-95-20-B	SS-95-20-C	SS-95-20-C
Si	-506	1112	3314	893	2056
S	320	1236	574	-68	304
Ti	89	256	705	182	543
Fe	16104	41024	82198	36239	59274
Co	2022	3079	4894	3781	3835
Cu	160	290	1689	151	928
Zn	3480	2401	4609	1410	4606
As	789	4840	7544	1564	4548
Se	79	23	110	156	86
Mo	49	221	468	115	230
Cd	33	20	21	24	6
Sb	20	79	236	48	133
Te	1	11	10	-7	3
Ba	2432	8372	5800	11477	12626
Ta					
Au					
Hg	49	60	-54	-89	23
Tl	28	38	78	24	33
Pb	2	181	599	237	389
Bi	6	32	99	10	67
U	20	87	117	94	123
Ce	3277	24005	27238	35452	31467
W	14	70	73	29	48

APPENDIX 111
MASS OF MN-FE-OXIDE COATINGS ON THE STREAM PEBBLES

Original volumes of samples for geochemical analysis

Sample Number	Mass of Pebble + Oxide (g)	Mass of Pebble (g)	Mass of Oxide (g)	Final Solution (g)	Volume Solution (ml)
DC-94-1	2.47045	2.41715	0.0533	49.1774	50
DC-94-1dp	3.65056	3.56346	0.0871	89.7156	90
DL-94-1Bdp	0.67954	0.67669	0.00285	19.80016	20
DC-94-2	6.4304	6.381	0.044	49.9793	50
DC-94-2dp	2.93038	2.89681	0.03357	40.3436	40
DC-94-3	10.05203	9.94248	0.10955	99.2329	100
DC-94-3dp	16.95807	16.85909	0.09898	100.0241	100
DC-94-4	4.51121	4.46482	0.04639	47.6226	50
DC-94-5	4.27743	4.21664	0.06079	59.886	60
DC-94-5dp	4.32738	4.28233	0.04505	49.5199	50
DC-94-6	5.18263	5.11661	0.06602	58.9587	60
DC-94-7	4.71962	4.69137	0.02825	29.5354	30
DC-94-7dp	4.56365	4.53682	0.02683	30.4306	30
DC-94-8A	3.75396	3.73959	0.01437	18.55022	20
DC-94-8B	4.80708	4.75646	0.05062	50.1095	50
DC-94-8Bdp	5.58826	5.54236	0.0459	49.1758	50
DC-94-8C	2.64764	2.49983	0.14781	100.0873	100
DC-94-8Cdp	2.58965	2.4767	0.11295	100.0897	100
DC-94-8D	1.72966	1.69473	0.03493	38.8076	40
DC-94-8Ddp	2.20444	2.17722	0.02722	30.1124	30
DC-94-9	8.913	8.8617	0.0513	50.3514	50
DC-94-10	3.66311	3.62659	0.03652	40.9541	40
DC-94-10dp	3.58056	3.54854	0.03202	30.2817	30
DC-94-11	5.71975	5.68328	0.03647	40.3479	40
DC-94-11B	1.84783	1.83335	0.01448	19.3167	20
DC-94-11Bdp	1.62301	1.61297	0.01004	18.95024	20
DC-94-12	3.90494	3.85186	0.05308	59.6075	60
DC-94-12dp	4.62377	4.55265	0.07112	69.8327	70
DC-94-13	5.94354	5.714	0.22954	105.7409	100
DC-94-14	4.04104	3.93605	0.10499	99.9068	100
DC-94-14dp	2.58933	2.55151	0.03782	39.4439	40

Sample Number	Mass of Pebble + Oxide (g)	Mass of Pebble (g)	Mass of Oxide (g)	Final Solution (g)	Volume Solution (ml)
DC-94-15	1.75858	1.70889	0.04969	49.7756	50
DC-94-15dp	2.0423	1.98454	0.05776	59.6231	60
DC-94-16	2.94285	2.8676	0.07525	79.5451	80
DC-94-16dp	2.04809	1.99298	0.05511	59.7495	60
DC-94-17	3.35339	3.31376	0.03963	40.5769	40
DC-94-18	3.22428	3.12299	0.10129	100.898	100
DC-94-18dp	4.94441	4.84311	0.1013	100.4681	100
DC-94-19	3.27596	3.1611	0.11486	100.5067	100
DC-94-20	3.59862	3.48053	0.11809	100.0041	100
DC-94-20dp	5.19819	5.0393	0.15889	100.5821	100
DC-94-21	1.60786	1.59308	0.01478	19.23481	20
DC-94-21dp	1.10128	1.09087	0.01041	19.17816	20
DC-94-22	2.73655	2.62197	0.11458	100.3215	100
DC-94-22dp	2.29683	2.18413	0.1127	100.6408	100
DC-94-23	3.99616	3.7911	0.20506	100.8773	100
DC-94-24	3.06367	2.96684	0.09683	100.4918	100
DC-94-24dp	2.57913	2.48189	0.09724	100.2269	100
DC-94-25	1.75001	1.66273	0.08728	89.7763	90
DC-94-25dp	1.78764	1.72815	0.05949	60.0776	60
DC-94-26	1.59393	1.57386	0.02007	20.0434	20
DC-94-26dp	1.45281	1.39525	0.05756	59.8909	60
DL-94-1	4.4725	4.45614	0.01636	19.48176	20
DL-94-1B	0.60274	0.59609	0.00665	22.69964	20
DL-94-2	7.41805	7.33266	0.08539	89.6316	90
DL-94-2dp	5.29636	5.28041	0.01595	18.92944	20

Sample Number	Mass of Pebble + Oxide (g)	Mass of Pebble (g)	Mass of Oxide (g)	Final Solution (g)	Volume Solution (ml)
WH-94-1	2.7122	2.68338	0.02882	29.3096	30
WH-94-1dp	3.49936	3.44582	0.05354	50.2388	50
WH-94-2	4.08022	4.06448	0.01574	19.73103	20
WH-94-3	0.97494	0.9704	0.00454	19.91207	20
WH-94-3dp	0.92962	0.92263	0.00699	19.0029	20
WH-94-4	3.84219	3.81893	0.02326	25.7537	25
WH-94-4dp	3.06876	3.04005	0.02871	28.7962	30
WH-94-5	3.17941	3.16499	0.01442	19.56432	20
WH-94-5dp	3.53455	3.52084	0.01371	19.87376	20
WH-94-6	3.06026	3.02965	0.03061	20.22089	30
WH-94-7	5.47266	5.44068	0.03198	28.9627	30
WH-94-7dp	4.53091	4.49805	0.03286	30.4513	30
WH-94-8	4.51056	4.48177	0.02879	30.8684	30
WH-94-8C	0.52763	0.51094	0.01669	19.54642	20
WH-94-8Cdp	0.59565	0.59116	0.00449	19.5989	20
WH-94-9	4.9291	4.88788	0.04122	39.5719	40
WH-94-9dp	2.99734	2.95237	0.04497	40.472	40
WH-94-10	3.59832	3.52628	0.07204	69.696	70
WH-94-11	5.66907	5.60673	0.06234	59.1318	60
WH-94-11dp	3.71869	3.65441	0.06428	65.0865	65
WH-94-12	3.39935	3.34482	0.05453	49.5134	50
WH-94-13	1.68498	1.66997	0.01501	19.7695	20
WH-94-13dp	1.82352	1.78171	0.04181	40.2092	40
WH-94-14	1.73271	1.67544	0.05727	60.3114	60
WH-94-14C	1.36741	1.33661	0.0308	30.3154	30
WH-94-14C	1.24401	1.22448	0.01953	19.65554	20
WH-94-15	2.97069	2.95961	0.01108	19.47622	20
WH-94-15dp	4.88172	4.85781	0.02391	24.5598	25
WH-94-16	3.05312	3.01142	0.0417	40.4202	40
WH-94-17	5.86354	5.84087	0.02267	19.52255	20
WH-94-17dp	2.94813	2.93575	0.01238	19.12618	20
WH-94-18	5.36617	5.34376	0.02241	19.63005	20
WH-94-19	2.8861	2.87398	0.01212	19.88335	20
WH-94-19dp	3.7469	3.72204	0.02486	24.32177	25

Sample Number	Mass of Pebble + Oxide (g)	Mass of Pebble (g)	Mass of Oxide (g)	Final Solution (g)	Volume Solution (ml)
WH-94-20	3.27639	3.21668	0.05971	60.289	60
WH-94-21	3.30576	3.28223	0.02353	19.97322	20
WH-94-22	2.55652	2.54163	0.01489	20.88047	20
WH-94-22dp	2.72208	2.70322	0.01886	19.36854	20
WH-94-23	2.79168	2.77664	0.01504	19.31073	20
WH-94-23B	2.45453	2.44913	0.0054	19.88511	20
WH-94-23Bdp	0.55659	0.55456	0.00203	19.38467	20
WH-94-24	1.63928	1.63048	0.0088	19.89641	20
WH-94-24dp	2.04611	2.03544	0.01067	19.47454	20
HB-94-1	2.4281	2.40627	0.02183	20.08905	20
HB-94-1dp	2.377	2.35753	0.01947	19.89508	20
HB-94-2	7.21816	7.18966	0.0285	30.3295	30
HB-94-3	1.59808	1.59203	0.00605	20.08405	20
HB-94-3dp	1.37524	1.3653	0.00994	19.84543	20
Blank 1	1 ml acid			20.93528	20
Blank 2	1 ml acid			20.17381	20
Blank 3	1 ml acid			40.6468	40
Blank 4	1 ml acid			40.3364	40
Blank 5	2 ml acid			60.8134	60
Blank 6	2 ml acid			21.67758	20
Blank 7	2 ml acid			80.7845	80
Blank 8	2 ml acid			100.1399	100
Blank 9	2 ml acid			100.0112	100
Blank 10	2 ml acid			50.8484	50
Blank 11	2 ml acid			90.1413	90

Sample Number	Mass of Pebble + Oxide (g)	Mass of Pebble (g)	Mass of Oxide (g)	Final Solution Wt. (g)	Volume Solution (ml)
SS-95-01	4.5541	4.55049	0.0037	19.18087	20
SS-95-02	5.5666	5.54478	0.0219	18.81985	20
SS-95-02dp	6.2729	6.22752	0.0454	40.3117	40
SS-95-03	5.2325	5.14157	0.091	89.9405	90
SS-95-04	7.6148	7.5469	0.0679	69.8018	70
SS-95-04dp	5.0575	5.00679	0.0508	49.6391	50
SS-95-05	3.7723	3.68394	0.0884	89.7459	90
SS-95-05A	3.1632	3.09548	0.0678	71.1532	70
SS-95-05Adp	1.56326	1.53444	0.02882	30.1075	30
SS-95-06	9.2261	8.88132	0.3448	100.8583	100
SS-95-06dp	6.2041	5.95166	0.2525	101.3592	100
SS-95-07	5.5246	5.32389	0.2008	100.5834	100
SS-95-08	7.2992	7.18624	0.113	100.7466	100
SS-95-08dp	6.8287	6.76232	0.0664	72.1217	70
SS-95-09	1.937	1.36536	0.5717	103.1144	100
SS-95-10	3.0468	2.79403	0.2528	103.5017	100
SS-95-10dp	1.75747	1.67493	0.08254	79.8623	80
SS-95-11	2.03999	2.02286	0.01713	19.41832	20
SS-95-11B	1.50016	1.49174	0.00842	19.45752	20
SS-95-11Bdp	1.26713	1.25682	0.01031	19.55415	20
SS-95-12	1.97292	1.95926	0.01366	20.1886	20
SS-95-12dp	1.37717	1.36649	0.01068	20.68045	20
SS-95-13	1.9351	1.90466	0.03044	30.3954	30
SS-95-14	1.66653	1.62974	0.03679	35.2898	35
SS-95-14dp	1.40653	1.38176	0.02477	24.8051	25
SS-95-15	1.66067	1.60382	0.05685	60.5734	60
SS-95-15C	0.91694	0.89854	0.0184	20.10335	20
SS-95-15Cdp	1.19015	1.14708	0.04307	45.1937	45
SS-95-16	1.97987	1.96507	0.0148	19.44015	20
SS-95-16dp	2.25808	2.24482	0.01326	19.00196	20
SS-95-17	1.93851	1.87001	0.0685	69.7528	70
SS-95-18	1.60174	1.59342	0.00832	19.23393	20
SS-95-18dp	1.71651	1.70612	0.01039	19.08232	20
SS-95-19	1.47801	1.45848	0.01953	19.53348	20
SS-95-20	1.10422	1.09011	0.01411	19.39547	20
SS-95-20dp	1.37796	1.35408	0.02388	24.4939	25

Sample Number	Mass of Pebble + Oxide (g)	Mass of Pebble (g)	Mass of Oxide (g)	Final Solution (g)	Volume Solution (ml)
SS-95-20A	1.11963	1.10771	0.01192	20.20173	20
SS-95-20Adp	0.93416	0.92435	0.00981	20.15025	20
Blank 12	N/A	N/A	0.015023	19.93936	20
Blank 13	N/A	N/A	0.04401	40.4794	40
Blank 14	N/A	N/A	0.06418	59.7632	60
Blank 15	N/A	N/A	0.07711	80.2982	80

The following chart is a list of samples which were diluted by a factor of 5 because some of the above samples were too concentrated to achieve accurate results.

Sample Number	Mass Oxide (g)	Mass Solution (0.5ml) (g)	Mass Solution (10 ml) (g)	Mass Original (g)
Blank 1	0.01428	N/A	7.28	20.93528
Blank 2	0.01428	N/A	6.3464	20.17381
Blank 3	0.03886	N/A	10.9373	40.6468
Blank 4	0.03886	N/A	10.4315	40.3364
Blank 5	0.0594	N/A	10.4019	60.8134
Blank 6	0.01428	N/A	8.4516	21.67758
Blank 7	0.07525	N/A	10.7378	80.7845
Blank 8	0.12654	N/A	10.4847	100.1399
Blank 9	0.12654	N/A	10.0223	100.0112
Blank 10	0.04947	N/A	10.564	50.8484
Blank 11	0.08659	N/A	10.1952	90.1413
Blank 12	0.015023	N/A	6.2521	19.93936
Blank 13	0.04401	N/A	10.8896	40.4794
Blank 14	0.06418	N/A	10.2869	59.7632
Blank 15	0.07711	N/A	10.4124	80.2982
DC-94-1	0.0533	0.519	10.5876	49.1774
DC-94-1dp	0.0871	0.4827	10.5318	89.7156
DC-94-1B	0.00665	0.5403	10.3044	22.69964
DC-94-2	0.0494	0.5288	10.4379	49.9793
DC-94-3	0.10955	0.532	10.9528	99.2329
DC-94-3dp	0.09898	0.5365	9.8629	100.0241
DC-94-4	0.04639	0.5325	10.8707	47.6226
DC-94-5	0.06079	0.5267	10.3165	59.886
DC-94-5dp	0.04505	0.5244	10.4954	49.5199
DC-94-6	0.06602	0.5376	10.2326	58.9587
DC-94-7	0.02825	0.5408	10.4454	29.5354
DC-94-8A	0.01437	0.5334	10.6611	18.55022
DC-94-8B	0.05062	0.5357	10.5559	50.1095
DC-94-8Bdp	0.0459	0.53	10.1898	49.1758
DC-94-8C	0.14781	0.5238	10.808	100.0873
DC-94-8Cdp	0.11295	0.5129	10.4504	100.0897
DC-94-8D	0.03493	0.5437	10.1998	38.8076
DC-94-8Ddp	0.02722	0.5324	10.2023	30.1124

Sample Number	Mass Oxide (g)	Mass Solution (0.5ml) (g)	Mass Solution (10 ml) (g)	Mass Original (g)
DC-94-9	0.0513	0.545	10.924	50.3514
DC-94-10	0.03652	0.5366	10.3329	40.9541
DC-94-11	0.03647	0.5494	10.2022	40.3579
DC-94-11B	0.01448	0.5661	10.5616	19.3167
DC-94-12	0.05308	0.5314	10.5376	59.6075
DC-94-12dp	0.07112	0.5402	10.4425	69.8327
DC-94-13	0.22954	0.5267	10.4047	105.7409
DC-94-14	0.10499	0.5715	10.6428	99.0968
DC-94-14dp	0.03782	0.5365	10.3314	39.4439
DC-94-15dp	0.05776	0.5249	10.3493	59.6231
DC-94-16	0.07525	0.5163	10.2706	79.5451
DC-94-16dp	0.05511	0.5686	10.3725	59.7495
DC-94-18	0.10129	0.5166	10.0167	100.898
DC-94-18dp	0.1013	0.5347	10.3356	100.4681
DC-94-19	0.11486	0.5223	10.442	100.5067
DC-94-20	0.11809	0.5176	10.7092	100.0041
DC-94-20dp	0.15889	0.5445	10.5033	100.5821
DC-94-21	0.01478	0.5332	10.3472	19.23481
DC-94-21dp	0.01041	0.6638	10.0159	19.17816
DC-94-22	0.11458	0.5096	10.6092	100.3215
DC-94-22dp	0.1127	0.5134	10.6514	100.6408
DC-94-23	0.20506	0.5166	10.1913	100.8773
DC-94-24	0.09683	0.5552	10.3038	100.4918
DC-94-24dp	0.09724	0.5016	10.365	100.2269
DC-94-25	0.08728	0.536	10.2663	89.7763
DC-94-26	0.02007	0.5555	10.6731	20.0434
WH-94-1	0.02882	0.5392	9.9862	29.3096
WH-94-1dp	0.05354	0.5413	10.7113	50.2388
WH-94-3	0.00454	0.5505	10.8249	19.91207
WH-94-3dp	0.00699	0.5914	10.3358	19.0029
WH-94-4	0.02326	0.614	10.3899	25.7537
WH-94-5dp	0.01371	0.7092	10.1695	19.87376
WH-94-6	0.03061	0.5395	10.5363	20.22089
WH-94-7	0.03198	0.5308	10.1223	28.9627
WH-94-8	0.02879	0.5431	9.9836	30.8684
WH-94-8C	0.01669	0.5363	10.1427	19.54642

Sample Number	Mass Oxide (g)	Mass Solution (0.5ml) (g)	Mass Solution (10 ml) (g)	Mass Original (g)
WH-94-9	0.04122	0.5334	10.0799	39.5719
WH-94-10	0.07204	0.5263	10.1327	69.696
WH-94-14	0.05727	0.5212	10.2784	60.3114
WH-94-14Cdp	0.01953	0.5642	10.3578	19.65554
WH-94-15dp	0.02391	0.5667	10.2601	24.5598
WH-94-16	0.0417	0.5333	10.6415	40.4204
WH-94-17	0.02267	0.5637	10.3023	19.52255
WH-94-18	0.02241	0.5333	10.9196	19.63005
WH-94-19	0.01212	0.8882	10.1871	19.88335
WH-94-19dp	0.02486	0.5406	10.5001	24.32177
WH-94-20	0.05971	0.5157	10.4484	60.289
WH-94-20dp	0.02473	0.5332	10.5451	24.4279
WH-94-22dp	0.01886	0.5237	10.2138	19.36854
WH-94-23B	0.0054	0.5282	10.4788	19.88511
WH-94-24	0.0088	0.569	10.567	19.89641
WH-94-24dp	0.01067	0.6197	10.3593	19.47454
HB-94-1	0.02183	0.5896	10.1152	20.08905
HB-94-3	0.006505	0.5729	10.3953	20.08405
SS-95-1	0.0037	0.5388	10.5263	19.18087
SS-95-2	0.0219	0.5354	10.382	18.81985
SS-95-3	0.091	0.5254	10.1705	89.9405
SS-95-4	0.0679	0.5534	10.1999	69.8018
SS-95-4dp	0.0508	0.5299	10.8335	49.6391
SS-95-5	0.0884	0.5393	10.5989	89.7459
SS-95-5Adp	0.02882	0.52	10.3388	30.1075
SS-95-6	0.3448	0.5649	10.8229	100.8583
SS-95-6dp	0.2525	0.5214	10.6902	101.3592
SS-95-7	0.2008	0.5246	10.6851	100.5834
SS-95-8	0.113	0.5289	10.0937	100.7466
SS-95-8dp	0.0664	0.6356	10.4552	72.1217
SS-95-9	0.5717	0.5191	10.0499	103.1144
SS-95-10	0.2528	0.5334	9.9096	103.5017
SS-95-10dp	0.08254	0.5163	10.7586	79.8623
SS-95-11	0.01713	0.5379	10.268	19.41832
SS-95-13	0.03044	0.5425	10.2876	30.3954

Sample Number	Mass Oxide (g)	Mass Solution (0.5ml) (g)	Mass Solution (10 ml) (g)	Mass Original (g)
SS-95-14	0.03679	0.6202	10.1223	35.2898
SS-95-14dp	0.02477	0.5321	10.4	24.8051
SS-95-15	0.05685	0.5747	9.9842	60.5734
SS-95-15C	0.0184	0.5607	10.9546	20.10338
SS-95-15Cdp	0.04307	0.5826	10.2614	45.1937
SS-95-17	0.0685	0.5218	10.5164	69.7528
SS-95-19	0.01953	0.546	10.1948	19.53348
SS-95-20dp	0.02388	0.5621	10.3054	24.4939